Oxidative Degradation of Aqueous Monoethanolamine in CO_2 Capture Processes: Iron and Copper Catalysis, Inhibition, and O_2 Mass Transfer

by

George Scott Goff, B.S.

Dissertation

Presented to the Faculty of the Graduate School of

The University of Texas at Austin

in Partial Fulfillment

of the Requirements

for the Degree of

Doctor of Philosophy

The University of Texas at Austin

May, 2005

The Dissertation Committee for George Scott Goff
certifies that this is the approved version of the following dissertation:

Oxidative Degradation of Aqueous Monoethanolamine in CO₂ Capture

Processes: Iron and Copper Catalysis, Inhibition, and O₂ Mass Transfer

Committee:

_____
Gary T. Rochelle, Supervisor

_____
Charles B. Mullins

_____
Benny D. Freeman

_____
James E. Critchfield

_____
Harovel G. Wheat

In memory of my grandmother,

Lucille Q. West

I hope I make you proud of me.

Acknowledgments

I would like to thank Dr. Gary Rochelle for his support and insight over the course of this project. Dr. Rochelle has always allowed me to pursue my own interests and has shown great patience with me. Our many brainstorming sessions were informative and always interesting, if not always productive. I appreciate that he saw the value in allowing me to develop my teaching skills by serving as a teaching assistant so many times, and that he allowed me to co-teach the senior design course with him. I have also enjoyed my many personal interactions with Dr. Rochelle, and I feel I have learned a lot from him in all aspects of my life. I want to thank him for being my mentor; it has been an experience I will always treasure.

Jody Lester has been a great comfort during my time at UT. She always has answers for my questions or can find the answers faster than I can. Not only does she keep the research group running smoothly, she has always been there professionally and personally for moral support. It has been one of my great pleasures to get to know Jody, and I thank her for making my UT experience much more enjoyable.

Mark Nelson, from Air Quality Analytical, Inc., has been an invaluable help. Mark is trained as a chemist, but he took this engineer under his wing and taught me about vibrational spectroscopy. Mark was always very patient with me and always went out of his way to help me whenever I called him. I could not have completed my project without his help and expertise and I thank him for that.

I would like to acknowledge several graduate students from our research group that I have had the pleasure of working with over the years: Dyron Hamlin, Eric Chen,

Tunde Oyenekan, Ross Dugas, Jennifer Lu, Akin Alawode, Andrew Sexton, John McLees, and Dr. Mohammed Al-Juaied. When I first came to graduate school, I shared a lab with Dr. Sanjay Bishnoi, and I would like to thank him for his friendship and for trying to prepare me for what was to come. Outside of my research group I would like to thank Michael Sigman, Holly Balasubramanian, Kelly O'Leary, Jenny Davila, and my fellow WVU alum Chris Taylor for their friendship. I also must thank everyone who has participated over the years in the greatly anticipated weekly ritual of Burrito Thursday. May the tradition never die!

The best part of my experience in graduate school has been making lasting friendships with some amazing people from Dr. Rochelle's research program. Dr. Norman Yeh was a senior graduate student when I came to UT and he has always been a great friend and mentor to me. Stefano Freguia is one of the funniest and most interesting individuals I have ever met. Things were never boring when he was around, and things have never been the same since he left. It has also been a great pleasure to interact with Marcus Hilliard, who has become a close friend and reminded me of the shocking concept that there is life outside of chemical engineering.

I must extend a special thanks to two of my best friends, Tim and Christa Cullinane, who I consider part of my family. Tim and I have shared a lab for almost our entire graduate experience, and I could not have asked for a better lab partner. He has always been a great sounding board and our technical discussions have been stimulating and valuable. At the least, I must thank Christa for putting up with all of our technical discussions outside of work. Beyond that, Tim and Christa have been my best friends

and I cannot thank them enough for their support, friendship, and everything else they have done for me. I could not have completed this work without them, and I will always treasure the times we spent together in Austin.

I have been fortunate to supervise two undergraduate students who worked on various parts of this project. Thad Urquhart worked with me during the summer of 2001, and Dan Ellenberger who almost single-handedly completed the UV-VIS work this past semester. I have enjoyed getting to know both Thad and Dan professionally and personally, and I thank them for their hard work.

I would like to thank Drs. Craig Schubert and Steve Bedell of The Dow Chemical Co., and Dr. Frank Geuzebroek of Shell Global Solutions for their insight into my research and for helping me develop my technical skills.

My happiest times at UT were probably the two semesters I spent working as a TA for Dr. Del Ottmers, who allowed me to TA the senior level design course with him in 2002 and 2003. He allowed me a great deal of freedom with teaching students and developing course work. Dr. Ottmers has been instrumental in showing me the joys of teaching and allowing me to begin to develop my skills as an educator. He is one of the most caring individuals I have ever met, and it has truly been an honor to interact with him both personally and professionally.

I would like to thank each of my committee members for their help over the years. The advanced kinetics course taught by Dr. Buddie Mullins was the best class I took during graduate school. Dr. Benny Freeman has been invaluable to my professional and personal development. He has taken a lot of time from his very busy

schedule to advise me on topics ranging from journal submissions, to job applications, and even the saké selection in the U.S. Dr. Jim Critchfield has always provided valuable feedback on a wide range of technical and personal issues. I want to thank him for his interest in my professional development and for his advice on some delicate problems. I have also truly enjoyed interacting with Dr. Harovel Wheat, whose enthusiasm for her research is contagious. I appreciate all the time she has spent teaching me about corrosion, even though it never became part of my research project.

I could not have completed this project without the love and support of my family. They gave me the courage to undertake this experience and the strength to finish it. I have watched both my parents return to college for advanced degrees while raising a family and working, and I now understand how truly difficult that was. I appreciate their support and all the opportunities they have given me. I also want to thank my sister for her support and friendship, and the many late night chats on the internet that made my extra-long lab experiments bearable. I am so proud of her and all she has accomplished. I also would like to thank my aunts and uncles for their support and encouragement, and for sharing their experiences in graduate school. I consider my other best friends Mike and Andrea Mirth part of my family. I would like to thank them for their support and friendship, which has been so important to me over the years.

Oxidative Degradation of Aqueous Monoethanolamine in CO_2 Capture Processes: Iron and Copper Catalysis, Inhibition, and O_2 Mass Transfer

Publication No. _____

George Scott Goff, Ph.D.

The University of Texas at Austin, 2005

Supervisor: Gary T. Rochelle

Oxidative degradation of monoethanolamine (MEA) was quantified by measuring NH_3 evolution using FT-IR analysis. This study used a sparged and an agitated reactor, controlled to within ±1°C. The rate of NH_3 evolution was quantified at 55°C, representative of absorber conditions in a typical MEA absorption/stripping process for CO_2 removal from flue gas. The effect of important process parameters, $Fe/Cu/MEA/O_2$ concentrations, CO_2 loading, pH, and agitation was studied. NH_3 evolution rates ranged from $0.15 - 8.7 \times 10^{-3}$ mol/L-hr.

Under significant experimental and industrial conditions, the rate of NH_3 evolution is controlled by the rate of O_2 absorption. Under some experimental conditions the rate of NH_3 evolution depends only on kinetics, and under other conditions the rate depends on both kinetics and O_2 mass transfer. NH_3 evolution rates increased with agitation and increased linearly with O_2 concentration. With low

catalyst (below 0.5 mM Fe/Cu) and MEA (less than 2.0 molal), NH_3 evolution was controlled by kinetics. With high catalyst (above 0.5 mM Fe/Cu) and MEA (above 7.0 molal), NH_3 evolution was controlled by the rate of O_2 mass transfer. Solutions between 2.0 and 7.0 m MEA showed effects of both O_2 mass transfer and degradation kinetics.

Previously reported degradation studies reported lower degradation rates under lower O_2 mass transfer conditions, indicating that these studies were also O_2 mass transfer limited. Industrial degradation rates were predicted for CO_2 capture from flue gas assuming degradation was limited by the rate of O_2 absorption. Results under-predict rates reported in the literature, indicating that in industrial applications oxidative degradation of MEA is likely controlled by the rate of O_2 absorption.

Chelating agents, stable salts, O_2 scavengers and reaction inhibitors, were tested as possible inhibitors. Only O_2 scavengers and reaction inhibitors show enough reduction in NH_3 evolution rates to be considered viable additives in an industrial application. Inhibitor A, a reaction inhibitor, is a stable inorganic compound. Na_2SO_3 and formaldehyde are both O_2 scavengers and are consumed stoichiometrically at the rate of O_2 mass transfer. All three inhibitors are more effective at reducing Cu catalyzed degradation and effectively reduce oxidative degradation at concentrations of approximately 100 to 250 mM.

Contents

Tables

Figures

Chapter 1: Introduction

This chapter gives an overview of CO_2 emission sources and the problems associated with these emissions. Emissions sources are identified and the best targets for emissions reductions are identified. A comparison of various removal technologies is presented along with various methods of CO_2 sequestration. Information on the traditional absorption/stripping process is given including information on solvent degradation. Finally, the objectives and scope of the current project are discussed.

1.1. Global Warming and CO_2 Emissions

1.1.1. Overview

The longest study of atmospheric CO_2 concentrations, measured at Mauna Loa, Hawaii since 1958, shows that CO_2 concentrations have risen by 19% over the last 45 years (Keeling and Whorf 2004). The Intergovernmental Panel on Climate Change (IPCC) has reported various environmental observations that indicate effects of global warming. Annual average temperatures of the Earth's surface, lower atmosphere and oceans are increasing, while areas with year round snow coverage is decreasing and

1

glaciers are retreating (IPCC 2001). These trends are significantly different from the long term trends in CO_2 concentrations. A new report shows that recent trends, over the last 200 years, in both CH_4 and CO_2 concentrations are significantly higher than what is expected based on past long term trends (Ruddiman 2005). The findings of the IPCC were supported by the National Research Council, who also agreed that greenhouse gases are accumulating in the atmosphere, which is "likely mostly due to human activities" (NRC 2001).

Global warming is increasingly becoming a policy issue, with debate centering on the 1997 Kyoto Protocol, which originally called for an overall 20% reduction CO_2 emissions, by 2010, relative to 1990 emission levels. The international response to mitigate global warming was to ratify the Kyoto Protocol, which came into effect on February 16, 2005 and requires at least a 5% reduction in 1990 level CO_2 emissions by 2012 for each signatory (Kyoto Protocol 2004). Even though the United States did not sign the Kyoto Protocol, regulations on CO_2 emissions are coming in the near future. The nature of the global economy means that U.S. companies will be affected by the Kyoto Protocol since many of these companies have plants in countries that have signed the treaty; therefore, there is a demand for research in the area of CO_2 capture technologies both within and outside the U.S.

1.1.2. *CO₂ Source and Sink Emissions*

In the global carbon cycle there are primarily three CO_2 sinks: the atmospheric, oceanic, and terrestrial ecosystems (bio-mass and soil accumulation) (Grace 2004).

Nearly all of the anthropogenic CO_2 is emitted directly to the atmosphere, but only about 40% of the CO_2 accumulates there. Another 30% of the CO_2 is dissolved into the oceans, and the remainder ends up being sequestered in biological ecosystems.

In 2002 the worldwide CO_2 emissions from anthropogenic sources was 24,533 million metric tons of CO_2 (Energy Information Administration 2004b). The U.S. emitted 23% of the worldwide CO_2 emissions with less than 5% of the world's population (U.S. Census Bureau 2004). Approximately 98% of the CO_2 emissions in the U.S. comes from the consumption and flaring of fossil fuels (Energy Information Administration 2004a). Figure 1.1 shows a breakdown of U.S. CO_2 emissions in 2002, which can be used to identify the best target applications for reducing CO_2 emissions.
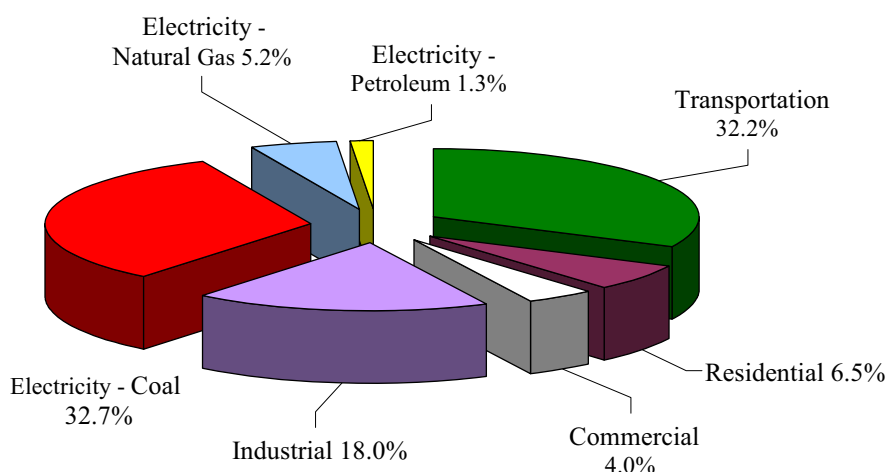
Figure 1.1 Breakdown of U.S. CO_2 Emissions from the Consumption and Flaring of Fossil Fuels in 2002 (Total = $5,729 \times 10^6$ mtons CO_2) (Energy Information Administration 2004a)

The largest source of CO_2 emissions is from electricity generation and the second is from transportation. Targeting the transportation sector for CO_2 removal is

problematic since each automobile itself is only a small source of emissions, and in order to significantly reduce CO_2 emissions a large economic investment must be made to develop and install removal systems for each vehicle. Fossil fuel fired power plants, however, are large point source emitters that represent the best target for reducing CO_2 emissions. The U.S. economy is heavily dependent on electricity, and electric power generation has increased by 13,000% since 1949 (Energy Information Administration 2004b). Figure 1.2 shows that only 10% of the electricity generated in the U.S. comes from renewable energy sources. While 50% of the electricity comes from coal fired power plants, these plants account for 83% of the CO_2 emissions produced from electricity generation. This makes coal fired power plants the most likely target for reducing CO_2 emissions from a point source.
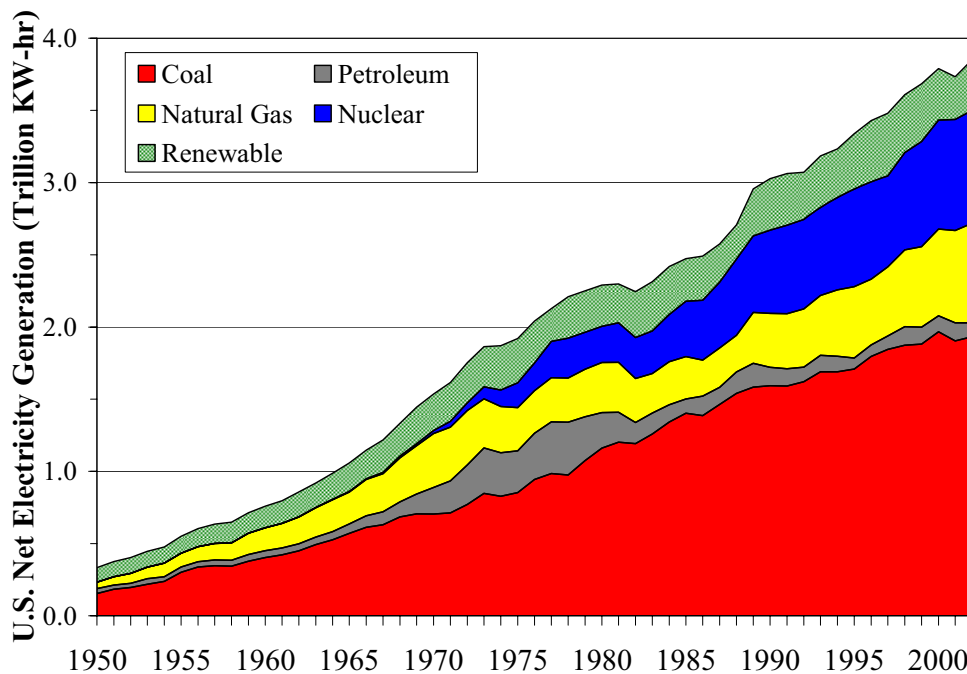
Figure 1.2 U.S. Net Electricity Generation since 1949 by Fuel Type
(Energy Information Administration 2004b)

1.1.3. CO_2 Capture and Sequestration

CO_2 capture from power plants represents the best target for emissions reduction since power plants represent large point source emissions that emit 39% of the total U.S. CO_2 emissions. There are two different scenarios for CO_2 removal from flue gas that are usually discussed, pre-combustion and post-combustion capture (Davison et al. 2001). Pre-combustion capture refers to gasifying a fuel with O_2 to form a syn-gas of CO and H_2. The CO can easily be converted to CO_2 and removed from the H_2 before the combustion process, since the syn-gas is produced at high pressure. This type of process is most commonly associated with a coal gasified power plant, or integrated gasification combined cycle (IGCC) power plant.

Post-combustion CO_2 capture involves various methods of removing the CO_2 from the flue gas at the end of the power plant cycle. This type of removal method is generally associated with a retrofit of a pulverized fuel (coal) power plant with flue gas desulphurization (PF+FGD) or a natural gas combined cycle (NGCC) power plant. A fourth type of power plant is generally discussed, which is a modification of the PF+FGD design. Instead of burning coal with air, this plant uses pure O_2 with recycled CO_2 to control the temperature of the boilers (CO_2/O_2). While producing pure O_2 is expensive, the CO_2 recycle gives a significant concentration increase in the flue gas, which can reduce the cost of post-combustion CO_2 capture.

Table 1.1 shows a comparison of a 500 MW power plant base case without CO_2 removal for each of the four types of plants discussed above (Alstom Power Inc. et al. 2001; IEA 1999; McGlamery et al. 1975). Not only do coal fired power plants emit the

most CO_2, but the CO_2 is more concentrated in the flue gas. This makes CO_2 easier to separate from a removal standpoint, and further supports that coal fired power plants are the best target for CO_2 emissions reductions.

Table 1.1 Comparison of Flue Gas Rates and Composition for 4 Power Plant Configurations (Alstom Power Inc. et al. 2001; IEA 1999; McGlamery et al. 1975)

	PF+FGD	**GTCC**	**IGCC**	**O_2/CO_2**
Flue Gas (scfm)	954,803	2,011,679	1,655,340	238,141
CO_2 (kg/s)	115	56	107	139
CO_2 (wet vol. %)	13	3	7	63
O_2 (wet vol. %)	5	10		
CO_2 (mton/day)	9,936	4,831	9,276	12,010

Several methods of post-combustion CO_2 capture are currently being developed. The most common technologies are cryogenics, membranes, adsorption, and aqueous absorption/stripping (Davison et al. 2001; IEA 1999; 2003). Cryogenic separation of CO_2 is generally only used for gas streams with high concentrations of CO_2. Due to the cold temperatures of the cryogenic solvents, the gas stream must be dehydrated, which is costly when treating the large gas volumes associated with power plant flues gas. Additionally, the cost of refrigeration is high in these processes and makes the economics of cryogenic CO_2 capture unsuitable for a flue gas application. It is difficult to achieve a high purity CO_2 product with membrane separation of flue gas without extensive process modifications like recycles and multiple stage separations. This would lead to increased costs associated with re-compression of the flue gas and large capital investments, making membrane separation an unsuitable technology.

Adsorbents are solids, such as zeolites or activated carbon, that selectively bind CO_2 from the flue gas. The adsorbent beds are regenerated by either applying heat to

liberate the CO_2, temperature swing adsorption (TSA), or by reducing the pressure to allow the CO_2 to desorb from the solid, pressure swing adsorption (PSA). The heat duty associated with TSA is large and PSA requires pulling a vacuum on the adsorbent bed or compressing the flues gas prior to the CO_2 separation step. Additionally, current adsorbents are limited by low selectivity and poor CO_2 capacity (Davison et al. 2001).

The final method of post-combustion capture is aqueous absorption/stripping. This process involves counter-currently contacting the flue gas with an aqueous solvent, typically an amine, that reacts reversibly with the CO_2 in an absorber column. The solvent is then regenerated in the stripper by applying heat to reverse the reaction and liberate the CO_2. Table 1.2 lists several amines commonly used in absorption/stripping for natural gas treating, H_2 purification, and NH_3 production to remove acidic impurities like CO_2 and H_2S (Kohl and Nielsen 1997). Aqueous absorption/stripping is currently the only technology that is developed enough for commercial application of CO_2 capture from flue gas. Monoethanolamine, the current solvent of choice, will be discussed in detail below.

Table 1.2 Common Amines used in Acid Gas Treating (Kohl and Nielsen 1997)

Monoethanolamine (MEA)	Di-isopropanolamine (DIIPA)
Diethanolamine (DEA)	Methyl-diethanolamine (MDEA)
Triethanolamine (TEA)	Di-glycolamine® (DGA®) is a registered trademark of Huntsman Chemical

After removing the CO_2 from the flue gas it must be permanently stored to ensure it will not be released to the atmosphere. The two methods of sequestration are either ocean storage or geological sequestration. Geological storage is currently accepted as the best sequestration method, which includes storage in depleted oil and gas reservoirs, deep saline reservoirs, and unminable coal seams (Davison et al. 2001). Injecting CO_2 into depleted oil and gas reservoirs can enhance the recovery of oil and gas by 10-15%. This technique, enhanced oil recovery (EOR), is an established technique but not widely in use today. Injection of CO_2 into unminable coal seams also recovers methane that is adsorbed on the coal. Deep saline aquifers are capped by a solid rock layer with low CO_2 permeability that would ensure the CO_2 stayed permanently sequestered. These aquifers are deep underground and contain salt water making them unsuitable for drinking water supply, and large volumes of reservoirs are available for CO_2 sequestration.

Both EOR and CO_2 injection into unminable coal seams results in the additional recovery of valuable products (oil and natural gas) which can help offset the cost of CO_2 capture and sequestration, but the capacities of these reservoirs are limited. Table 1.3 shows the capacity of the three types of reservoirs worldwide and the percentage of the projected CO_2 emissions from 2000 to 2050 each type of reservoir could sequester (Davison et al. 2001).

Table 1.3 Capacity of Natural Reservoirs for CO_2 Sequestration (Davison et al. 2001)

	Global Capacity	
	10^9 mtons CO_2	% of emissions to 2050
Depleted oil and gas fields	920	45
Deep saline reservoirs	400 – 10,000	20 – 500
Unminable coal seams	> 15	> 1

1.2. CO_2 Capture by Aqueous Absorption/Stripping

Alkanolamine systems are the current technology of choice for CO_2 capture from flue gas, with monoethanolamine (MEA) being the most widely used solvent. MEA is chosen as the current solvent of choice for flue gas treating because of its high capacity for CO_2, fast reaction kinetics, and high removal efficiencies (Kohl and Nielsen 1997). In the aqueous absorption/stripping process, shown in Figure 1.3, the flue gas, containing up to 15 vol. % CO_2 and 5 – 10 vol. % O_2 (from Table 1.1), is counter-currently contacted with the aqueous amine solution in an absorber column. The CO_2 reacts reversibly with MEA to form an MEA carbamate, shown in Equation 1.1. The rich amine solution, with a CO_2 loading (α) of around 0.40 moles CO_2/mole MEA, is then sent through a counter-current heat exchanger, where it is pre-heated by the lean amine solution before being sent to the stripper column.

$$2\ H_2NCH_2CH_2OH + CO_2 \leftrightarrow HOCH_2CH_2NH\text{-}COO^- + HOCH_2CH_2NH_3^+ \qquad 1.1$$

In the stripper heat is provided in the reboiler by steam, and is used to reverse the chemical equilibrium between MEA and the MEA-carbamate, thus liberating the

CO$_2$. The gas leaving the stripper contains CO$_2$ and water, and is de-hydrated and compressed before being pumped to an aquifer for geological sequestration. The hot lean amine solution, $\alpha \approx 0.15$, is then sent through the counter-current heat exchanger where it is cooled before being recycled to the absorber. Additionally, a reclaimer takes a slip stream from the stripper to remove heat stable salts (such as formate and sulfate) and high molecular weight degradation products.
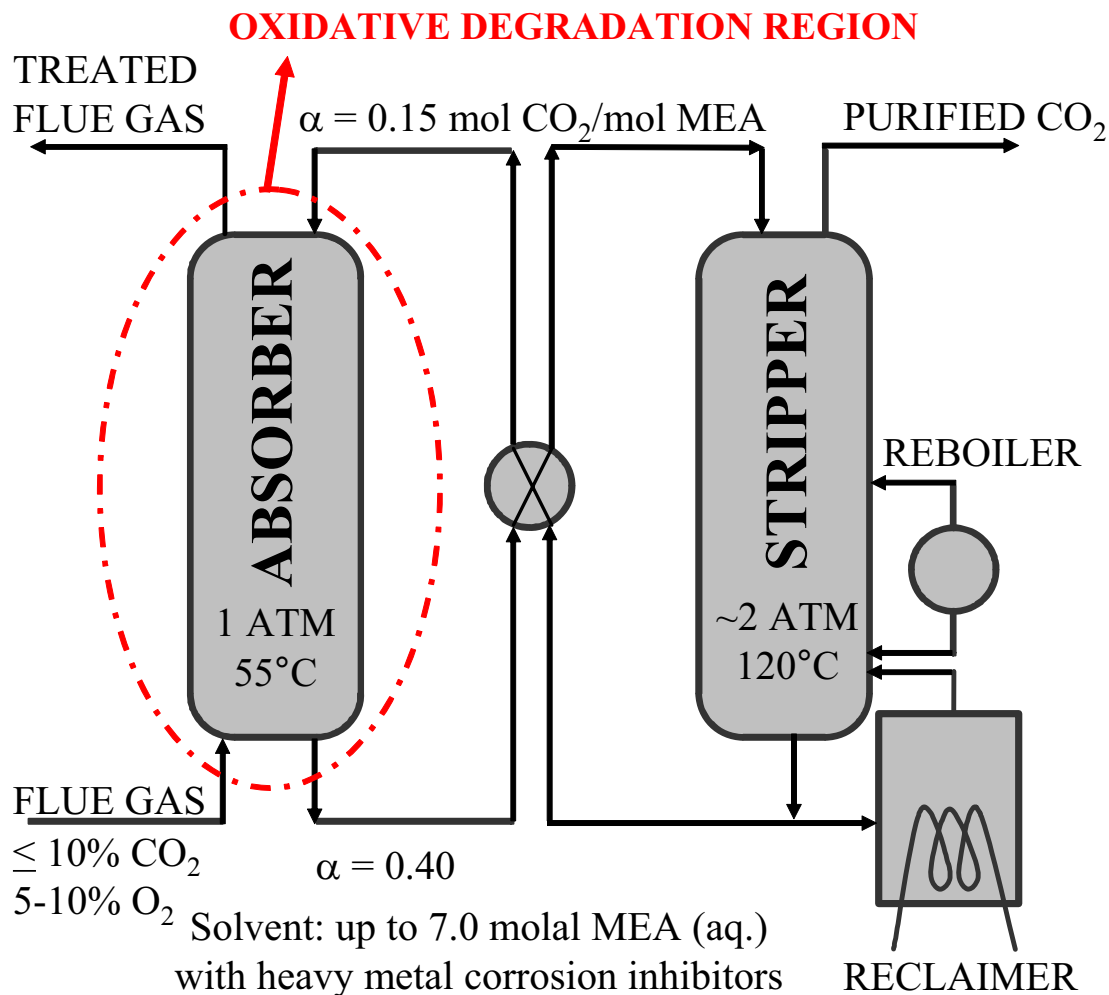
Figure 1.3 Process Flow Diagram for CO$_2$ Capture with Aqueous Absorption/Stripping

Alkanolamine systems for acid gas removal have severe corrosion problems associated with them. MEA by itself is a known corrosion inhibitor in aqueous solutions in the absence of CO_2 (Riggs 1973). This would suggest that neither the amine nor the protonated amine is responsible for iron corrosion; however, amine carbamates are known complexing agents, and could cause the increase in the corrosion rates (Nakayanagi 1996). Plant tests have indicated a much higher dissolved iron concentration than would be expected based on pH speciation calculations (Comeaux 1962; Hofmeyer et al. 1956; Wong et al. 1985). This increased solubility is most likely explained by the complexing of the MEA carbamate with the Fe. Because of this, corrosion inhibitors are used in these systems. Corrosion inhibitors used in acid gas treating systems are primarily heavy metal based. Copper salts are the most commonly used (Cringle et al. 1987; Pearce 1984; Pearce et al. 1984; Wolcott et al. 1985) while vanadium salts, usually in the form of vanadate, are also known corrosion inhibitors for acid gas treating (Ranney 1976).

The CO_2 absorption reaction (Equation 1.1) is highly exothermic, resulting in a large heat duty for solvent regeneration. The high heat duty associated with solvent regeneration is the largest economic factor in the cost of CO_2 capture and results in an efficiency loss of 8 – 13 % for the power plant (IEA 2003). The overall cost of CO_2 capture from a PF+FGD or NGCC power plant is estimated at \$35 to \$50 / mton CO_2 (IEA 2003).

Amine solvents in these processes are subject to three types of degradation: thermal, carbamate polymerization, and oxidative (Rochelle et al. 2001). Thermal

degradation only occurs at temperatures in excess of 200ºC, and should not be a problem in flue gas applications. Carbamate polymerization results in the formation of high molecular weight degradation products, and will occur in any process where an alkanolamine forms a carbamate with CO_2. Oxidative degradation occurs in the presence of oxygen, and results in fragmentation of the amine solvent. This process is not normally encountered in most acid gas treating processes, such as natural gas purification, since these processes do not contain O_2; therefore, oxidative degradation provides an additional mechanism for MEA degradation in CO_2 capture from flue gas which contains O_2 (Table 1.1).

1.3. Research Objectives and Scope

In carbon dioxide removal systems using amine solvents, degradation of the amine contributes a significant cost associated with the make-up rate for the solvent. This make-up rate can depend on several factors such as thermal degradation, oxidative degradation, amine carbamate polymerization, and evaporative losses. The loaded amine solutions will corrode carbon steel equipment, which will in turn catalyze the degradation rates. Since most gas treating processes that use alkanolamines for CO_2 removal are applications without oxygen, oxidative degradation is an additional source of solvent degradation in flue gas treating applications that has not been properly quantified. There are three main reasons the oxidative degradation of MEA must be quantified: potential adverse environmental impact of degradation products, process economics, and process performance.

Known oxidative degradation products of MEA include various aldehydes, NH_3, and nitrosamines (Rochelle et al. 2001). Any release of the volatile degradation products can have adverse environmental impact. Nitrosamines are known carcinogens, and NH_3 forms particulates which are regulated by the U.S. EPA. Most of the degradation products are removed from the process through solvent reclaiming. The liquid and solid waste from this process must be disposed of, and currently the composition, toxicity, and volume of this waste is not well known, and is potentially considered hazardous waste.

Economic losses come from solvent purification and replacement. MEA costs around \$1.48/kg (CMR 2003), and must be continually fed to the process to replace the degraded solvent. Currently solvent degradation is estimated to be around 10% of the total cost of CO_2 capture (Rao and Rubin 2002). It was stated above that the primary economic cost is the heat duty associated with solvent regeneration, but the reclaiming process also uses steam at a higher temperature than the reboiler. While this heat duty is much smaller than the heat duty of the reboiler, any decrease in steam requirements is beneficial to the process. The cost of waste disposal is not cheap, especially for hazardous waste, and has not accurately been accounted for in economic models of CO_2 capture since the degradation process is not well understood.

Another significant cost is associated with equipment corrosion. The MEA solvents are highly corrosive, and the degradation products have been shown to significantly increase the rate of corrosion of process equipment (Hofmeyer et al. 1956; Tanthapanichakoon and Veawab 2003; Veawab and Aroonwilas 2002; Veawab et al.

1999). Both Fe, present in solution as a corrosion product, and the Cu corrosion inhibitors have been shown to catalyze the rate of oxidative degradation of MEA (Blachly and Ravner 1963; Chi 2000; Goff and Rochelle 2004). This represents a serious dilemma in the overall design of the process and can seriously affect the process economics. The corrosion and degradation mechanisms are not understood, so this represents a large technology gap that must be filled.

Oxidative degradation also affects the performance of the system. As the MEA degrades the solvent has a reduced capacity for CO_2 absorption and must be replaced. Freguia showed that the accumulation of heat stable salts (degradation products) can have a catalytic effect on the CO_2 absorption kinetics (Freguia 2002). This is again a major tradeoff since the degradation products increase corrosion and solvent-make-up increases operating costs.

Most previous studies on the oxidative degradation of MEA were long time experiments, taking anywhere from several days to several weeks for a single data point. Some works have been focused only on identifying the liquid phase degradation products (Bello and Idem 2005; Strazisar et al. 2003), while other studies have attempted to quantify degradation rates by measuring the rate of formation of these products (Lawal and Idem 2005; Lawal et al. 2005; Rooney et al. 1998). In an effort to improve the efficiency of degradation experiments, the current study will quantify the rate of oxidative degradation by measuring the rate of NH_3 evolution from the degraded MEA solutions. This is a proven method that has been used previously by several

investigators (Blachly and Ravner 1963; Chi 2000; Hofmeyer et al. 1956), and is valid since NH_3 is the primary amino degradation product of MEA (Petryaev et al. 1984).

The overall goal of this project is to quantify the significance of MEA oxidative degradation and to examine potential methods of minimizing the oxidative degradation rates of monoethanolamine. This study does not include investigations of the other methods of solvent degradation, carbamate polymerization or thermal degradation. Additionally, the effect of other flue gas impurities, such as NO_x, SO_x, etc., on the oxidative degradation of MEA is not included in the scope of this work. The catalysts of interest are Fe and Cu since these will be present in industrial applications. Chi only quantified the effect of Fe on the oxidative degradation of MEA (Chi 2000), and the early studies by the U.S. Navy only quantified Cu over a narrow set of conditions (Blachly and Ravner 1963; 1964; 1965; 1966). The current work proposes to expand upon this work and also quantify the effect of the mixed catalyst system on the rate of NH_3 evolution. Vanadium, while a known corrosion inhibitor (Ranney 1976), is not known to be used commercially in any MEA CO_2 removal application and was not included in this study.

The experimental conditions in this study are representative of conditions encountered in an actual CO_2 capture from flue gas process. An average absorber temperature of 55°C will be used exclusively throughout this study. CO_2 loadings of 0.0, 0.15, and 0.40 will be used along with MEA concentrations ranging from 1.0 to 14.0 molal (m). O_2 concentrations will be varied from zero to 18 wet vol. % (air).

The specific goals of the project are as follows:

- Quantify the effect of process variables such as temperature, oxygen concentration, CO_2 loading, amine concentration, as well as dissolved iron and copper on the oxidative degradation rate of MEA by measuring the rate of NH_3 evolution.

- Determine where in the CO_2 removal process oxidative degradation is most likely to occur.

- To identify oxidative degradation inhibitors suitable for use in an industrial CO_2 capture process and to quantify the effect of these inhibitors on the oxidative degradation rate in the presence of Fe and Cu alone and together.

Chapter 2: Literature Review

This chapter introduces the current body of knowledge on the oxidative degradation of MEA. Information on degradation chemistry, degradation products, and O_2 stoichiometry is presented. A review of previous studies on the oxidative degradation of MEA is presented, as well as a comparison of the oxidative degradation resistance for various amines. Finally, this chapter introduces the basic theory of mass transfer with chemical reaction and how this applies to the current study when interpreting experimental results.

2.1. Degradation Chemistry

The mechanism for the oxidative fragmentation of MEA is still unclear. There are primarily two different mechanisms that give the same degradation products. The first degradation mechanism involves the abstraction of an electron from the lone pair of the nitrogen, while the second mechanism involves the abstraction of a hydrogen atom from the nitrogen, α-carbon, or β-carbon.

2.1.1. Electron Abstraction Mechanism

Figure 2.1, illustrating the proposed mechanism involving the electron abstraction, is based largely on a series of studies performed at the Edgewood Arsenal by the U.S. Army Chemical Research and Development Laboratories. While these experiments studied the oxidation of amines using chlorine dioxide and other single electron oxidants, these studies focused primarily on the oxidation of tertiary amines (Dennis et al. 1967; Hull et al. 1967; Rosenblatt et al. 1963; Rosenblatt et al. 1967). The studies concluded that the rate-limiting step is the electron abstraction, rather than the hydrogen abstraction (Hull et al. 1967). In this mechanism a free radical, such as Fe^{+3}, removes an electron from the nitrogen of the amine, forming an amine radical. The amine radical then de-protonates to form an imine radical. From here, the studies show that the imine radical reacts with a second free radical to form an imine, which reacts with water to form an aldehyde and ammonia. In addition to the imine radical reacting with a free radical, Chi and Rochelle (Chi and Rochelle 2002) propose that the imine radical can react with oxygen to form an amino-peroxide radical. The peroxide radical could then react with another molecule of MEA to form an amino-peroxide and another aminium radical. The peroxide could then decompose to form hydrogen peroxide and an imine, which would in turn react with water to form an aldehyde and ammonia.
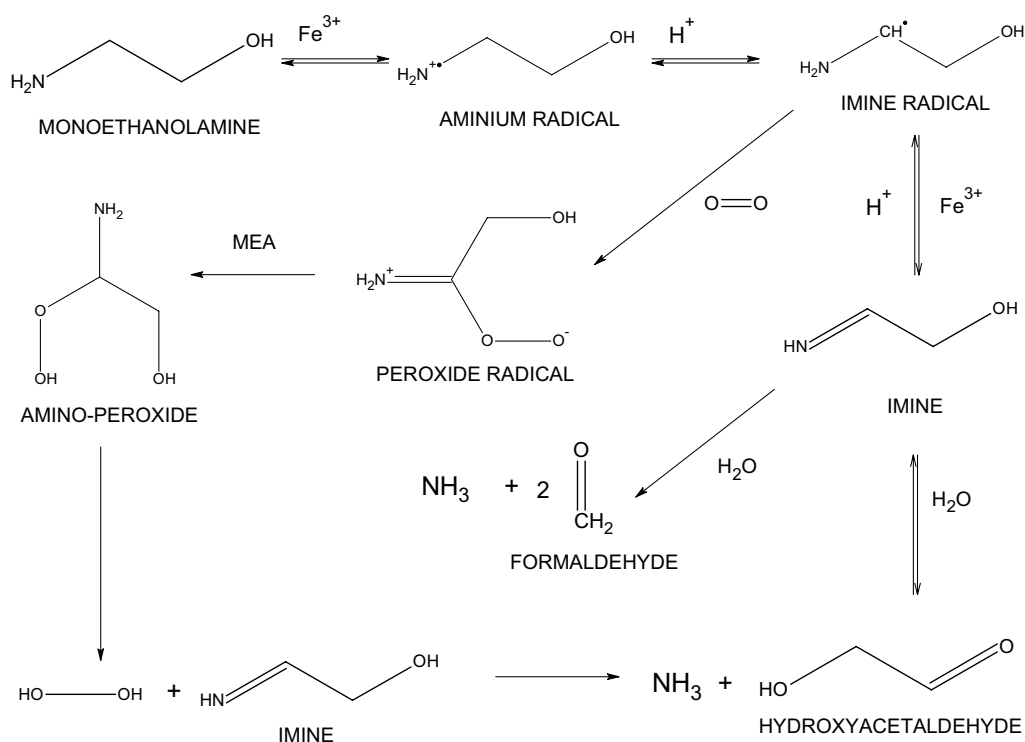
Figure 2.1 Electron Abstraction Mechanism for the Oxidative Degradation of MEA (Chi and Rochelle 2002)

2.1.2. *Hydrogen Abstraction Mechanism*

As stated previously, most of the amines studied at Edgewood Arsenal were tertiary amines. The investigators recognized the hydrogen abstraction mechanism, but determined for tertiary amines the electron abstraction dominated. Only one primary amine was tested, benzylamine, and the study showed that 73% of the amine that degraded proceeded via hydrogen abstraction from the α-carbon (Hull et al. 1967). Another study has shown that MEA will degrade via the hydrogen abstraction mechanism (Petryaev et al. 1984). In this study, aqueous solutions of alkanolamines were degraded by using ionization radiation as the initiation step. The radiation formed

initiating radicals from the aqueous amine solutions, such as H·, OH·, $e^-_{(aq.)}$, H_2, and H_2O_2. The investigators proposed that the mechanism proceeded through a 5-membered cyclic, hydrogen bonded conformation of MEA at pH's greater than 6. In aqueous solution, MEA can form a cyclic conformation by hydrogen bonds between HN---O or OH---N. Free radicals can abstract a hydrogen atom from the nitrogen, the α-carbon, or the β-carbon. The newly formed amine radical can then transfer the radical internally through the ring structure, which ultimately results in cleavage of the N---C bond. The degradation products are NH_3 and an aldehyde or aldehyde radical, which can be seen in Figure 2.2. In the case of the aldehyde radical formation, this radical would act as an initiator by abstracting another hydrogen from a second molecule of MEA, forming the MEA radical and the aldehyde.

The validity of the cyclic transition state is supported by several molecular simulation studies (Alejandre et al. 2000; Button et al. 1996; Vorobyov et al. 2002). These studies predicted and validated the existence of the cyclic conformation in aqueous solutions by spectroscopic methods. The properties predicted by the molecular simulations have been able to reproduce observed data with good accuracy. The mechanism of hydrogen abstraction is further supported by these studies by validating the formation of the 5-membered ring. Specifically, one study shows that there are 2 conformations of the OH---N ring, and 4 conformations of the NH---O ring (Vorobyov et al. 2002). Additionally, Vorobyov predicts that the strength of the hydrogen bond in one of the OH---N conformations is at least 4 times stronger than any of the other conformations. In the hydrogen abstraction mechanism above, two of the three

intermediates involve the OH---N conformation and result in ammonia as the primary amino degradation compound. Since the molecular simulations predict that this is the most stable of the conformations, ammonia, and not methyl-amine, is the most likely amino degradation product from the oxidative degradation of MEA.
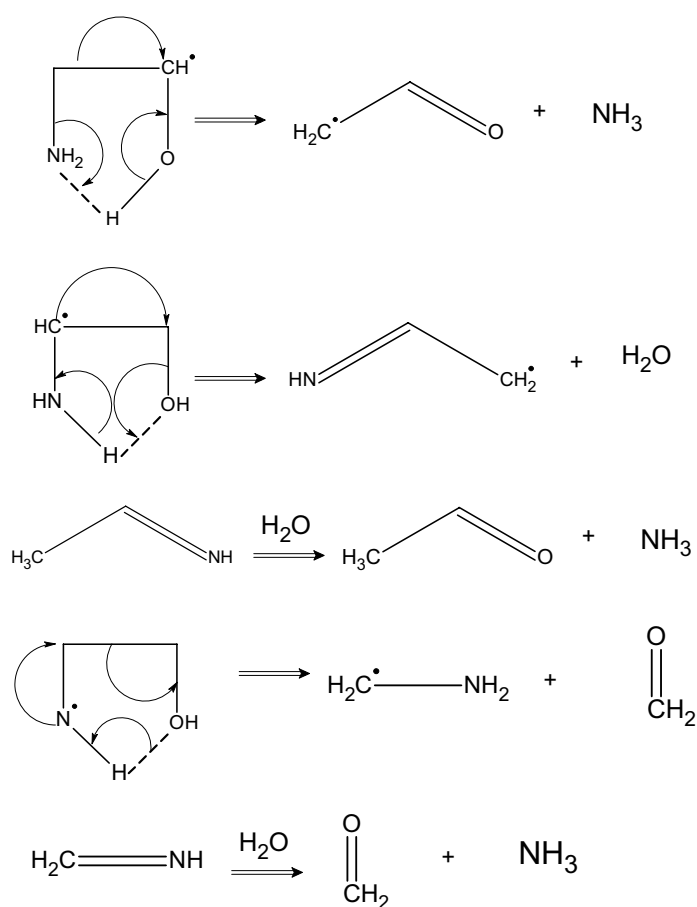
Figure 2.2 Hydrogen Abstraction Mechanism for the Oxidative Degradation of MEA (Petryaev et al. 1984)

2.1.3. Degradation Products

Both of the previously presented mechanisms predict the primary degradation product of MEA is ammonia, followed by various aldehydes. It has been well established that aldehydes are very susceptible to autoxidation in the presence of oxygen (Fessenden and Fessenden 1994). Oxygen has two unpaired electrons in its ground state and is therefore considered a diradical, often represented as ·O-O·. The oxygen will react with aldehydes to form carboxylic acids via a peroxy acid intermediate. Since the MEA solutions have high pH (9-12), the carboxylic acids would dissociate in solution to form heat stable salts with MEA, partially neutralizing the amine and reducing the capacity for CO_2 absorption. The presence of organic acids in degraded MEA solutions has been documented by several investigators, particularly a study by The Dow Chemical Co. (Rooney et al. 1998), and will discussed in detail below in Section 2.2.

While the two mechanisms presented above are useful in qualitatively showing the route to the degradation products, neither of these mechanisms directly accounts for the role of oxygen or the dissolved metals. Additionally, the mechanisms are written only in terms of free MEA degrading, while in fact there are actually three MEA species present in CO_2 loaded solutions. The effects of speciation and pH will need to be included in a comprehensive degradation mechanism.

2.1.4. O_2 Stoichiometry

It is important to note that while the pathway described by both of the above mechanisms is different, the degradation products are the same. Both of the mechanisms predict the primary amino degradation product of MEA is ammonia, followed by various aldehydes, which will be oxidized to carboxylic acids in the presence of oxygen. The formation of the carboxylic acids has a strong effect on the overall oxygen stoichiometry of the system, depending on which acid is formed.

Table 2.2 shows the formation of various organic acids in loaded and unloaded amine solutions. This study was able to identify the most common anions being formed as acetate, formate, glycolate, and oxalate. These experiments also show that the primary anion that is formed for MEA degradation is formate, in both loaded and unloaded solutions. Another minor degradation product formed for both the loaded and unloaded solutions is acetate, while oxalate was only detected in the unloaded solutions.

The oxygen stoichiometry is extremely important when trying to extract kinetics from degradation measurements. Table 2.1 shows a comparison of the O_2 stoichiometry involved in the formation of various degradation products, based on the elementary reaction of O_2 with one molecule of MEA. This reaction represents a minimum stoichiometry to achieve the given degradation product. All of the degradation products listed in Table 2.1 are predicted from the mechanisms presented above with the exception of CO and CO_2. These products have been included as final oxidation products and should represent the highest oxidation state of products that could possibly be formed. The stoichiometry can vary from 0.5 to 2.5 depending on what degradation

23

product is being formed, with the 2.5 representing an extreme upper limit on the expected stoichiometry. It should also be noted that degradation products will be formed in parallel, so the actual stoichiometry of the process should fall somewhere in the range of 0.5 to 2.5. It should be noted that the stoichiometry for acetaldehyde is 0.0, which means acetaldehyde can be formed by any free radical and this reaction can occur in the absence of O_2.

Table 2.1 Oxygen Stoichiometry for the Formation of Various Degradation Products

MEA + $\nu O_2 \rightarrow NH_3$ + Degradation Products	
Product	**Stoichiometry (ν)**
Acetaldehyde	0.0
Formaldehyde	0.5
Acetic Acid	0.5
Hydroxyacetaldehyde	0.5
Glycolic Acid	1.0
Formic Acid	1.5
CO	1.5
Oxalic Acid	2.0
CO_2	2.5

Since the rate of oxidative degradation in this study is quantified by the rate of NH_3 evolution from the MEA solution, the O_2 stoichiometry relates this rate to the rate of O_2 consumption by Equation 2.1. The uncertainty of the factor of 5 associated with the oxygen stoichiometry must be accounted for when interpreting measured degradation rates or predicting MEA degradation rates from the rate of O_2 absorption based on process conditions.

$$\text{Rate of NH}_3 \text{ Evolution} = \frac{\text{Rate of O}_2 \text{ Consumption}}{\nu} \qquad\qquad 2.1$$

2.2. Previous MEA Oxidative Degradation Studies

Several different studies have previously been performed on the oxidative degradation of MEA. These studies were performed over a wide range of experimental conditions, making direct comparison of the results difficult. No mechanistic studies for the oxidative degradation of MEA have been performed, and only one study unsuccessfully attempted to extract kinetics from the experimental data. Several studies have partially or completely analyzed the liquid solution for aqueous, non-volatile degradation products; however, no study has been conducted that was able to close the gas and liquid phase material balances for the MEA solution. A summary of each of these studies follows.

2.2.1. The Dow Chemical Co.

Two studies on MEA degradation were performed by The Dow Chemical Co. The first study quantified the rate of oxidative degradation by measuring the rate of NH_3 evolution from the amine solution and the basicity loss of the liquid amine solution (Hofmeyer et al. 1956; Lloyd 1956). The rates reported in this study are the highest rates reported in the literature besides rates reported by studies in the current research group. In this study it was shown that the NH_3 loss from the MEA solution accounted for 40% of the total basicity loss of the solvent. The rest of the basicity loss came from neutralization of free MEA by the formation of heat stable carboxylic acid salts.

Corrosion tests performed with MEA solutions showed a significant increase in corrosion rate with the degraded solutions.

The second study performed by The Dow Chemical Co. is the most complete and accurate experimental study of the aqueous degradation products of MEA performed to date (Rooney et al. 1998). The formation of carboxylic acids in CO_2 loaded ($\alpha = 0.25$) and unloaded solutions of 20 wt. % MEA, 50 wt. % di-glycol amine® (DGA®), 30 wt. % diethanolamine (DEA), as well as 30 and 50 wt. % methyl-diethanolamine (MDEA) over a 28 day period was quantified by liquid analysis with ion chromatography. Solutions were degraded by bubbling air through the amine solutions at 180ºF.

The study showed that of the unloaded solutions, MEA degraded the fastest. Both of the MDEA solutions degraded faster than the MEA solutions for the loaded solutions, and all of the loaded solutions had lower degradation rates than the unloaded solutions. A summary of the total anions formed at the end of the 28 day experiment for all of the solutions tested can be found in Table 2.1. The study was able to identify some of the anions being formed as acetate, formate, glycolate, and oxalate. Based on this data, it can be seen that the primary anion that is formed for MEA is formate, regardless of loading. Another minor degradation product formed for both the loaded and unloaded solutions is acetate, while no oxalate was detected for MEA degradation. Interestingly enough, glycolate is only detected in the unloaded solutions.

Since this study was able to quantify the distribution of carboxylic acid degradation products for loaded and unloaded MEA solutions, the O_2 stoichiometry for

these solutions can be calculated using the information in Table 2.1 and Equation 2.1. Since NH_3 is not expected to be the only amino degradation product for MDEA, DGA®, and DEA, Equation 2.1 cannot be used to estimate O_2 stoichiometry for these amines. The O_2 stoichiometry for MEA is 1.17 for the unloaded solution, and 1.44 for the loaded solution. While the degradation rate for the unloaded solution is higher, the O_2 stoichiometry is lower.

Table 2.2 Comparison of Anion Formation for Various Alkanolamine Solutions over 28 Days of Oxidation (935 g Solution, Air Sparging, 180°F) (Rooney et al. 1998)

Rates of Formation ($\mu mol/kg_{solution}$-hr)	Acetate	Formate	Glycolate	Oxalate	Total Anions
50 wt.% MDEA unloaded	2.8	7.8	10.2	0.0	20.8
50 wt.% MDEA loaded	2.3	10.3	8.6	0.0	21.2
30 wt.% MDEA unloaded (1)	11.3	7.3	13.2	0.0	31.8
30 wt.% MDEA unloaded (2)	11.0	8.2	14.0	0.0	33.2
30 wt.% MDEA loaded	6.7	6.9	10.0	0.0	23.6
30 wt.% DEA unloaded	1.5	7.4	1.9	0.0	10.8
30 wt.% DEA loaded	1.2	1.8	0.2	0.0	3.2
50 wt.% DGA® unloaded	3.4	31.5	3.8	0.2	39.0
50 wt.% DGA® loaded	5.2	6.8	0.0	0.2	12.2
20 wt.% MEA unloaded	1.4	27.3	19.5	0.0	48.2
20 wt.% MEA loaded	1.5	16.5	0.0	0.0	18.0

for the loaded solutions $\alpha = 0.25$

2.2.2. U.S. Department of Energy

The study by the National Energy Technology Laboratory performed comprehensive liquid analysis on degraded samples from an industrial application (Strazisar et al. 2003). The IMC Chemicals Facility in Trona, CA removes CO_2 from a coal-fired power plant using an aqueous MEA solvent, and uses the purified CO_2 to

carbonate brine for the sale of commercial sodium carbonate. This facility has been removing CO_2 from flue gas since 1978, which is longer than any other facility.

Solution analysis was performed on make-up MEA (clean), lean MEA (inlet to the absorber), and the liquid waste from the reclaimer. Volatile compounds were identified using gas chromatography combined with mass spectrometry (GC-MS), FT-IR, or atomic emission detection. Ionic species in the liquid were quantified using ion chromatography and inductively coupled plasma-atomic emission spectroscopy. This is the first published study to attempt a quantitative analysis of degraded industrial solutions. In addition to the known carboxylic acid degradation products, several new degradation compounds were detected in this experiment, but using this data to extract kinetics or mechanisms for oxidative degradation is problematic.

First, since this analysis was done using an actual flue gas, many of the degradation products are attributable to reactions with impurities in the flue gas such as SO_X and NO_X. Sulfate was found in the liquid solution, as well as nitrosamines. No solution analysis was performed on the rich MEA solution. This makes it impossible to determine whether the "new" degradation products are being formed in the absorber/stripper process or in the solvent reclaimer. Additionally, the solid precipitate in the reclaimer was not analyzed so a complete material balance around the reclaimer is impossible. No analysis was done on the treated flue gas or the purified CO_2 stream to analyze for volatile degradation products like NH_3.

Many of the degradation products identified in this study are likely the result of carbamate polymerization, CO_2 side reactions, or from thermal degradation in the

reclaimer. While quantitative data on rates of oxidative degradation of MEA cannot be determined from this study, the study does show the presence of carboxylic acids in the degraded solution, which matches the expected degradation products predicted above.

2.2.3. University of Regina

Two studies were performed by different principle investigators at the University of Regina. The first study was as an attempt to quantify the kinetics of the oxidative degradation of MEA under conditions encountered in a typical flue gas treating process (Supap 1999; Supap et al. 2001). Experiments were performed with an autoclave reactor at elevated temperatures and pressures. Degradation was quantified by measuring the concentration of MEA using GC-MS. Kinetics were regressed from the experiments based on the rate of MEA loss and O_2 consumption. As the O_2 was consumed, O_2 was added to the reactor to maintain constant pressure. Since the partial pressure of volatile degradation compounds, namely NH_3, was not accounted for in the total pressure measurements, there is some question as to the accuracy of the O_2 consumption rate. Additionally, some of the kinetic parameters of the degradation reactions only have a statistical significance of $\sim \pm 200\%$. Using the kinetics from this study to predict the degradation rates expected in the reactors used in this work under-predicts the degradation rate by an order of magnitude. Based on these results and the data presented in Chapter 4, these experiments were performed under conditions controlled by the rate of O_2 mass transfer, and the degradation kinetics should not be assumed to be accurate.

The second study was performed more recently and analyzed the liquid solution to determine the degradation products and mechanism of degradation for MEA and mixtures of MEA/MDEA (Bello and Idem 2005; Lawal and Idem 2005; Lawal et al. 2005). Experiments were again performed with an autoclave reactor at temperatures of 55°C, 100°C, and 120°C and O_2 pressures of 250 or 350 kPa over a several day time frame. Degradation experiments were performed with and without O_2 and CO_2 to quantify the effect of CO_2 loading and degradation in the absence of O_2. Degradation products were identified using a GC-MS with methods developed by previous investigators in the research group (Supap 1999). Concentrations and rates of formation of the degradation products were not quantified, and MEA/MDEA degradation rates were quantified by the concentration change of the amine with time.

A significant number of degradation products were identified, most of which had not previously been identified and reported in the literature, ranging from NH_3 and formate to a 15-member cyclic crown ether. Noticeably absent in the identified compounds are thermal degradation products and carbamate polymerization products that have been identified previously by several investigators (Polderman et al. 1955; Yazvikova et al. 1975). It is unclear whether the products identified in the earlier studies were included in the sample analysis or not, but complex mechanisms were also presented to show the formation pathway for all of the measured degradation products.

Compound analysis was performed by doing a library search to mass spectra in the NIST database. The original work by Supap shows that the statistical match for the MEA sample spectrum to the NIST reference spectrum is only as good as 86%, and that

the statistical match of some of the reported major degradation products is as low as 10%. This brings into question the accuracy of the analytical method, with such a poor statistical match with the reference spectra of the degradation compounds.

Excluding the difficulties with the analytical methods, several trends were apparent from the data. Degradation rates increased with increasing temperature and O_2 partial pressure; however, the degradation rates decreased when the MEA concentration increased. Unloaded MEA solutions in the presence of O_2 degraded the fastest, followed by loaded MEA with O_2, and the slowest was loaded MEA with no O_2. The addition of MDEA to the MEA solutions appears to decrease the rate of MEA oxidation as the MDEA is preferentially oxidized. Since the oxidation kinetics of tertiary amines are faster than primary amines, MDEA should degrade preferentially to MEA in the blended solvent under O_2 mass transfer controlled conditions.

2.2.4. Girdler Corporation

Early studies on the oxidative degradation of alkanolamines were primarily driven by the U.S. Department of the Navy starting in the early 1950's (Girdler Corporation 1950). Alkanolamine systems were being used to remove CO_2 from the air supply of nuclear submarines. Oxidative degradation in these types of systems is particularly important since ammonia, which is a known toxic air pollutant, is volatile and can be released into the closed atmosphere of the submarine. The study performed by the Girdler Corporation was intended to screen a wide range of potential amine

31

absorbents based on several properties including resistance to oxidative degradation. Oxidative degradation tests were performed on 39 amines and 11 blends of amines.

Experiments were performed by sparging a 50/50 blend of CO_2/O_2 through amine solutions for seven days. Degradation was quantified by measuring free amine concentration, primary amine concentration, total organic nitrogen content, and NH_3 evolution. Results from the experiments showed significant degradation of MEA when studied alone and in blends with other amines. MEA was not recommended for further study as a CO_2 capture solvent in nuclear submarines due to the high degradation rates.

2.2.5. Navy Studies

Despite the findings of the Girdler Corporation, MEA was selected as a solvent for air purification in nuclear submarines. Degradation of MEA solutions in nuclear-powered submarines was noticed by the smell of ammonia in the atmosphere, as well as a darkening of the solution color, decreased CO_2 capture efficiencies, and an increase in amine make-up rates (Blachly and Ravner 1964). A series of studies was conducted in the early 1960's to attempt to quantify and inhibit the oxidative degradation of MEA (Blachly and Ravner 1963; 1964; 1965; 1966; Lockhart and Piatt 1965).

Studies were performed by sparging gas (with various O_2 and CO_2 concentration) through MEA solutions. Degradation was quantified by measuring the rate of NH_3 evolution over several days. These studies are important because they are the first to quantify the catalytic effect of a range of dissolved metals. In particular, iron, chromium, and nickel were studied since the submarines use stainless steel

equipment for the CO_2 removal process. Copper was also found to be an important contaminant, and was shown to come primarily from the ships water supply (from the copper piping). Of the four metals studied, Cu was the only metal that showed unacceptably high catalytic activity under conditions normally found in a nuclear submarine (Blachly and Ravner 1964). This is also the first study to show the presence of peroxide production during the degradation mechanism, although the structure of the peroxide was not identified.

An inhibitor package was developed based on two additives, the tetra-sodium salt of ethylene-diamine-tetra-acetic acid (EDTA), and the monosodium salt of N,N-diethanol glycine (VFS, or bicine). The EDTA was used as a chelating agent to bind the Cu and other dissolved metals to prevent them from acting as catalysts, and VFS functioned as a peroxide scavenger to inhibit the degradation mechanism. These inhibitors were both found to be more effective at inhibiting Cu catalyzed degradation than any of the other three metals. Specifications were developed for an additive package consisting of both EDTA and VFS, which was subsequently employed in nuclear submarines to minimize oxidative degradation of MEA.

2.2.6. The University of Texas at Austin (Rochelle Group)

Until recently, most degradation studies were long-term experiments. The experiments were performed by sparging a gas containing CO_2 and O_2 through a loaded amine solution, or using pressurized reactors with elevated temperatures and partial pressure of O_2. Studies that analyzed NH_3 evolution from the MEA solutions did so by

passing the reaction gas through a weak acid solution to dissolve the ammonia, and periodically titrating with a strong acid. Most of these studies were performed at low gas rates, and subsequently low mass transfer conditions. Degradation rates were low and required long experimental times to accumulate enough degradation products for accurate detection.

The studies performed by Chi and Rochelle were able to decrease the experimental time by instantaneously measuring the concentration of evolved ammonia by Fourier-Transform Infra-Red (FT-IR) analysis (Chi 2000; Chi and Rochelle 2002). The degradation rate was quantified by analyzing the rate of evolved NH_3 normalized to the liquid volume of amine solution. The benefit of this method is that it allows instantaneous measurements of gas-phase products (NH_3), without having to run experiments for long periods of time. Data points were obtained in a matter of hours as opposed to weeks. Since these experiments were run at conditions with much higher mass transfer conditions, volatile compounds were stripped from the MEA solutions so that the concentration of dissolved NH_3 is negligible. This method allows amine degradation rates to be quantified only by gas analysis, and eliminates the messy and complex liquid analysis. Only primary amines that form NH_3 as the primary degradation product can use this analysis method.

Chi studied the effect of dissolved Fe on the oxidative degradation of MEA, and found that dissolved iron, over a concentration range of 0.0001 to 3.2 mM, catalyzed the degradation rates from 0.12 to 1.10 mmoles NH_3 evolved / liter of solution-hr. This degradation rate is significantly higher than the rates encountered in the other reported

studies. The effect of EDTA and VFS were also studied to confirm the inhibiting potential in MEA solutions under conditions found in flue gas applications. These studies showed that a ratio of bicine to total dissolved iron of 100 to 1 cut the degradation rate by half. EDTA studies by these investigators somewhat contradicted the findings of Blachly and Ravner. Chi found that in solutions with a CO_2 loading of 0.40, a ratio of EDTA to total dissolved iron of 22.5 to 1 cut the degradation rate by 40%. A second experiment at a lower total iron concentration showed that at a ratio of EDTA to iron of 130 to 1, the rate was also decreased by 40%. This data shows that further study on the effectiveness of EDTA as a degradation inhibitor is needed, since it appears that EDTA is potentially as strong an inhibitor as VFS for Fe catalyzed degradation.

A second study carried out co-currently with this work examined the effect of vanadium as an oxidation catalyst (Ho 2003). The study by Ho used the same Sparged Reactor as the current study, described in detail in Chapter 3, and combinations of V, Fe, and Cu. Results from the experiments show that V is a catalyst for oxidative degradation and rates reported were equivalent to rates with Fe or Cu alone. These experiments also appear to be limited by the rate of O_2 mass transfer.

2.3. Oxidative Degradation Stability of Various Solvents

A comprehensive review of the oxidative degradation of a wide range of amines has been presented elsewhere, but will be summarized here (Rochelle et al. 2001). Reported data on the resistance to oxidative degradation of various amines used in CO_2

35

removal processes is inconclusive and conflicting. The original study by the Girdler Corporation showed that DEA degraded faster than MEA, and tertiary amines (MDEA) were significantly slower (Girdler Corporation 1950). Hofmeyer et al. reported that the resistance increased from MEA < DEA < TEA (Hofmeyer et al. 1956). The study by Rooney et al. (Rooney et al. 1998) contradicts these findings and shows that in unloaded solutions, resistance to oxidative degradation follows the following trend: 30% DEA > 50% MDEA > 30% MDEA > 50% DGA® > 20% MEA. The trend changes in the presence of CO_2 to: 30% DEA > 50% DGA® > 20% MEA > 50% MDEA > 30% MDEA. Recent studies in the Rochelle Group have shown that oxidative degradation of aqueous piperazine, a cyclic secondary diamine, in concentrated K_2CO_3 is approximately the same as aqueous MEA (Alawode 2005 (in progress); Jones 2003).

Studies on the fundamental reaction mechanisms of various amines with free radicals suggests that rate constants increase in the order of primary amines < secondary amines < tertiary amines (Hull et al. 1969a; Hull et al. 1969b; Hull et al. 1967; Hull et al. 1969c). Hindered and substituted amines are more resistant to degradation and amines with hydroxyl groups (alkanolamines) are more likely to degrade than the corresponding alkylamine.

Kinetic studies suggest that primary amines are expected to react with free radicals slower than secondary and tertiary amines, which is contradictory to the results from oxidative degradation experiments presented above. This is possibly due to the degradation experiments being O_2 mass transfer limited, discussed in detail in Chapter 4. Secondary and tertiary amines generally have higher viscosities and surface tensions,

and lower O_2 diffusivities than primary amines. If the degradation kinetics for these amines are even higher than primary amines, these systems are even more likely to be O_2 mass transfer limited than the MEA system.

2.4. Mass Transfer with Chemical Reaction

When trying to look at the reaction of aqueous MEA with O_2, it is important to understand the two types of physical processes that occur and how they interact. First, the O_2 must dissolve into the amine solution, and then it can react with MEA to form the degradation products. This means that the system depends on both the rate of O_2 mass transfer from the flue gas into the liquid solution as well as the kinetics of the interaction of O_2 with the amine. In order to correctly interpret the results of degradation experiments and to be able to accurately predict degradation rates in an actual CO_2 removal process, it is necessary to understand how the overall degradation rate depends on the physical absorption rate and the kinetics of the degradation reactions.

2.4.1. Mass Transfer Theory

The simplest mass transfer theory assumes that all transport between two different phases occurs in two films of finite thickness, with each film having a different resistance to mass transfer (Lewis and Whitman 1924). The concentration profile for a gas absorbing into a liquid with no chemical reaction (physical absorption) is represented in Figure 2.3. The subscript i refers to concentrations at the gas-liquid

interface. If the system is at steady state the concentration in the liquid at the gas-liquid interface is in equilibrium with the concentration of the gas at the interface. Since gases are sparingly soluble in most liquids, the solubility can be represented by Henry's law, where H_{O_2} is the Henry's constant of O_2. The concentration of O_2 in the bulk liquid can be represented by either C_{O_2} or $P_{O_2}^*$, which is the partial pressure of O_2 that is in equilibrium with the bulk liquid composition ($P_{O_{2,i}} = C_{O_{2,i}}/H_{O_2}$).
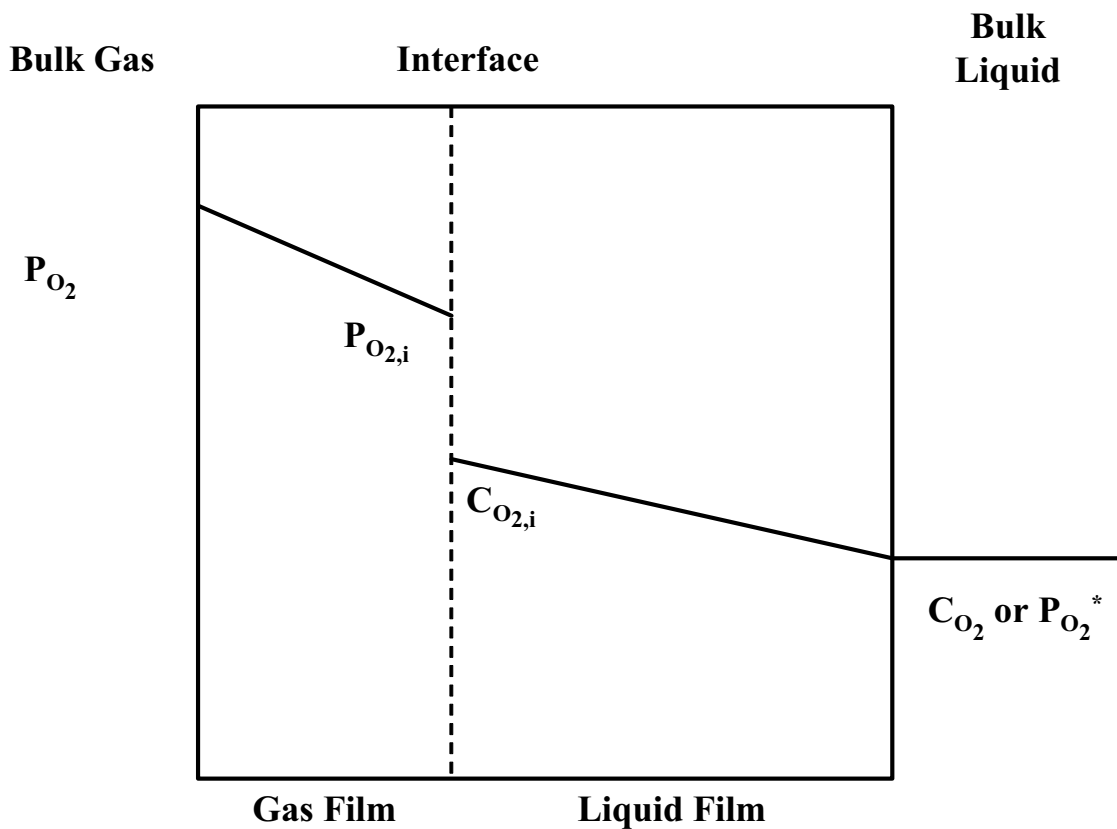
Figure 2.3 Concentration Profile for Physical Absorption of O_2 into MEA

In the case of the oxidative degradation of MEA, the O_2 diffusing into the amine solution is reacting with the MEA. There are five different regimes of mass transfer

38

with chemical reaction: Kinetic, Diffusion, Fast Reaction, Instantaneous Reaction, and Surface Reaction (Astarita 1966).

The Kinetic Regime occurs when the reaction kinetics are slow enough that all of the liquid phase is saturated with the diffusing component, O_2, or $C_{O_2} \approx C_{O_{2,i}}$. The kinetics in this regime still show a dependence on reactant or catalyst concentration, but are slow enough so that all of the reactions take place in the bulk liquid, and the overall rate of O_2 consumption can be represented by Equation 2.2.

$$\text{Rate of } O_2 \text{ Consumption} = f(k_i, catalyst, MEA, O_2) \qquad 2.2$$

Where: k_i is the intrinsic rate constant

As the kinetics are increased, the system enters the Diffusion Regime. The reactions still take place in the bulk liquid, but now the kinetics are fast enough that O_2 reacts as quickly as it can diffuse into the bulk liquid. In the Diffusion Regime the value of C_{O_2} is much smaller than $C_{O_2}^*$, i.e. the bulk liquid is no longer saturated with dissolved O_2. An increase in the reaction kinetics does not affect the overall rate of consumption of O_2, since the controlling process is diffusion of O_2 into the bulk liquid. At this point the rate of O_2 consumption can be represented by Equation 2.3.

$$\text{Rate of } O_2 \text{ Consumption} = \frac{K_G a V}{H_{O_2}} (P_{O_2} - P_{O_2}^*) \qquad 2.3$$

Where: K_G is the overall gas phase mass transfer coefficient,

$K_G = f(diffusion\ coefficient,\ viscosity,\ surface\ tension,\ etc.)$

a is the contact area/volume,

and V is the total volume of solution

As the kinetics continue to increase, the system enters the Fast Reaction Regime. At this point the reactions are fast enough that the reaction takes place in the liquid film and not the bulk liquid. If the kinetics are further increased, the system again becomes diffusion limited and enters the Instantaneous Reaction Regime. At this point, the kinetics are so fast that the liquid reactant is being depleted in the liquid film, and the kinetics are so fast that the reaction occurs as soon as O_2 and MEA are brought together by diffusion transport. If the kinetics are again increased so that the concentration of A in the liquid film is negligible, the system is in the Surface Reaction Regime. At this point, the overall rate of consumption of A is controlled by the diffusion of A to the gas-liquid interface where the reaction takes place instantaneously. The rate of consumption of A can be considered gas-film controlled, and the rate of mass transfer is determined by the overall gas-film mass transfer coefficient, K_G.

2.4.2. *O_2 Mass Transfer and the Oxidative Degradation of MEA*

Since the mechanisms for the oxidative degradation of MEA involve a series of free radical reactions, the overall reaction rate is expected to be very fast. In Chapter 4 it will be shown that under laboratory conditions the degradation rate of MEA is controlled by the rate of O_2 mass transfer. One of the primary variables tested in this study is catalyst concentration (iron and copper). Based on the data presented in Chapter 4, the reported overall degradation rates range fall in the Kinetic Regime, Diffusion Regime, or Fast Reaction Regime. Figure 2.4 represents qualitatively the effect of catalyst concentration over these three mass transfer with chemical reaction

regimes. At low catalyst concentrations the degradation rate is slow enough to be in the Kinetic Regime, but as the concentration of catalyst increases, the overall rate begins to be diffusion controlled. In this regime an increase in the catalyst concentration has little effect on the overall reaction rate. At high catalyst concentrations the rate begins to increase again as the system enters the Fast Reaction Regime.

Kinetic Regime

Rate of O_2 Consumption $= f(k_i, catalyst, MEA, O_2)$

Fast Reaction Regime

Diffusion Regime

Rate of O_2 Consumption $= \dfrac{K_G a V}{H_{O_2}}(P_{O_2} - P_{O_2}^*)$

Overall Reaction Rate

Catalyst Concentration ⟶
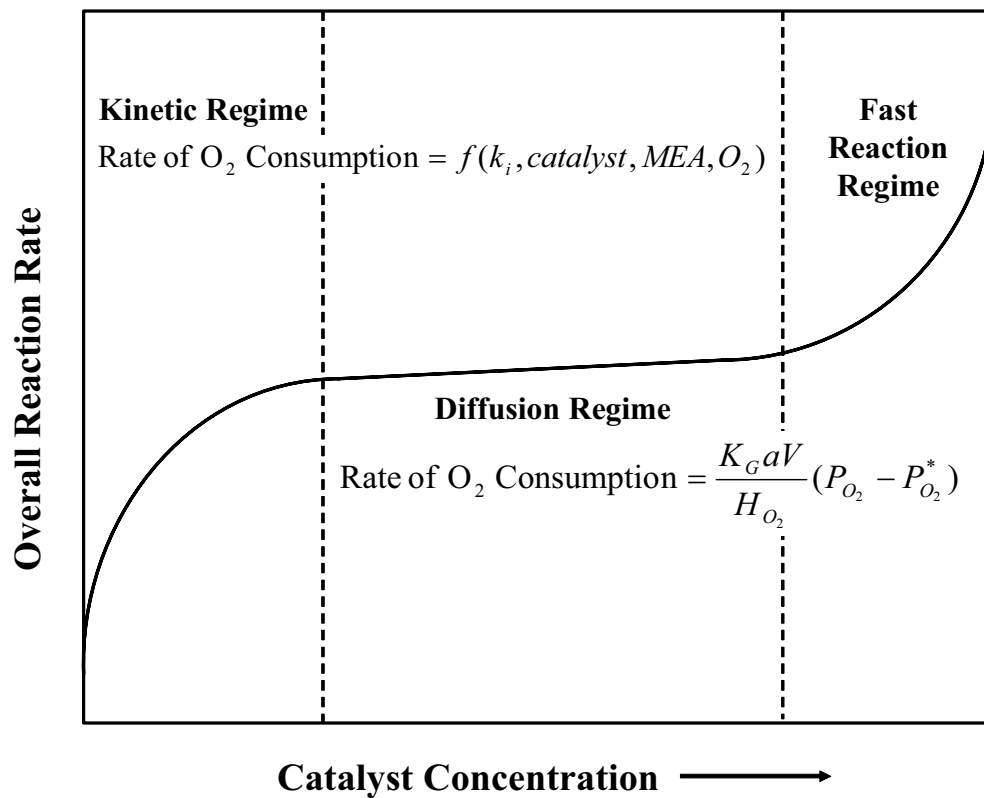
Figure 2.4 Effect of Catalyst Concentration on the Overall Reaction Rate

The rate of physical absorption of O_2 into a sparged or agitated tank, the case shown in Figure 2.3, is described by Equation 2.4. The rate of absorption depends on the overall gas-side mass transfer coefficient, K_G, the gas-liquid contact area per unit volume of liquid, a, the total liquid volume, V, and the Henry's constant for O_2

solubility in the amine solution, H_{O_2}. All of these depend on the physical properties of the amine solution and the fluid hydraulics of the gas-liquid contactor. The driving force for mass transfer in Equation 2.4 is written in terms of O_2 partial pressure, where P_{O_2} is the partial pressure of O_2 in the bulk gas, and $P_{O_2}^*$ is the partial pressure of O_2 that is in equilibrium with the dissolved O_2 in the bulk liquid.

$$\text{Rate of } O_2 \text{ Absorption} = \frac{K_G aV}{H_{O_2}}(P_{O_2} - P_{O_2}^*) \qquad \qquad 2.4$$

For a system with mass transfer with chemical reaction that is operating in either the Kinetic or Fast Reaction Regime, the overall rate is also equal to the kinetics. When the kinetics are slow, the bulk solution is close to being at equilibrium with bulk gas and $P_{O_2}^* \approx P_{O_2}$. However, as the kinetics increase, the mass transfer rate is not able to supply O_2 fast enough to the bulk liquid and the dissolved O_2 begins to decrease. In the Fast Reaction Regime, the dissolved O_2 in the bulk solution approaches zero, and Equation 2.4 reduces to Equation 2.5.

$$\text{Rate of } O_2 \text{ Consumption} = \frac{K_G aV P_{O_2}}{H_{O_2}} \qquad \qquad 2.5$$

Many of the reported degradation rates in this study fall within the regimes where the degradation rate can be described by Equations 2.4 and 2.5. These results will be presented in Chapter 4, and the above equations will be referred to again in this chapter.

Chapter 3: Experimental Methods and Apparatus

This chapter details the experimental methods used to measure the oxidative degradation of monoethanolamine used throughout this project. Information on chemicals, solution preparation, equipment calibration, reactor design, and data interpretation are presented in detail.

3.1. Chemicals

In order to accurately quantify the effect of dissolved metals on the degradation rate of MEA, a highly purified solvent with known concentrations of impurities was used. Table 3.1 shows a typical analysis of the LCI (low chloride iron) grade MEA supplied by Huntsman Chemical. This grade of MEA was used in all experiments.

House air, available at 7.17 barg (104 psig), was used as the primary reaction gas. CO_2 was purchased from an industrial gas supplier at 99.9 vol. % purity and N_2, purchased from the Cryo-lab in the Department of Physics, was available at 16.2 barg (235 psig).

Table 3.1 Certificate of Analysis for LCI Grade Monoethanolamine

Shipment/Tank Lot:	1241603	
Container Prefix:	3A30	
Container Number:	1 Drum	
<u>Analysis</u>	<u>Result</u>	<u>Units</u>
Appearance	Passes	
Monoethanolamine	99.92	wt. %
Water	0.12	wt. %
Iron	31	ppb_m
Chloride, as Cl	< 0.5	ppm_m
Sulfate	< 0.1	ppm_m
Cobalt	3	Pt - Co
Al, Sb, Ba, B, Cd, Ca, Cr, Cu, Ga, Ge, Au, Pb, Li, Mg, Mn, Ni, K, Si, Ag, Na, Sr, Ta, Sn, Ti, Zn	< 10	ppm_m

A number of solutes were added to the amine solutions to quantify catalytic and inhibitory effects. These solutes were added to the reactor either directly as a solid or as an aqueous solution. The metal catalysts were purchased as $FeSO_4 \times 7\ H_2O$ and $CuSO_4 \times 5\ H_2O$ and injected directly into the reactors as aqueous solutions. All solutions were made gravimetrically using de-ionized water. Details for these additives can be found in Table 3.2.

Table 3.2 Chemical Reagent Specifications

Chemical	CAS #	Manufacturer	FW	Assay	Lot
Cupric Sulfate	7758-99-8	Mallinckrodt AR	249.68	0.995	4844N06693
Iron(II) Sulfate	7782-63-0	Acros	278.02	0.995	A012451702
Ethylenedinitrilo-tetraacetic Acid, Disodium Salt	6381-92-6	EM Science	372.24	0.99	38139842
Bicine	150-25-4	Acros	163.17		A014372601
Glycine	56-40-6	EM Science	75.07	0.985	39141937
Inhibitor A		MCB Reagents		0.999	
Inhibitor A		Fisher Scientific		0.994	
Inhibitor A		Acros			
Formaldehyde	50-0-0	Fisher Scientific	30.03	0.378	023454
Paraformaldehyde	30525-89-4	Fisher Scientific	30.03	0.954	037435
Potassium Formate	590-29-4	Alfa Aesar		0.99	10099291
Magnesium Chloride	7791-18-6	Fisher Scientific	203.31	0.999	026132
Magnesium Sulfate	10034-99-8	Acros	246.48		A016693301
Manganese Sulfate	10034-96-5	EM Science	169.02	0.99	33060323
Hydroquinone	123-31-9	Eastman Organic Chemicals	110.11		
Ascorbic Acid	50-81-7	Eastman Chemicals	176.13		
tri-Potassium Phosphate Heptahydrate	22763-02-6	EM Science	338.38	0.98	9299
Potassium Permanganate	7722-64-7	Mallinckrodt AR	158.03	0.995	7068KMDC
Sodium Chloride	7647-14-5	EM Science	58.44	0.99	37255742
Sodium Sulfite	7757-83-7	EM Science	125.05	0.98	33233390
Sodium Bisulfite	7631-90-5	Mallinckrodt AR	104.07		7448KJCD
Sodium Tetrasulfide	12034-39-8	PPG Industries	174.20		
Potassium Chloride	7447-40-7	Fisher Scientific	74.56	1.003	020948
Potassium Bromide	7758-02-3	Fisher Scientific	119.01	1.01	037496
tri-Sodium Phosphate	22763-02-6	EM Science	338.38	0.98	PX1575-1

3.1.1. Solution Preparation

All of the solutions in this study were prepared gravimetrically. Amine solutions were loaded with CO_2 by sparging pure CO_2 through the solutions inside an ice bath. The temperature of the solution was kept cold in order to minimize discoloration of the loaded MEA solution due to formation of irreversible CO_2 by-products or carbamate polymerization products. CO_2 loadings were quantified by TIC

(total inorganic carbon) analysis using a Model 525 Analyzer from Oceanography International Corp. and a Horiba PIR-2000 gas phase CO_2 analyzer using a previously described procedure (Chi 2000).

Solutions were run with CO_2 loadings of 0, 0.15, and 0.40 mol CO_2 / mole MEA. The last two loadings correspond to the top and bottom of the absorber respectively. The CO_2 partial pressure at 55°C was set to 2 vol. % for solutions with α = 0.40 and to the concentration in air for solutions when α = 0.15 (Jou et al. 1995). Solutions with α = 0 were run with either air or N_2.

3.2. Experimental Equipment

Degradation experiments were performed by bubbling gas through the amine solution in a temperature controlled semi-batch reactor. Figure 3.1 shows a simple process flowsheet diagram for the oxidative degradation experiments. Reaction gas, consisting of house air, N_2, CO_2, or a mixture of the three, was bubbled through water to pre-saturate the gas before being sparged through the amine solution in order to minimize water losses. After the gas was bubbled through the amine solution in the semi-batch reactor, it entered a heated sample line before being pumped through the FT-IR for gas analysis and vented into the fume hood. The pre-saturator was a stainless steel calorimetric bomb located in the reservoir of the heat bath. Temperature was controlled in the reactor by circulating a heat transfer fluid between the heat bath and the jacket of the glass reactor. Several different configurations of this apparatus were

used throughout the course of this study, but all of them followed the same basic principles illustrated in Figure 3.1.
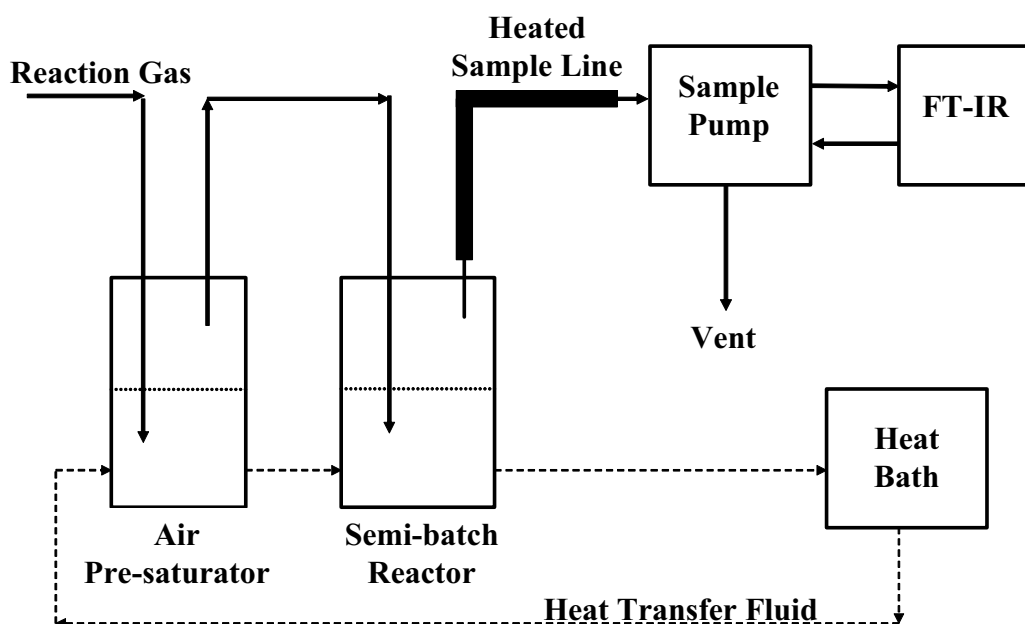
Figure 3.1 Oxidative Degradation Experiments Simplified Process Flowsheet

3.2.1. Mass Flow Controllers

Gas flowrates were regulated using Brooks mass flow controllers connected to a 4 channel Brose control box (model 5878). The control box displayed a digital readout corresponding to the % open of the mass flow controller. Air and N_2 flowrates were controlled by a 15 SLPM flow controller (model 5850E) and CO_2 was controlled with either a 0.5 SLPM or a 1.0 SLPM flow controller (model 5850E). Flow controllers were calibrated every 12 months or as needed. Calibrations were performed by connecting the flow controllers to the appropriate source gas, changing the setting on the control box, and measuring the volume displacement of soap bubbles in a graduated

burette as a function of time. The volumetric flowrate of gas was then converted to a molar flowrate based on the Ideal Gas law. Figure 3.2 shows a typical calibration curve for air and the 15 SLPM mass flow controller.

$$y = -71.473x^2 + 152.388x + 0.300$$
$$R^2 = 0.999$$
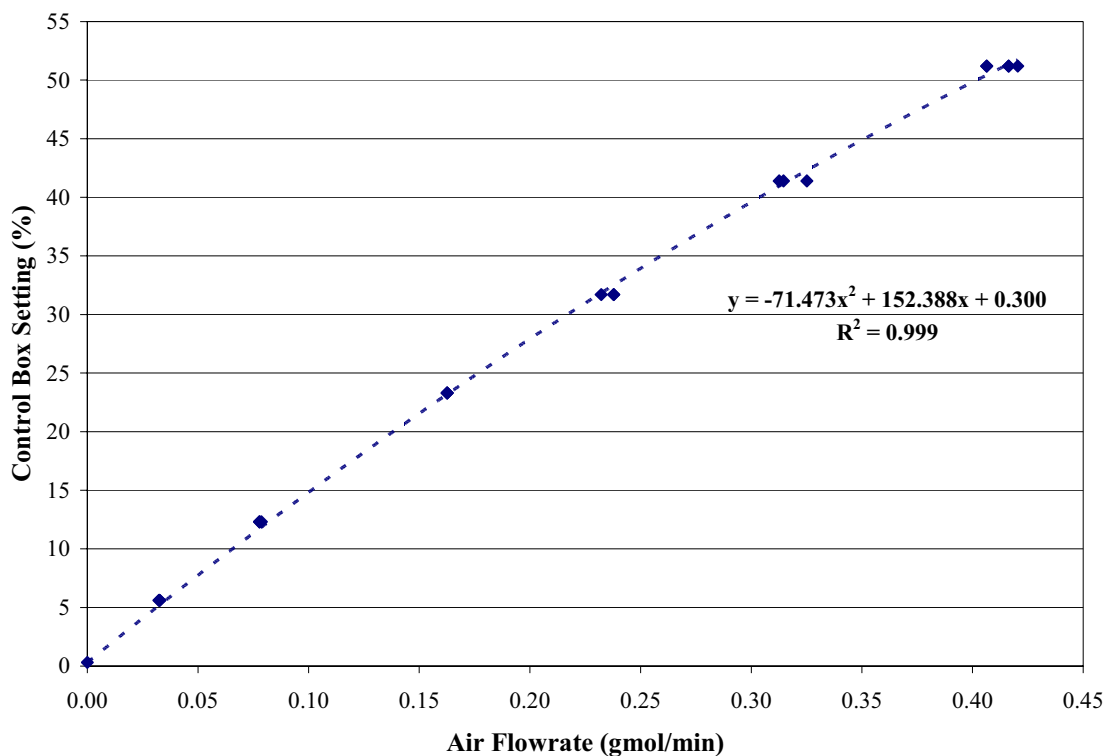
Figure 3.2 Calibration Curve for the 15 SLPM Brooks Mass Flow Controller and Air

3.2.2. Temperature Control Equipment

Two different temperature baths were used in this study. The temperature was monitored continuously throughout an experiment, for both reactor systems, and the temperature of the heat baths were adjusted as needed to keep the reactor at a constant temperature.

The Agitated Reactor system used an IsoTemp 3016H temperature bath manufactured by Fisher Scientific International. The heat transfer fluid was a di-methyl

silicone oil (50 cSt viscosity) purchased from Krayden, Inc. Temperature was controlled within ±1°C by monitoring the temperature in the reactor with a thermistor. For this system, in order to maintain a reactor temperature of 55°C, the temperature bath was set at a temperature of approximately 63°C depending on ambient conditions. Temperature was monitored continuously throughout an experiment and the temperature of the heat bath was adjusted as needed to keep the reactor at a constant temperature.

The Sparged Reactor used a Lauda MS heat bath with a mixture of ethylene glycol and water as the heat transfer fluid. Temperature was also controlled to within ±1°C by monitoring the temperature in the reactor with a Type "K" thermocouple connected to an Omega Engineering 10 channel digital readout box (model 199).

3.2.3. Agitated Reactor System

Figure 3.3 below shows the entire Agitated Reactor system and associated equipment. The Agitated Reactor, purchased from Ace Glass Inc., was a 1 L jacketed glass reactor with a 5 neck (threaded, 1 large, 3 medium, and 1 small) top and an 8 mm bottom drain tube, which served as the gas inlet to the reactor. The reactor is rated for a pressure of 3.10 barg (45 psig) at 100°C and had an inside diameter of 10 cm and a depth of 15 cm. The reactor jacket was equipped with 2 threaded "Ace-Safe" taps for easy connection to tubing. The standard FETFE o-rings which were recommended for use with MEA dissolved when they came in contact with the pure amine, so all o-rings

and rubber seals were replaced with CHEMRAZ® perfluorelastomer polymers in order to ensure proper chemical compatibility.

The center neck of the reactor was equipped with a StedFast™ Stirrer (model SL 1200) by Fisher Scientific International, capable of agitation speeds up to 1450 RPM. The agitator used a stainless steel stir shaft with a single flat-blade paddle. The impeller blade rotated parallel to the axis of the drive shaft, and was 5 cm wide and 13 mm high. The reactor was sealed by inserting the stir shaft through a rubber septum stopper (sleeve type, outer joints 24/40–24/25, from Chemglass Inc.) lubricated with vacuum grease. The septum was replaced every 1-2 experiments, or during the experiment if the septum tore around the rotating agitator shaft.

One of the three medium necks was used for inserting the thermistor into the reactor, and a second neck was used as the gas outlet. The remaining two openings were used for additions to the reactor through the course of the experiment. Plugs and connectors were made of either nylon or Teflon®, and both have proven to be compatible with MEA. The plug for the gas outlet was packed with air filter media (NaturalAire Cut-to-fit) to serve as a mist eliminator and eliminate liquid entrainment into the heated sample line.
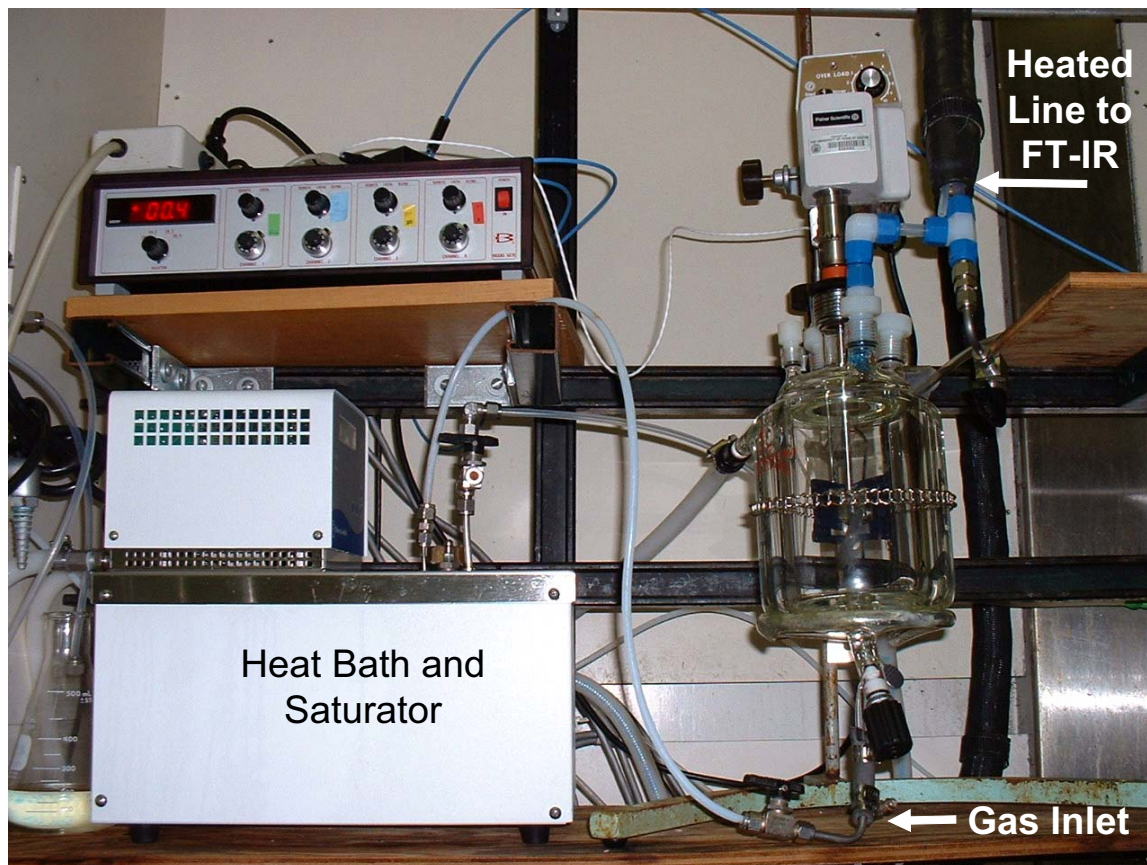
Figure 3.3 Agitated Reactor System and Associated Equipment

3.2.4. Sparged Reactor System

The Sparged Reactor system was a modified version of an earlier system used to study MEA degradation catalyzed by iron (Chi 2000). The system was modified to include a pre-saturator and portable multi-component FT-IR (instead of a desktop model with fixed wavelength analysis) and also eliminated the condenser used on the gas outlet. Details of the previous apparatus can be found in Chi's thesis (Chi 2000).

The Sparged Reactor was a semi-batch 500 ml glass jacketed reactor, sealed with a Number 14 rubber stopper. The stopper contained ports for a thermometer, gas

inlet, gas outlet (including a mist eliminator made of the same material used in the Agitated Reactor), and a sample injection/removal port. Gas was sparged through the amine solution using a 6.35 mm (1/4") Teflon® tee with rates ranging from 7.5 to 8.0 LPM. The reactor had a quiescent liquid depth of 3.8 to 5.0 cm (250 to 350 ml of amine solution). Since the sample pump, located on the discharge end of the sample line, was used with the Sparged Reactor system, a vacuum pressure gauge was placed on the gas outlet to measure the reactor pressure. Under normal operation the sample pump maintained a slight vacuum of 1 to 3 mm Hg in the reactor. Figure 3.4 shows a detailed representation of the Sparged Reactor.
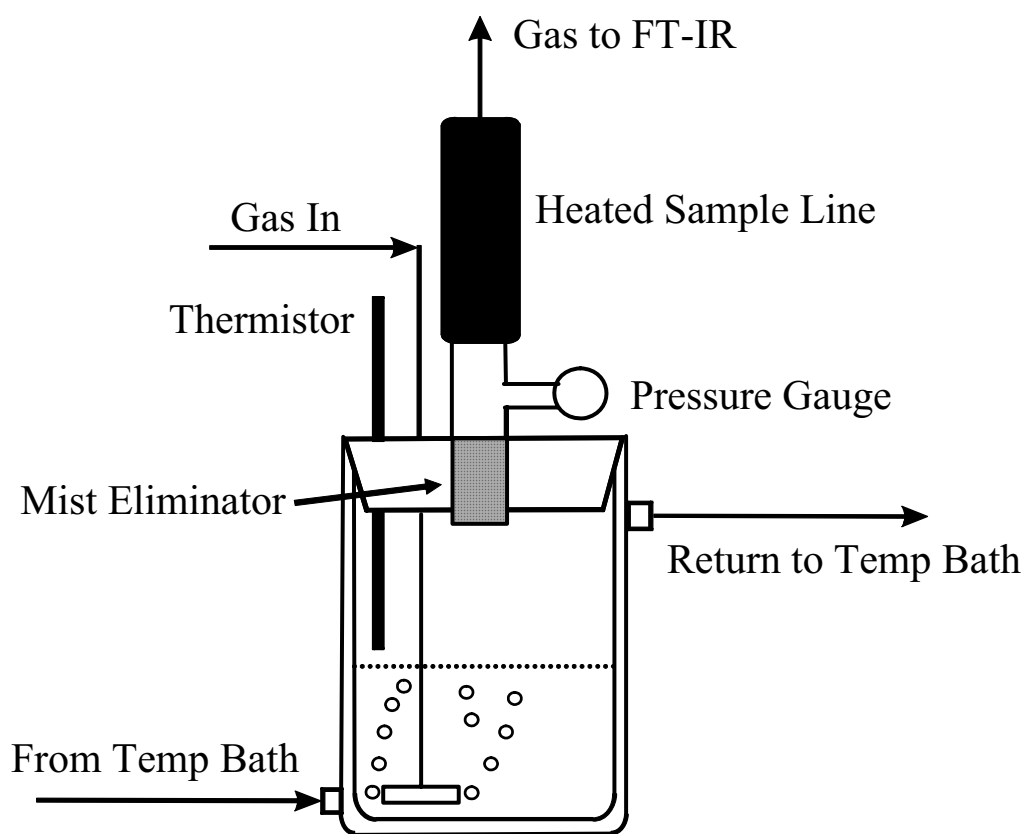
Figure 3.4 Sparged Reactor for Oxidative Degradation Experiments

3.2.5. FT-IR Analyzer System

The gas phase portable FT-IR analyzer and sample pump were purchased from Air Quality Analytical, Inc. The portable FT-IR analyzer, a Temet Gasmet™ Dx-4000 (Serial Number 01253), allows for simultaneous analysis of up to 50 components and the gas cell is temperature controlled at 180°C. The high temperature analysis allows for direct sample measurement without having to dry or dilute the gas stream to avoid IR interference due to water absorption. Table 3.3 below gives detailed specifications for the FT-IR analyzer.

The gas sampler had dual temperature control (for the sample pump and the heated sample line) as well as pressure gauges for the sample inlet and the vent line. The heated sample line was a 15 ft. long insulated Teflon® tube with PFA tubing for the gas sample. Both the sample pump and the sample line were controlled at a temperature of 180°C to avoid any liquid entrainment into the gas sample cell or condensation of liquid onto the gold plated mirrors.

Table 3.3 Temet Gasmet™ Dx-4000 FT-IR Gas Analyzer Technical Specifications

General Parameters	
Model	DX-4000
Serial Number	01253
Supplier	Air Quality Analytical, Inc. (www.airqa.com)
Measurement principle	FT-IR (Fourier Transform Infrared)
Performance	Simultaneous analysis of up to 50 compounds
Operating temperature	20 ± 20°C, optimum 15 - 25°C non condensing
Storage temperature	-20 – 60°C, non condensing
Power supply	12 VDC or 100-240 VAC / 50 - 60 Hz
Software	Calcmet™ for Windows v 4.41
Spectrometer	
Interferometer	Temet Carousel Interferometer
Resolution	$8\ cm^{-1}$ ($7.76\ cm^{-1}$)
Scan frequency	10 spectra/s
Aperture	2.54 cm
Detector	MCTP (Mercury, Cadmium, Tellurium, Pelletier Cooled)
IR-source	Ceramic, SiC, 1550 K temperature
Beamsplitter	ZnSe
Window material	BaF_2
Wavenumber range	$900 – 4200\ cm^{-1}$
Sample Cell	
Structure	Multi-pass, fixed path length 5.0 m
Material	Gold/Ruthenium/Nickel coated extruded Aluminum
Mirrors	fixed, protected gold coating
Volume	1.0 L nominal
Connectors	Swagelok 6.35 mm (1/4")
Gaskets	Teflon® coated Viton®
Temperature	180°C
Maximum sample gas pressure	2 bar
Flow rate	1-5 L/min
Response time	3 cell flushes (depends on gas rate)
Required gas filtration	Filtration of particulates (2 microns)
Sample condition	non condensing
Measuring parameters	
Zero point calibration	Every 24 hours calibrate with N_2 (minimum)
Zero point drift	2 % of smallest measuring range per zero point calibration interval
Sensitivity drift	None
Accuracy	2 % of smallest measuring range
Temperature drift	2 % of smallest measuring range per 10 °C temperature change
Pressure influence	1 % change of measuring value for 1 % sample pressure change
Enclosure	
Material/Weight	Aluminum/16 kg
Dimensions (mm)	433 ∗ 185 ∗ 425

3.3. Analytical Methods

Several different analytical methods were used throughout this project, with infrared spectroscopy being the most important and widely used. This section details the types of measurements that were made and detailed analytical methods.

3.3.1. Infrared spectroscopy

The composition of gas leaving the degradation reactor was quantified using the Temet Gasmet™ Dx-4000 FT-IR gas analyzer detailed above. The application of infrared radiation ($600 - 4200$ cm^{-1}) to a molecule excites both the rotational and vibrational energy levels of the molecule. The transition from a lower energy level to a higher energy level requires a discrete amount of energy, which corresponds to a given wavelength, or wavenumber (the inverse wavelength), in the infrared region. Every molecule absorbs radiation over a distinct set of wavelengths, providing a unique spectrum with which to identify the molecule. In order for a molecule to undergo a transition in its vibrational or rotational energy level, it must exhibit a net dipole moment to allow interaction with the electric field of the infrared radiation. Since homo-nuclear diatomic molecules do not exhibit a net dipole moment with any vibrational or rotational changes, these molecules are IR inactive and show no absorption spectra in the IR region.

The absorption spectra from IR radiation can be used quantitatively to determine the concentration of a compound using the Beer-Lambert law (Equation 3.1). Radiation of a known intensity is measured before and after the radiation has come in contact with

the gas sample. Transmittance, T, is defined as the fraction of radiation that passes through the gas. Absorbance, A, is the logarithm of the inverse transmittance, and is proportional to a constant, the optical path length, and the concentration of the species in the gas sample. The molar absorptivity, *a*, is unique for each molecule and each wavelength.

The Beer-Lambert law states that for a given optical path length, the absorbance is proportional to the concentration of the species in the gas sample at a fixed wavelength. This is true only if the molar absorptivity, *a*, does not change with concentration. At high concentrations, or for strongly absorbing wavelengths, this will no longer be true and the value for the molar absorptivity is only good over a narrow concentration range. Additionally, changes in temperature and pressure can affect the absorptivity and must be accounted for to accurately calculate the concentration.

$$A = \log_{10}\left(\frac{I_0}{I}\right) = \log\left(\frac{1}{T}\right) = abc \qquad\qquad 3.1$$

Where: A = absorbance
  I_0 = incident radiation intensity
  I = intensity of radiation after contacting sample
  T = transmittance
  a = molar absorptivity, dependent on wavelength
  b = optical path length
  c = concentration of species in the sample

Reactions between gas species generally do not occur; therefore, the total absorbance of the gas sample is the sum of the absorbance by each species. This allows for simultaneous analysis of multiple compounds in the gas sample. Quantification of the gas species and their concentrations requires the availability of reference absorption

spectra for each component over the concentration range of interest. Simple compounds over small concentration ranges require fewer spectra since the molar absorptivity is nearly constant, but other species such as water and CO_2 will require more reference spectra to account for the changing molar absorptivity at some wavelengths.

Using the Beer-Lambert law (Equation 3.1), an absorbance of 1.0 corresponds to a transmittance of 10%, meaning that the compound is absorbing 90% of the incident radiation at that wavelength. Two problems will occur at an absorbance above 1.0. The first problem is that, in general, above 1.0 absorbance units, the compound is generally not obeying the Beer-Lambert law anymore, and the molar absorptivity for that wavenumber is no longer a linear function of concentration. In order to accurately account for this, reference spectra must be generated over much smaller concentration intervals.

The second problem that arises at an absorbance over 1.0 has to do with physical limitations of the detector. In order to have meaningful results, the absorbance signal generally needs to be 3 times the noise, (or a signal-to-noise ratio of 3.0). For a current top of the line analyzer, the noise level might be 1% (absorbance basis), resulting in a maximum absorbance of 1.52 (keeping the signal-to-noise ratio at 3.0). The Temet Gasmet™ Dx-4000 has a noise level of ~ 2% (absorbance basis), resulting in a maximum absorbance of approximately 1.2 absorbance units; therefore, a spectrum containing an absorbance above 1.2 absorbance units will not contain useful information (Nelson 2005).

Even though the physical limitations of the detector allow for detection of compounds above 1.0 absorbance units, for this study a maximum absorbance of 1.0 was used in order to account for deviations from the Beer-Lambert law and possible noise level fluctuations. For very strongly absorbing compounds, such as water and CO_2, the absorbance maximum is generally set lower than 1.0. The details of absorbance maxima will be covered later in this chapter.

3.3.1.3. Reference Spectra Generation

Reference spectra for gas compounds were generated by blending the gas with nitrogen in known ratios using the mass flow controllers detailed above. The flow controllers were re-calibrated for each gas to ensure accurate flow measurements. The spectra were recorded using the FT-IR until the concentration reached steady state. Steady state spectra were then examined, and the cleanest average spectrum (no baseline shift or interference from background CO_2 or H_2O) was then selected to be the reference spectrum in the software library for that particular concentration.

Compounds that are a liquid at standard conditions, such as monoethanolamine, must be vaporized in order to obtain reference spectra. An apparatus supplied by Air Quality Analytical Inc. was used to generate reference spectra for MEA. The apparatus consisted of a syringe connected to a gear pump, a Brooks mass flow controller, a furnace, and a heated sample line run at 180°C. MEA was loaded into the syringe, and a volumetric flowrate was set for the gear pump. The MEA was pumped into the furnace where it was evaporated and mixed with N_2 (controlled by the mass flow

controller) before passing through the heated line to the FT-IR. The same procedure for selecting the reference spectra was used for MEA as for the gas compounds.

Spectra generated on other FT-IR analyzers can also be used as reference spectra as long as corrections are made for path length, temperature, and pressure. This assumes that the sample and reference are at a concentration where the Beer-Lambert law still holds. Air Quality Analytical, Inc. provides a library of reference spectra with the purchase of the gas analyzer. Several reference spectra that were not generated on the Dx-4000 (SN 01253) were used during this analysis. Any reference spectra in the library titled "Library 01253" were generated on the FT-IR used in this study, while reference spectra from the library titled "Library 180" were generated on other analyzers at a temperature of 180°C.

In Chapter 2, NH_3 was shown to be the primary amino degradation product for MEA and is used in this study to quantify the oxidative degradation rate. Figure 3.5 shows a 214 ppm_v reference spectrum for NH_3. Vibrational-rotational transitions occur at lower energy levels (600 – 1300 cm^{-1}) and are closely spaced resulting in many narrow line peaks. The two sharp absorption peaks at 934 and 965 cm^{-1} are from the inversion transition of the ammonia hydrogen atoms and are the primary peaks used in the IR analysis of NH_3. The other noticeable absorption peak at 3200 to 3600 cm^{-1} results from the N-H stretch. The absorption peak is the second region used for IR analysis of NH_3. Analysis regions are discussed in more detail in the next session. Reference spectra for water, CO_2, and MEA can be found in Figure 3.6, Figure 3.7, and Figure 3.8 respectively. Additional reference spectra used throughout this study for gas

analysis can be found in Appendix A, including concentration ranges and reference

spectra library locations.
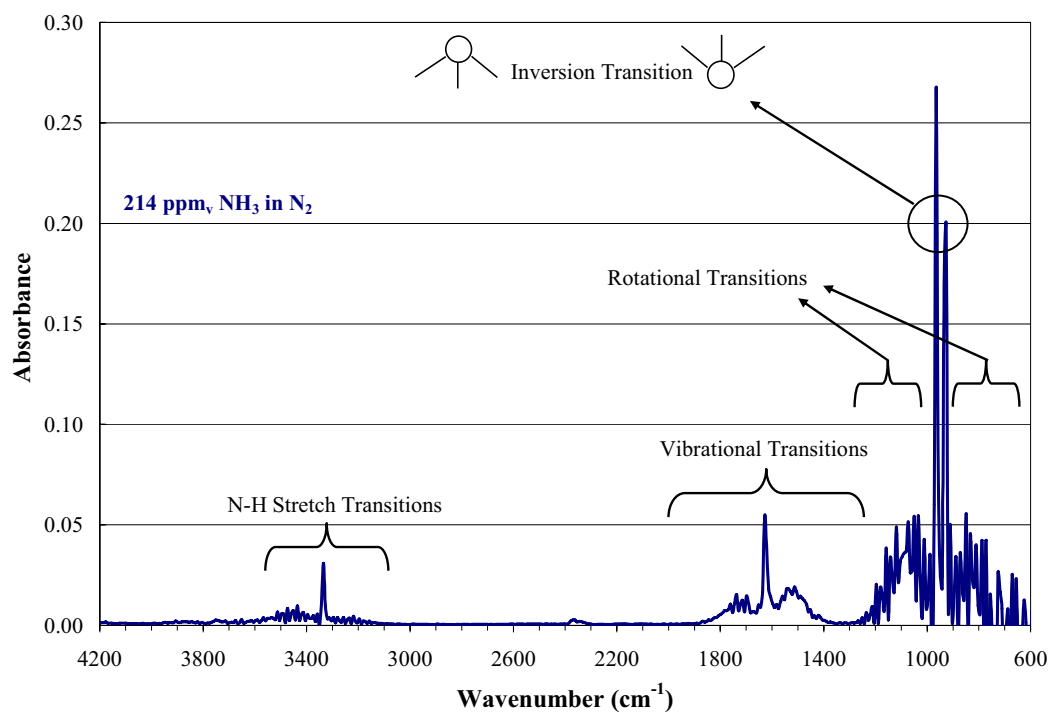
Figure 3.5 Reference Spectrum for NH_3 (214 ppm$_v$, 180°C, 5 m path length)
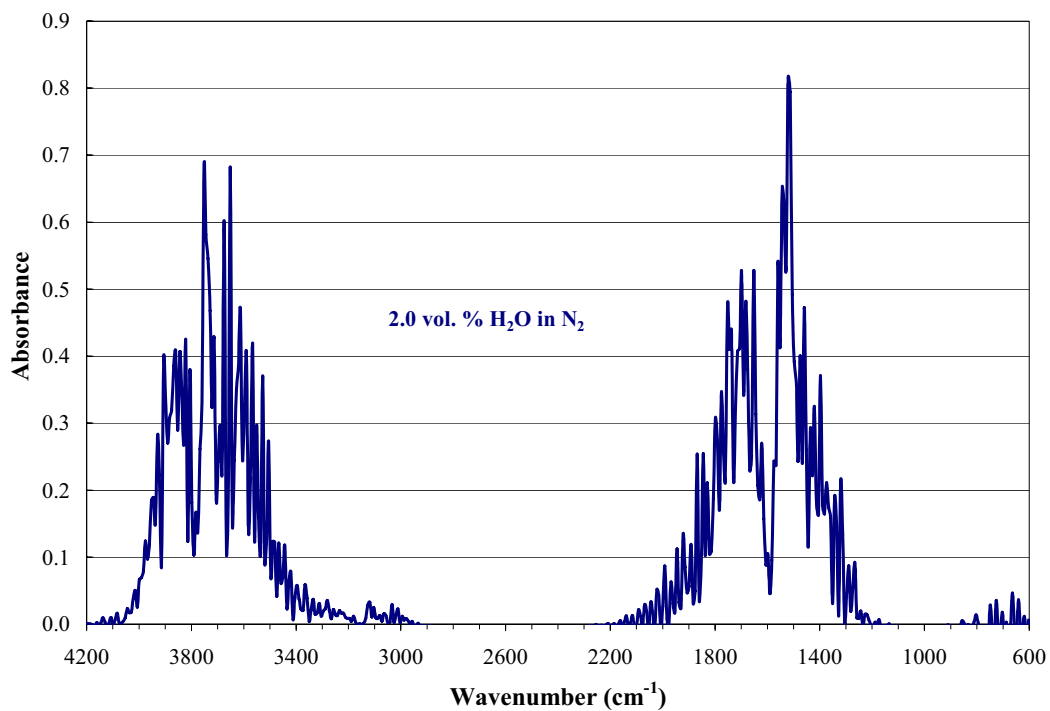
Figure 3.6 Reference Spectrum for Water (2.0 vol. %, 180°C, 5 m path length)
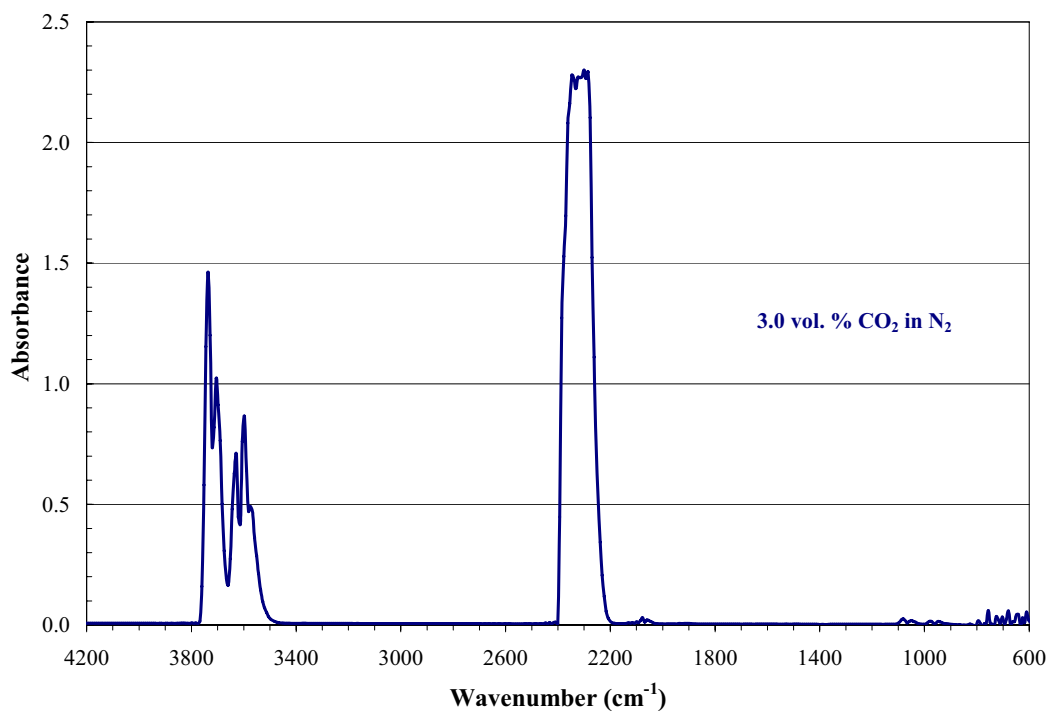
Figure 3.7 Reference Spectrum for CO_2 (3.0 vol. %, 180°C, 5 m path length)

61
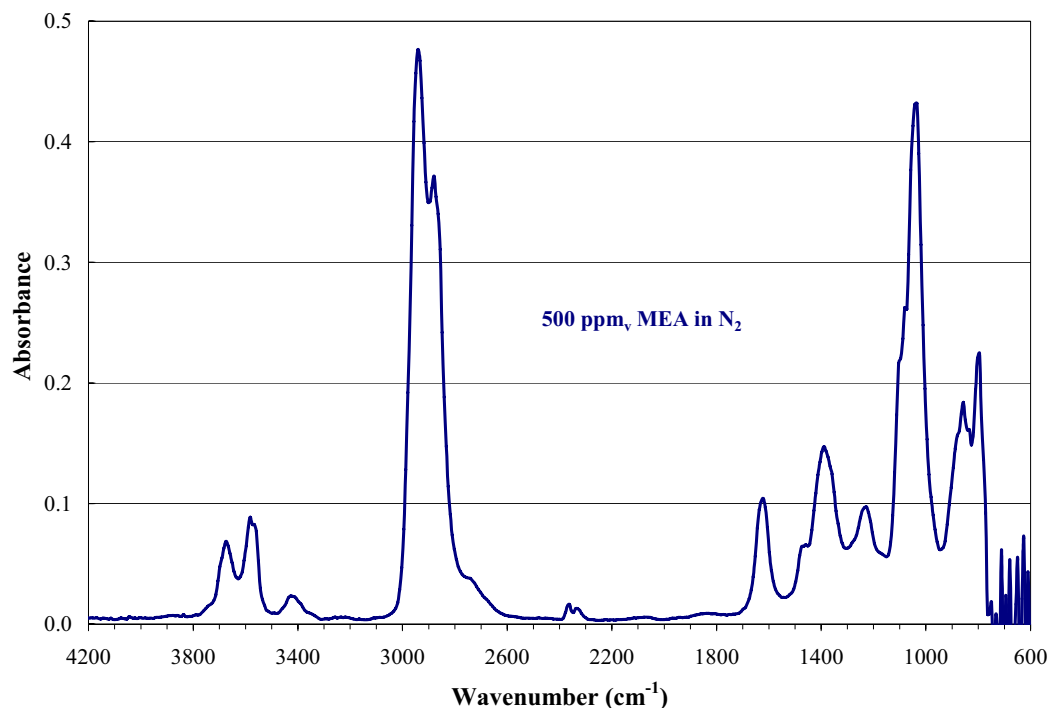
Figure 3.8 Reference Spectrum for MEA (500 ppm$_v$, 180°C, 5 m path length)

3.3.1.4. Multiple Component Analysis

Each compound in the gas sample absorbs infrared radiation independently of each of the other compounds, resulting in a cumulative absorption spectrum. Specifically, the FT-IR detects the transmittance of the infrared radiation from 900 to 4200 cm^{-1} and converts this to absorbance via the Beer-Lambert law (Equation 3.1). This absorbance spectrum is the sum of the absorbance spectra for each compound in the gas sample. Multiple components can be resolved from this combined spectrum by multiplying a reference spectrum for each compound by a factor X_i (to change the concentration) and subtracting the result from the combined absorbance spectrum. The multipliers and reference spectra are changed to minimize the residual absorbance

spectrum that is left after all the components have been subtracted from the absorbance spectrum. Details of the mathematical methods used by the Calcmet™ software for resolving multiple components from a single absorbance spectrum can be found elsewhere (Saarinen and Kauppinen 1991), while a sample analysis will be shown later in this section.

In order to properly resolve multiple compounds, different analysis areas (wavenumber regions) can be set for each component. The Calcmet™ software allows for up to 3 analysis areas to be set for each compound, each with a different absorbance maximum. If the absorbance of the sample spectrum goes above the set maximum, the software will no longer use this analysis region for that compound. The analysis regions are also determined by choosing regions where absorption peaks for multiple compounds do not overlap or interfere with each other. These regions have been identified and refined multiple times over the course of the project, and all of the data was re-analyzed after each change. This has resulted in an analysis method that is valid for all of the experiments performed in this study. One method was developed and optimized for the Sparged Reactor and a second for the Agitated Reactor, and are detailed in Appendix B. Table 3.4 shows the analysis regions used for each compound in the multi-component analysis for the Agitated Reactor application along with the associated absorbance limit for each measuring range and the number of references used for each component.

Table 3.4 Analysis Regions and Absorbance Limits for Compounds Studied in the Agitated Reactor Oxidative Degradation Experiments

Compound	Conc.	Measuring Range 1		Abs. limit	Measuring Range 2		Abs. limit	Measuring Range 3		Abs. limit	Refs.
		cm^{-1}			cm^{-1}			cm^{-1}			
Water	vol. %	1883	2161	1.0	3142	3319	0.5				13
CO_2	vol. %	980	1130	1.0	1999	2208	0.5	2450	2650	0.5	3
CO	ppm_v	2007	2207	0.5	2624	2750	1.0				8
N_2O	ppm_v	2107	2246	0.5	2647	2900	0.5				5
NO	ppm_v	1760	1868	0.8	1869	1991	0.8	2550	2650	1.0	4
NO_2	ppm_v	2550	2933	0.5							3
NH_3	ppm_v	910	964	1.0	980	1196	0.5	3219	3396	0.5	4
Formaldehyde	ppm_v	988	1111	1.0	2450	2600	0.6	2650	3211	0.5	3
Acetaldehyde	ppm_v	1034	1243	1.0	2638	2916	1.0				3
MEA	ppm_v	980	1119	1.0	2624	3150	1.0				1
Methanol	ppm_v	980	1281	1.0	2450	2650	1.0	2763	3304	1.0	7
Methylamine	ppm_v	980	1303	1.0	2450	2650	1.0	2800	3450	1.0	3
CH_4	ppm_v	2833	3203	0.5	3018	3203	0.5				2

Since the absorbance peaks for different compounds can overlap, it is necessary to specify possible interferences from other compounds. For example, water has two major absorption peaks that stretch over almost the entire IR region, as shown previously in Figure 3.6. These major peaks of water will interfere with every component in the analysis, and must be specified as a possible interference for these compounds. Conversely, not every component is an interference for water. Take the example of methylamine and water, shown in Figure 3.9 below where the regions being used for analysis are shown with bold lines and regions not used for analysis are shown in dashed or light solid lines. The three analysis regions for methylamine, and the significant absorbance peaks, do not interfere with the significant absorbance peaks used in water analysis; therefore, methylamine is not a significant source of interference with water. This kind of analysis was completed for all of the components and entered

into the Calcmet™ software prior to sample analysis. A correlation matrix of the interferences between the compounds studied in the oxidative degradation experiments is shown in Table 3.5.
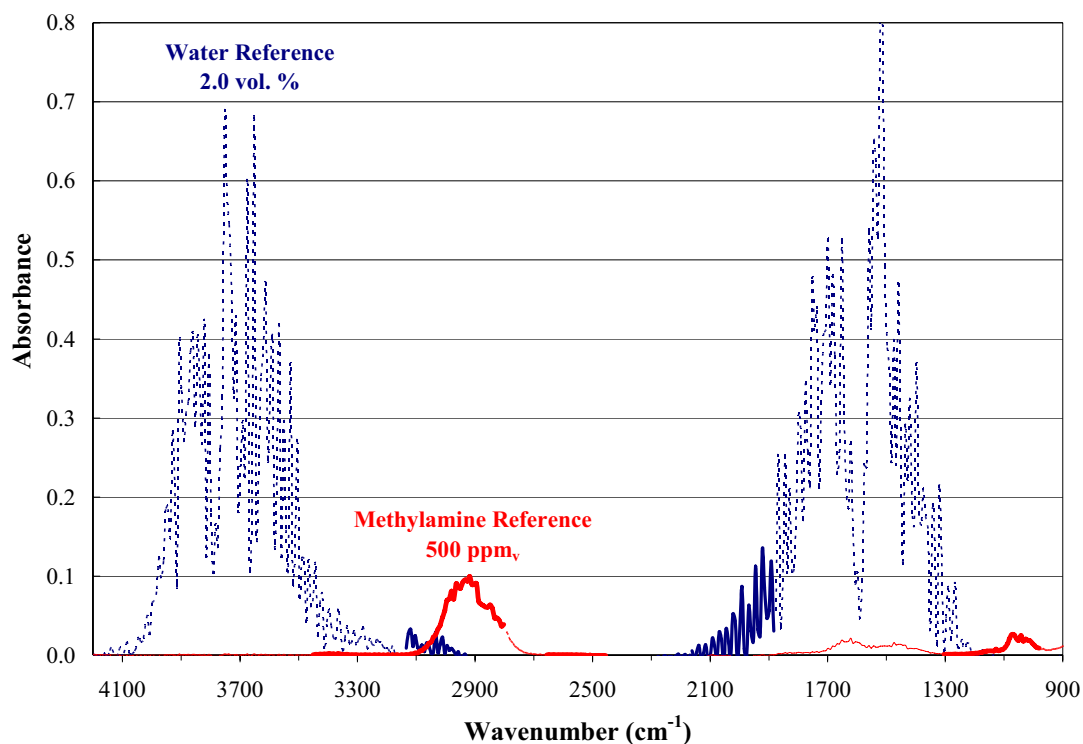
Figure 3.9 Comparison of IR Reference Spectra for Water and Methylamine
(solid lines are regions used for analysis)

The Calcmet™ software also allows for corrections due to pressure, temperature and path length. Temperature and pressure corrections are made using the Ideal Gas law to calculate the new concentration, and then path length corrections are made using the Beer-Lambert law (Equation 3.1). Each reference file has a temperature, pressure and path length assigned to it, and if these conditions are different from the sample

conditions, the sample data is transformed to match the conditions of the reference spectrum.

Table 3.5 Correlation Matrix for Interfering Compounds for FT-IR Analysis

Compound \ Interference	H₂O	CO₂	CO	N₂O	NO	NO₂	NH₃	Fo	Ac	MEA	M	MA	CH₄
Water		X	X	X	X		X			X			
CO₂	X		X	X		X	X		X	X	X	X	
CO	X	X		X	X	X		X	X	X	X	X	
N₂O	X	X	X		X	X		X	X	X	X	X	X
NO	X	X	X	X			X		X	X			
NO₂	X	X		X				X	X	X	X	X	X
NH₃	X	X		X	X			X	X	X	X	X	
Formaldehyde	X	X	X		X	X		X	X	X	X	X	X
Acetaldehyde	X	X	X		X	X	X		X	X	X	X	X
MEA	X	X	X		X	X	X	X		X	X	X	X
Methanol	X	X	X		X	X	X	X	X		X	X	X
Methylamine	X	X	X		X	X	X	X	X	X			X
Methane	X	X	X		X	X	X	X	X	X	X		

3.3.1.5. Example of Multi-component Analysis

Once the reference spectra, analysis regions, and interferences have been specified for each component, the Calcmet™ software can analyze any sample spectrum. The first thing in each experiment is to take a background scan. This is done by flowing N_2 through the heated sample line and heated sample cell. The raw data for the background scan, shown in Figure 3.10, shows the intensity count for a single beam of the analyzer. The peaks in the range of 1300 to 1800 cm^{-1} and 3550 to 3800 cm^{-1} are from water absorbance and the small peak around 2350 cm^{-1} is from CO_2 absorbance. Even though the analyzer optics are being purged with N_2, the optics casings are not

hermetically sealed, so some air (water and CO_2) will still be present. The observed spectrum utilizing the N_2 purge shows a significant improvement in these analysis regions when compared to a background scan without the purge.
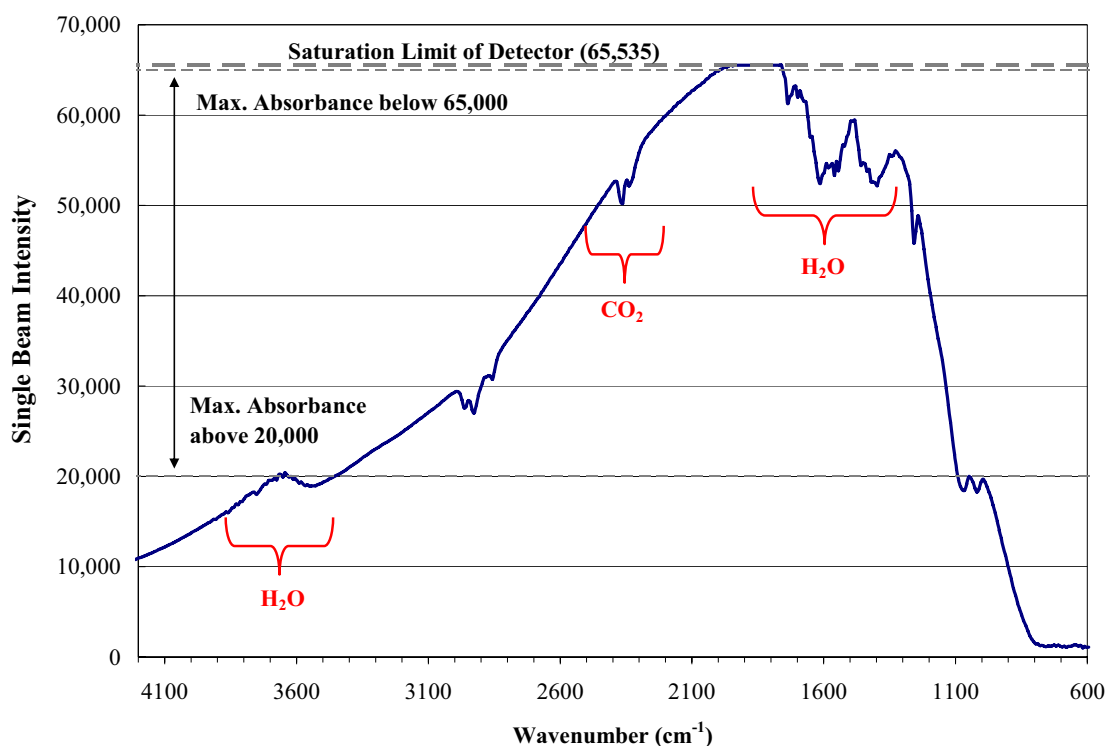
Figure 3.10 Background Scan for Experiment 20040607 (5 minute scan at 180°C)

The MCTP detector has a physical saturation limit of 65,535 for the incident radiation intensity (I_0). If the intensity is above this value, meaningful data (transmittance or absorbance) cannot be gathered at that wavenumber since the true value of I_0 is unknown. In order to correct this, the gain of the instrumentation should be decreased. The desired values of the maximum I_0 should be above 20,000 and below 65,000, and are also shown in Figure 3.10. The background scan for Experiment 20040607 shows that between 1760 and 1938 cm^{-1} the detector is saturated and data

between these wavenumbers should not be used for analysis. This was corrected subsequently by reducing the gain of the X Digital Trimmer for future experiments.

After the background scan has been completed, the experiment can be started. For this example, analysis will be shown for Sample 060704_00534 taken from Experiment 20040607, detailed later in this chapter. Figure 3.11 shows the raw absorbance spectrum for this sample prior to analysis. Absorbance spectra are saved for each experiment, as well as the component analysis. This is particularly useful since additional compounds can be added to the analysis at a later date, and the samples can be re-analyzed to determine the presence or absence of the new component in the old gas sample.

Table 3.4 shows that the maximum absorbance for any component in the analysis is 1.0. The spectrum in Figure 3.11 shows that from 1450 to 1775 cm^{-1} and 3574 to 3906 cm^{-1} the absorbance is above this limit and no data from these regions will be used in the regression for resolving multiple components. Looking at the absorbance spectrum and comparing it to the reference for water, it is clear that the sample has a high concentration of water which results in the absorbance above 1.0. The results for the multi-component analysis performed by Calcmet™ are shown in Table 3.6 (located on Page 70). The residual shown for each compound is the absolute value of the maximum residual in the analysis ranges used for that compound. This shows a "worst case" residual for each component.
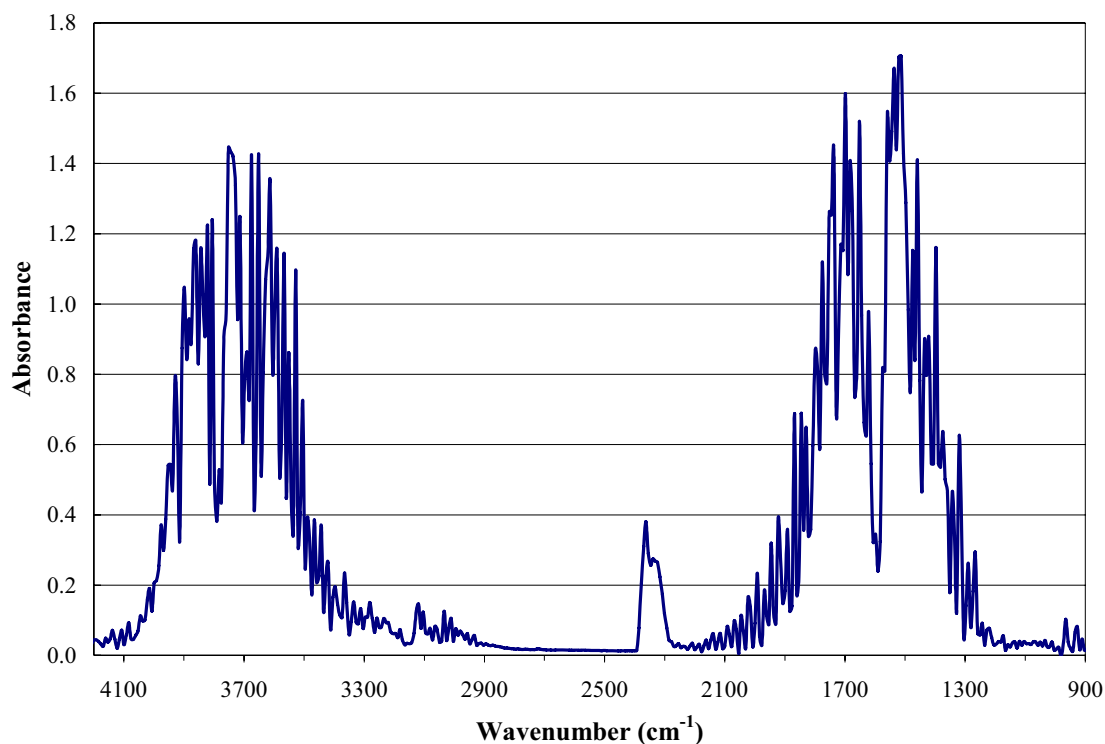
Figure 3.11 Absorbance Spectrum for Sample 060704_00534 (1 minute scan at 180°C)

In this particular analysis, Calcmet™ has calculated a negative concentration for both NO and formaldehyde. In the software settings for the Calcmet™ program, there is an option to allow negative concentrations to be calculated. The benefit in using this setting is that it enables a powerful troubleshooting method. If the analysis calculates negative concentrations, whose magnitude exceeds the noise amplitude, this could indicate a baseline drift in the IR signal or an interference with another compound (either an incorrect specification in the interference table or an interference with a compound not currently specified in the application settings). In this example, formaldehyde shows a slightly negative concentration (-0.99 ppm$_v$). With such a small

negative deviation, this is likely due to noise in the spectrum, indicating that the analysis is working correctly and there is no formaldehyde in the sample.

Table 3.6 Component Analysis Results for Sample 060704_00534

Compound	Concentration		Max. Residual $\lvert$ Absorbance $\rvert$
Water	10.91	vol. %	0.0055
CO_2	0.01	vol. %	0.0047
CO	0.36	ppm_v	0.0017
N_2O	0.59	ppm_v	0.0010
NO	-8.30	ppm_v	0.0044
NO_2	0.66	ppm_v	0.0007
NH_3	63.06	ppm_v	0.0044
Formaldehyde	-0.99	ppm_v	0.0035
Acetaldehyde	3.92	ppm_v	0.0041
MEA	13.69	ppm_v	0.0038
Methanol	0.12	ppm_v	0.0038
Methylamine	0.02	ppm_v	0.0039
CH_4	4.22	ppm_v	0.0016

Recall from Table 3.3 that the detection limit for a compound is ~ 2% of the smallest measuring range specified as long as this is above the noise level of the detector. The lowest concentration reference spectrum for NO used in the analysis is 10 ppm_v (Appendix B), so the detection limit for NO is 0.2 ppm_v. This is below the noise level, so the noise actually determines the detection of NO in this analysis method. Since the analysis calculates a large negative value for NO, -8.30 ppm_v, which is above magnitude of the noise, this indicates a problem with the analysis. In order to

troubleshoot this problem, examine the component residual spectrum and compare this to the reference spectrum for NO. This comparison can be seen in Figure 3.12.

Table 3.4 shows the analysis region for NO starts at 1760 cm^{-1} with an absorption limit of 0.8 in this analysis region; however, the sample spectrum is above this absorbance until 1806 cm^{-1}, which is where the analysis of this sample starts for NO. The residual for NO is larger than the absorbance spectrum for NO at almost every wavelength. The largest residual, -0.0044, occurs at 1883 cm^{-1} in the trough of the NO double peak. This is easily explained by recalling that the background spectrum was saturated between 1760 and 1938 cm^{-1}, making analysis in this region impossible. NO is a very weak IR absorber and only displays one signature absorption peak. The analysis region from 2550 to 2650 cm^{-1} is used primarily as a baseline check. The only analysis region for NO that is not saturating the detector and for which the background scan is not saturated is from 1938 – 1991 cm^{-1}. Since an analysis region of 200 cm^{-1} is generally needed for a quantitative analysis, the concentration of NO will not be able to be determined for this experiment.
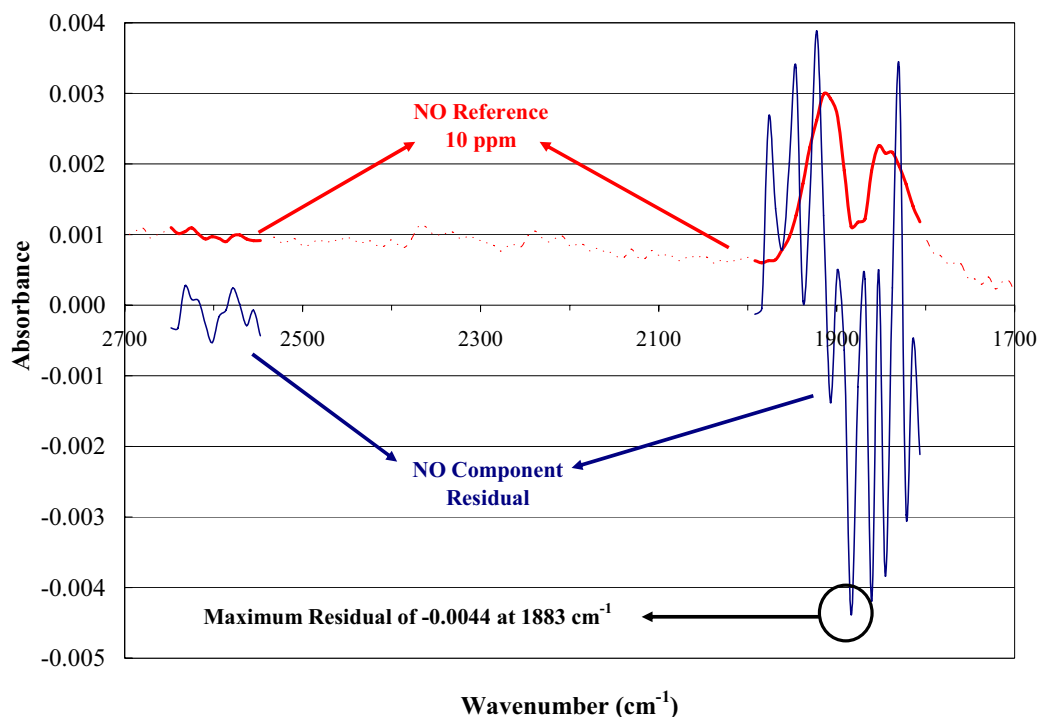
Figure 3.12 Comparison of Reference and Component Residual Spectra for NO

3.3.2. Ultraviolet-Visible Spectroscopy

Ultraviolet-Visible (UV-VIS) spectroscopy is often used to quantify the color and composition of transition metal complexes in aqueous solution. The principles of UV-VIS are the same as IR spectroscopy except that the radiation here involves electronic transitions of bonding electrons. These transitions are higher energy than the rotational and vibrational transitions encountered in IR spectroscopy, and generally occur in the region of 200 to 800 nm. The oxidative degradation of MEA is catalyzed by metals like Cu and Fe, both of which are transition metals and will complex with MEA and other degradation products. Degraded solutions are always strongly colored and the solutions range from a clear light yellow to a nearly opaque dark purple color.

72

In order to qualitatively compare these solutions, UV-VIS was performed on a number of the samples to account for these color changes.

Analysis was performed using a HP 8452A Diode Array Spectrophotometer equipped with a deuterium lamp, and capable of a 2 nm resolution. Data was collected in the range of 200 - 800 nm using 5 ml polycarbonate cuvettes with a 1 cm path length. The sample time was 0.5 sec. Samples with an absorbance above 1.0 cannot be used for qualitative analysis as described previously due to deviations from the Beer-Lambert law. Details of the UV-VIS scans can be found in Appendix H.

3.4. Experimental Data Interpretation

Section 3.3.1.5 gave a detailed example of multi-component analysis of Sample 20040607_00534. This type of analysis is performed for each sample spectrum collected during the experiment. In Chapter 2 it was shown that the primary amino degradation product of MEA is expected to be NH_3. The rate of oxidative degradation of MEA is quantified in these experiments by measuring the rate of NH_3 evolution from the amine solution. By operating the reactor at high mass transfer conditions, this ensures the amount of NH_3 left in solution is negligible compared to the amount of NH_3 being stripped by the reaction gas.

The gas rate being fed to the reactor is calculated from the calibrations on the Brooks mass flow controllers. This gas is dry and is partially saturated by being bubbled through the heated saturator bomb. Using the water concentration from the FT-

IR analysis, the total gas flowrate through the reactor is back calculated. The moles of NH_3 in the outlet were calculated by multiplying the flowrate by the NH_3 concentration.

Since the saturator bomb does not completely saturate the inlet gas some water loss from the amine solutions occurs. The average mass of the solution, subtracting additions made throughout the experiment, is used to calculate the average volume of MEA solution in the reactor. Density calculations are based on experimental data from existing correlations (Weiland 1996). The rate of NH_3 evolution is then calculated by normalizing the moles of NH_3 leaving the reactor by the average volume of MEA solution. Rates are reported in units of mmoles NH_3 evolved / liter of MEA solution-hour, or mM/hr. Detailed tabulations for the experiments can be found in the appendix. Figure 3.13 shows a sample analysis for Experiment 20040607.

The initial spike in the degradation rate comes from stripping NH_3 from the solution which has accumulated during solvent storage. The first steady state is reached after approximately 2 hours. At this point, the system can be perturbed by changing the agitation rate, or adding a catalyst or inhibitor to the solution. After approximately 160 minutes, 0.01 mM Cu was added to the reactor, and the NH_3 evolution rate began to increase, and reached the next steady state at 400 minutes.

The initial steady state for this experiment with no added catalyst (0.0002 mM Fe) represents a baseline degradation rate that is always encountered. The lowest measured rate for these experiments is 0.15 mM/hr, which is used as a baseline degradation rate in Chapter 5. This represents the minimum amount of oxidative degradation that will occur for aqueous MEA.
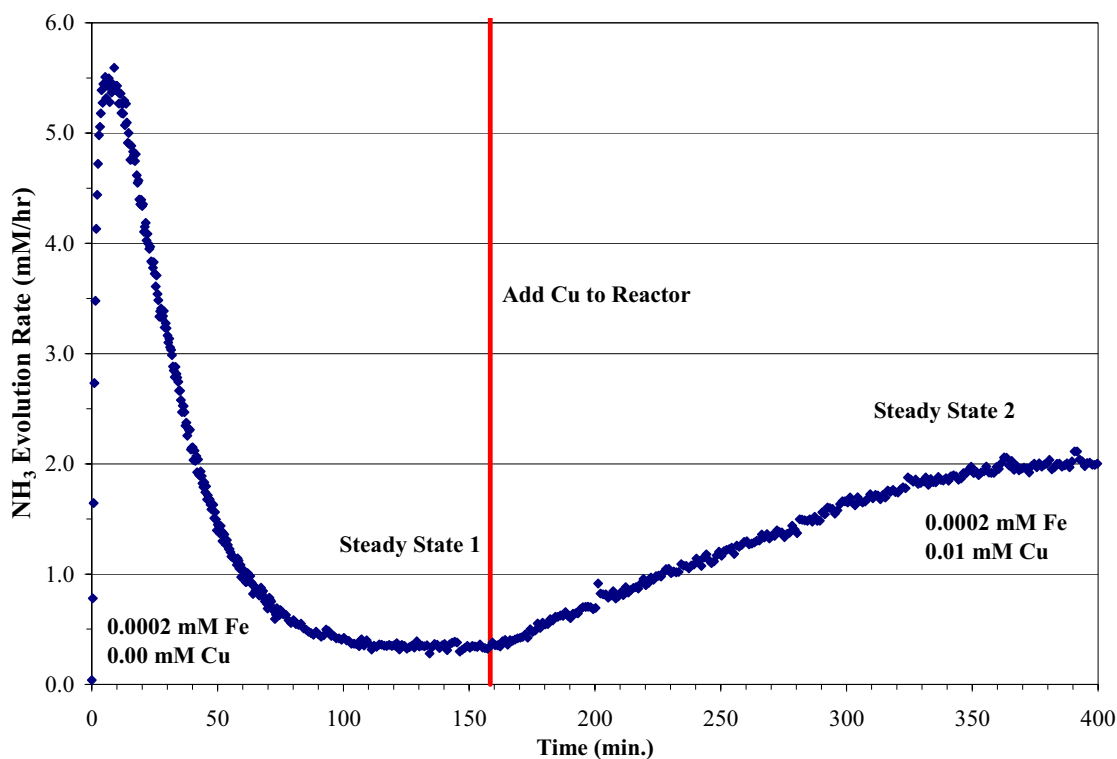
Figure 3.13 Sample Analysis for Experiment 20040607
(55°C, 7.0 m MEA, $\alpha = 0.15$, Air, Agitated Reactor Data, 1400 RPM)

Experiment 20040607 is a typical representative degradation experiment for the Agitated Reactor. Under these conditions the concentrations of MEA, acetaldehyde, and formaldehyde remain relatively unchanged throughout the experiment and are approximately 3 ppm$_v$, 3.6 ppm$_v$ and 0.5 ppm$_v$ respectively.

Chapter 4: Oxygen Mass Transfer

This chapter details key results that show the rate of MEA degradation is controlled by the rate of O_2 absorption under significant industrial and laboratory conditions. The effect of important process parameters, catalyst/MEA/O_2 concentrations, CO_2 loading (α), pH, and agitation is presented. Re-analysis of previous studies shows that they were also mass transfer limited. Predicted degradation rates in an industrial application match reported solvent make-up rates.

4.1. Introduction

The mechanism for the oxidative degradation of MEA presented in Chapter 2 showed that the reactions can be considered as a set of free radical reactions. Reactions involving free radicals are generally very fast due to the instability of the intermediates. In processes involving both mass transfer and chemical reactions, it is necessary to determine which process dominates the overall observed rates. Experiments were performed to quantify the effect of catalyst concentration (both Cu and Fe), MEA concentration, gas phase O_2 concentration, CO_2 loading (α), pH, and agitation on the

rate of NH_3 evolution from MEA solutions at 55°C. Results from these studies suggest that the rate of NH_3 evolution is controlled by the rate of O_2 mass transfer into the amine solution and not the kinetics of the degradation reactions.

These results were then compared to results from previous experiments by other investigators, which were discussed in Chapter 2. This comparison shows that the mass transfer capabilities of both the Sparged Reactor system and the Agitated Reactor system are much higher than what was observed in previous studies. Additionally, degradation rates in this work are much higher than rates observed by previous investigators, indicating that the previous studies were actually reporting O_2 mass transfer rates and not kinetics.

The final validation of the O_2 mass transfer findings comes from estimating the rate of oxidative degradation in an actual flue gas treating application. The rate of O_2 absorption was estimated using the rigorous AspenPlus simulation developed by Freguia for CO_2 absorption with aqueous MEA (Freguia 2002). Results from the estimate were compared with literature values, and were found to be larger than the rates calculated by assuming that the oxidative degradation of MEA is controlled by rate of O_2 absorption under typical industrial operating conditions.

4.1.1. Evolution of the Degradation Apparatus

Initial experiments were performed using the apparatus developed to study oxidative degradation of MEA catalyzed by iron (Chi 2000). Results from these initial screening experiments indicated that better analytical methods were needed to

accurately quantify the rate of NH_3 evolution, and the new Gasmet™ FT-IR system was added to the apparatus. The sparged apparatus described in Chapter 3 was then used to expand upon the initial findings. Results from the initial experiments using the apparatus developed by Chi can be found in Appendix C and are not presented in detail in this chapter.

Experiments performed with the Sparged Reactor showed two problems. The first problem was reproducibility and the second was water loss from the reactor. Appendix D shows that experiments with the Sparged Reactor show significant mass loss, as high as 33% (data from experiments with mass loss greater than this were not reported). Additionally, the spread in the data was significant for experiments performed under similar conditions. The results from the experiments using the Sparged Reactor, however, were able to show effects of O_2 mass transfer. In order to attempt to validate these findings, experiments were performed to measure the rate of O_2 absorption in the sparged rector by measuring the rate of sulfite oxidation. These results indicated that the Sparged Reactor results were likely controlled by O_2 mass transfer rate.

In order to quantify the mass transfer effects, the Agitated Reactor was built, and several experiments from the Sparged Reactor experiments were repeated. The Agitated Reactor experiments show better reproducibility, higher mass transfer capabilities, and less water loss from the amine solution than the Sparged Reactor experiments. The experiments were then expanded to quantify the effect of O_2 mass transfer over a wider range of conditions.

4.2. Experimental Results

This section will present key results from O_2 mass transfer experiments carried out in both the Sparged Reactor and the Agitated Reactor. Details from all these experiments can be found in the appendix. A summary of the experiments performed, including the date and experimental conditions can be found below in Table 4.1 and Table 4.2 for the Sparged Reactor and the Agitated Reactor systems respectively.

Table 4.1 Summary of Sparged Reactor Experiments (7.0 molal MEA, 55°C)

Date	Variable	α^1	Catalysts		Comments
06/25/02	Catalyst	0.40	Fe		
06/26/02	Catalyst	0.40	Fe	Cu	
06/27/02	Catalyst	0.40	Fe	Cu	
07/01/02	Catalyst	0.40	Fe	Cu	
07/11/02	Catalyst	0.40	Fe		
07/15/02	Catalyst	0.40	Fe	Cu	
07/17/02	Catalyst	0.15	Fe		precipitate formed
07/18/02	Catalyst	0.15	Fe	Cu	foaming problems
07/19/02	Catalyst	0.15	Fe	Cu	
10/15/02	Catalyst	0.40	Fe	Cu	highest Cu conc. tested
10/18/02^2	Catalyst and pH	0.21	Fe	Cu	pH = 10.3, precipitate forms, foaming problems
10/21/02^2	Catalyst and pH	0.50	Fe	Cu	pH = 8.9
10/30/02^2	Catalyst and pH	0.05	Fe	Cu	pH = 11.0
11/13/02	O_2	0.15	Fe	Cu	
11/18/02	O_2	0.15	Fe	Cu	
12/05/02	Catalyst	0.15	Fe	Cu	
12/06/02	Catalyst	0.40	Fe	Cu	
12/09/02	Catalyst	0.15	Fe	Cu	
12/10/02	Catalyst	0.00	Fe	Cu	foaming problems

[1] α = moles CO_2 / mole MEA
[2] Loading for these experiments is moles SO_3^{-2} / mol MEA

Table 4.2 Summary of Agitated Reactor Experiments (7.0 molal MEA, 55°C)

Date	MEA (m)	α^1	Fe [mM]	Cu [mM]	O$_2$ (%)	RPM
09/16/03	7.0	0.15	0.0002	0.00	air	vary
09/22/03	7.0	0.15	0.0002	0.00	air	vary
09/23/03	7.0	0.15	0.0002	0.00	air	vary
09/24/03	7.0	0.15	0.0002	0.00	air	vary
09/29/03[2]	7.0	0.15	0.0002	0.18	air	vary
09/30/03[2]	7.0	0.15	0.0002	0.18	air	vary
10/03/03[2]	7.0	0.15	0.0002	0.18	air	vary
10/20/03	7.0	0.15	0.1429	0.00	air	vary
10/21/03	7.0	0.15	0.1429	0.00	air	vary
10/24/03	7.0	0.15	0.0002	0.17	8.2%	vary
10/27/03	7.0	0.15	0.0002	0.20	vary	1400
10/28/03	3.5	0.15	0.0001	0.22	vary	1400
10/30/03	3.5	0.15	0.0001	0.24	vary	1400
11/01/03	14.0	0.15	0.0003	0.20	vary	1400
11/03/03	14.0	0.15	0.0003	0.20	vary	1400
11/10/03	7.0	0.15	0.0002	0.19	air	vary
11/13/03	7.0	0.15	0.0002	0.20	vary	1400
11/14/03[3]	3.5	0.15	0.0001	0.20	vary	1400
05/26/04[4]	2.0	0.15	0.0001	0.21	vary	vary
06/03/04	1.0	0.15	0.0000	0.21	air	vary
06/04/04	1.0	0.15	0.0000	0.20	4.6%	vary
06/07/04	7.0	0.15	0.0002	vary	air	1400
06/26/04	7.0	0.15	Vary	0.00	air	1400
06/28/04	7.0	0.00	0.0002	vary	air	1400

[1] α = moles CO_2 / mole MEA
[2] solution contains 37 mM Formaldehyde
[3] solution contains 0.5 molal NaCl
[4] solution contains 1.6 molal Nacl

The metal catalysts were purchased as $FeSO_4 \times 7\ H_2O$ and $CuSO_4 \times 5\ H_2O$ and injected directly into the reactors as aqueous solutions. All solutions were made gravimetrically using de-ionized water.

4.2.1. Catalyst Concentrations and CO_2 Loading

The first variable studied in the Sparged Reactor was catalyst concentration. Dissolved metals catalyze the oxidative degradation of MEA. Dissolved iron is present in industrial applications because the amine solution is corrosive to the steel process equipment; therefore, Cu corrosion inhibitors are added to the MEA solution to decrease the corrosion rates (Cringle et al. 1987; Pearce 1984; Pearce et al. 1984; Wolcott et al. 1985). Both of these metals have been shown to catalyze the oxidative degradation of MEA (Blachly and Ravner 1963; Chi 2000), but no quantitative study has been performed to determine the effect of Cu on the oxidative degradation of MEA. Experiments were carried out using the Sparged Reactor at CO_2 loadings of 0.00, 0.15, and 0.40 mol CO_2/mol MEA, corresponding to the conditions at the top and bottom of the absorber at 55°C with 7.0 molal MEA solutions. Figure 4.1 and Figure 4.2 show the results from the solutions with rich and lean CO_2 loadings respectively.

Up to ~ 0.2 mM Fe all of the solutions show a strong dependence on the catalyst concentration, although the increase in NH_3 evolution rate is less than first order with respect to both Fe and Cu concentration for both the rich and the lean solutions. Solutions containing only Fe degrade slower than solutions that contain both Fe and Cu, and the rate of NH_3 evolution shows a stronger dependence on the Cu concentration than the concentration of dissolved Fe. Another major observation from Figure 4.1 and Figure 4.2 is that the solutions with lean loading appear to degrade 1.5 to 2 times faster than the solutions with rich loading.
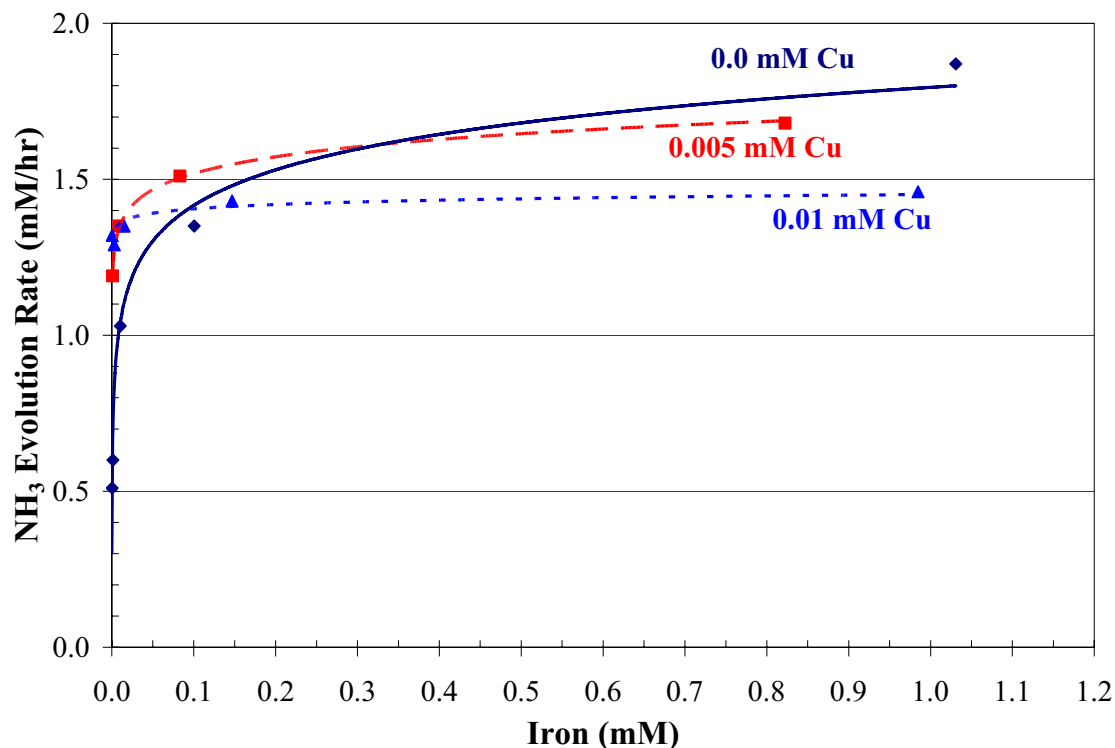
Figure 4.1 Effect of Fe and Cu on the Oxidative Degradation Rate of Rich MEA
(55°C, 7.0 m MEA, α = 0.40, Air, Sparged Reactor)

For all of the solutions shown in Figure 4.1 and Figure 4.2 the rate of NH_3 evolution increases exponentially up to ~ 0.2 mM Fe and then flattens off. This is a strong indication that the degradation of solutions above 0.2 mM Fe is controlled by the rate of O_2 absorption. Solutions with concentrations above 0.2 mM Fe still show a dependence on the Cu concentration, which seems to contradict the observation that these solutions are controlled by the rate of O_2 mass transfer. The rate of NH_3 evolution is related to the rate of O_2 consumption by the O_2 stoichiometry of the degradation reactions. If the stoichiometry of the degradation reactions changes, the rate of NH_3 evolution will be directly affected. The addition of a second catalyst to the amine

solution can change the overall stoichiometry of the degradation reactions, and thus the rate of NH_3 evolution, even if the system is mass transfer controlled. Different catalysts can promote different steps in the reaction mechanism, have a stronger effect on the same reaction, or completely change the reaction pathway; therefore, copper could either be changing the rate limiting step in the reaction, or simply be changing the selectivity of the formation of degradation products, thereby changing the overall O_2 stoichiometry of the degradation reactions.
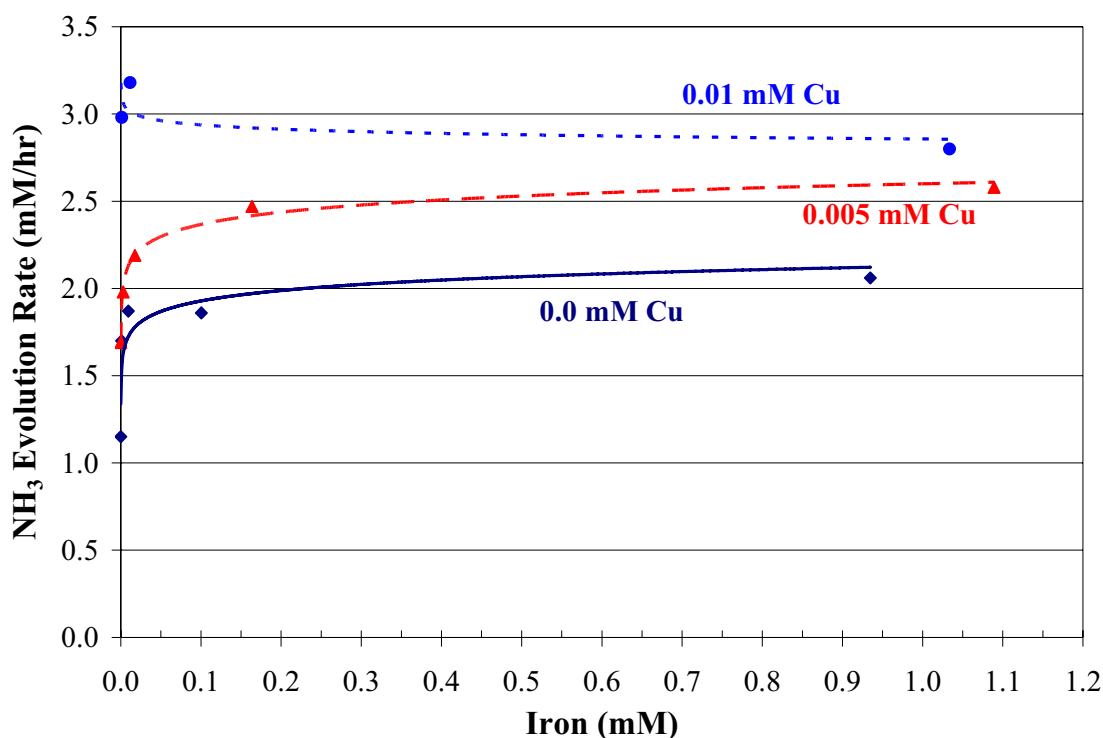
Figure 4.2 Effect of Fe and Cu on the Oxidative Degradation Rate of Lean MEA (55°C, 7.0 m MEA, $\alpha = 0.15$, Air, Sparged Reactor)

The results in Figure 4.1 and Figure 4.2 show that the rate of NH_3 evolution decreases with increasing CO_2 loading. Figure 4.3 shows the effect of CO_2 loading in a

mixed Cu/Fe catalyst system. The rich solutions show the lowest degradation rates, while the lean solutions show the highest degradation rates. The unloaded solution shows an increase in NH_3 evolution as the concentration of Fe increases, but the lean and rich solutions are essentially independent of Fe concentration. This indicates that the loaded solutions are in an O_2 mass transfer controlled regime, while the unloaded solutions are still in a regime where the kinetics at least partially determine the NH_3 evolution rate. Since the carbamate is playing a role in rate of oxidative degradation of MEA, it is necessary to examine the effect of MEA speciation on the overall oxidative degradation rate.
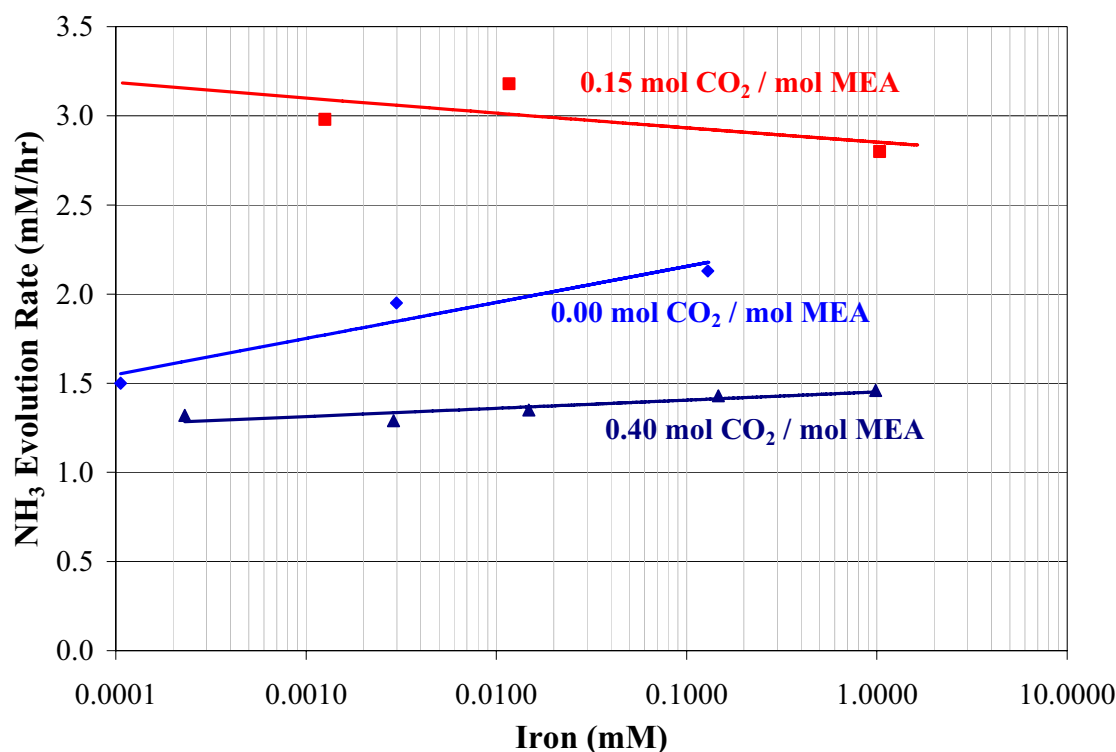
Figure 4.3 Effect of CO_2 Loading on the Rate of NH_3 Evolution from 7.0 m MEA (55°C, 0.01 mM Cu, Air, Sparged Reactor)

4.2.2. Speciation and pH

The degradation mechanism discussed in Chapter 2 was written in terms of free MEA as the actively degrading species. In loaded solutions there are three species of MEA that could undergo oxidative degradation: free MEA, protonated MEA ($MEAH^+$), and the MEA carbamate ($MEACOO^-$). Figure 4.4 shows the distribution of these species as a function of CO_2 loading at 55°C for a 7.0 molal solution calculated using the equilibrium constants reported by Freguia (Freguia 2002) which were modified from the original data of Austgen (Austgen 1989). As the CO_2 reacts with the MEA, the relative concentrations of carbamate and protonated MEA both increase. The carbamate concentration passes through a maximum at a loading of approximately 0.5 mol CO_2/mol MEA. At higher loadings, the buffer capacity of the free amine reaction is surpassed, and the dominant absorption mechanism is the conversion of CO_2 to bicarbonate, resulting in the maxima in carbamate concentration.

The degradation rates presented above clearly show that the rate of NH_3 evolution is a function of CO_2 loading. Degradation rates are highest for solutions with $\alpha = 0.15$, lowest for solutions with $\alpha = 0.40$, and in between for solutions with $\alpha = 0.0$. From the speciation data in Figure 4.4, it can be seen that above $\alpha \sim 0.35$, $MEAH^+$ is the dominant species, and below $\alpha \sim 0.35$ free MEA is the dominant species. The dominant amine species for both the lean solutions ($\alpha = 0.15$) and the unloaded solutions is free MEA. The primary difference is that the lean solutions contain carbamate, with a ratio of $MEAH^+$/MEA = 0.2. Since the solutions where MEA is the

dominant amine species in aqueous solution show the highest rates of oxidative degradation, this would suggest that free MEA is the active species being degraded.
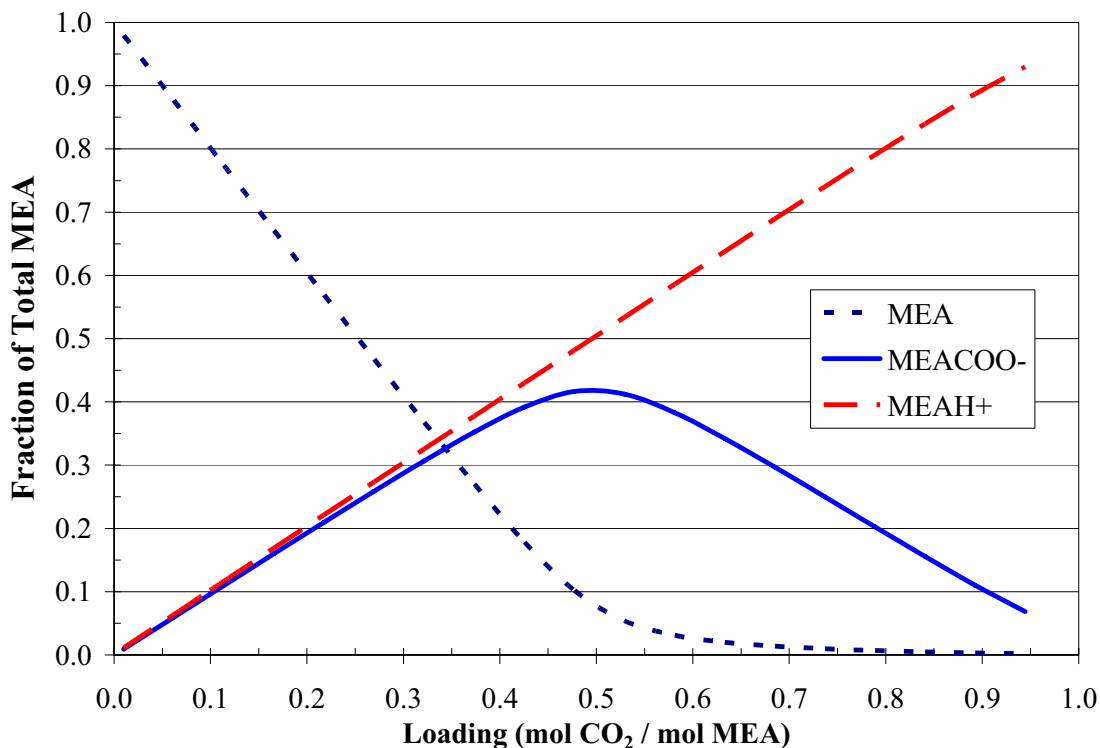
Figure 4.4 Speciation of CO_2 Loaded 7.0 molal MEA Solutions at 55°C

In order to verify this observation, unloaded solutions of 7.0 m MEA were titrated with sulfuric acid to manipulate the ratio of $MEAH^+$/MEA in the absence of CO_2. The solution pH was measured before the degradation experiments, and was compared to the measured pH of the loaded solutions. Table 4.3 shows a comparison of speciation for the pH experiments and typical MEA solutions, while Figure 4.5 shows the results for the pH experiments.

Table 4.3 Speciation Comparison for CO_2 and H_2SO_4 Loaded 7.0 m MEA

pH	mol CO_2/ mol MEA	mol H_2SO_4/ mol MEA	$MEAH^+$/MEA
9	0.00	0.41	4.4
10	0.00	0.18	0.6
11	0.00	0.05	0.1
10	0.40	0.00	2.0
11	0.15	0.00	0.2
12	0.00	0.00	---

The ratio of $MEAH^+$/MEA follows the expected trends. Namely, as the pH becomes more acidic the ratio of $MEAH^+$/MEA increases and the rate of NH_3 evolution decreases. This matches the trends observed in CO_2 loaded solutions. The primary difference in these experiments is the magnitude of the degradation rates; the loaded solutions appear to degrade faster. The ionic strength in the H_2SO_4 loaded solutions is much higher than the equivalent MEA solutions, which can account for the lower rates in all of these solutions.

Solutions with a CO_2 loading = 0.40 have a ratio of $MEAH^+$/MEA = 2.0 and solutions with $\alpha = 0.15$ have a ratio of 0.2. Comparing Figure 4.5 to Figure 4.1 and Figure 4.2 above, the degradation rates with CO_2 present are higher than the solutions with no CO_2 at the same ratio of $MEAH^+$/MEA. If O_2 solubility alone were accounting for the change in degradation rates, the solutions with $\alpha = 0$ should degrade the fastest, followed by solutions with $\alpha = 0.15$ and then $\alpha = 0.40$. This clearly indicates that the carbamate is affecting the degradation rate and explains why solutions with zero loading degrade slower than the lean solutions. While it does not appear that the carbamate is

the actively degrading species in aqueous solution, it could be playing a catalytic role by stabilizing an intermediate in the degradation mechanism.
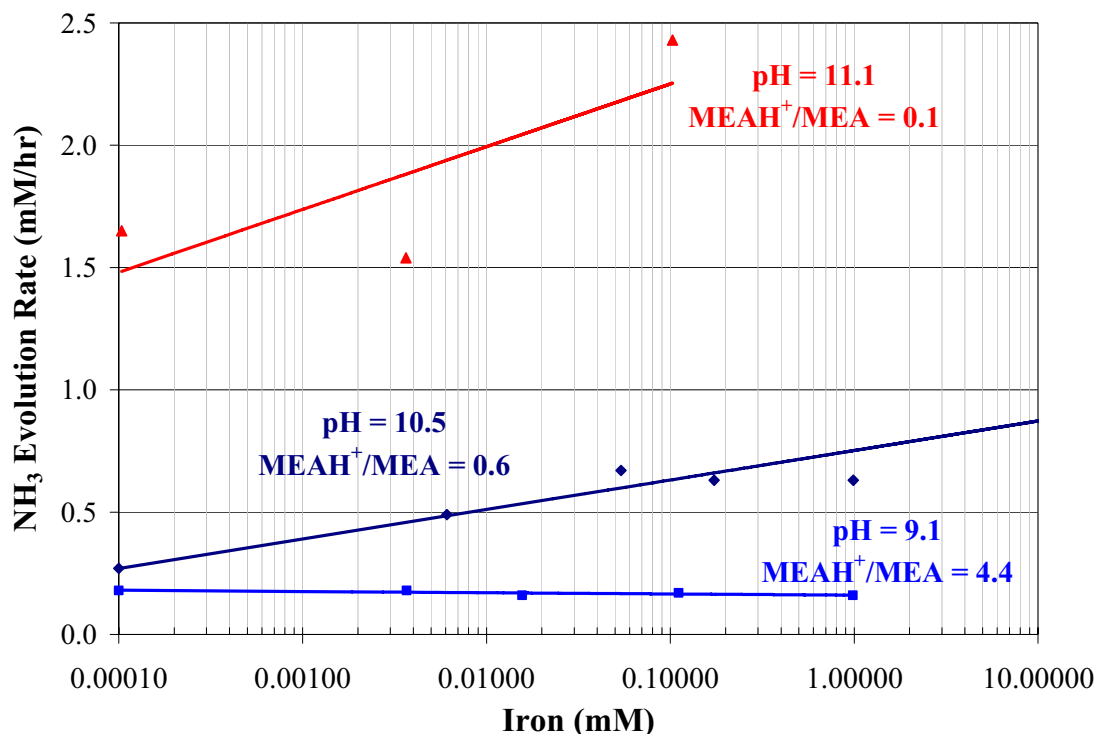
Figure 4.5 Effect of MEA Speciation on Oxidative Degradation
(7.0 m MEA, $55°C$, 0.001 mM Cu, titrated with H_2SO_4, Air, Sparged Reactor)

4.2.3. Sulfite Oxidation Experiments

The results from the Sparged Reactor experiments, presented above in Section 4.2.1 indicate that the observed rates of NH_3 evolution are controlled by the rate of O_2 absorption into the MEA solutions. In order to validate this observation, experiments were performed to attempt to quantify the rate of O_2 absorption into the Sparged Reactor. This was done by measuring the rate of sulfite oxidation in aqueous solution, a widely used method for determining mass transfer coefficients in gas-liquid contactors.

88

The sulfite oxidation kinetics are very fast, and this system is controlled by the rate of O_2 absorption. Unlike the MEA system, the O_2 stoichiometry for sulfite oxidation is known; therefore, by measuring the rate of sulfite oxidation, the rate of O_2 absorption is also known. The overall reaction is shown below in Equation 4.1.

$$SO_3^{-2} + \frac{1}{2}O_2 \xrightarrow{\;catalyst\;} SO_4^{-2} \qquad\qquad 4.1$$

In order to accurately model the mass transfer characteristics of the Sparged Reactor, it would be desirable to measure the O_2 uptake in situ; however, since the O_2 would be competitively reacting with both MEA and sulfite, this would not allow for an accurate measurement of the total rate of O_2 absorption. A solvent system was selected that closely matched the physical properties of MEA that are important in determining mass transfer coefficients, namely viscosity, surface tension, and O_2 solubility (Henry's constant). Concentrated aqueous solutions of $MgSO_4$ were used for the sulfite oxidation experiments. Viscosities for the concentrated solutions were measured in a Cannon-Fenske viscometer (Cannon Instrument Co., No. 100, 3-15 cSt) using a previously detailed method (Cullinane 2005). A comparison of the viscosities for various $MgSO_4$ solutions (both experimental and literature values) to both water and loaded MEA solutions (from literature data) is shown below in Figure 4.6.

At 55°C the viscosity of water is around 0.5 cP, while the viscosity of the lean MEA solutions is 1.4 cP and the rich solutions is 3.0 cP. The viscosity of the $MgSO_4$ solutions increases with increasing salt concentration. Figure 4.6 shows that the 15 wt. % $MgSO_4$ solutions have nearly the same viscosity as the lean MEA solution (α =

0.15), with a difference of only ~ 7 % at 55°C. Similarly, the 20 wt. % $MgSO_4$ solutions closely match the viscosity of the rich MEA solution (α = 0.40) with only ~ 3% difference at 55°C. Since the viscosity of the 15 wt. % $MgSO_4$ matches the lean loaded amine solutions, which show the highest degradation rates and therefore the highest rate of O_2 absorption, this solvent was chosen as a suitable choice to compare to the MEA solutions.
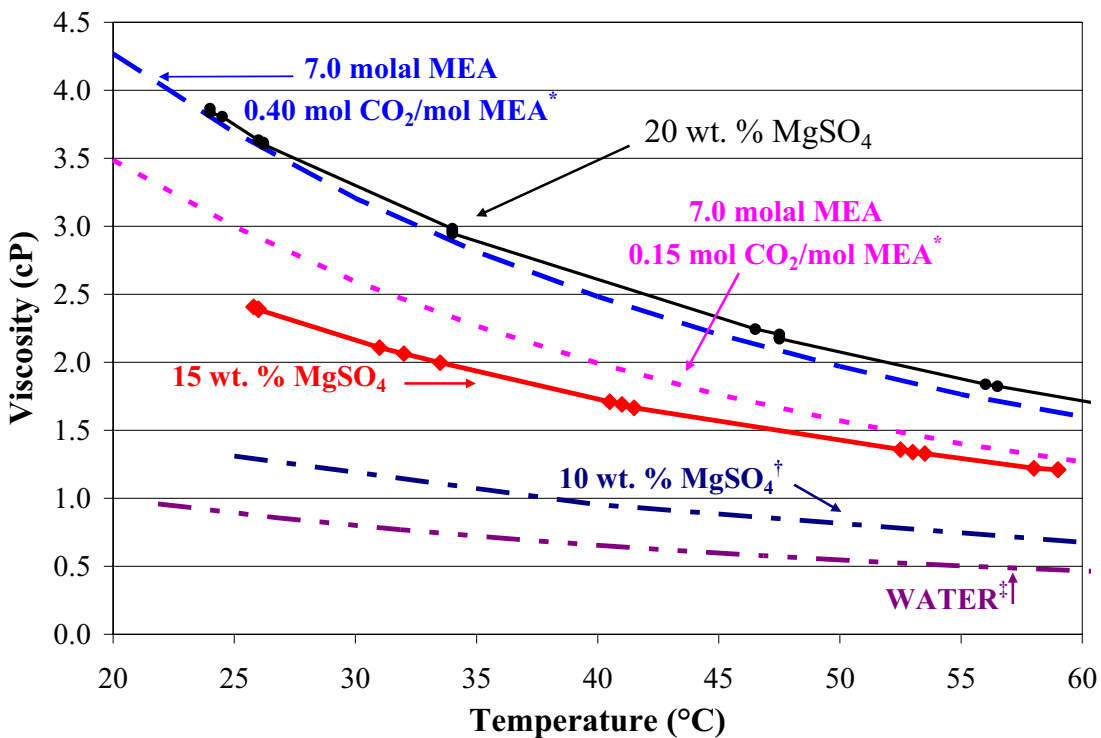
Figure 4.6 Viscosities of Water, Loaded Mea, and $MgSO_4$ (aq.) Solutions
[*] (Weiland 1996), [†] (Korosi and Fabuss 1968), [‡] (Perry et al. 1997)

The second physical property to match is surface tension. Surface tension measurements of loaded amine solutions are difficult to measure due to CO_2 desorption during the measurements. Measurements have been made in unloaded solutions

(Vazquez et al. 1997), but no reproducible measurements have been made in loaded solutions (Weiland 1996). Surface tension measurements of $MgSO_4$ (aq.) are available in the literature (Jones and Ray 1942), and a comparison between these measurements and the surface tension of unloaded MEA solutions is shown in Figure 4.7.
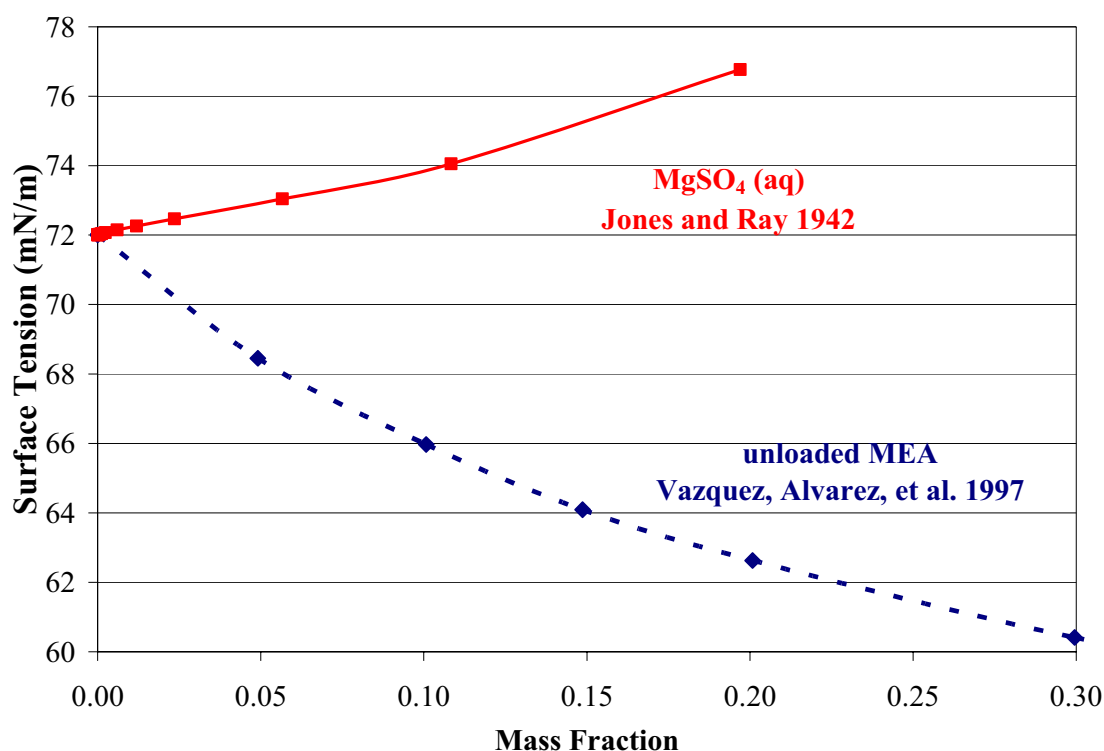
Figure 4.7 Surface Tension of $MgSO_4$ and Unloaded MEA at 25°C

The surface tension increases as the concentration of $MgSO_4$ increases, while the surface tension of MEA solutions decreases with increasing amine concentration. In general, a lower surface tension results in an increased gas-liquid contact area (larger bubbles are more stable) and a higher mass transfer coefficient. Unloaded MEA solutions have a low ionic strength, but loaded solutions have a much higher ionic strength, which tends to increase the surface tension. It might be expected that the

surface tension of loaded solutions would be higher than what is predicted by the unloaded solutions. This has been observed in other alkanolamine solutions where the surface tension has increased by 10 – 20 % from a loading of 0.0 to 0.40 (Weiland 1996). The 15 wt. % $MgSO_4$ solution is only 20% higher than the unloaded 7 molal MEA (30 wt. %). The surface tension will be even closer to the loaded solutions, and matches the surface tension of the MEA solutions adequately enough to use this solution for the sulfite oxidation experiments.

The final physical property to match is O_2 solubility. Gas solubility in electrolyte solutions is generally calculated by modifying the Henry's constant for the gas in pure water to account for increased or decreased solubility from the electrolytes. These constants are called van Krevelen constants and have been shown to accurately model the solubility of gases in electrolyte systems over a wide range on conditions. These constants have been measured for both the $MgSO_4$ system (Tromans 2000) and loaded amine solutions (Weiland 1996). No value of the Henry's constant for O_2 solubility in aqueous MEA has been reported in the literature; therefore, it was assumed that the solubility in MEA (aq.) was the same as water. The same Henry's constant was used for both the $MgSO_4$ system and the MEA system (Dean 1992). Figure 4.8 shows the solubility of O_2 in $MgSO_4$ (aq.) and loaded 7.0 molal MEA solutions relative to pure water ($\phi = C_{Iaq} / C_{aq}$ = solubility in electrolyte solution / solubility in water).
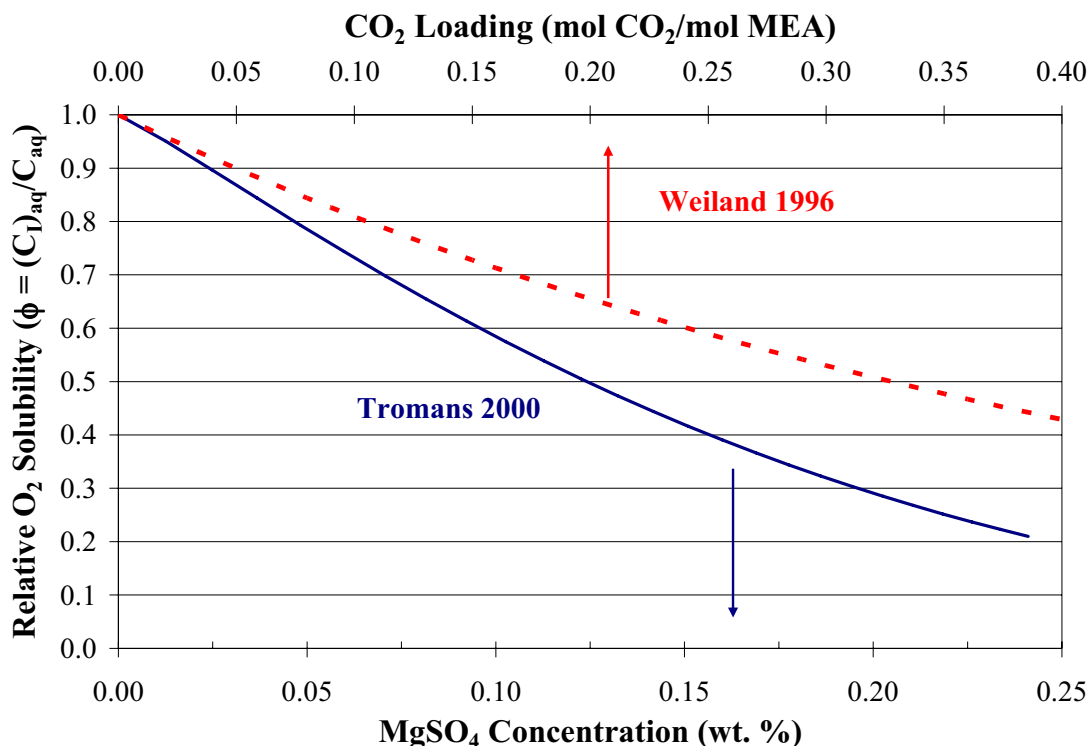
Figure 4.8 O_2 Solubility in $MgSO_4$ (aq.) and Loaded 7.0 molal MEA Relative to Water

In both the MEA and $MgSO_4$ solutions, the O_2 solubility decreases with increasing ionic strength. The relative solubility of O_2 decreases by 60% when the $MgSO_4$ concentration is increased to 15 wt. % and the CO_2 loading is increased to 0.40. The relative solubility in the lean MEA solutions ($\alpha = 0.15$) is roughly half of that with $\phi = 0.7$. If the solubility of O_2 in unloaded 7.0 m MEA is the same as water, this means that the 15 wt. % $MgSO_4$ closely matches the solubility in the MEA solutions.

Since the 15 wt. % $MgSO_4$ solutions closely matches the viscosity, surface tension, and O_2 solubility of loaded MEA solutions, this solvent was selected for use in the sulfite oxidation experiments. The experiments were run using a 0.05 m Na_2SO_3 solution, which is buffered by 0.20 m $NaHSO_3$. Air was bubbled through a saturator

and then sparged through the reactor solution over a range of flow rates. The pH was measured continuously through the experiment. As the sulfite was oxidized, the pH of the solution decreased as the bisulfite was converted to sulfite to maintain thermodynamic equilibrium. The reactor solution was then titrated with a 1.0 m Na_2SO_3 solution to replace the oxidized sulfite. The solution was then brought back to the original pH as some of the sulfite converted back to bisulfite. The O_2 absorption rate was then calculated by relating the rate of sulfite addition to the rate of oxygen absorption by the O_2 stoichiometry shown in Equation 4.1. Detailed results from the sulfite oxidation experiments can be found in Appendix E, and Figure 4.9 shows representative results from these experiments.
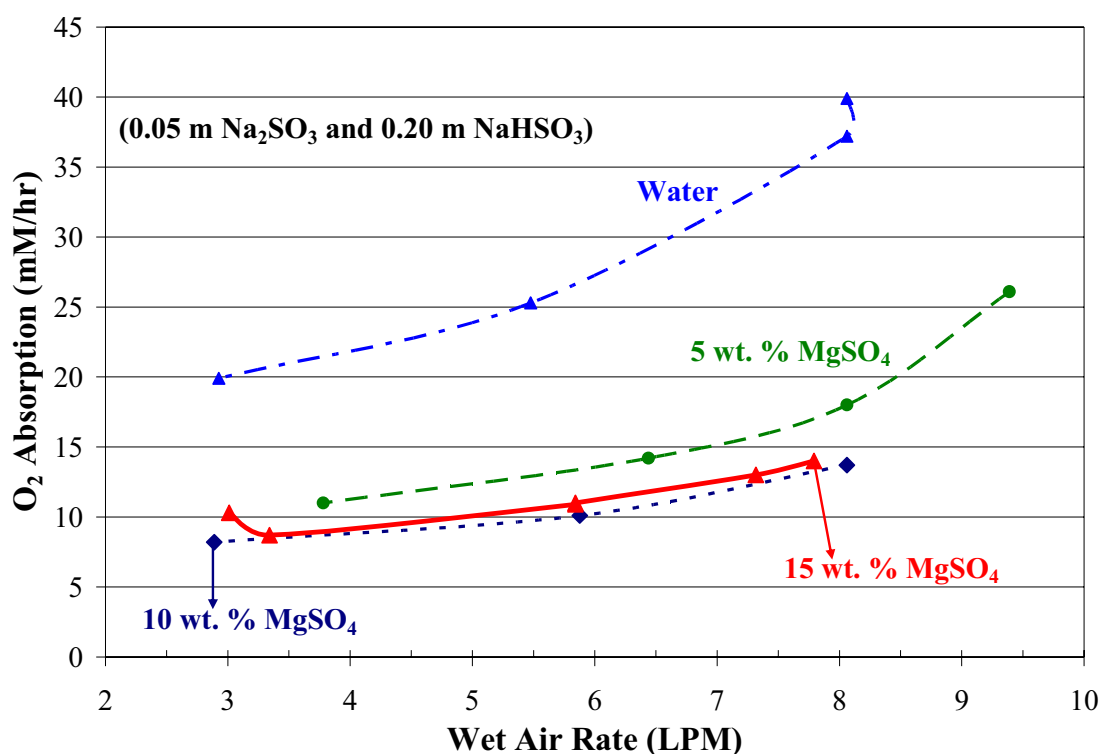
Figure 4.9 O_2 Absorption into Concentrated $MgSO_4$ Measured by Sulfite Oxidation (Sparged Reactor, 55°C, 0.05 m Na_2SO_3 / 0.20 m $NaHSO_3$)

The rate of O_2 absorption decreases dramatically in the $MgSO_4$ solutions compared to the rate in pure water. There is no observable difference in the rate of O_2 absorption between the 10 and 15 wt. % $MgSO_4$ solutions. Since there is no artificial agitation of the amine solution, gas-liquid mixing and agitation is directly dependent on the air flow rate. The rate of O_2 absorption increases with air flow rate for each of the systems, proving that the rate of sulfite oxidation is mass transfer controlled.

The NH_3 evolution rates shown above in Section 4.2.1 are as high as 3.3 mM/hr and air flow rates ranged from 6.6 to 8.8 LPM. Recall from Chapter 2 that the O_2 stoichiometry for MEA oxidation is unknown and ranges from 0.5 to 2.5 depending on the degradation product. Assuming that the rate of O_2 absorption into the loaded MEA solutions matches the rates for the 15 wt. % $MgSO_4$ solutions, the rate of NH_3 evolution could be as high as twice the rates in Figure 4.4. Since the observed NH_3 evolution rates in the Sparged Reactor system are on the same order as the O_2 absorption into the $MgSO_4$ solutions, this further suggests that the degradation rates are at least partially controlled by O_2 mass transfer and not the kinetics of the amine solution. In order to attempt to measure NH_3 evolution rates under kinetic controlled conditions, a new reactor system was built with artificial agitation of the amine solution.

4.2.4. Comparison of Reactor Systems

In order to compare the mass transfer capabilities of the two reactor systems, a number of experiments were run in the Agitated Reactor at the same conditions as experiments in the Sparged Reactor. Figure 4.10 shows a comparison of NH_3 evolution

from several solutions with lean CO_2 loading and varying catalyst concentrations in the Agitated Reactor and the Sparged Reactor. The bottom three curves are the same data from Figure 4.2 and the top two curves are data from the Agitated Reactor, where the agitation rate was set to 1400 RPM.
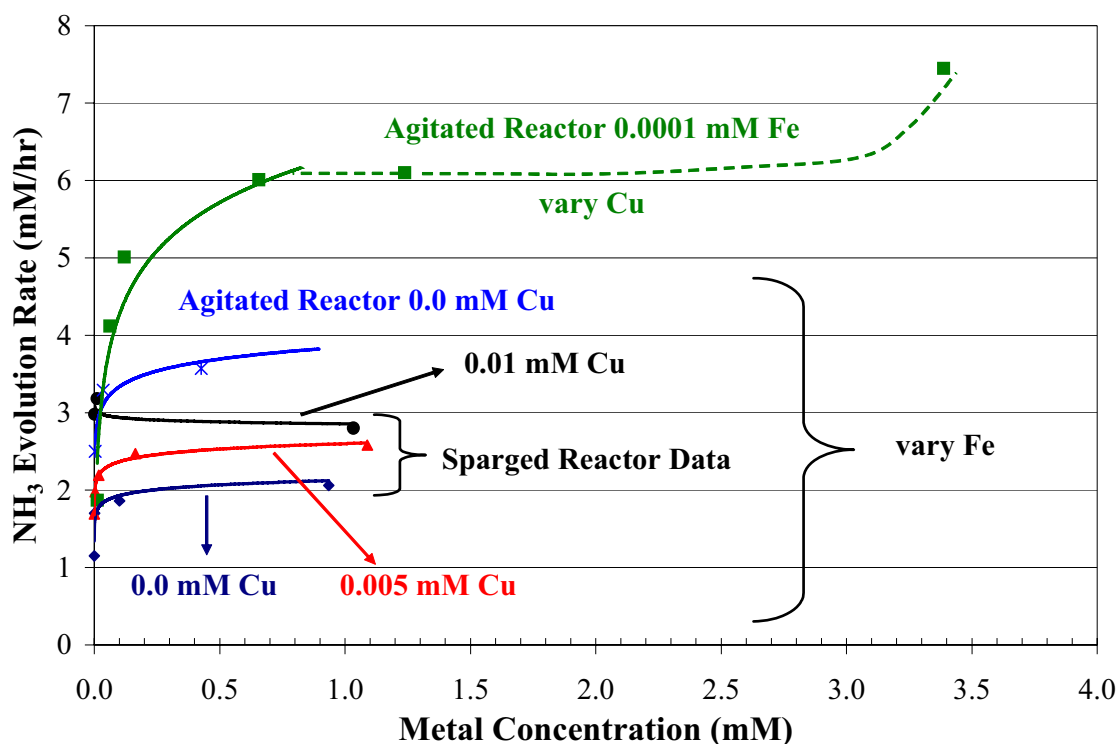
Figure 4.10 Comparison of NH_3 Evolution in Lean MEA Solutions in the Sparged and Agitated Reactor Systems (55°C, $\alpha = 0.15$, Air, Agitated Reactor Data at 1400 RPM)

Both of the solutions run in the Agitated Reactor show significantly higher degradation rates than the three solutions from the Sparged Reactor. The Fe only solutions from the Agitated Reactor, fourth series from the bottom, show degradation rates twice as high as the same solution from the Sparged Reactor, the bottom series, at 1 mM Fe. The system with only Cu, the top series, shows the highest degradation rates

yet observed, reaching 7.5 mM/hr when the Cu concentration is 3.4 mM. The solid portion of the curve represents a regressed trendline for the Cu data excluding the last data point at 3.3 mM. The dashed portion of the curve shows that the measured data fits the expected trend of a system controlled by the rate of O_2 mass transfer, as discussed in Chapter 2. For Cu concentrations below 0.6 mM, the rate of NH_3 evolution is controlled by the kinetics of the degradation reactions. Between 0.6 and 3 mM Cu the rate of NH_3 evolution is controlled by the rate of O_2 mass transfer into the amine solution, and for Cu concentrations above 3 mM the rate is controlled again by the kinetics as the reaction begins to take place in the liquid boundary layer instead of the bulk solution, resulting in enhanced mass transfer.

Since the Agitated Reactor has a much higher mass transfer capability than the Sparged Reactor, and reactor systems from other previous studies, this indicates the experimentally determined oxidative degradation rates of MEA are likely reporting the rate of O_2 mass transfer and not degradation kinetics as was previously believed.

4.2.5. Agitation and Time of Experiments

In order to investigate the possibility that the data being measured is actually the O_2 mass transfer rates and not the degradation kinetics, the Agitated Reactor was built. This reactor system allows for independent control of the O_2 mass transfer via the external agitator. Additionally, experiments performed in the Agitated Reactor were more reproducible and the mass balance was generally better than experiments performed with the Sparged Reactor system. In order to test the effect of O_2 mass

transfer on the observed degradation rates, it was necessary to select solutions that gave the highest rates for this study. If these solutions show that they are not controlled by the rate of O_2 mass transfer, solutions that give lower rates of NH_3 evolution are also not controlled by the rate of O_2 absorption.   Since it was shown above that solutions with lean CO_2 loading degrade faster than solutions with high CO_2 loading, experiments performed with the Agitated Reactor focused primarily on using MEA solutions with α = 0.15.   Figure 4.11 shows the effect of changing the agitation rate on the NH_3 evolution rate in 7.0 m MEA at 55°C.
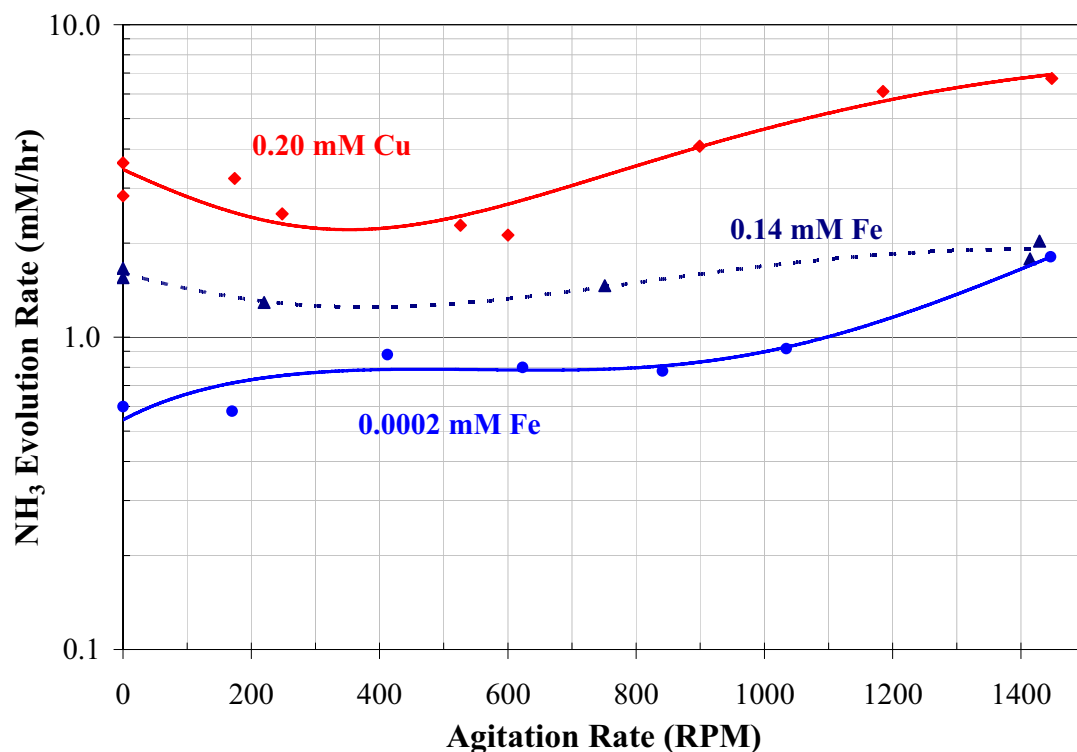
Figure 4.11 Effect of Agitation on the Rate of NH_3 Evolution from MEA Solutions in the Presence of Fe and Cu (α = 0.15, 55°C, 7.0 m MEA, Air, Agitated Reactor)

The data generated in the Agitated Reactor again shows the same trends as the data shown in Figure 4.1 and Figure 4.2, but NH_3 evolution rates are a factor of 2 higher than the data with the Sparged Reactor. The degradation rates increase as the Fe concentration increases and the solutions with copper degrade faster than the solutions with only iron at a fixed agitation rate. For the baseline Fe solution, 0.0002 mM, the NH_3 evolution rate appears to follow the classic curve for mass transfer effects with a reactive system. The degradation rate increases from 0 to 300 RPM and then levels off and shows little effect until around 900 RPM when the rate begins to increase again. This is analogous to the trends discussed in Chapter 2 which illustrate the effect of concentration on overall reaction rates. Below 300 RPM the baseline Fe solution is likely mass transfer controlled, from 300 to 900 RPM the system is controlled by both kinetics and mass transfer, and above 900 RPM the solution shows effects of O_2 mass transfer again. The increase in degradation rates at higher agitation rates will be discussed below.

As the Fe concentration is increased, the degradation rate increases. The solution containing 0.14 mM Fe shows only a weak effect of agitation on degradation rates, but the rate increases by 60% when the agitation rate is increased from 200 to 1400 RPM. This solution appears to show a minimum in NH_3 evolution around 400 RPM, and above this the rate begins to increase just like the solution with lower Fe.

The solution containing 0.20 mM Cu shows the highest NH_3 evolution rates and the most pronounced effect of agitation. As the agitation rate is increased from 0 to 250

RPM the rate of NH_3 evolution decreases. As the agitation is further increased, the degradation rate increases by more than a factor of 3 between 350 and 1400 RPM.

The minimum in the NH_3 evolution rate can easily be explained by the observed fluid mechanics. At low agitation rates, there are actually fewer bubbles in the solution, and the observed mass transfer is less than with no agitation. As the agitation is further increased and the solution begins to vortex, the gas is better dispersed in the amine solution and there are visibly more bubbles with a smaller diameter. At high agitation rates, above 900 RPM, the rate of NH_3 evolution increases for all three solutions. This is likely due to increased back mixing of the gas with the liquid, increasing the gas-liquid contact time and allowing for more O_2 to be absorbed into the amine solution. This again directly supports that the observed rates are in fact measuring the rate of O_2 mass transfer instead of degradation kinetics.

In order to validate the current method of gas phase analysis for determining the degradation rates of MEA, it was necessary to check the effect of time on the degradation rates. Degradation rates were observed over the course of 2 days for several sets of experiments, and showed that time has little or no effect on the degradation rates. The results for iron catalyzed degradation can be seen in Figure 4.12. Again the NH_3 evolution rates show the same dependence on the agitation rates as in Figure 4.11. Over the course of 33 hours, the degradation rate is virtually unaffected since the data appears to be within $\pm$ 0.2 mM/hr, which is within the error of this experiment. This would suggest that degradation products, which accumulate during the course of a run, have no effect on the degradation of MEA.
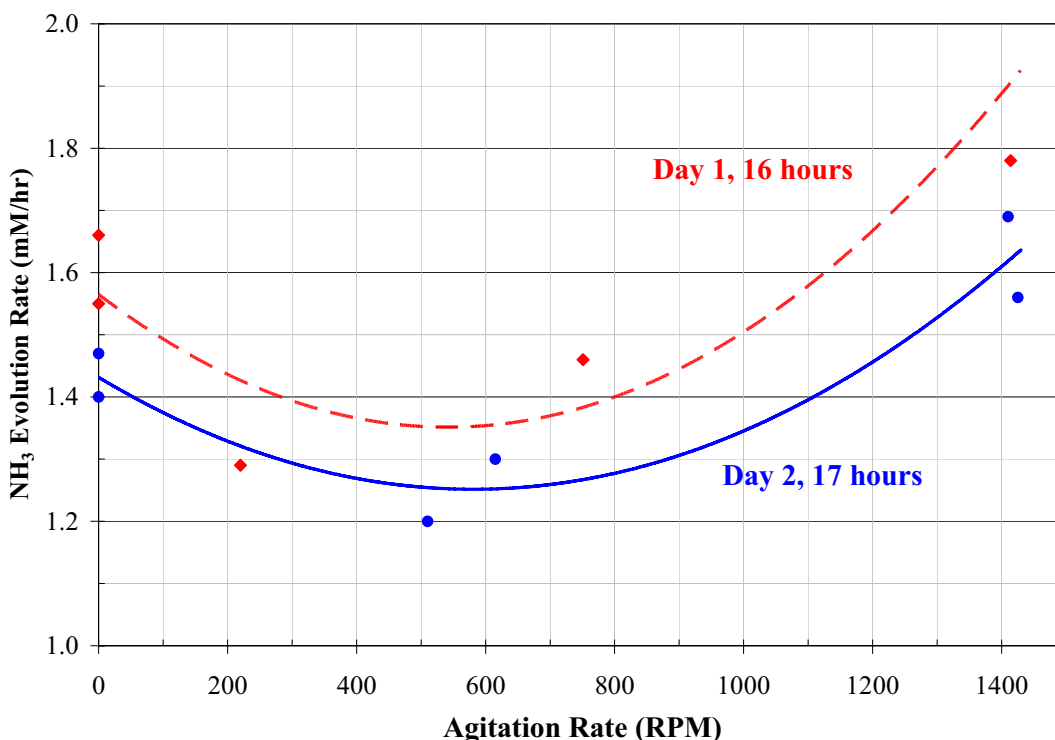
Figure 4.12 Effect of Time on the Rate of NH_3 Evolution from MEA Solutions in the Presence of 0.14 mM Fe ($\alpha = 0.15$, 55°C, 7.0 m MEA, Air, Agitated Reactor)

This is further supported by the data in Figure 4.13, which compares the NH_3 evolution rates during the second day of an experiment where formaldehyde was added to the MEA solution at the beginning of the experiment to an experiment where no formaldehyde was added. Enough formaldehyde was added to approximate the accumulated concentration of formate after one day of operation. Both solutions show a strong effect of agitation on the rate of NH_3 evolution, indicating they are both controlled by the rate of O_2 mass transfer. Since the formaldehyde will oxidize to formate, the primary carboxylic acid degradation product of MEA, this experiment represents a partially degraded solution. Again, there is no difference between the

experiments with and without formaldehyde below 600 RPM. At higher agitation rates, the solution with formaldehyde present appears to give lower NH_3 evolution rates, which could indicate that kinetics begin to be important under these conditions; however, the data point at 1200 RPM could just be an outlier. Additional experiments with formaldehyde are detailed in Chapter 5. The results from Figure 4.13 indicate that the accumulation of degradation products in the amine solution likely has little or no effect on the oxidative degradation rate.
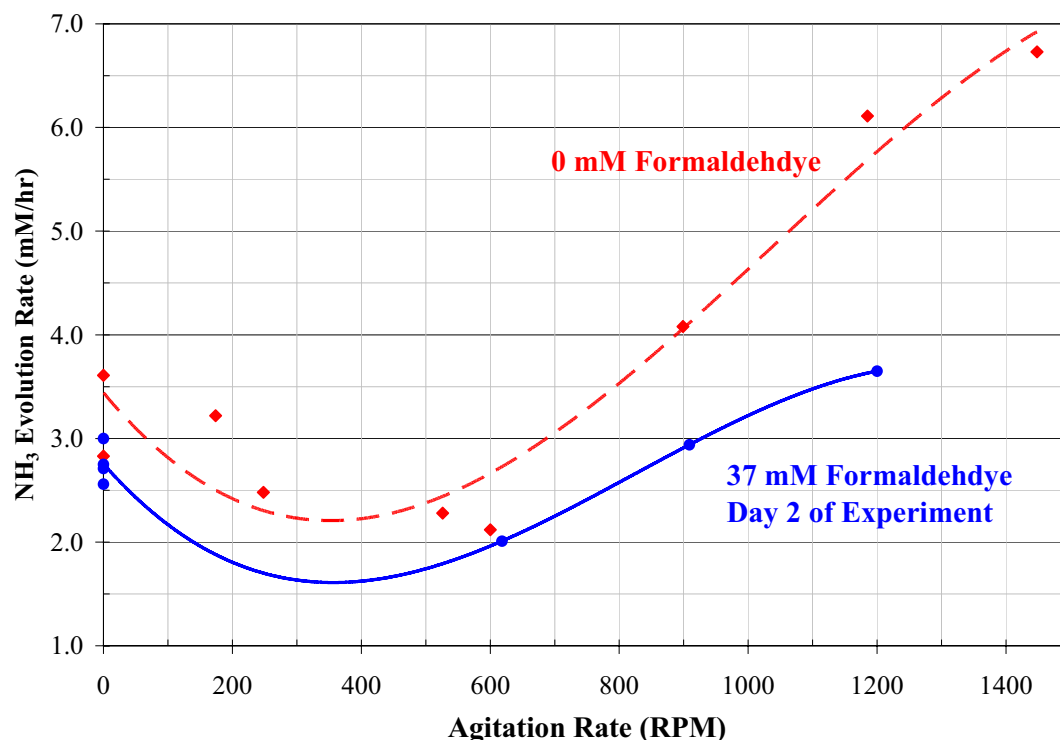
Figure 4.13 Effect of Formaldehyde on the NH_3 Evolution Rate from MEA Solutions ($\alpha = 0.15$, 55°C, 7.0 m MEA, Air, 0.0002 mM Fe, 0.2 mM Cu, Agitated Reactor)

4.2.6. O_2 Partial Pressure and MEA Concentration

In order to further quantify the observed mass transfer phenomenon, experiments were performed to look at the effect of O_2 concentration and MEA concentration on the rate of NH_3 evolution. The results from these experiments are shown in Figure 4.14. For all experiments, the total gas rate was held constant, and air was diluted with N_2 to change the O_2 concentration. If the system is in a region where the rates are controlled by the rate of O_2 mass transfer, the NH_3 evolution rate should have a linear dependence on the O_2 concentration. This is exactly the behavior observed in Figure 4.14 for all amine concentrations.
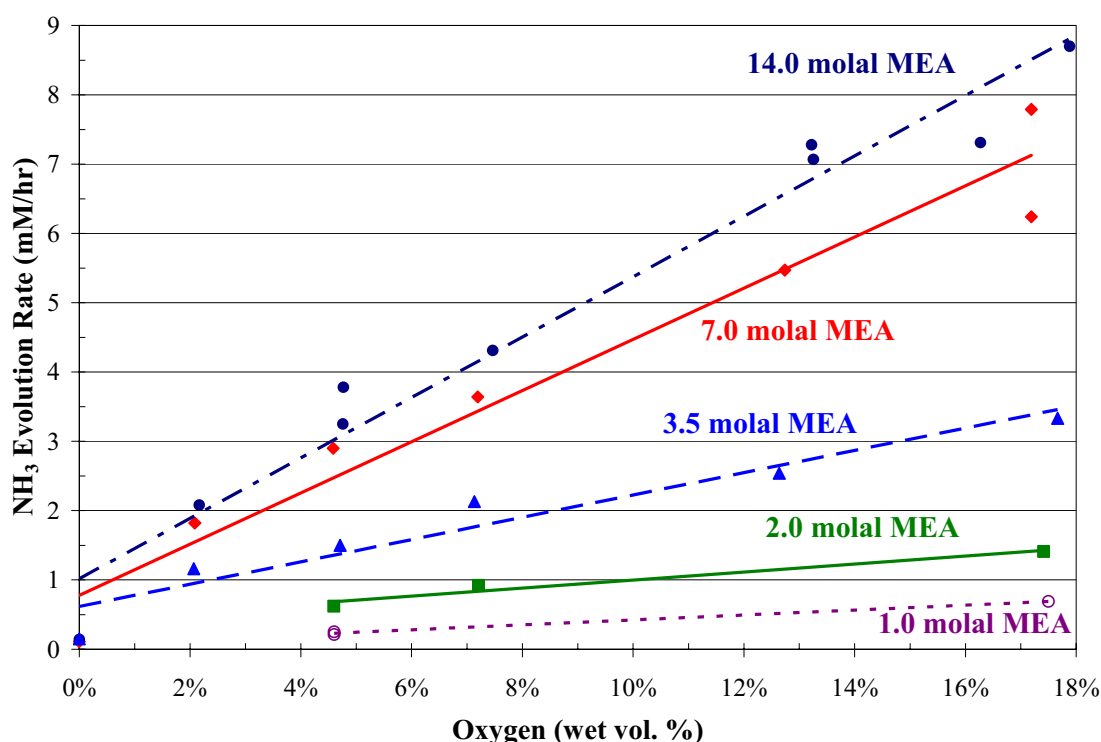
Figure 4.14 Effect of O_2 and MEA Concentrations on the Rate of NH_3 Evolution from MEA Solutions ($\alpha = 0.15$, 55°C, ≤ 0.0002 mM Fe, 0.2 mM Cu, 1400 RPM)

Solutions below 3.5 m MEA show a weaker dependence on the O_2 concentration and could be in the region where the kinetics partially or totally control the rate of NH_3 evolution. Figure 4.15 shows the effect of agitation on several MEA solutions with reduced concentrations of O_2.
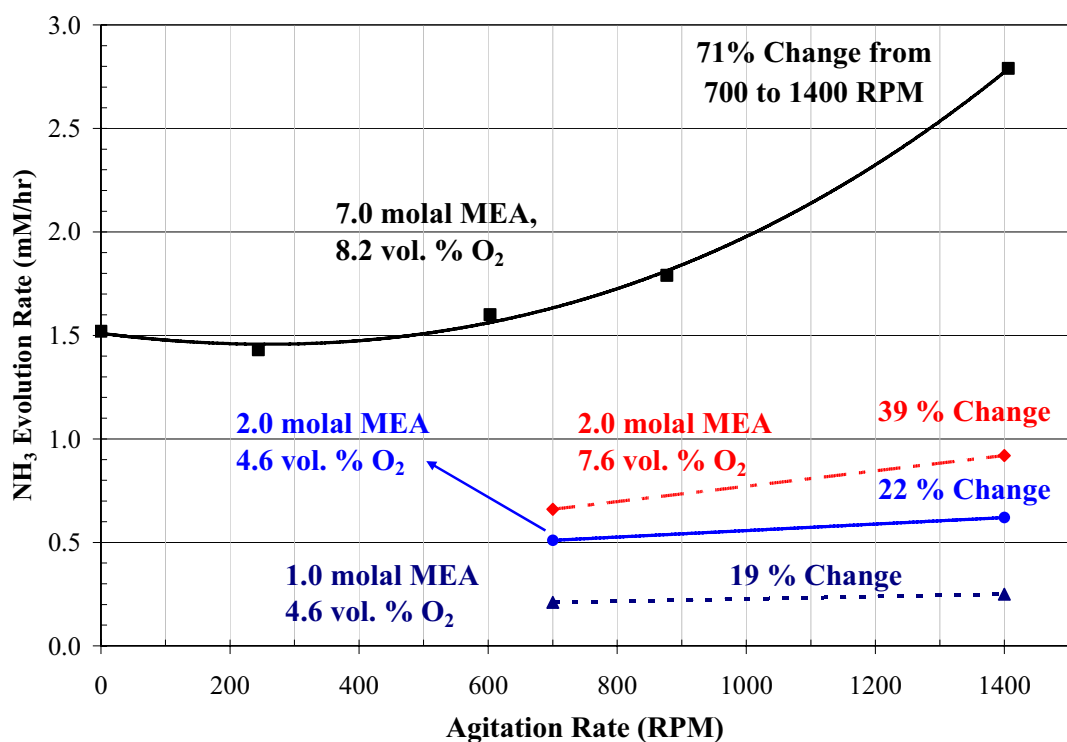
Figure 4.15 Effect of Agitation on NH_3 Evolution from MEA Solutions with Reduced O_2 Concentration ($\alpha = 0.15$, 55°C, ≤ 0.0002 mM Fe, 0.2 mM Cu, Agitated Reactor)

The 7.0 m solution with 8.2 vol. % O_2 (roughly half that of air) still shows a strong dependence on agitation, decreasing by 71% from 1400 to 700 RPM. The 1.0 m and 2.0 m MEA solutions showed a less pronounced effect of agitation on the degradation rates. The 2.0 m MEA solution with 7.6 vol. % O_2 decreased by 39% when the agitation rate changed from 1400 to 700 RPM. The solutions with 4.6 vol. % O_2

104

showed a decrease of 22% and 19% for the 2.0 m and 1.0 m MEA solutions when the agitation rate was changed from 1400 to 700 RPM. This indicates that the 1.0 m and 2.0 m MEA solutions are in a region where the rate of NH_3 evolution is kinetic controlled. The 1.0 m solution in particular shows NH_3 evolution rates approaching the baseline rates observed in this study, indicating that the kinetics are important in these solutions.

MEA solutions below 7.0 m MEA show a dependence on MEA concentration, indicating that they are at least partially controlled by kinetics of the degradation reactions. Solutions below 3.5 molal show a weak dependence on O_2 concentration and agitation rate, indicating that they are likely kinetic controlled. The 3.5 m MEA solution appears to be in the middle of the two regimes. The ionic strength is changing considerably in these solutions between 1.0 and 14.0 m MEA, and it was shown above in Figure 4.8 that ionic strength plays a significant role in O_2 solubility. To test the effect of ionic strength on the 3.5 m MEA solution, 1.6 m NaCl was added to increase the ionic strength of the 3.5 m MEA solution to be equal to the 7.0 m MEA solution. The results of this experiment are shown in Figure 4.16.

The rate of NH_3 evolution was only slightly lower in the 1.6 m NaCl solution, with the exception of the air data point ($O_2 = 17.5\%$) which could be an outlier. If the kinetics are fast enough so that all of the O_2 has reacted before it diffuses into the bulk solution (Diffusion Regime), an increase in the ionic strength, and subsequent decrease in the bulk solution O_2 solubility, should have no effect on the rate of NH_3 evolution.

The slightly lower rates in the 1.6 m NaCl can be explained by a decrease in the the Henry's constant of O_2 (Equation 2.3). Since the solutions do show a dependence on the bulk gas phase concentration of O_2 and the MEA concentration, this indicates that both kinetics and O_2 mass transfer contribute to the rate of NH_3 evolution in the 3.5 m MEA solutions.
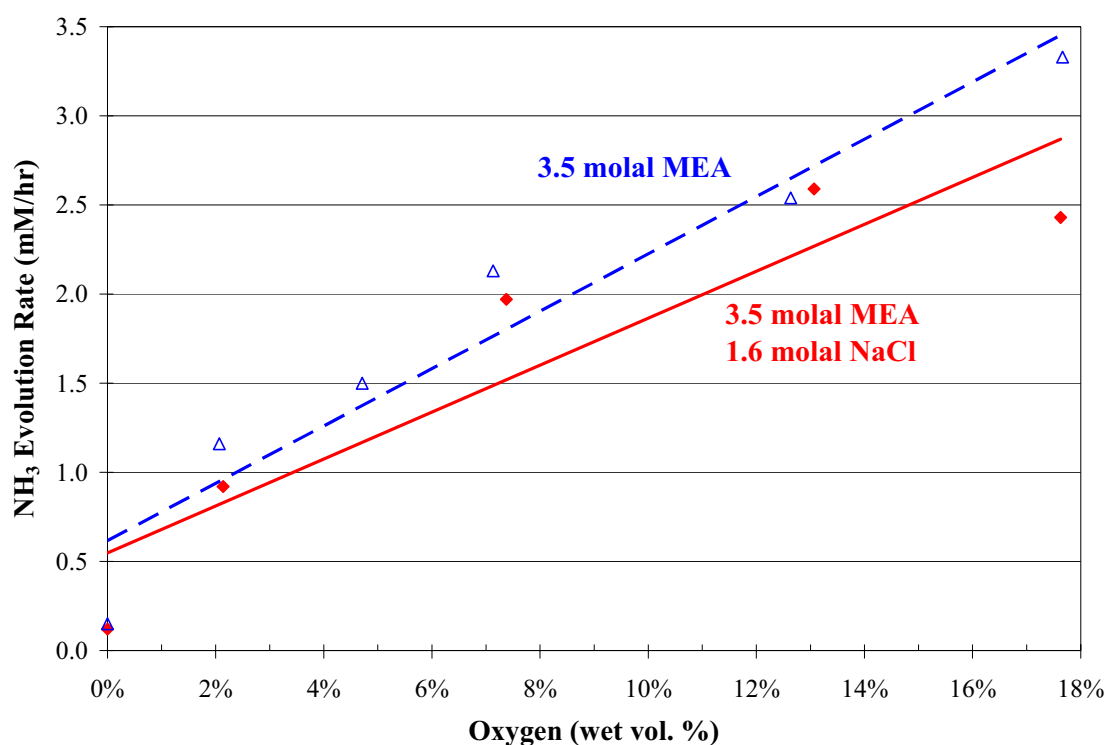
Figure 4.16 Effect of Ionic Strength on NH_3 evolution from a 3.5 m MEA Solution ($\alpha = 0.15$, 55°C, ≤ 0.0002 mM Fe, 0.2 mM Cu, 1400 RPM)

Solutions with high MEA concentrations (7.0 m and 14.0 m) showed degradation rates that would indicate they are in the regime controlled by mass transfer rates only. At low amine concentrations, the ionic strength is low and O_2 is more soluble and has a higher diffusion coefficient, suggesting that the degradation rates are

106

controlled by kinetics. At high amine concentrations, the ionic strength goes up and the diffusion coefficient goes down, resulting in lower O_2 solubility. This suggests that at high MEA concentrations, the degradation rates are controlled by the rate of O_2 mass transfer. For solutions of intermediate MEA concentrations, around 3.5 m MEA, the degradation rates show some dependence on agitation as well as MEA and O_2 concentration, indicating that the oxidative degradation rate depends on both the rate of O_2 mass transfer and the degradation kinetics.

4.3. Comparison with Previous Degradation Studies

Previous oxidative degradation studies have all been interpreted as being kinetic controlled. Based on the data presented above, the degradation process is likely controlled by the rate of O_2 mass transfer and not kinetics; therefore, the results from previous studies need to be re-evaluated to determine if they also support this finding. In order to do this, several key degradation studies will be compared to the current work.

Most of the previous studies performed long term degradation studies at low gas rates relative to the volume of amine solution. Primarily, analysis was done on the liquid solution instead of analyzing for NH_3 in the gas. Since the degradation rates are relatively slow, and liquid analysis is complicated, the experiments take a long time to accumulate enough of the degradation products to make an accurate measurement. Additionally, the previous degradation studies were performed at inconsistent conditions, i.e. various amine concentrations, temperatures, and gas compositions.

While all of the experiments used loaded MEA solutions, the value of the CO_2 loading also varied. In order to compare these various studies on the same basis, mass transfer coefficients for each study were estimated.

Recall from Chapter 2 that for a reacting system that is controlled by the rate of mass transfer, the rate of O_2 absorption/consumption can be determined using Equation 4.2 below.

$$\text{Rate of } O_2 \text{ Consumption} = \frac{K_G aV}{H_{O_2}}(P_{O_2} - P_{O_2}^*) \qquad 4.2$$

If the kinetics are fast enough that the bulk concentration of O_2 is negligible, Equation 4.2 reduces to Equation 4.3:

$$\text{Rate of } O_2 \text{ Consumption} = \frac{K_G aVP_{O_2}}{H_{O_2}} \qquad 4.3$$

Since all of the previous studies report both degradation rates and oxygen partial pressure, a comparison between studies can be made by using an apparent overall gas phase mass transfer coefficient K_G', shown below, and the space time (liquid volume / gas flow rate). A comparison of some of the key parameters from these studies can be found in Table 4.4.

$$K_G' = \frac{(\text{Rate of } O_2 \text{ Consumption})}{P_{O_2}} = \frac{K_G aV}{H_{O_2}} = \text{Apparent Mass Transfer Coefficient} \qquad 4.4$$

With the exception of the current study, all of the studies in Table 4.4 were performed by sparging a gas through the amine solution with no additional agitation.

The studies by Hofmeyer, Chi and Rochelle, Goff and Rochelle, and the Current Study analyzed the outlet gas for NH_3 evolution instead of doing liquid analysis, while the rest of the studies used some kind of liquid analysis and were long term degradation studies.

Table 4.4 Comparison of Key Parameters for Various Experiments Measuring the Oxidative Degradation of MEA

Study	T (°C)	MEA (m)	Reaction Gas	Liq. Vol. (L)	Space Time (min)	Rate (mM/hr)	K_G' (mM/hr-bar)
(Rooney et al. 1998)	82	5.4	Air	1.0	181.82	0.03 – 0.07	0.2 - 0.4
(Blachly and Ravner 1964)	55	5.4	Air	0.3	1.00	0.02 – 0.14	0.1 - 0.8
(Girdler Corporation 1950)	80	3.1	50% O_2	0.1	1.00	0.36 – 1.32	0.7 - 2.6
(Hofmeyer et al. 1956; Lloyd 1956)	75	5.4	Pure O_2	0.2	0.35	5.00	5.0
(Chi and Rochelle 2002)	55	7.0	Air	0.4	0.05	0.10 – 2.32	0.6 - 12.9
(Goff and Rochelle 2003)	55	7.0	Air	0.3	0.04	0.48 – 5.00	2.7 - 27.8
Current Study	55	7.0	Air	0.5	0.06	0.25 – 8.25	1.4 - 45.8

Space Time = Liquid Volume/Gas Flowrate
K_G' = Apparent Mass Transfer Coefficient = Rate/P_{O_2}
    this assumes no dissolved O_2 in the bulk liquid

In order to compare the mass transfer characteristics of the various studies, one can compare the space time and the apparent mass transfer coefficient, K_G', for each of the experiments. Simply speaking, at low space times, the system should have a relatively high amount of agitation and mixing, and therefore a higher value of K_G'. Conversely, at high space times, the gas is very slowly sparged through the solution, and there is likely minimum mixing and agitation, resulting in much lower values of

K_G'. While it is recognized that most of the methods for predicting mass transfer coefficients in gas-liquid contactors depend on the superficial gas velocity (Gaddis 1999; Van't Riet 1979), the space time was used in the current analysis since the geometry of the degradation reactor was not reported in any of the compared studies.

Figure 4.17 shows that the apparent mass transfer coefficient does in fact correlate with the space time for the studies in Table 4.4, and that K_G', the apparent mass transfer coefficient, depends on the square root of the space time. All of the studies fit this trend with the exception of the current study. This is easily explained as the current study uses additional agitation which accounts for the much higher values of K_G' at a space time similar to the studies by Chi and Rochelle and Goff and Rochelle.

All of the previous studies report degradation rates lower than those reported in the current study under conditions with smaller values of K_G'. As the space time increases, K_G' decreases, and the degradation rate goes down. This is consistent with the assumption that the experiments are operating in the mass transfer controlled regime. Since it is clear that all of the previous experiments had smaller degradation rates than the current study, which was shown above to be O_2 mass transfer limited, and had larger space velocities and smaller values of K_G', the data suggests that all of these previous studies were also performed under conditions that were actually measuring the rate of O_2 mass transfer and not the kinetics of MEA degradation.
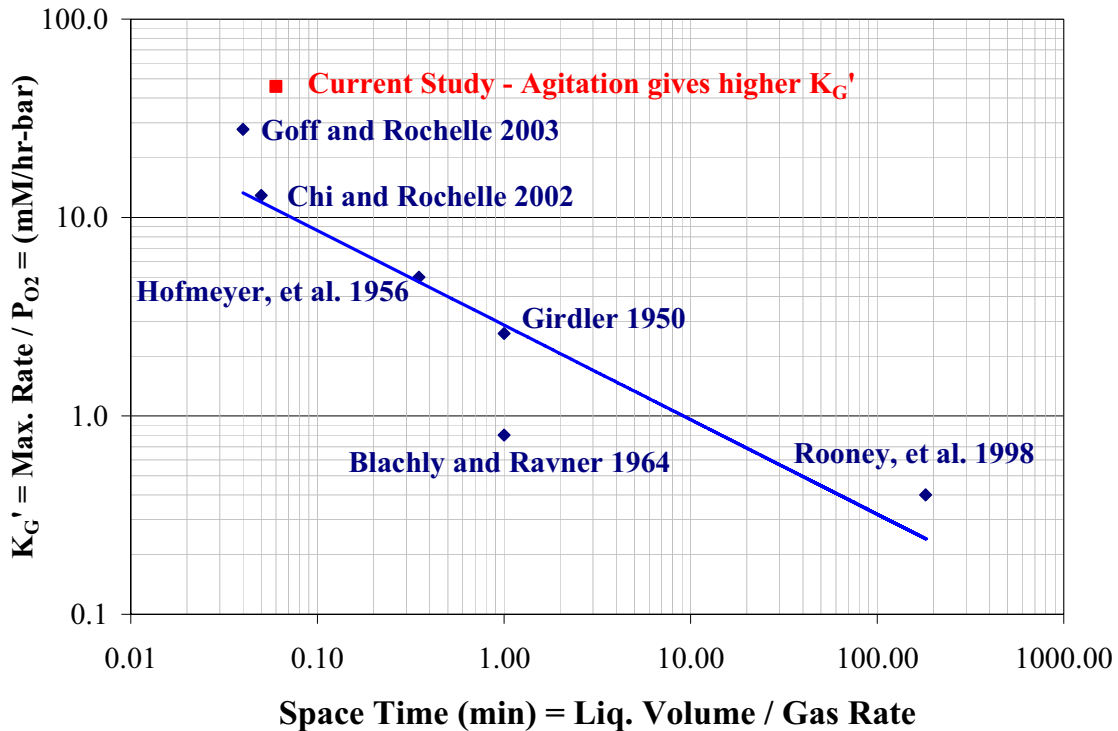
Figure 4.17 Correlation of Space Time and the Apparent Mass Transfer Coefficient, K_G', from Various Studies on the Oxidative Degradation of MEA Using Sparged or Agitated Reactors

4.4. Estimation of Industrial Degradation Rates

As a final verification that the oxidative degradation of MEA is controlled by the rate of O_2 mass transfer instead of the degradation kinetics, a comparison of predicted degradation rates for an industrial application was made with literature values of observed degradation rates. In order to make this calculation, details of the physical performance of an absorber column must be known. The information for this calculation came from the base case of the rigorous model developed by Freguia for modeling CO_2 removal from flue gas using MEA (Freguia 2002).

The calculations were made assuming 85% CO_2 removal from a flue gas containing 3% CO_2 and 5% O_2 on a wet volume basis. The solvent was a 7.0 m MEA solution, and the absorber operated with a lean CO_2 loading of 0.15 and a rich loading of 0.40. The column had 15.2 m (50 ft.) of stainless steel CMR#2 packing, and operated at atmospheric pressure. The absorber operated with a nominal temperature of 55°C, and the superficial liquid and gas velocities were 8.7×10^3 kg/m^2-hr and 10.8×10^3 kg/m^{2}hr respectively. In order to complete the estimation of the degradation rates, the following assumptions were made:

- Degradation occurred only in the absorber packing. No degradation occurs in the absorber sump.

- The bulk liquid O_2 concentration was negligible. This assumed fast reaction kinetics, but not fast enough to have enhanced mass transfer. This represented a worst case scenario for fast kinetics, as this gave the largest possible partial pressure driving force, and the O_2 consumption rate was then estimated by Equation 4.3.

- Mass transfer coefficients and wetted packing area were estimated using the method of Onda in order to calculate the performance of the packing (Onda et al. 1968).

- Calculations were performed using the average physical properties of the amine solution (i.e. $\alpha = 0.275$ and 55°C). The viscosity and density of the amine solution was estimated using the correlations by Weiland (Weiland

112

1996) and the surface tension of MEA was calculated from data gathered by Vazquez et al. (Vazquez et al. 1997).

- Since no literature data could be found on the diffusivity of O_2 in aqueous solutions of MEA, the diffusion coefficient was estimated using the Wilke-Chang Equation and the average physical properties of the solvent and was calculated to be 2.98×10^{-6} cm^2/sec (Seader and Henley 1997).

- Physical solubility of O_2 in the amine solution was assumed to be the same as the solubility in water, 1116 L-atm/mol (Dean 1992). The Henry's Constant was then corrected for the effect of ionic strength on the physical solubility to 1436 L-atm/mol, using the values of the van Krevelan Constants for aqueous MEA species (Weiland 1996).

- In order to calculate the total degradation rate, the amount of liquid holdup in the packing was estimated to be 4.7% using the correlation developed by Billet and Schultes (Billet 1997).

Based on these assumptions, a fractional liquid holdup of 4.7% was calculated, which gave a liquid residence time of 5.1 minutes in the packing. The calculation also estimated that the packing yields a total of 18.7 overall liquid transfer units, or a height equivalent of a theoretical plate (HETP) of 0.82 m. These estimates all fall within the expected values for the design of a CO_2 absorber system, and therefore should provide an accurate estimate of the performance of the absorber.

Using the mass transfer coefficients estimated from the above calculation, the rate of O_2 absorption is 7.1 mM/hr. In order to relate the O_2 absorption to MEA loss,

the stoichiometry must be known. As stated previously, the actual stoichiometry for the MEA system is not known, so we can estimate a range of degradation rates based on the O_2 stoichiometry from Chapter 2. Using a stoichiometry range of 0.5 to 2.5 moles of O_2 per mole of MEA, the MEA loss is somewhere between 2.9 and 14.2 mmol MEA/L_{holdup}-hr. Multiplying this by the total estimated amount of liquid holdup gives a MEA degradation rate of 0.29 to 0.73 kg MEA/mton CO_2 captured. In economic terms, this amounts to $0.40 to $2.00 per mton CO_2 captured assuming a price of $1.48/kg MEA (CMR 2003).

The degradation rate estimated for the physical absorption of O_2 in an amine scrubber unit is approximately the same as the observed rates in the current experimental study. One literature value reports a degradation rate of 3.6 kg MEA per mton CO_2 captured (Arnold et al. 1982). This value is reported for CO_2 capture using a 5.4 m MEA solution (20 wt. %), and is much higher than the estimated degradation rates because it includes MEA losses from other types of degradation, evaporative losses, spills, etc. A more recent estimate of degradation losses for the same solvent is 0.45 kg MEA per mton CO_2 captured for the same solvent system (ABB 1998). It should also be noted that the literature values of MEA degradation also include MEA loss from the formation of heat stable salts from the reaction of MEA with SO_2 in the flue gas. The solvent loss associated with heat stable salt formation is not insignificant; therefore, the rate of MEA loss due to the oxidative degradation of the solvent can be significantly less than what is reported as the total solvent makeup rate.

Literature values for MEA solvent makeup in industrial applications are either within or larger than the rates predicted when assuming physical absorption of O_2 into MEA. This would suggest that the oxidative degradation of MEA is controlled by the rate of O_2 absorption and not the kinetics of the degradation reactions in an industrial process. Additionally it would suggest that the O_2 is not completely depleted in the bulk solution since this assumption causes an over-estimation of the degradation rates.

4.5. Conclusions

Experiments were performed in both the Sparged Reactor and the Agitated Reactor to quantify the effect of catalyst concentration (both Cu and Fe), MEA concentration, gas phase O_2 concentration, CO_2 loading, pH, and agitation on the rate of NH_3 evolution from MEA solutions at 55°C. Results from these experiments show that the oxidative degradation of MEA can be O_2 mass transfer limited under laboratory conditions. Under some experimental conditions the rate of NH_3 evolution depends on only kinetics or O_2 mass transfer, and under other conditions the rate shows effects of both kinetics and O_2 mass transfer.

In general, the rate of NH_3 evolution increased as the agitation rate was increased, and also increased linearly with increasing O_2 concentration. At low concentrations of catalyst (less than 0.5 mM Fe or Cu) and MEA (less than 2.0 molal), the rate of NH_3 evolution was controlled by the degradation kinetics. At high concentrations of catalyst (above 0.5 mM Fe or Cu) and MEA (above 7.0 m) the rate of

NH$_3$ evolution was controlled by the rate of O$_2$ mass transfer. Solutions between 2.0 and 7.0 m MEA showed effects of both O$_2$ mass transfer and degradation kinetics.

The rate of NH$_3$ evolution increases when the concentration of dissolved Fe and Cu are increased, and the rate is less than first order with respect to catalyst concentration. In the Sparged Reactor, it was observed that kinetics controlled the rate of NH$_3$ evolution for concentrations of Fe below 0.2 mM regardless of Cu concentration. Above 0.2 mM Fe the rates were independent of Fe concentration, indicating the rate is limited by the rate of O$_2$ absorption. The rate of NH$_3$ evolution shows a stronger dependence on Cu concentration than iron concentration, which can be attributed to a change in the overall O$_2$ stoichiometry from the Fe system, the rate limiting reaction step, or the reaction mechanism itself.

Solutions with lean CO$_2$ loading, $\alpha = 0.15$, degrade 1.5 to 2 times faster than solutions with rich CO$_2$ loading, $\alpha = 0.40$. Unloaded MEA solutions degrade faster than the rich solutions but slower than the lean solutions. MEA solutions partially neutralized with H$_2$SO$_4$ show that as the ratio of protonated MEA to MEA increases the rate of NH$_3$ evolution decreases. Solutions of SO$_4$ loaded MEA with the same MEAH$^+$/MEA ratio as CO$_2$ loaded MEA solutions showed a slower rate of NH$_3$ evolution. This indicates that while the free MEA is likely the degrading species in solution, the presence of the MEA carbamate appears to increase the rate of NH$_3$ evolution.

The mass transfer capability of the Sparged Reactor was quantified by measuring the rate of sulfite oxidation in concentrated MgSO$_4$ (aq.) solutions. This

solvent system was chosen because the viscosity, surface tension, and O_2 solubility closely match the properties of loaded MEA solutions. Results from these experiments show that given the factor of 5 uncertainty in the O_2 stoichiometry of the MEA system, the observed NH_3 evolution rates are on the same order as the O_2 absorption rates in the sulfite experiments. This further suggests that the degradation rates are at least partially controlled by O_2 mass transfer and not the kinetics of the amine solution. In order to attempt to measure NH_3 evolution rates under kinetic controlled conditions, a new reactor system was built with artificial agitation of the amine solution.

Experiments in the Agitated Reactor showed the same trends as the experiments with the Sparged Reactor, but the NH_3 evolution rates were approximately twice as high for the same catalyst concentrations. This increase in NH_3 evolution rates from the Sparged Reactor to the Agitated Reactor with solution of the same catalyst concentration can only be explained by O_2 mass transfer limitations in the Sparged Reactor. Experiments with Cu alone showed that the NH_3 evolution rate appeared to be controlled by oxidation kinetics below 0.6 mM Cu. The rate was controlled by O_2 mass transfer between 0.6 and 3.0 mM Cu, and above this the system enters the Fast Reaction Regime where the reactions take place primarily in the liquid film.

Experiments in the Agitated Reactor showed that as the agitation rate increases, the rate of NH_3 evolution increases with both Fe and Cu catalyzed solutions. The Cu catalysis resulted in significantly higher degradation rates, which again can be explained by a change in the O_2 stoichiometry. The O_2 stoichiometry for these systems was never verified independently, and was beyond the scope of this project. Since increasing the

agitation rate increases the rate of NH_3 evolution, this indicates that oxidative degradation is at least partially controlled by the rate of O_2 mass transfer.

The addition of formaldehyde to the MEA solution does not significantly change the rate of NH_3 evolution over a 2 day experiment when compared to solutions without formaldehyde. This indicates that the accumulation of formate in the MEA solution does not significantly affect the oxidative degradation of MEA.

Additional experiments in the Agitated Reactor examined the effect of MEA concentration and O_2 concentration on the rate of NH_3 evolution in lean loaded solutions catalyzed by 0.20 mM Cu. MEA solutions ranging from 1.0 m to 14.0 m show a linear dependence on the O_2 concentration up to 17 vol. %, following the expected trend if the rate of NH_3 evolution is O_2 mass transfer limited. MEA solutions below 7.0 m show a dependence on MEA concentration. Solutions between 2.0 m and 7.0 m appear to show effects of both O_2 mass transfer and kinetics on the rate of NH_3 evolution. Solutions with 1.0 m MEA show only a weak dependence on both agitation and O_2 concentration, indicating that kinetics dominate the rate of NH_3 from these solutions.

Since the current study shows the experimentally observed degradation rates are partially or completely controlled by the rate of O_2 absorption over a range of significant conditions, previously published investigations were re-examined to determine if they too were actually reporting the rate of O_2 absorption instead of degradation kinetics. In order to compare studies that differed in experimental conditions on the same basis, apparent mass transfer coefficients (calculated by taking

the maximum reported rate and normalizing by the gas O_2 concentration) were correlated with the gas space time (liquid volume / gas rate). The results showed that the both the Sparged Reactor and Agitated Reactor had higher apparent mass transfer coefficients and reported higher degradation rates than any of the previous studies. Since the current work is O_2 mass transfer limited, data suggests that all of these previous studies were also performed under conditions that were actually measuring the rate of O_2 mass transfer and not the kinetics of MEA degradation.

As a final verification that the oxidative degradation of MEA is controlled by the rate of O_2 mass transfer instead of the degradation kinetics, a comparison of predicted degradation rates for an industrial application was made with literature values of observed industrial degradation rates. Estimates were made using a rigorous AspenPlus simulation developed by Freguia for CO_2 absorption from flue gas using MEA. Oxidative degradation rates of MEA in industrial applications are predicted to be 0.29 to 0.73 kg MEA/mton CO_2. This was estimated assuming the rate of O_2 absorption limited the degradation rates and that degradation only occurred in the packing of the absorber. Reported industrial makeup rates are within or greater than the estimated range of degradation rates for O_2 mass transfer limited degradation. Since reported MEA makeup rates match the rates predicted by assuming an O_2 mass transfer limitation, this indicates that MEA degradation is likely determined by the rate of O_2 absorption under typical industrial conditions.

Chapter 5: Inhibitors for Oxidative Degradation

This chapter details the experimental results for a number of additives tested to inhibit the oxidative degradation of MEA using the Agitated Reactor. In addition, observations on heats of reactions, solution color, and trends of other gas phase degradation products are included.

5.1. Inhibitor Screening

In Chapter 4 it was shown that the oxidative degradation of monoethanolamine is likely controlled by the rate of O_2 absorption under typical conditions in a flue gas treating application. This finding influences the way degradation can be inhibited in an industrial process: instead of making process modifications, an additive can be added to the solution to further decrease the reaction rates. A scavenger could be added to the solution to either react competitively with O_2 or to react with another free radical or intermediate in the reaction mechanism. The scavenger must react faster with O_2/free radicals than MEA. The second method of inhibition is to add a chelating agent to bind with the dissolved metals and prevent them from participating in the reaction

mechanism. The final method of inhibition involves salting out the O_2. Gases generally have decreasing solubility in aqueous solutions as the ionic strength increases, so the addition of a stable salt could effectively reduce O_2 solubility and the rate of absorption.

Table 5.1 shows the compounds examined in this study categorized by O_2 scavengers and reaction inhibitors, chelating agents, and stable salts. Only three compounds were successful at inhibiting the oxidative degradation of MEA at concentrations low enough to be suitable for an industrial application: one reaction inhibitor, Inhibitor A, and two O_2 scavengers, Na_2SO_3 and formaldehyde.

Table 5.1 Additives Screened for Inhibiting the Oxidative Degradation of MEA.

O_2 Scavengers and Reaction Inhibitors		Chelating Agents	Stable Salts
Quinone	Manganese Salts	EDTA	Potassium Chloride
Ascorbic Acid	Inhibitor A	(ethylene-diamine-tetra-acetic acid)	Potassium Bromide
Na_2SO_3		Sodium Phosphate	Potassium Formate
Formaldehyde		Na_2S_4	

Screening experiments were first performed under conditions that gave the highest observed degradation rates in a single metal system, i.e. 7.0 m MEA, 0.20 mM Cu, $\alpha = 0.15$ mol CO_2 / mol MEA, 1400 RPM. Successful inhibitors were then tested over a range of conditions including Fe concentration. Results are presented normalized to the baseline degradation rate of 0.15 mM/hr, which represents the lowest degradation rate achievable (refer to Figure 3.13). Table 5.2 shows a comprehensive list of experiments performed during the inhibitor study; detailed analysis for each experiment can be found in Appendix G.

Table 5.2 Degradation Inhibitor Experiments (7.0 molal MEA, 55°C, 1400 RPM)

Date	Inhibitor	α	Metal	Comments
01/28/04	Na$_2$SO$_3$	0.15	Cu	
01/29/04	Na$_2$SO$_3$	0.15	Cu	Continuation of 01/28/04
02/05/04	Na$_2$SO$_3$	0.15	Cu	
02/06/04	Na$_2$SO$_3$	0.15	Cu	Continuation of 02/05/04
02/09/04	Na$_2$SO$_3$	0.15	Cu	
02/20/04	Na$_2$SO$_3$	0.15	Cu	Some problems with mist eliminator
02/21/04	Ascorbic Acid / Inhibitor A	0.15	Cu	AA was possible catalyst
02/23/04	Inhibitor A	0.15	Cu	
02/27/04	Na$_2$SO$_3$	0.40	Cu	
03/16/04	Inhibitor A	0.40	Cu	
03/22/04	Inhibitor A	0.40	Cu	
07/06/04	KBr / KBrO$_3$	0.15	Cu	
07/07/04	KCl	0.15	Cu	
07/08/04	MnSO$_4$	0.15	Cu	Solid formation. Clean with EDTA
07/12/04	MnSO$_4$	0.15	Cu	
07/14/04	KMnO$_4$	0.15	Cu	
07/19/04	EDTA	0.15	Cu	
07/21/04	KHCO	0.15	Cu	
07/22/04	KHCO	0.15	Cu	Continuation of 07/21/04
07/26/04	Quinone	0.15	Cu	
07/28/04	Formaldehyde	0.15	Cu	MEA + Formalin for stock soln.
07/29/04	Formaldehyde	0.15	Cu	Continuation of 07/28/04
07/31/04	Inhibitor A	0.15	Cu	
08/02/04	Inhibitor A	0.15	Cu	Continuation of 07/31/04
08/04/04	K$_3$PO$_4$	0.15	Cu	
08/07/04	Inhibitor A	0.15	Cu	
08/08/04	Inhibitor A	0.15	Cu	Continuation of 08/07/04
08/09/04	Inhibitor A	0.15	Cu	
08/10/04	Inhibitor A	0.15	Cu	Continuation of 08/09/04
08/12/04	MnSO$_4$	0.15	Cu	
08/13/04	MnSO$_4$	0.15	Cu	Continuation of 08/12/04
08/19/04	Inhibitor A	0.15	Cu	Use new KI instead of old KI
08/20/04	Inhibitor A	0.15	Cu	Continuation of 08/19/04
08/24/04	MnSO$_4$	0.15	Cu	Middle conc. Range for Mn.
08/25/04	MnSO$_4$	0.15	Cu	Continuation of 08/24/04
10/25/04	Inhibitor A	0.15	Fe	
10/26/04	Inhibitor A	0.15	Fe	Continuation of 10/25/04
11/01/04	Inhibitor A	0.40	Fe	
11/02/04	Inhibitor A	0.40	Fe	Continuation of 11/01/04
12/01/04	Formaldehyde	0.15	Fe	
12/02/04	Formaldehyde	0.15	Fe	Continuation of 12/01/04
12/07/04	Inhibitor A	0.15	Fe	
12/08/04	Inhibitor A	0.15	Fe	Continuation of 12/07/04
1/10/05	Inhibitor A / Formaldehyde	0.15	Fe	
1/11/05	Inhibitor A / Formaldehyde	0.15	Fe	Continuation of 1/10/05
1/13/05	Inhibitor A / Formaldehyde	0.15	Fe	
1/14/05	Inhibitor A / Formaldehyde	0.15	Fe	Continuation of 1/13/05
1/24/05	Na$_2$SO$_3$	0.15	Fe	
1/31/05	Inhibitor A	0.15	Fe & Cu	

5.2. O_2 Scavengers and Reaction Inhibitors

5.2.1. Inhibitor A

Inhibitor A is an inorganic additive that effectively inhibits oxidative degradation. Results from the Inhibitor A experiments can be seen in Figure 5.1, where the solid lines represent lean solutions with $\alpha = 0.15$ mol CO_2/mol MEA and the dashed lines represent rich solutions with $\alpha = 0.40$. As the concentration of Inhibitor A increases, the NH_3 production decreases for all of the solutions. Rich solutions show a lower NH_3 evolution rate and are more easily inhibited than lean solutions. Solutions containing dissolved Cu also show higher degradation rates than solutions with dissolved Fe and are more easily inhibited by Inhibitor A. With Cu solutions, the NH_3 evolution is reduced to 1.5 times the baseline rate at 9 mM Inhibitor A with rich solutions and 2.3 times the baseline rate at 280 mM Inhibitor A with lean solutions. The Fe solutions are reduced to 1.5 times the baseline rate at 100 mM Inhibitor A with rich solutions and 3.7 times the baseline rate at ~ 270 mM Inhibitor A with lean solutions. When the concentration of Inhibitor A is increased by an order of magnitude in the lean solutions, this amounts to a factor of 5.6 decrease in degradation for the Cu solutions and 2.8 for the Fe solutions.

Inhibitor A is not expected to degrade; therefore, it will not need to be continuously fed to the process. This makes Inhibitor A an attractive additive for industrial applications. Since the effectiveness of Inhibitor A depends on both the catalyst present and the concentration of MEA (represented here as CO_2 loading), this

additive functions as a reaction mechanism inhibitor. Additionally, available literature suggests that there is no mechanism by which Inhibitor A could act as an O_2 scavenger. The concentrations used for Inhibitor A are less than 5 wt. %, making this inhibitor a viable additive to MEA solutions for industrial applications.
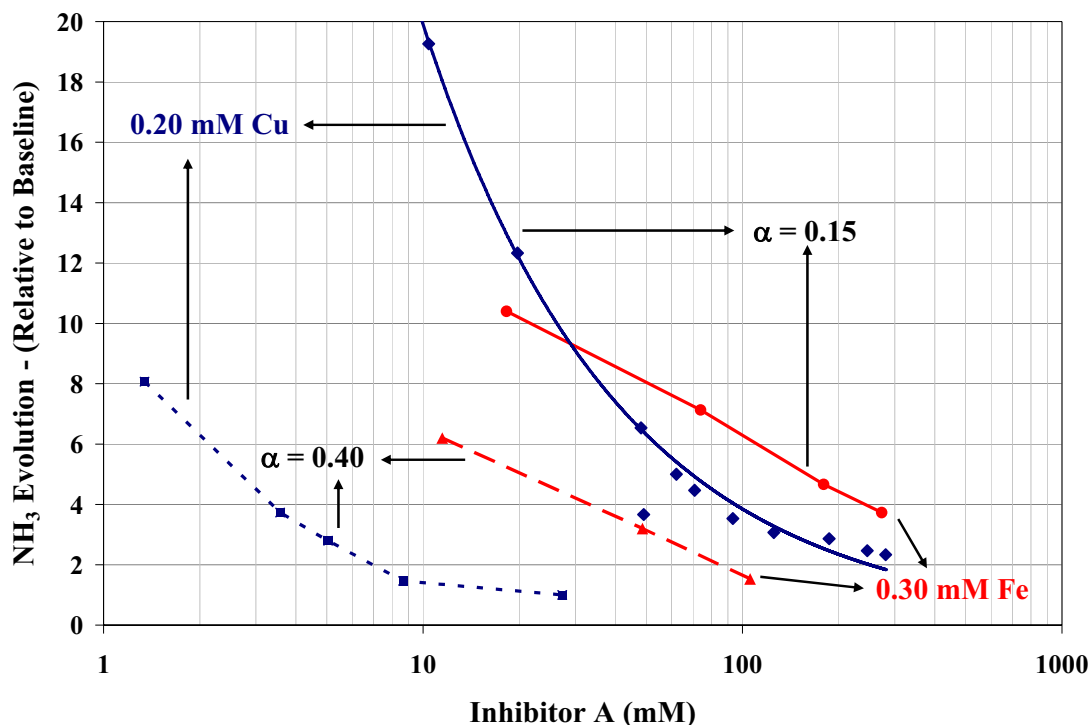
Figure 5.1 Effect of Inhibitor A on the Oxidative Degradation of MEA in the Presence of Copper or Iron (55°C, 7.0 m MEA, 1400 RPM, Baseline = 0.15 mM/hr)

Since Cu is added to the MEA process to inhibit corrosion, both Cu and Fe will be present in solution in industrial applications. Any degradation inhibitor added to this process needs to be effective in the presence of both Cu and Fe and should not interfere with Cu inhibiting the corrosion of carbon steel. Figure 5.2 shows the results of the

three different systems, Cu by itself, Fe by itself, and Cu and Fe mixed, with lean CO_2 loadings.
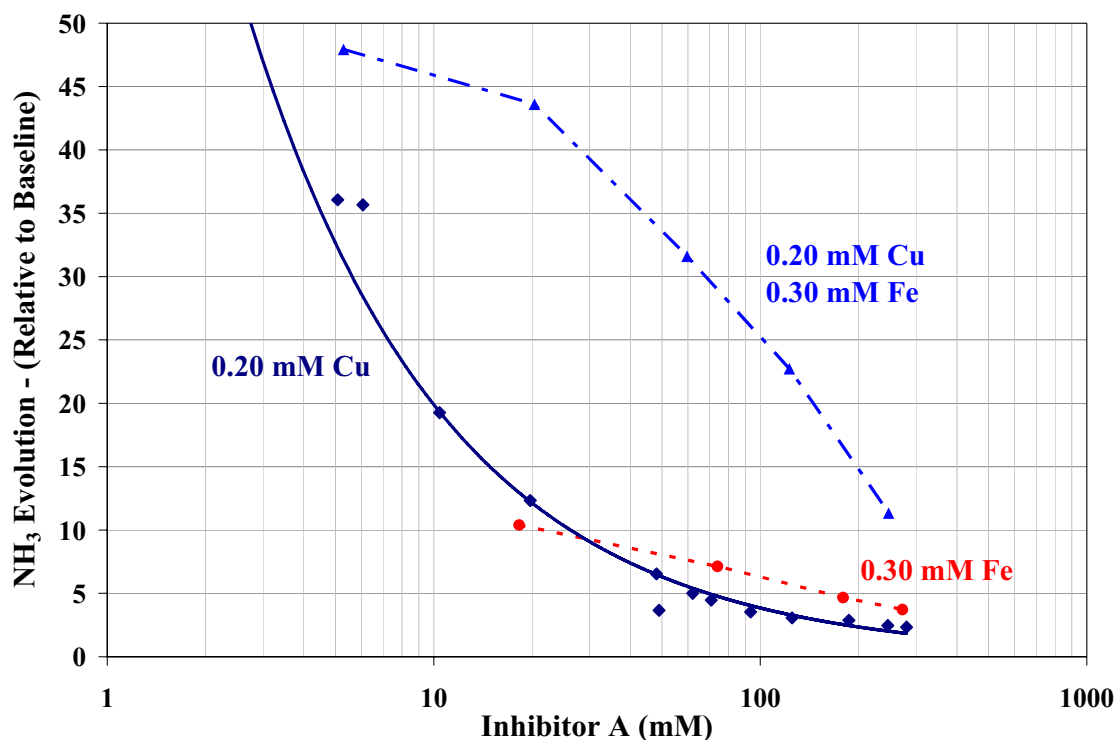
Figure 5.2 Effect of Inhibitor A on the Oxidative Degradation of MEA with both Copper and Iron (55°C, 7.0 m MEA, $\alpha = 0.15$, 1400 RPM, Baseline = 0.15 mM/hr)

The system with the mixed metals shows a higher degradation rate at each concentration of Inhibitor A than either system with only one metal. Inhibitor A is also less effective with the mixed system than the Cu only system, as shown by the shallower slope of the curve. For example, compare the change in the rate of NH_3 evolution for the three catalyst systems when the concentration of Inhibitor A is increased from ~ 20 mM to 200 mM. The NH_3 evolution rate decreases by a factor of 4 for catalysis by both Fe and Cu, while the rate decreases by a factor of 6 and 3 for the

Cu only solutions and the Fe only solutions respectively. While it does take a higher concentration of Inhibitor A to reduce the NH$_3$ evolution rate in the presence of both Fe and Cu, this inhibitor is still effective at reducing the oxidative degradation of MEA.

Three different oxidation states of Inhibitor A were selected for study, ranging from a moderately reduced oxidation state to a high oxidation state. Two different salts with different reduced oxidation states were tested, and both salts behaved the same way in terms of the inhibiting behavior. The oxidized form of the salt was less effective at inhibiting the oxidative degradation of MEA for the Cu catalyzed system, as shown in Figure 5.3.
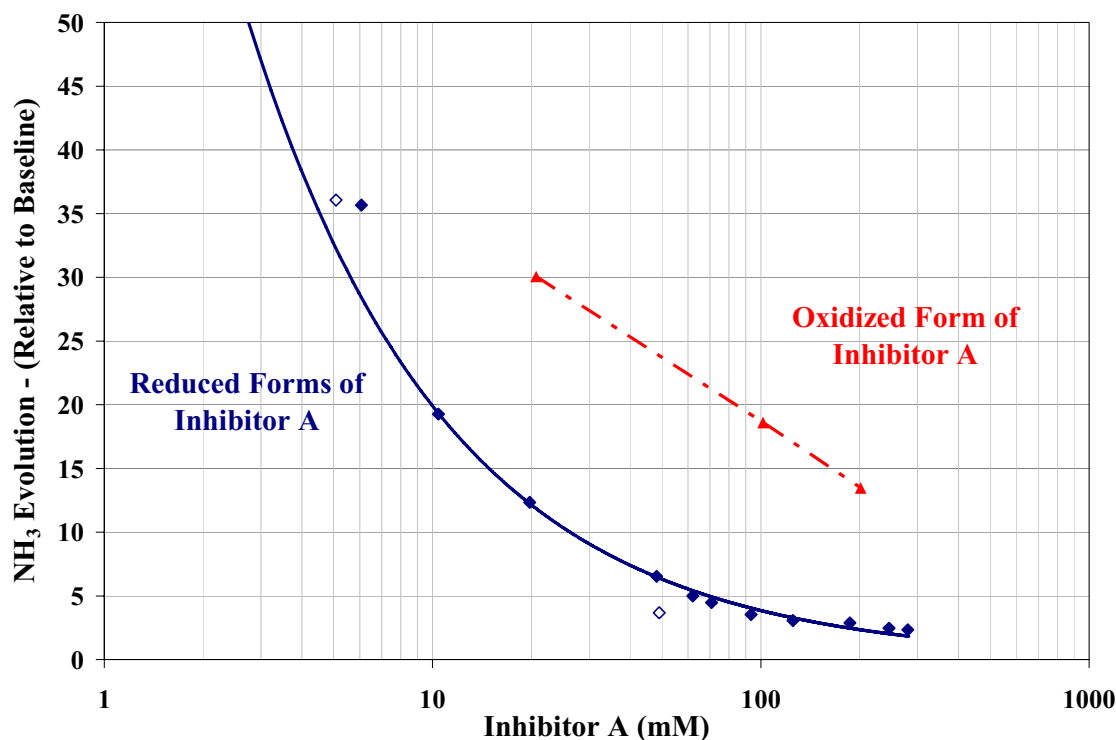
Figure 5.3 Effect of the Oxidation State of Inhibitor A on the Oxidative Degradation of MEA with Copper (55°C, 7.0 m MEA, $\alpha = 0.15$, 1400 RPM, Baseline = 0.15 mM/hr)

5.2.1.1. Miscellaneous Solution Observations with Inhibitor A

The gas phase FT-IR analysis looked at a range of compounds detailed in Chapter 3. In general, the only detectable compounds were acetaldehyde and formaldehyde (occasionally). The acetaldehyde was present at a concentration of less than 5 ppm_v and decreased as the rate of NH_3 evolution decreased. Formaldehyde was generally not detectable. When solutions containing Inhibitor A were sealed overnight, there was a spike of acetaldehyde and formaldehyde when the experiment was started the next day. After this initial inventory had been stripped from the solution, the concentration of the compounds in the gas phase was undetectable.

When neutral salts of Inhibitor A were added to the Agitated Reactor, no significant temperature change was observed for one of the reduced oxidation state salts, however, the second form of the reduced salt showed a noticeable temperature spike upon addition to the MEA solution. The oxidized form of Inhibitor A showed a temperature decrease upon addition and the temperature of the heat bath had to be increased by $\sim 0.5°C$ in order to keep the temperature constant in the reactor.

For systems containing no inhibitor, the solution is a clear orange color when the system reaches the initial steady state. Upon the addition of Inhibitor A, the solutions change color, sometimes slowly, to a clear yellow color (straw colored). This transition generally occurs between a concentration of 25 mM and 100 mM of Inhibitor A. The oxidized form of Inhibitor A made the solutions a yellowish-orange color (approximately the color of orange juice), but these solutions were more orange than any of the other solutions. Solutions containing only Cu were stable when sealed

overnight and did not change color. Solutions containing Fe, including the mixed Cu and Fe solutions, turned a dark red color (sometimes a very dark purple) when sealed overnight. These solutions were so dark that they almost appeared to be opaque, but in actuality were clear. When the solutions were again sparged with air, the color turned back to a light orange color, but never completely turned yellow. When the air sparging was turned off, these solutions again turned the dark red color within a half hour. UV-VIS analysis was performed on samples after the end of the experiments in order to attempt to quantify the observed colors. Details can be found in Appendix H.

5.2.2. Na_2SO_3

Na_2SO_3 is a known oxygen scavenger that is used in a range of applications varying from boiler feed-water treating to food packaging (Hakka and Ouimet 2004; Somogyi 2004; White 2001). One drawback of O_2 scavengers is that they are consumed at the rate of O_2 absorption and must be constantly fed to the system. Additionally, they form oxidized degradation products that accumulate and must be purged from the solution. The kinetics of sulfite oxidation in aqueous solutions is known to be very fast and the rate of oxidation is controlled by the rate of O_2 absorption (Lee 1986; Ulrich 1983).

SO_2 is regulated pollutant in flue gas, and is currently removed by absorption in a limestone slurry scrubber. SO_2 reacts quickly with O_2 in MEA solutions to form sulfate (SO_4^{-2}), forming a heat stable salt with MEA (Kohl and Nielsen 1997). This heat stable salt binds up the amine and prevents it from reacting with CO_2, effectively

reducing the capacity of the solvent. In order to regenerate the solvent, a slip stream from the stripper bottoms is sent to a reclaimer. For applications containing SO_2 the minimum rate of reclaiming is equal to the moles of SO_2 absorbed into the MEA solvent. Typical coal fired flue gas will contain approximately 100 ppm_v SO_2 after the limestone slurry scrubber, but most estimates suggest that this will need to be reduced to less than 10 ppm_v to reduce the rate of solvent reclaiming (ABB 1998). Since there is always some SO_2 present in coal fired power plant flue gas, SO_2 represents a viable additive for reducing the oxidative degradation of MEA since this scavenger will not need to be bought and added continuously to the solvent.

Figure 5.4 shows the effect of Na_2SO_3 on the rate of NH_3 evolution from 7.0 m MEA solutions. With Cu catalysis the relative rate of NH_3 evolution decreases as more Na_2SO_3 is added to solution up to 100 mM, resulting in a decrease in NH_3 evolution by a factor of 6 from 20 mM to 100 mM. Above 100 mM, the rate begins to increase until the solubility limit is reached, between 0.8 M and 1.0 M. Since this additive is an O_2 scavenger and does not affect or participate in the mechanism of MEA degradation, the inhibiting power is independent of CO_2 loading. The increase in the relative rate of NH_3 evolution above 100 mM could be explained by conjugated oxidation or enhanced O_2 mass transfer. It has been observed that both Cu and Fe can enhance the rate of O_2 absorption into aqueous solutions of sulfite at concentrations as low as 0.1 mM (Ulrich 1983). The increase in NH_3 evolution at higher concentrations of Na_2SO_3 with Cu could be due to enhanced O_2 mass transfer into the amine solution. This continues to increase until the solubility limit of Na_2SO_3 is reached between 0.8 M and 1.0 M.
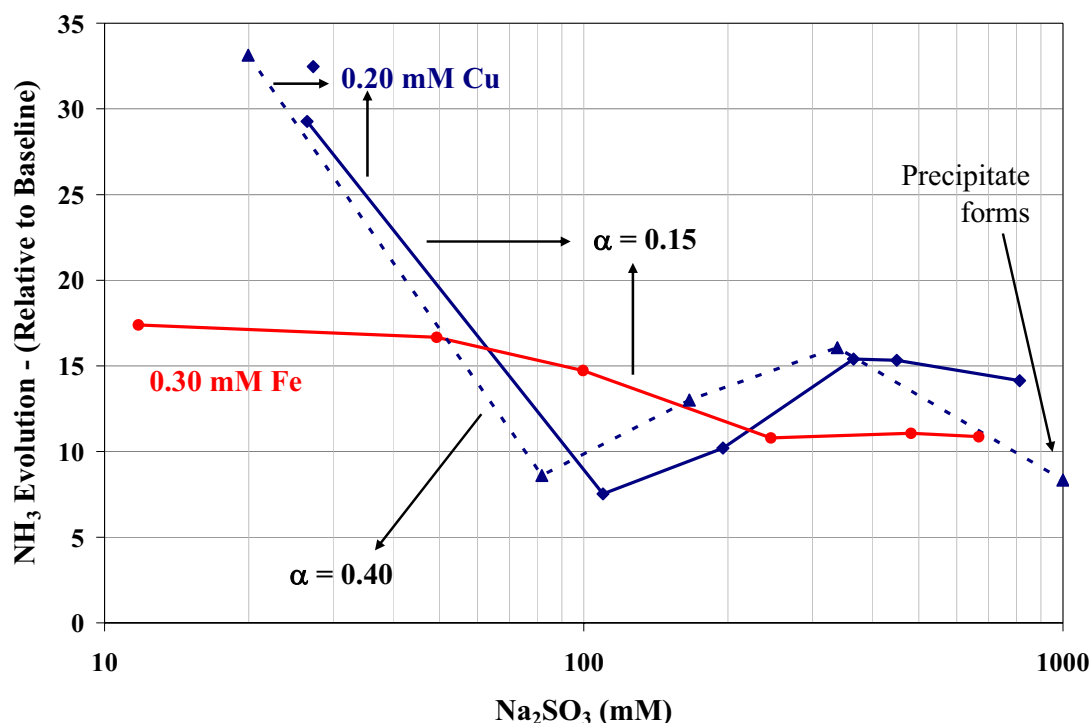
Figure 5.4 Effect of Sulfite on the Oxidative Degradation of MEA in the Presence of Copper or Iron (55°C, 7.0 m MEA, 1400 RPM, Baseline = 0.15 mM/hr)

Na_2SO_3 also decreases NH_3 evolution catalyzed by Fe, although it is not as effective at inhibiting Fe as Cu. The rate of NH_3 evolution decreases by approximately 40% when the Na_2SO_3 concentration is increased from 12 mM to 670 mM. The Fe system does not appear to exhibit the same minimum in NH_3 evolution as the Cu catalyzed degradation. Since the slope of the Na_2SO_3 / Cu system is much steeper than the curve for Na_2SO_3 / Fe this also indicates that Cu is a better catalyst for sulfite oxidation. In a previous study measuring the effect of transition metals on the rate of sulfite oxidation in aqueous solutions, the rate constant for Cu was shown to be more than an order of magnitude higher than the rate constant for Fe (Ulrich 1983). Other

studies have shown that sulfite oxidation shows a square root dependence on the catalyst concentration, independent of the metal being used, and the dependence on O_2 and SO_3^{-2} concentration is also independent of catalyst (Barron and O'Hern 1966; Bengtsson and Bjerle 1975; Chen and Barron 1972; Conklin and Hoffmann 1988). For the scavenger systems, the O_2 can react with the scavenger or the amine. Assuming that the rate of O_2 consumption is constant for the cases in Figure 5.4, the larger slope of the Cu curve further confirms that Cu is a better catalyst than Fe for sulfite oxidation.

Na_2SO_3 inhibits both Cu and Fe catalyzed degradation of MEA to some extent; therefore, the presence of SO_2 in the absorber feed may be helping to reduce the rate of oxidative degradation of MEA in commercial CO_2 capture systems. While Na_2SO_3 is not as effective an inhibitor as Inhibitor A, it is a "free" additive in coal fired power plant applications, and some benefit may be derived by allowing some SO_2 to enter the CO_2 removal process.

5.2.2.1. Miscellaneous Solution Observations with Na_2SO_3

Na_2SO_3 was added to the Agitated Reactor as a solid. No significant temperature change was observed for either Cu or Fe solutions upon addition of Na_2SO_3. Gas phase concentrations of formaldehyde were generally undetectable, and the concentration of acetaldehyde ranged from 2 to 4 ppm_v. Unlike the behavior of acetaldehyde in the presence of Inhibitor A, acetaldehyde concentrations remained constant through the sulfite experiments and did not noticeably change with increasing Na_2SO_3 concentration.

For systems containing no inhibitor, the solution is a clear orange color when the system reaches the initial steady state. Upon the addition of Na_2SO_3, the solutions behave like the solutions with Inhibitor A, changing to a clear yellow color (straw colored). When solutions containing Na_2SO_3 and either Cu or Fe were sealed overnight, the solutions returned to the orange color. If the solutions were then sparged with air again, they stayed orange and did not turn yellow again. In experiments with higher Cu concentrations (2.3 mM Cu on 01/28/04 and 01/29/04) the solutions turned emerald green when the solution was sealed overnight, and turned back to yellow the next day when it was sparged with air. Unlike solutions with Inhibitor A and Fe, solutions with Na_2SO_3 and Fe did not turn red when sealed overnight. Details of UV-VIS scans for these samples can be found in Appendix H.

5.2.3. Formaldehyde

In Chapter 2 it was shown that formaldehyde is an expected intermediate in the oxidative degradation of MEA. It has also been shown that formate is an observed degradation product in industrial processes, and it likely comes from the oxidation of formaldehyde. Since aldehydes are easily oxidized to the corresponding carboxylic acids in the presence of O_2 (Fessenden and Fessenden 1994), and since formaldehyde should be present to some extent in industrial CO_2 capture applications as a degradation intermediate, formaldehyde is a suitable compound to screen as a possible degradation inhibitor. While formaldehyde itself is considered an air toxic under the Clean Air Act (EPA 1990), the presence of O_2 should oxidize the formaldehyde to formate and thus

132

minimize the potential environmental impact from releasing formaldehyde to the atmosphere. Since formate is also a heat stable salt that neutralizes MEA just like sulfate, it must also be removed from the solution via solvent reclaiming.

Figure 5.5 shows the effect of formaldehyde on the relative rate of NH_3 evolution with 7.0 molal MEA solutions at lean CO_2 loadings. With both Cu and Fe the rate of NH_3 evolution decreases as the concentration of formaldehyde is increased. Just like Inhibitor A and Na_2SO_3, formaldehyde is a more effective inhibitor for Cu than for Fe catalyzed degradation. When the concentration of formaldehyde is increased from ~ 50 mM to ~ 250 mM the Cu catalyzed degradation is decreased by a factor of 5, while the Fe catalyzed degradation is only decreased by a factor of 1.5. Assuming that the form of the kinetic expression for formaldehyde oxidation is the same for both Cu and Fe and that the total rate of O_2 consumption is unchanged for each data point, Figure 5.5 indicates that Cu is a better catalyst than Fe for oxidizing formaldehyde.

Formaldehyde is potentially a better inhibitor than Na_2SO_3 since it is not solubility limited at higher concentrations, and appears to shut down Cu catalyzed degradation at 500 mM. Na_2SO_3 is more effective at lower concentrations than formaldehyde, but both show significant inhibiting effects at concentrations of 100 mM. Since formaldehyde is an intermediate in the degradation mechanism, this means that the oxidative degradation of MEA is possibly self limiting, in that that the degradation products being formed begin to compete with MEA for the available oxygen.
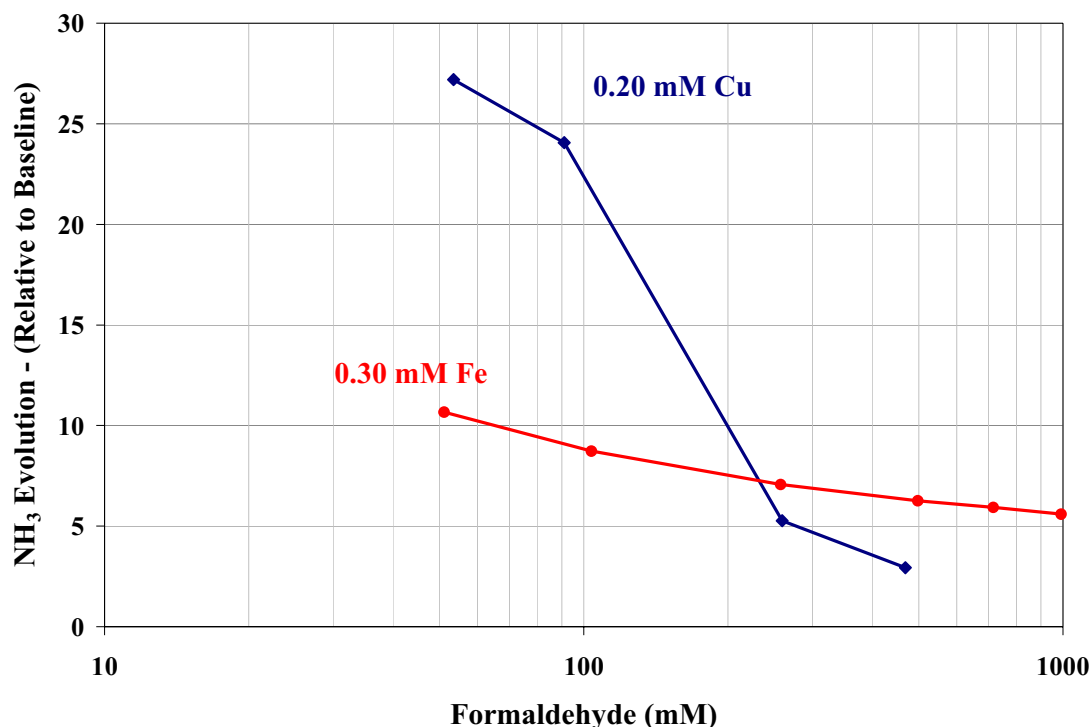
Figure 5.5 Effect of Formaldehyde on Copper or Iron Catalyzed Oxidative Degradation of MEA (55°C, 7.0 m MEA, α = 0.15, 1400 RPM, Baseline = 0.15 mM/hr)

5.2.3.1. Gas Phase Aldehyde Analysis

Several forms of formaldehyde were used in these experiments. Initially, formaldehyde was added to the reactor as formalin solution (37.8 wt. % formaldehyde, 11.0 % methanol, 51.2 wt. % water), but the methanol made IR analysis very difficult and the formaldehyde was easily stripped from the solution. In order to help combat this, a solution was prepared containing 30 wt. % MEA by adding MEA to the formalin solution. When the MEA was added to the solution a gas was evolved and the solution heated to the point where the solution was almost boiling. Experiments 07/28/04 and 07/29/04 were run with this solution, and the formaldehyde volatility was decreased, but

the methanol still interfered with the IR analysis. All other experiments were run using paraformaldehyde solid as the source of formaldehyde to minimize volatility losses.

Generally, formaldehyde and acetaldehyde vapor concentrations are less than 5 ppm_v. When formaldehyde is added to the MEA solution, there is a spike in acetaldehyde concentration which decreases to a concentration lower than the steady state value before formaldehyde addition. This trend was consistently observed, and the concentration of formaldehyde was always less than 10 ppm_v. At concentrations of formaldehyde below ~ 100 mM, acetaldehyde has a higher gas concentration, and somewhere between 100 mM and 250 mM formaldehyde has the highest gas concentration. Figure 5.6 shows an example of this from the 7/29/04 experiment. At a formaldehyde concentration of 91 mM, the gas concentrations of formaldehyde and acetaldehyde are 1 ppm_v and 3.8 ppm_v respectively. After then next addition, bringing the dissolved formaldehyde concentration to 260 mM, the gas concentrations of formaldehyde and acetaldehyde are 2.8 ppm_v and 0.8 ppm_v respectively.
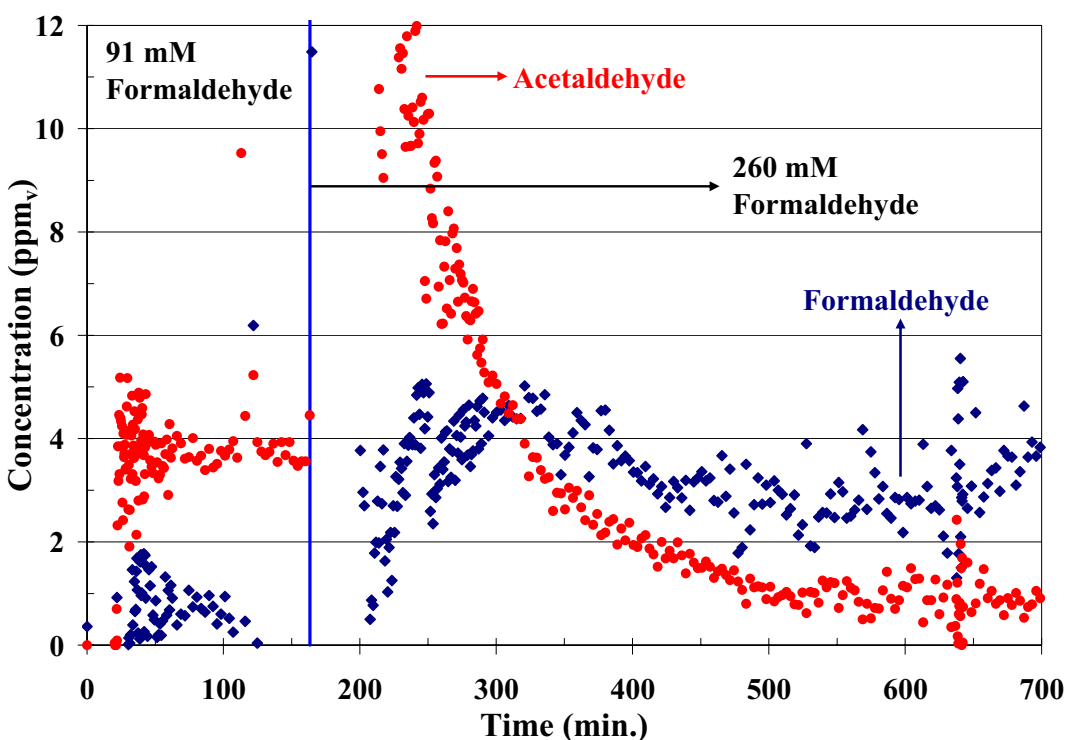
Figure 5.6 Example of Gas Concentrations of Acetaldehyde and Formaldehyde
(55°C, 7.0 m MEA, α = 0.15, 0.22 mM Cu, 1400 RPM, 07/29/04)

5.2.3.2. Formaldehyde and Inhibitor A

Since formaldehyde is a better inhibitor than Na_2SO_3, it was desired to try a

blend of Inhibitor A and formaldehyde. Inhibitor A was added at a concentration of

48.0 mM, which was selected by examining Figure 5.1. This concentration was enough

to significantly inhibit the NH_3 rate, but the rate is still ~ 6 times the baseline rate of

0.15 mM/hr. Formaldehyde was then added to the solution, and the results are shown in

Figure 5.7. At concentrations of formaldehyde below 150 mM the system behaves as if

the solution only contained Inhibitor A, while at concentrations above 150 mM

formaldehyde the solution behaves as if there were no Inhibitor A in solution. Based on

this, there is no benefit of using a blend of Inhibitor A and formaldehyde.

136
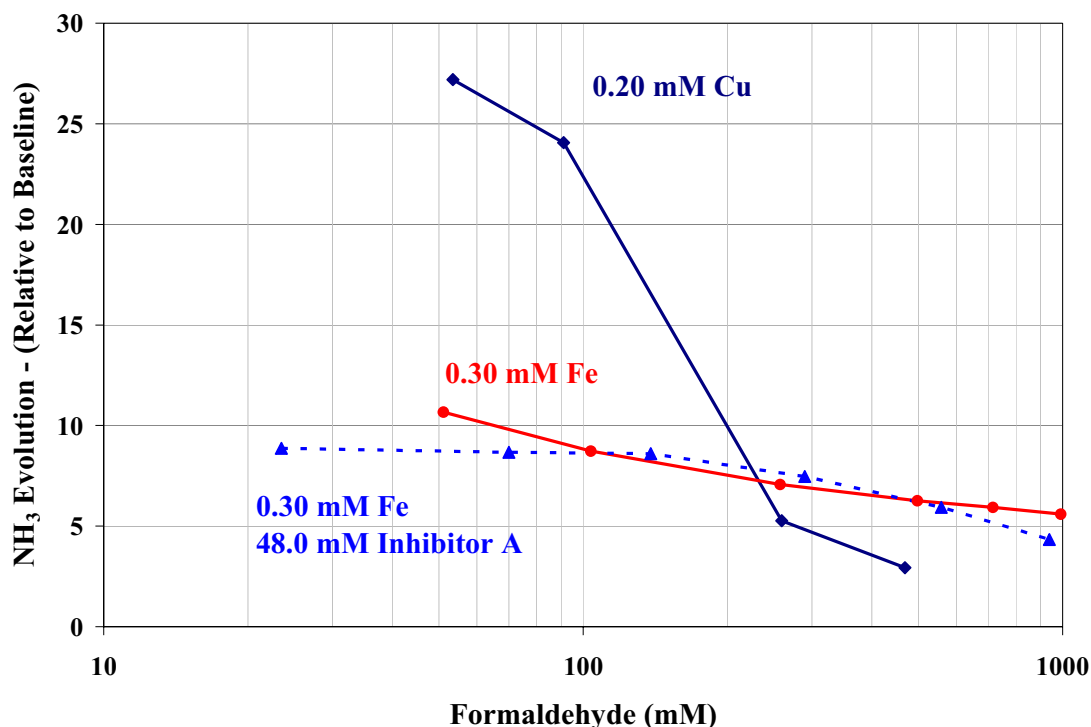
Figure 5.7 Inhibitor A/Formaldehyde Mixed System for Inhibiting Fe Catalyzed Degradation of MEA (55°C, 7.0 m MEA, $\alpha = 0.15$, 1400 RPM, Baseline = 0.15 mM/hr)

5.2.3.3. Miscellaneous Solution Observations with Formaldehyde

The addition of the MEA/formalin mixture to the Agitated Reactor did not result in any noticeable temperature change. Just as the addition of MEA to formalin was exothermic, the addition of paraformaldehyde to the reactor resulted in a noticeable temperature spike of 0.5 to 1.2°C, depending on the amount of solid added. The reactor temperature exponentially decreased over a matter of several minutes to the temperature prior to addition.

The color of solutions containing formaldehyde follows basically the same trend as solutions with Inhibitor A and Na_2SO_3. The solutions start out orange and turn yellow as the NH_3 evolution rate decreases. Fe solutions turn dark red when sealed

overnight, and remain orange (although a lighter shade of orange than the color before the initial addition of formaldehyde) when sparged with air the next day. Details of the UV-VIS scans for these experiments can be found in Appendix H.

5.2.4. Hydroquinone and Ascorbic Acid

Not all O_2 scavengers are effective at inhibiting the oxidative degradation of MEA. Hydroquinone is a known O_2 scavenger in alkanolamine systems (Veldman and Trahan 1997; Veldman and Trahan 2001). Industrial applications that use hydroquinone are typically O_2 starved, so the behavior of hydroquinone in a flue gas application with excess O_2 could be quite different. Figure 5.8 shows that upon addition of 11 mM hydroquinone to an MEA solution, the rate of NH_3 evolution actually increases by more than a factor of 4. As the hydroquinone is oxidized, the rate of NH_3 evolution decreases and eventually returns to the original value. Similar behavior is also observed for ascorbic acid, a known free radical scavenger used as an antioxidant in food packaging (Somogyi 2004). When 65.5 mM ascorbic acid was added to a 7.0 molal MEA solution the rate of NH_3 evolution increased by more than a factor of 2.5 and decreases to the original value as the ascorbic acid is consumed.
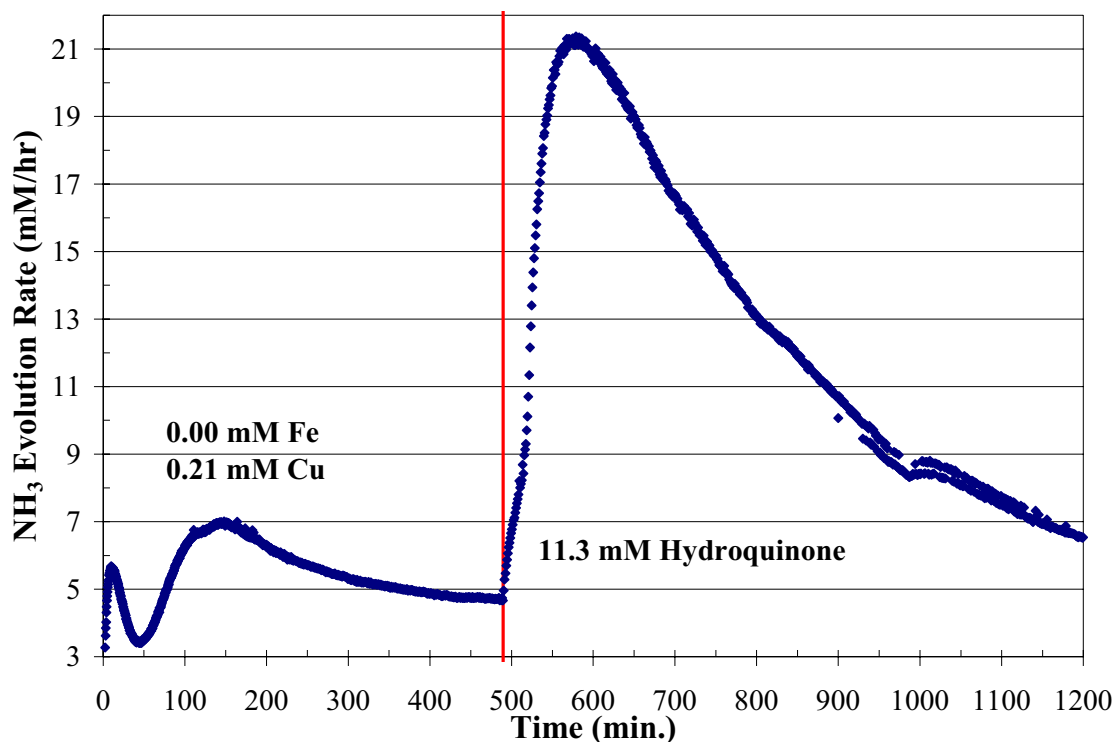
Figure 5.8 Effect of Hydroquinone on the Oxidative Degradation of MEA in the Presence of Copper (55°C, 7.0 m MEA, α = 0.15, 0.21 mM Cu, 1400 RPM)

Hydroquinone and ascorbic acid do not contain nitrogen, so the increase in NH_3 evolution must come from the degradation of MEA. Both of these additives form "stable radicals" when they interact with O_2. Since the mechanism of the oxidative degradation of MEA is initiated by free radicals, the intermediates from hydroquinone and ascorbic acid oxidation catalyze the degradation of MEA. The addition of either of these compounds appears to produce a stoichiometric concentration of NH_3 which will be addressed in more detail in Section 5.2.6. Since these O_2 scavengers increase the rate of NH_3 evolution, they are not suitable additives for an industrial process to inhibit the oxidative degradation of MEA.

5.2.4.1. Miscellaneous Solution Observations with Hydroquinone and Ascorbic Acid

No observable temperature change was detected when the hydroquinone was added to the Agitated Reactor. Prior to the hydroquinone addition, the gas concentration of acetaldehyde was 3 ppm_v and formaldehyde was undetectable. After the addition, the formaldehyde spiked to 9 ppm_v and slowly decreased back to zero (at a time of ~ 1100 min. in Figure 5.8) as the hydroquinone was consumed. As the formaldehyde concentration spiked, the concentration of acetaldehyde fell to zero and remained undetectable for nearly 3 hours (time of 700 min.) and rose to the initial value of 3 ppm_v by the time the formaldehyde had disappeared. After the hydroquinone was added to the reactor, the solution went from the usual orange color to a brownish red that was nearly opaque. This solution resembled prune juice in consistency and color. After the experiment was over, the reactor was coated with a brown residue, and the reactor had to be flushed several times with a dilute acid solution.

The addition of ascorbic acid caused a temperature increase of approximately 0.8°C, which decreased to the original value as the ascorbic acid was consumed. Along with an increase in NH_3 evolution, the concentration of acetaldehyde increased from approximately 3 to 6 ppm_v, while formaldehyde increased from 0 to 7.5 ppm_v. CO also increased in concentration from 0 to 2.5 ppm_v. The solution also changed color from the usual orange to a very dark orange, almost red color. Details of the UV-VIS scans for both hydroquinone and ascorbic acid can be found in Appendix H.

5.2.5. *Manganese Salts*

The final additive examined as a possible inhibitor for oxidative degradation of MEA is manganese. Limestone slurry scrubbers for SO_x removal from flue gas use organic acids as pH buffers, and Mn^{+2} has been shown to be an effective inhibitor for organic acid oxidation (Lee 1986). Manganese was added to the oxidative degradation experiments separately as $MnSO_4$ and $KMnO_4$, and both forms of Mn showed catalytic effects on the oxidation of MEA. Figure 5.9 shows the results from one experiment with $KMnO_4$.
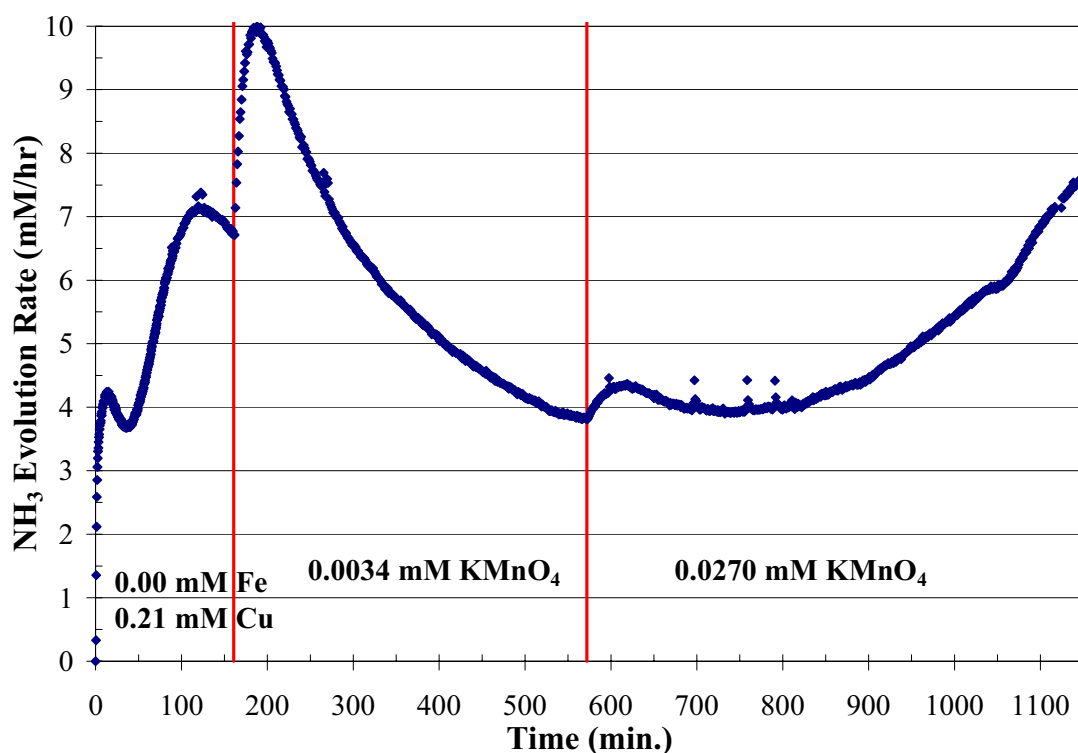
Figure 5.9 Effect of $KMnO_4$ on the Oxidative Degradation of MEA
(55°C, 7.0 m MEA, $\alpha = 0.15$, 0.21 mM Cu, 1400 RPM)

Upon addition of Mn, NH_3 evolution increased, decreased to a minimum, and increased again. The maximum rate for Mn catalyzed degradation is higher than rates observed for Cu catalyzed degradation at equivalent concentrations (recall data from Chapter 4). Unlike Cu or Fe catalyzed degradation, the NH_3 rate changes with time for Mn catalyzed degradation. This would indicate that Mn is participating in the oxidation mechanism in a different way than either Cu or Fe.

The initial increase in rate indicates that Mn is reacting with an intermediate or oxidizing a degradation product. If this reaction is faster than the Cu and MEA reactions, the degradation rate would then decrease as the intermediate or degradation product is consumed, and the oxidation state of Mn changes. In the absence of the degradation product, Mn would be regenerated to the active oxidation state by reacting with MEA or O_2. If this Mn reaction is slower than the Cu and MEA reactions, the intermediate or degradation product can accumulate. Mn then begins to react with this compound increasing the rate of NH_3 evolution again. Once the degradation product/reaction intermediate had again accumulated, Mn is regenerated by reacting with the intermediate. Both Mn^{+2} and MnO_4^- are known catalysts for the oxidation of formate (Taylor and Halpern 1959; Wiberg and Stewart 1955), which is the primary carboxylic acid degradation product of MEA (Rooney et al. 1998). This supports the likelihood that Mn is oxidizing one of the degradation products or intermediates of MEA degradation.

NH_3 produced from adding Mn is not stoichiometric, which can be seen in Figure 5.9. Since Mn shows catalytic effects on the rate of NH_3 evolution, it is an unsuitable additive for inhibiting oxidative degradation.

5.2.5.1. Miscellaneous Solution Observations with Mn Salts

The addition of either Mn salt produced no noticeable effect on the temperature of the reactor. Additionally, no noticeable trends were observed with the gas phase concentration of other degradation products. Solutions turned from the normal orange color to a brown color. At concentrations above 6 mM Mn, a black solid formed, and a brownish scale was observed coating the inside of the glass reactor for all the Mn experiments. Cleaning was difficult and usually required rinsing with a strong chelating agent, EDTA, then a dilute acid rinse, and then flushing several times with water. This was repeated up to three times to ensure the reactor was completely clean. Details of the UV-VIS scans for the Mn experiments can be found in Appendix H.

5.2.6. Scavenger Consumption and Stoichiometry

Inhibitor A is not consumed by O_2; however, the O_2 scavengers tested, Na_2SO_3, formaldehyde, hydroquinone, and ascorbic acid, are consumed stoichiometrically at the rate of O_2 absorption. Scavengers that are oxidized must be continually replaced, and the degradation products must be removed to avoid accumulation in the circulating solvent. This makes Na_2SO_3 and formaldehyde less attractive as oxidation inhibitors than Inhibitor A, but they are still viable alternatives. The reclaimer, shown in the PFD in Figure 1.3, serves a dual purpose in the MEA process. The first is to remove the

MEA degradation products and the second is to remove sulfate which accumulates from the absorption of SO_2 in the flue gas. If the degradation of MEA is completely inhibited, the reclaimer must still be run in order to purge the sulfate. While adding an O_2 scavenger which degrades creates additional degradation products that must also be purged, the net effect on the reclaimer heat duty can still be decreased.

Both Na_2SO_3 and formaldehyde are consumed over time, and show a stoichiometric decrease in NH_3 production. Hydroquinone and ascorbic acid increase the rate of NH_3 evolution, and also show a stoichiometric relationship to the amount of NH_3 produced. Table 2 shows a comparison of the stoichiometry for additives tested in this section. The stoichiometry was calculated by taking the difference between the expected NH_3 evolution (at the base rate conditions) and the actual observed NH_3 evolution over the observed time of the inhibition/catalysis, and normalized by the moles of additive.

Table 5.3 Stoichiometric Effects of Various Additives on NH_3 Evolution from Oxidizing MEA Solutions (55°C, 7.0 m MEA, $\alpha = 0.15$, 0.21 mM Cu, 1400 RPM)

| Additive | Molar Stoichiometry | |
	Additive / NH_3 Avoided	Additive / NH_3 Produced
Inhibitor A	---	---
Na_2SO_3	5.8	---
Formaldehyde	15.5	---
Hydroquinone	---	2.6
Ascorbic Acid	---	0.7
Manganese	---	not stoichiometric

144

5.3. Chelating Agents

Chelating agents are compounds that chemically bond with dissolved metals. An effective chelator for oxidation inhibition would render the metal catalysts inactive. For this study, a representative organic and inorganic chelating agent was selected for analysis. The tetra-sodium salt of ethylene-diamine-tetra-acetic acid (EDTA) was selected as the organic chelator. EDTA is widely acknowledged as a strong chelating compound, having four carboxylic acid groups available to co-ordinate with dissolved metals. Experiments from the 1960's, performed by the U.S. Department of the Navy, identified EDTA as an additive to stabilize MEA solutions to oxidative degradation (Blachly and Ravner 1964; 1965; 1966). These studies also identified bicine as a stabilizer, but it was much less effective. Previous studies in this research group confirmed these findings, and found that EDTA was the most effective chelating agent for both Fe and Cu (Chi 2000; Goff and Rochelle 2003). Two inorganic chelating agents were selected: tri-sodium phosphate (Na_3PO_4) and sodium tetra-sulfide (Na_2S_4). Figure 5.10 compares the results for the inhibiting effect of EDTA and phosphate.

EDTA is clearly a more effective inhibitor than phosphate. Relative to the initial rate, EDTA shows a 65% reduction in NH_3 evolution at a 0.9:1.0 ratio of EDTA to Cu, but the rate is still 14 times the baseline rate. This is much higher than the rates observed with Inhibitor A, Na_2SO_3, or formaldehyde, although the concentration of EDTA is significantly lower. Phosphate is only a weak inhibitor, resulting in an NH_3 evolution rate 24 times that of the baseline case (23% reduction) at a 474:1 ratio of phosphate to Cu. Phosphate is a stable compound that is not oxidized and doesn't

degrade. While EDTA shows a significant decrease in NH_3 evolution at low concentrations, experiments showed that over time EDTA was no longer inhibiting the degradation.
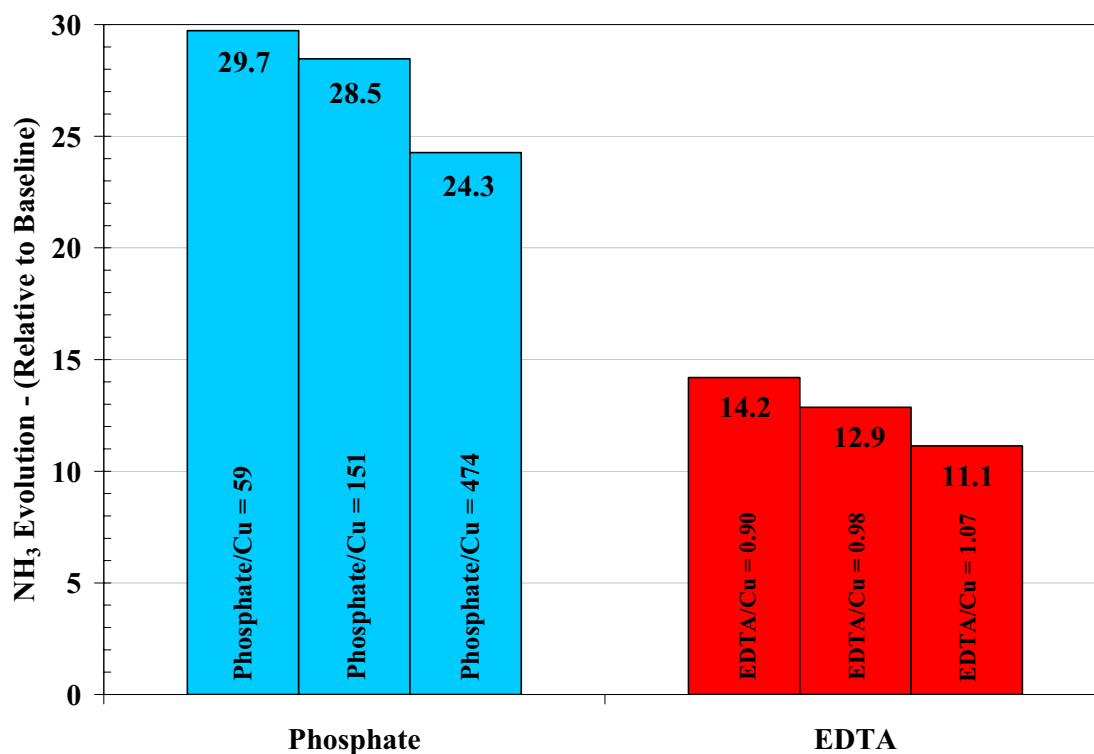
Figure 5.10 Inhibiting the Oxidative Degradation of MEA with EDTA or Phosphate (55°C, 7.0 m MEA, α = 0.15, 0.20 mM Cu, 1400 RPM, Baseline = 0.15 mM/hr)

Fe is a known catalyst for EDTA oxidation (Seibig and van Eldik 1997), and Cu could also be a catalyst. It appeared that over the course of the experiment the rate of NH_3 evolution increased as EDTA was being consumed. The Navy studies from the 1960's did not observe the consumption of EDTA since the rate of O_2 mass transfer in these experiments was significantly less than rates in the current apparatus (Goff and Rochelle 2004). If EDTA is oxidized, the degradation products would accumulate in an

absorber/stripper system and must be removed, and the EDTA must be replaced. A second possibility to explain the decline in inhibition is that the complexed form of Cu is still an active catalyst. This could result in a change in stoichiometry or mechanism, resulting in a time lag in NH_3 production. Since EDTA is consumed over time and both EDTA and phosphate are weak inhibitors compared to Inhibitor A, Na_2SO_3, and formaldehyde, chelating agents appear to be unsuitable alternatives for minimizing oxidative degradation of MEA in an industrial application.

Na_2S_4 is a known compound for precipitating metal compounds. Experiments performed with loaded MEA solutions showed that a precipitate formed when Na_2S_4 was added to solutions containing Cu. This would effectively decrease the oxidative degradation rates, but would eliminate the corrosion inhibitor, which was added to the process in the first place. While this experiment shows that Na_2S_4 is an effective compound for precipitating metals from loaded MEA solutions, it is an unacceptable solution for implementation in a CO_2 capture process.

5.3.1. *Miscellaneous Solution Observations with EDTA and Na_3PO_4*

The addition of EDTA and K_3PO_4 did not result in any noticeable temperature difference in the reactor. Additionally, no noticeable trends were observed with the gas phase concentration of other degradation products. Solutions did not change color noticeably upon the addition of either EDTA, while the K_3PO_4 solution turned a darker orange color. Details of the UV-VIS scans can be found in Appendix H.

5.4. Stable Salts

Three stable salts, potassium chloride, potassium bromide, and potassium formate, were added to MEA solutions at concentrations up to 1.1 M. The results of the salt experiments can be seen in Figure 5.11. The addition of KCl resulted in an increase in the rate of NH3 evolution. Neutral salts are known to increase the rate constants in reactions involving charged intermediates. A recent study has shown a significant catalytic effect with the addition of KCl on the rate constant of piperazine, a cyclic diamine, with CO_2 (Cullinane 2005). While the salts can increase the rate constants of the kinetics, the increase in ionic strength generally decreases the solubility of gases in water. If the increase in the kinetics is larger than the decrease in the solubility of O_2, the overall rate of NH_3 evolution can increase.

Both potassium formate and potassium bromide slightly decrease the rate of NH_3 evolution. The relative rate of NH_3 evolution is still 34 times the base rate (15% reduction) at a potassium formate concentration of 775 mM and 29 times the base rate at a potassium bromide concentration of 1.0 M. Potassium formate is of particular interest since formate has been shown as a significant degradation product of MEA and will accumulate in the amine solution in an industrial application (Rooney et al. 1998).

While both KBr and potassium formate show an ability to inhibit NH_3 evolution, the effect is very weak compared to the scavengers that were tested. The high concentrations required to achieve even a minimal reduction in degradation rates makes stable salts an unsuitable method for minimizing oxidative degradation of MEA. While adding salts that are not normally present is economically unfeasible, Figure 5.11 shows

that allowing formate to accumulate to significant concentrations will give some benefit

by mildly reducing NH_3 evolution.
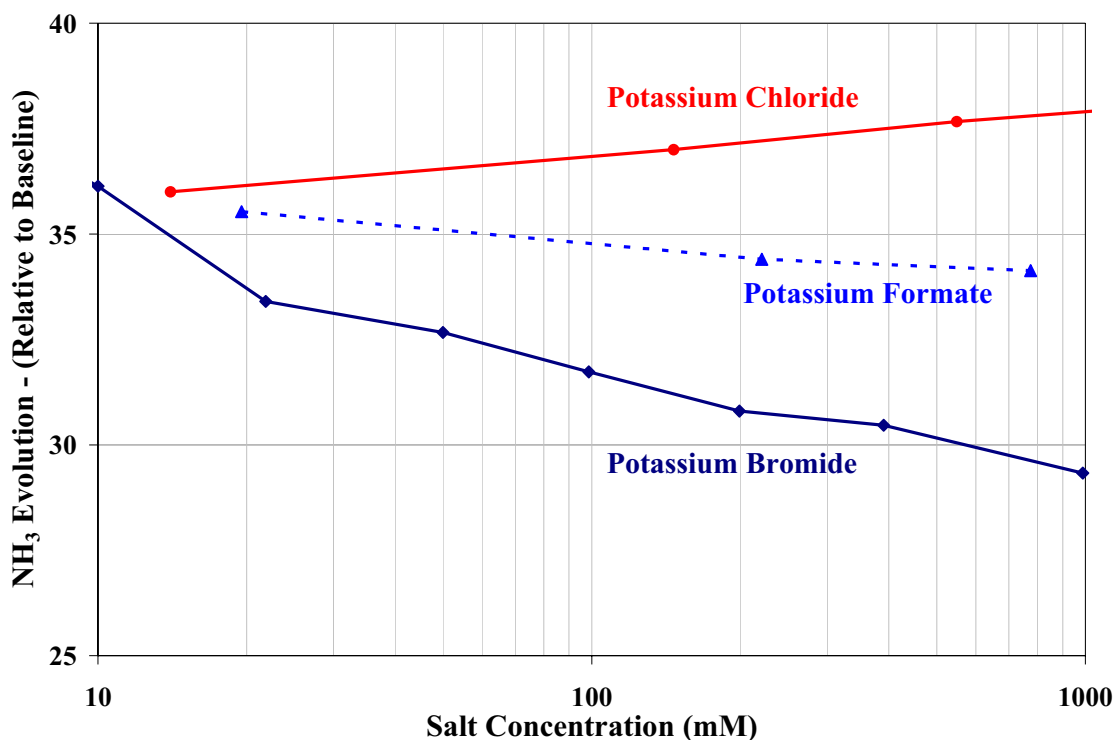
Figure 5.11 Stable Salt Effect on Copper Catalyzed Oxidative Degradation of MEA
(55°C, 7.0 m MEA, α = 0.15, 0.21 mM Cu, 1400 RPM, Baseline = 0.15 mM/hr)

5.4.1. *Miscellaneous Solution Observations with Stable Salts*

The addition of potassium chloride, bromide, and formate did not result in any

noticeable temperature difference in the reactor. Additionally, no noticeable trends

were observed with the gas phase concentration of other degradation products.

Solutions containing potassium chloride and bromide did not change color noticeably

and remained an orange color. Solutions containing potassium formate remained an

orange color, but the solution containing 775 mM formate turned a dark red after the air

sparging and agitation were stopped. Details of the UV-VIS scans can be found in Appendix H.

5.5. Degradation Inhibitors and Corrosion

While Inhibitor A, Na_2SO_3, and formaldehyde all show promise as viable additives for oxidative degradation inhibition, the effect of the compounds on corrosion is unknown. No corrosion experiments have been performed with these additives in an MEA solution. Initial literature findings suggest that Inhibitor A is also a corrosion inhibitor. This dual inhibition capacity makes Inhibitor A an extremely attractive additive for MEA solutions; however, detailed corrosion studies must be performed before any of these compounds could be put into service in an industrial CO_2 capture plant. Since both heat stable salts and chelating agents would likely increase the corrosion rates of steel, this gives an additional reason for excluding these classes of compounds as possible additives to decrease oxidative degradation of MEA.

5.6. Conclusions

In Chapter 4 it was shown that the rate of oxidative degradation of MEA is likely controlled by rate of O_2 absorption under typical conditions in a flue gas treating application. In order to minimize oxidative degradation, several categories of additives have been tested as possible inhibitors: O_2 scavengers and reaction inhibitors, chelating agents, and stable salts. Of the additives tested, only the O_2 scavengers and reaction

inhibitors show a significant enough reduction in the rate of NH_3 evolution to make these viable additives in an industrial application.

Inhibitor A is an inorganic compound that is stable and not consumed, and acts as a reaction mechanism inhibitor. It was shown to be effective at inhibiting oxidative degradation catalyzed by Cu, Fe, and both Cu and Fe. The NH_3 evolution rate was equal to the baseline rate at 250 mM Inhibitor A for solutions with $\alpha = 0.15$ and at 100 mM Inhibitor A for solutions with $\alpha = 0.40$. Inhibitor A is also more effective at inhibiting Cu catalyzed degradation than Fe catalyzed degradation.

Na_2SO_3 and formaldehyde were also shown to be effective degradation inhibitors, and were independent of CO_2 loading. Like Inhibitor A, these O_2 scavengers were more effective at inhibiting Cu catalyzed degradation than Fe catalyzed degradation. Neither of the scavengers were as effective as Inhibitor A and both are consumed stoichiometrically at the rate of O_2 absorption. For the Cu solutions the relative rate of NH_3 evolution decreases as more Na_2SO_3 is added to solution, up to 100 mM, resulting in a factor of 6 decrease in NH_3 evolution from 20 mM to 100 mM. Above this concentration the NH_3 evolution increases until the solubility limit between 0.8 M and 1.0 M. The rate of NH_3 evolution decreases by approximately 40% when the Na_2SO_3 concentration is increased from 12 mM to 670 mM. The Fe system does not appear to exhibit the same minimum in NH_3 evolution as the Cu catalyzed degradation.

When the concentration of formaldehyde is increased from $\sim$ 50 mM to $\sim$ 250 mM the Cu catalyzed degradation is decreased by a factor of 5, while the Fe catalyzed degradation is only decreased by a factor of 1.5 when $\alpha = 0.15$. Formaldehyde is

potentially a better inhibitor than Na_2SO_3 since it is not solubility limited at higher concentrations, and appears to shut down Cu catalyzed degradation at concentrations 500 mM. Na_2SO_3 is more effective at lower concentrations than formaldehyde, but both show significant inhibiting effects at concentrations of 100 mM.

Two other well known oxidation inhibitors, hydroquinone and ascorbic acid, increase the rate of NH_3 evolution. Hydroquinone increases the rate by more than a factor of 4 at a concentration of 11 mM, while ascorbic acid increases the rate by a factor 2.5 at a concentration of 65.5 mM. As hydroquinone and ascorbic acid are consumed the rate decreases to its original value. Since both hydroquinone and ascorbic acid increase the rate of NH_3 evolution, they are ineffective oxidation inhibitors.

Under experimental conditions in this study, $MnSO_4$ and $KMnO_4$ both showed complex catalytic activity by increasing the rate of NH_3 evolution. The increase in NH_3 evolution is not stoichiometric to the amount of Mn added to solution. The catalytic activity of Mn makes this an unsuitable additive for inhibiting oxidative degradation.

Scavengers are consumed stoichiometrically at the rate of O_2 mass transfer. In an industrial application the scavengers must be replaced, and the degradation products must be removed to avoid accumulation in the circulating solvent. The molar ratio of additive to NH_3 avoided is 5.8 and 15.5 for Na_2SO_3 and formaldehyde respectively. Hydroquinone and ascorbic acid have a molar stoichiometry of 2.6 and 0.7 additive/NH_3 produced.

EDTA can inhibit NH_3 production by 65% at a 0.9 to 1 ratio of EDTA to Cu, while phosphate only reduces NH_3 evolution by 23% at a 500 to 1 ratio. While phosphate is a stable compound, EDTA loses inhibiting capacity with time. Since EDTA is consumed by reacting with O_2 and phosphate is a weak inhibitor, chelating agents are not viable additives for reducing oxidative degradation of MEA in an industrial process.

Three stable potassium salts, chloride, bromide, and formate, were chosen to increase the ionic strength and decrease the dissolved O_2 solubility. These salts proved to be ineffective inhibitors even at concentrations above 1.0 M. While KCl appears to weakly increase the degradation rates, both KBr and potassium formate are weak inhibitors. Formate, the primary carboxylic acid degradation product of MEA, decreases the NH_3 evolution by 15% at 0.55 M.

While Inhibitor A, Na_2SO_3, and formaldehyde show promise as additives for reducing the oxidative degradation of MEA, the effect of these compounds on the corrosion of steel has not been tested. Although initial literature findings indicate that Inhibitor A is also a corrosion inhibitor, detailed corrosion studies must be performed before these chemicals could be used in an industrial application.

Chapter 6: Conclusions and Recommendations

This chapter details the key findings of this study on the oxidative degradation of monoethanolamine. Results are presented from the O_2 mass transfer study and the study on degradation inhibitors. This project shows that under significant laboratory and industrial conditions, the rate of oxidative degradation is controlled by the rate of O_2 mass transfer. Three compounds were identified as potential additives in an industrial application to inhibit oxidative degradation. Finally, recommendations are made for future work on oxidative degradation of MEA.

6.1. Conclusions Summary

The oxidative degradation rate of MEA was quantified by measuring the rate of NH_3 using FT-IR gas analysis. This study used a Sparged Reactor and an Agitated reactor, both of which were jacketed and temperature controlled to within $\pm1°C$. The rate of NH_3 evolution was quantified at 55°C, which was representative of absorber conditions in a typical MEA absorption/stripping process for CO_2 removal from flue gas. The first part of the work focused on quantifying the effect of O_2 mass transfer

rates on the rate of NH_3 evolution, and the second part of the study examined a number of chemical additives as potential degradation inhibitors.

The study on O_2 mass transfer shows that under significant experimental and industrial conditions, the rate of NH_3 evolution is controlled by the rate of O_2 absorption. Under some experimental conditions the rate of NH_3 evolution depends on only kinetics, and under other conditions the rate shows effects of both kinetics and O_2 mass transfer. In general, the rate of NH_3 evolution increased as the agitation rate was increased, and also increased linearly with increasing O_2 concentration. At low concentrations of catalyst (less than 0.5 mM Fe or Cu) and MEA (less than 2.0 m), the rate of NH_3 evolution was controlled by the degradation kinetics. At high concentrations of catalyst (above 0.5 mM Fe or Cu) and MEA (above 7.0 m) the rate of NH_3 evolution was controlled by the rate of O_2 mass transfer. Solutions between 2.0 and 7.0 m MEA showed effects of both O_2 mass transfer and degradation kinetics.

Previously reported degradation studies using sparged reactors were compared to the current study, and were found to report lower degradation rates at conditions expected to give lower rates of O_2 mass transfer. This indicates that the previous studies were also mass transfer limited and were reporting O_2 absorption rates and not degradation kinetics. Industrial degradation rates were predicted for CO_2 capture from a natural gas fired power plant assuming degradation occurs only in the packing and is limited by the rate of O_2 absorption. The results under-predict the rates reported in the literature, indicating that under industrial conditions the oxidative degradation of MEA is probably controlled by the rate of O_2 absorption into the amine solution.

155

In order to minimize oxidative degradation, several categories of additives have been tested as possible inhibitors: O_2 scavengers and reaction inhibitors, chelating agents, and stable salts. Of the additives tested, only the O_2 scavengers and reaction inhibitors show a significant enough reduction in the rate of NH_3 evolution to make these viable additives in an industrial application. Inhibitor A acts as a reaction mechanism inhibitor, is a stable inorganic compound, and is the best of the tested additives for inhibiting oxidative degradation of MEA. Na_2SO_3 and formaldehyde both act as O_2 scavengers and are consumed stoichiometrically at the rate of O_2 mass transfer. All three inhibitors are more effective at reducing Cu catalyzed degradation and effectively reduce oxidative degradation at concentrations of approximately 100 to 250 mM for all three inhibitors.

6.2. O_2 Mass Transfer Conclusions

Experiments performed in the Sparged Reactor and the Agitated Reactor indicate that over a range of significant laboratory and industrial conditions the oxidative degradation of MEA is controlled by the rate of O_2 absorption. Under some experimental conditions the rate of NH_3 evolution appears to be controlled by the degradation kinetics, and under other conditions the rate shows effects of both kinetics and O_2 mass transfer. The conditions for these three sets of data are detailed below.

6.2.1. Effects of Degradation Kinetics

Below 0.2 mM Fe or Cu in the Sparged Reactor, the rate of NH_3 evolution shows a dependence on the catalyst concentration consistent with kinetic control. The same phenomenon is observed in the Agitated Reactor for Fe and Cu below 0.5 mM. The rates of NH_3 evolution by Cu catalysis are always higher than the rates observed with Fe catalysis at the same concentrations in the Kinetic Regime and the Diffusion Regime. A change in the overall O_2 stoichiometry with different catalysts (Fe compared to Cu) would result in a change in NH_3 evolution even if the system were mass transfer controlled.

The concentration of free MEA appears to affect the rate of NH_3 evolution. This was measured in three different ways. For solutions of 7.0 m MEA the rate of NH_3 evolution varied with CO_2 loading as follows: $\alpha = 0.40 < 0.0 < 0.15$. This is different from the expected results based on mass transfer conditions; as α increases the viscosity and ionic strength increase, and the O_2 solubility and diffusivity should decrease. This is consistent when comparing the results for the loaded solutions, but does not explain the high rates observed in solutions with zero loading. To examine the effect of the MEA carbamate, solutions were loaded with sulfuric acid (instead of CO_2) to match both pH and CO_2 loadings. The order of the rate of NH_3 evolution as a function of equivalent CO_2 loading changed in these solutions to: $\alpha = 0.40 < 0.15 < 0.0$. This follows the trend of NH_3 evolution increasing with free MEA concentration, but

indicates the presence of the MEA carbamate can be affecting the degradation mechanism or kinetics.

For 1.0 and 2.0 m MEA at $\alpha = 0.15$, the rate of NH_3 evolution shows only a very weak dependence on the rate of agitation ($\sim 20\%$ change when agitation changes from 700 to 1400 RPM) and O_2 concentration. Under these conditions the rate appears to be approximately pseudo-first-order with O_2 and first order with MEA. The pseudo-first-order dependence on O_2 is consistent with operating in the Kinetic Regime, where the bulk liquid is saturated with O_2.

6.2.2. Effects of O_2 Mass Transfer

The rate of NH_3 evolution from solutions in the Sparged Reactor is a factor of 2 lower than the rate from the same solutions in the Agitated Reactor at 1400 RPM. This can only be explained by O_2 mass transfer limitations in the Sparged Reactor. Above 0.2 mM and 0.5 mM catalyst for the Sparged Reactor and Agitated Reactor respectively, the rate of NH_3 evolution is independent of catalyst concentration. This indicates that the system is operating in the Diffusion Regime and the rate of NH_3 evolution is controlled by the rate of O_2 absorption into the bulk solution. At concentrations above 3.5 mM Cu, the rate begins to increase again as the system enters the Fast Reaction Regime and kinetics again control the overall rate of NH_3 evolution.

Solutions of 7.0 m MEA with lean CO_2 loading show significant dependence of the rate of NH_3 evolution on the agitation rate. When no additional Fe is added to the solution, the agitation shows no effect on the rate of NH_3 evolution below 800 RPM.

The rate of NH_3 evolution from solutions with 0.14 mM Fe show a weak dependence on agitation rate over the entire range, while solutions with 0.20 mM Cu show a strong dependence on agitation increasing by a factor of 3 up to 1400 RPM.

Lean loaded amine solutions with 3.5 to 14.0 m MEA show a linear dependence of the rate of NH_3 evolution on the bulk gas O_2 concentration. For systems controlled by the rate of O_2 absorption, the rate of NH_3 evolution depends on a partial pressure driving force of O_2 concentration. A decrease in the gas concentration of O_2 results in a decrease in NH_3 evolution, which is consistent with the observed results. When the MEA concentration is increased from 7.0 to 14.0 m MEA at 1400 RPM the rate of NH_3 evolution does not significantly increase. This indicates a mass transfer limitation since the rates no longer follow the trends observed in the Kinetic Regime. As the viscosity and ionic strength increase, the O_2 solubility and diffusivity decrease, and the rate of NH_3 evolution should decrease. Since other important mass transfer parameters, like surface tension and O_2 solubility, are unknown for this system, a slight increase in the overall NH_3 evolution rate still indicates mass transfer control.

Previously reported degradation studies reported lower degradation rates under lower O_2 mass transfer conditions, indicating that these studies were also O_2 mass transfer limited. Results from the previous studies were re-analyzed to determine the mass transfer capabilities of the respective systems. To compare results from studies performed over a wide range of conditions, the maximum reported degradation rate was normalized by the bulk gas O_2 concentration, to assume mass transfer control. Results from this analysis show that the current study reports significantly higher degradation

rates under higher mass transfer conditions than any other reported study. Since the current work shows evidence of being mass transfer controlled, the previous studies are also limited by the rate of O_2 mass transfer and not the degradation kinetics.

Estimated MEA degradation rates for a typical CO_2 capture process, assuming O_2 mass transfer control, under-predict reported degradation rates. This indicates that in industrial applications the rate of oxidative degradation of MEA is likely controlled by the rate of O_2 absorption. The degradation of MEA in an industrial CO_2 absorber was predicted assuming the rate was controlled by the rate of O_2 mass transfer into the amine solution, that degradation takes place only in the packing of the absorber column, and that the bulk concentration of dissolved O_2 is negligible. This represents a worst case scenario, since all of the absorbed O_2 reacts with MEA, and an upper limit of the expected degradation rate. O_2 absorption rates were predicting using performance properties from CO_2 absorption from a natural gas fired power plant into a 7.0 m MEA solution using the model developed by Freguia (Freguia 2002). The predicted degradation rate of 0.29 to 0.73 kg MEA / mton CO_2 captured is significantly less than rates reported in the literature (ABB 1998; Arnold et al. 1982). Assuming O_2 mass transfer control, which gives higher degradation rates than kinetic controlled rates, under-predicts industrial solvent make-up rates. This indicates that under industrial conditions the rate of oxidative degradation of MEA is controlled by the rate of O_2 absorption.

6.2.3. Effects of both Degradation Kinetics and O_2 Mass Transfer

Several sets of experiments show effects of both kinetics and O_2 mass transfer, indicating the system is not fully in either the Kinetic or Diffusion Regime. One clear example of this is the speciation and pH study performed in the Sparged Reactor. The order of the rate of NH_3 evolution as a function of equivalent CO_2 loading changed in these solutions to: $\alpha = 0.40 < 0.15 < 0.0$. As the ratio of free MEA increased, the rate of NH_3 evolution increased. The solutions loaded with H_2SO_4 degrade significantly slower than the solutions with equivalent CO_2 loadings, and they also have significantly higher ionic strength. The O_2 solubility should be lower in the H_2SO_4 loaded solutions, which could account for the decreased NH_3 rates in these solutions. The order of the NH_3 evolution rates with respect to loading is different in the two systems. The rate of NH_3 evolution varied with CO_2 loading as follows: $\alpha = 0.40 < 0.0 < 0.15$. This trend does not follow the expected trends based on O_2 solubility or free MEA alone. The presence of the MEA carbamate appears to have an effect on the degradation kinetics for solutions with moderate CO_2 loadings, and the decrease in NH_3 evolution for the rich solutions is accounted for in the low concentration of free MEA in these solutions.

Experiments that vary the concentration of both MEA and O_2 also exhibit effects of both O_2 mass transfer and degradation kinetics. These experiments were performed with 0.20 mM Cu and $\alpha = 0.15$ and 1400 RPM. The rate of NH_3 evolution appears to exhibit a first order dependence on MEA between 2.0 and 7.0 m, which is consistent with a kinetic effect. Increasing the agitation rate also increases the rate of NH_3

161

evolution, which is consistent with an O_2 mass transfer effect. These solutions also show a linear, nearly first order, dependence on O_2 concentration which is the expected effect in the Diffusion Regime, but this could also be a kinetic effect where the kinetics are nearly first order with respect to O_2 concentration. Additionally, increasing the ionic strength in these solutions appears to have no effect, which is inconsistent with expected results for a system operating in either the Kinetic or Diffusion Regime.

The physical properties of the amine solution are changing significantly over these concentration ranges. Values for the surface tension, O_2 solubility, and O_2 diffusivity are unknown. Additionally, the system is operated at constant agitation rate, not constant power input, and the effect of MEA concentration on the mass transfer coefficients for the Agitated Reactor are unknown. This makes clear analysis of data in the regions that exhibit effects of both O_2 mass transfer and degradation kinetics difficult.

6.2.4. Oxidative Degradation of Other Amine Solvents

The oxidative degradation of other aqueous amine solvents is likely controlled by the rate of O_2 mass transfer. This includes solvents used in CO_2 removal from flue gas, natural gas processing, and other applications at both low and high O_2 partial pressures. The rate of O_2 absorption into the amine solution can be estimated from physical properties of the amine solutions and performance of the CO_2 absorber. The O_2 absorption rate can then be converted to an MEA degradation rate by the O_2 stoichiometry, which ranges from 0.5 to 2.5 mol O_2/mol MEA. Other alkanolamine

systems, including blended amine systems, generally have higher viscosities than MEA systems (Weiland 1996; Weiland et al. 1998). In these systems the rate of O_2 mass transfer should be even slower than the MEA solutions. Since the kinetic studies presented in Chapter 2 suggest that secondary and tertiary amines react even faster than MEA with O_2, the oxidative degradation rates of these amines should also be controlled by the rate of physical absorption of O_2 into the amine solution. This implies that for any amine system, the oxidative degradation rate can be estimated from the rate of O_2 absorption and the O_2 stoichiometry of the degradation reactions.

In blended amine solutions the amine with the fastest kinetics will react with O_2 preferentially over the amine with slower kinetics. This was observed in blends of MEA/MDEA where the MDEA was preferentially oxidized over MEA (Lawal and Idem 2005; Lawal et al. 2005). This has serious implications when selecting mixed amine solvents for use in flue gas treating applications. Sterically hindered amines and other amines with faster CO_2 reaction kinetics, such as piperazine, can be added to MEA as a promoter for CO_2 absorption (Cullinane 2005; Dang 2000). These amines are several times more expensive than MEA and can potentially preferentially react with O_2 and act as O_2 scavengers in a blended solvent. In this case, the added cost of solvent replacement from oxidative degradation becomes a much more significant factor in the overall economics of CO_2 capture than in the MEA solvent alone. For some promoted or blended solvents, the benefit to CO_2 absorption rates can be overcome by the added cost of solvent replacement, and could dictate which amine is ultimately selected to use as a rate promoter in flue gas applications.

6.3. Degradation Inhibitor Conclusions

In order to minimize oxidative degradation, several categories of additives were tested as possible inhibitors: O_2 scavengers and reaction inhibitors, chelating agents, and stable salts. Of the additives tested, only the O_2 scavengers and reaction inhibitors show enough reduction in NH_3 evolution rates to make these viable additives in an industrial application.

Inhibitor A is an inorganic compound that is not consumed, and acts as a reaction mechanism inhibitor. It was shown to be effective at inhibiting oxidative degradation catalyzed by Cu, Fe, and both Cu and Fe. At 250 mM Inhibitor A the NH_3 evolution rate was equal to the baseline rate with $\alpha = 0.15$ and at 100 mM Inhibitor A with $\alpha = 0.40$. Inhibitor A is also more effective at inhibiting Cu catalyzed degradation than Fe catalyzed degradation.

Na_2SO_3 and formaldehyde were also shown to be effective degradation inhibitors, and were independent of CO_2 loading. Like Inhibitor A, these O_2 scavengers were more effective at inhibiting Cu catalyzed degradation than Fe catalyzed degradation. Neither of the scavengers were as effective as Inhibitor A and both are consumed stoichiometrically at the rate of O_2 absorption. With Cu solutions the relative rate of NH_3 evolution decreases as more Na_2SO_3 is added to solution, up to 100 mM, resulting in a factor of 6 decrease in NH_3 evolution from 20 mM to 100 mM Na_2SO_3. Above this concentration the NH_3 evolution increases until the solubility limit between 0.8 M and 1.0 M. The rate of NH_3 evolution decreases by approximately 40% when the

Na$_2$SO$_3$ concentration is increased from 12 mM to 670 mM. The Fe system does not appear to exhibit the same minimum in NH$_3$ evolution as the Cu catalyzed degradation.

When the concentration of formaldehyde is increased from ~ 50 mM to ~ 250 mM the Cu catalyzed degradation is decreased by a factor of 5, while the Fe catalyzed degradation is only decreased by a factor of 1.5 when α = 0.15. Formaldehyde is potentially a better inhibitor than Na$_2$SO$_3$ since it is not solubility limited at higher concentrations, and appears to shut down Cu catalyzed degradation at concentrations 500 mM. Na$_2$SO$_3$ is more effective at lower concentrations than formaldehyde, but both show significant inhibiting effects at concentrations of 100 mM.

Scavengers are consumed stoichiometrically at the rate of O$_2$ mass transfer. In an industrial application the scavengers must be replaced, and the degradation products must be removed to avoid accumulation in the circulating solvent. The molar ratio of additive to NH$_3$ avoided is 5.8 and 15.5 for Na$_2$SO$_3$ and formaldehyde respectively. Since Inhibitor A is a stable compound that does not need to be continuously fed to the process, it is a very attractive additive for use in an industrial process.

While Inhibitor A, Na$_2$SO$_3$, and formaldehyde show promise as additives for reducing the oxidative degradation of MEA, the effect of these compounds on the corrosion of steel has not been tested. Although initial literature findings indicate that Inhibitor A is also a corrosion inhibitor, detailed corrosion studies must be performed before these chemicals could be used in an industrial application.

6.4. Process Design Implications

When designing and optimizing a CO_2 capture process, the rate of solvent degradation is important from an economic and environmental standpoint. The findings presented in this work have several major implications on the overall process design of an absorption/stripping system.

The concentration of O_2 in the gas to be treated should be minimized. The presence of excess O_2 has no detrimental effects on current NO_x control and flue gas desulphurization processes; however, it was shown in this work that the rate of oxidative degradation of MEA increases linearly with O_2 concentration. The combustion process should be optimized to operate as close as possible to the stoichiometric O_2 concentration. If additional dilution gas is needed, such as in natural gas fired power plants, the CO_2 recycle (O_2/CO_2 power plant) option could be a very attractive alternative for CO_2 capture applications.

The CO_2 absorber should not be over-designed. Since both CO_2 and O_2 absorption into MEA solutions is controlled by the rate of mass transfer across the liquid film, over-design of the absorber (for CO_2 absorption) will result in increased solvent degradation. Contactor selection is also important since the mass transfer coefficients in tray towers are typically much higher than packing. Oxidative degradation should occur faster with trays than packing. Most absorbers use structured or random packing to minimize pressure drop, but selection is also important for oxidative degradation. Packing should be selected that has a high wetted area, but gives

low liquid hold-up inside the tower. An increase in liquid hold-up corresponds to a larger volume of MEA that is in contact with O_2 and results in more degradation.

O_2 stripping from the absorber sump is not likely to significantly affect the rate of oxidative degradation. It was previously believed that the degradation kinetics were slow enough that the majority of the oxidative degradation occurred in the sump of the absorber. The MEA solution was assumed to be saturated with O_2 as it entered the sump, and the O_2 was consumed after the solution was no longer contacting the flue gas. One idea proposed sparging the absorber sump with an inert gas, like N_2, to strip out the dissolved O_2 before it could react with MEA (Chakravarti and Gupta 2001). Based on the findings in this work, the oxidative degradation takes place in the absorber packing, and the dissolved O_2 is sufficiently depleted by the time the MEA solution enters the absorber sump; therefore, O_2 stripping is not likely to have much affect on reducing solvent degradation.

Process equipment should be constructed from corrosion resistant materials or use non-metallic corrosion inhibitors. It has been shown that Cu and V corrosion inhibitors catalyze the rate of oxidative degradation of MEA. Building the process equipment out of materials resistant to corrosion, possibly stainless steel, FRP, or more expensive metal alloys, will increase the capital investment for the process but could result in decreased operating costs associated with solvent make-up and reclaiming. This would eliminate the need for the metal corrosion inhibitors. Using a non-metallic corrosion inhibitor that does not participate in oxidative degradation would still allow the use of carbon steel process equipment, while decreasing the rate of oxidative

degradation relative to the current process. The corrosion mechanism is not well understood; however, and serious work must be done to identify effective corrosion inhibitors that are stable and do not catalyze oxidative degradation.

Solvents with high viscosity and/or ionic strength should have lower oxidative degradation rates. While it is expected that secondary and tertiary amines have faster degradation kinetics, the decreased O_2 absorption rates in these solvents should result in an overall decrease in the rate of oxidative degradation. The use of hindered amines, promoted K_2CO_3 solvents, promoted secondary or tertiary alkanolamines, or alkanolamine blends could be very attractive alternatives to the traditional MEA process from an oxidative degradation standpoint.

6.5. Recommendations

6.5.1. Characterization of Agitated Reactor Mass Transfer Coefficients

The mass transfer characteristics of the Agitated Reactor should be measured and correlated. The O_2 absorption rate was measured in the Sparged Reactor by measuring the rate of sulfite oxidation in concentrated $MgSO_4$ (aq.), but the upper limit for the rate of O_2 absorption in the Agitated Reactor was never independently measured or predicted. Extensive amounts of literature are available on predicting mass transfer coefficients in agitated reactors that do not vortex or have gas back mixing (Chapman et al. 1982; Gaddis 1999; Garcia-Ochoa and Gomez 1998; Linek and Vacek 1981; Van't Riet 1979). Most of these studies explicitly state that correlations for the mass transfer coefficients are no longer valid for reactors that form a vortex.

Several of the literature studies state that measuring mass transfer coefficients in one solvent and extending the correlations to other solvents, even solvent with similar physical properties, can result in significant error in estimating mass transfer coefficients. O_2 absorption rates cannot be measured in situ with MEA solutions since the O_2 immediately begins to react with MEA. In order to pick a suitable solvent to measure equivalent O_2 uptake rates, data should be collected to provide a better understanding of the physical properties of MEA solutions. Specifically, measurements should be made to measure the surface tension of loaded MEA solutions. This is a difficult measurement and has not been reproducible in the past (Weiland 1996).

The O_2 solubility in MEA solutions is also currently unknown. In order to accurately model absorption rate in a system that is in the Diffusion Regime, the bulk liquid concentration of O_2 must be known. Two different methods were used unsuccessfully in the study to attempt to measure O_2 solubility in MEA. Two different dissolved O_2 electrodes were used as well as a fiber optic O_2 sensor from Ocean Optics, Inc. The O_2 electrodes gave slow response times and samples had to be withdrawn from the reactor to perform the measurements. Since the O_2 reactions are very fast, most of the O_2 was gone by the time the measurement was made and an accurate value of the dissolved O_2 could not be made. The fiber optic O_2 sensor was found to be chemically incompatible with the MEA solution. This system would have allowed for in-situ measurements of dissolved O_2 in the Agitated Reactor up to 80°C, but the protective overcoat on the probe was dissolved by the amine. Several different configurations were used and none of them worked. A new formulation that allegedly

is compatible with the amine may be forthcoming from Ocean Optics, Inc. This system could possibly be used to measure O_2 solubility, but other methods might have to be used.

6.5.2. Determination of O_2 Stoichiometry

The most important piece of information missing from this study is the value of the O_2 stoichiometry for Cu and Fe catalyzed reactions. This parameter is essential for estimating degradation rates in industrial applications and extraction of kinetics information from the mass transfer controlled data. A known value for the O_2 stoichiometry can also help to accurately explain the rate differences observed for Cu and Fe catalyzed solutions in the Diffusion Regime. Liquid analysis for degradation products is extremely difficult and development of analytical methods is slow and tedious. Difficulties of this type of analysis are evident from any of the studies that attempted to perform liquid analysis (Alawode 2005; Bello and Idem 2005; Jones 2003; Lawal and Idem 2005; Lawal et al. 2005; Supap 1999).

In order to accumulate degradation products to concentrations high enough for accurate detection longer time experiments must be performed. This is currently limited in the Agitated Reactor by control of the water balance. The saturator bomb must be refilled every 1-2 hours and the system cannot be run unattended. Modifications must be made to correct this, or a new apparatus must be built. Some of the current analytical methods that can be used for detection of various liquid phase degradation products are: ion-chromatography, gas-chromatography/mass spec, FT-IR,

and NMR. NMR is the most powerful tool for component identification but is hindered by the presence of paramagnetic ions such as Fe and Cu which cause severe peak broadening at low concentrations.

The O_2 stoichiometry should be determined for Cu alone, Fe alone, and in the mixed catalyst system. Additionally, since Inhibitor A acts as a reaction inhibitor, the effect of this additive on the O_2 stoichiometry should be determined. Experiments should be performed up to the boiling point of the amine solution to account for possible reactions encountered in the solvent reclaimer. Experiments should be run with and without O_2 and in loaded and unloaded MEA solutions.

6.5.3. Kinetic Study

An experimental study should be performed to quantify the kinetics for the rate of formation of the major degradation products after they have been identified by the O_2 stoichiometry study. The role of O_2 and metal catalysts is not well defined in the degradation mechanisms presented in Chapter 2. The oxidation state of the metals in solution as well as what amine species the metal is complexed to can have a significant affect on the catalytic properties of the metal. Rate constants and activation energies for the primary reactions will allow for direct calculation of changing O_2 stoichiometry based on the selectivity of the reactions at different process conditions. A complete understanding of the degradation mechanism will allow for selection of additional reaction inhibitors, potentially more environmentally friendly than the three additives determined in the current work, as possible additives for use in an industrial application.

6.5.4. Computer Modeling

The AspenPlus simulation developed by Freguia (Freguia 2002) allows for prediction of process performance of CO_2 absorption with MEA. The addition of reaction kinetics for the primary degradation reaction into this model would allow for more accurate estimation of oxidative degradation rates under actual operating conditions in a CO_2 capture process. This model could be used for a systematic study to identify beneficial process modifications to minimize the degradation rates. Additionally, this model would allow for more accurate quantification of solvent make-up rates and would improve the accuracy of the CO_2 capture economics. The economic impact of degradation inhibitors could also accurately be modeled and would allow for advanced screening of degradation inhibitors based on overall process economics.

6.5.5. General Laboratory Considerations

Several experimental difficulties were encountered throughout this work and should be addressed if the Agitated Reactor is used for additional future studies. The first issue is the water balance. The current pre-saturator is a small calorimeter bomb that must be refilled every 1–2 hours. If the bomb is filled too full the high gas rate entrains the liquid and floods the reactor, but if the liquid level in the bomb is too low the gas does not saturate, which results in water loss from the reactor. A better saturator should be designed with automatic liquid level control. If this system worked properly, the Agitated Reactor could be run unattended, which would allow for longer experiments to be conducted.

The current apparatus is sealed using a rubber septum around the agitator shaft. This septum has to be replaced at least every day or it will tear and allow more water to escape from the reactor. When the septum tears the concentration of all of the measured compounds decreases in the FT-IR significantly, and the experiment must be interrupted so the septum can be replaced. Replacing the seal with a more compatible tighter seal will eliminate this problem as well as allow the reactor to be sealed and operated at elevated temperatures and pressure.

The de-ionized (DI) water supply at the university is connected to the cooling water system, which is made of copper tubing. Since Cu has been shown to be a potent catalyst for oxidative degradation, contamination of Cu in the DI water can lead to increased degradation rates in the experiments. This is a possible explanation for baseline fluctuations encountered during the current study. It is recommended that future experiments be performed using ultra-high purity water, the same quality used for ion-chromatography, in order to reduce the potential of un-quantified metal contamination.

The current system uses house air as a source of oxygen. It is recommended that future studies use a blend of N_2, O_2, and CO_2. NO_x species have been observed at low concentrations throughout the course of this study and the source of the NO_x has not been determined. Some of the NO_x could be formed during the degradation reactions, but it is more probable that the source is from the house air supply. NOx are known free radicals, which can initiate the degradation reactions, and also form nitrosamines by reacting with secondary amines (Fessenden and Fessenden 1994). By artificially

creating a synthesis gas from pure gas cylinders of N_2, O_2, and CO_2 the possibility of NO_x contamination is significantly reduced and the presence of these species in the gas product can be attributed to formation in the reactor.

Appendix A: FT-IR Reference Spectra

This appendix presents an example of a reference FT-IR spectrum for each compound included in the analysis of gas-phase degradation products for both the Sparged and Agitated Reactors. Details on sample temperature, concentration and path length are included for each sample spectrum.
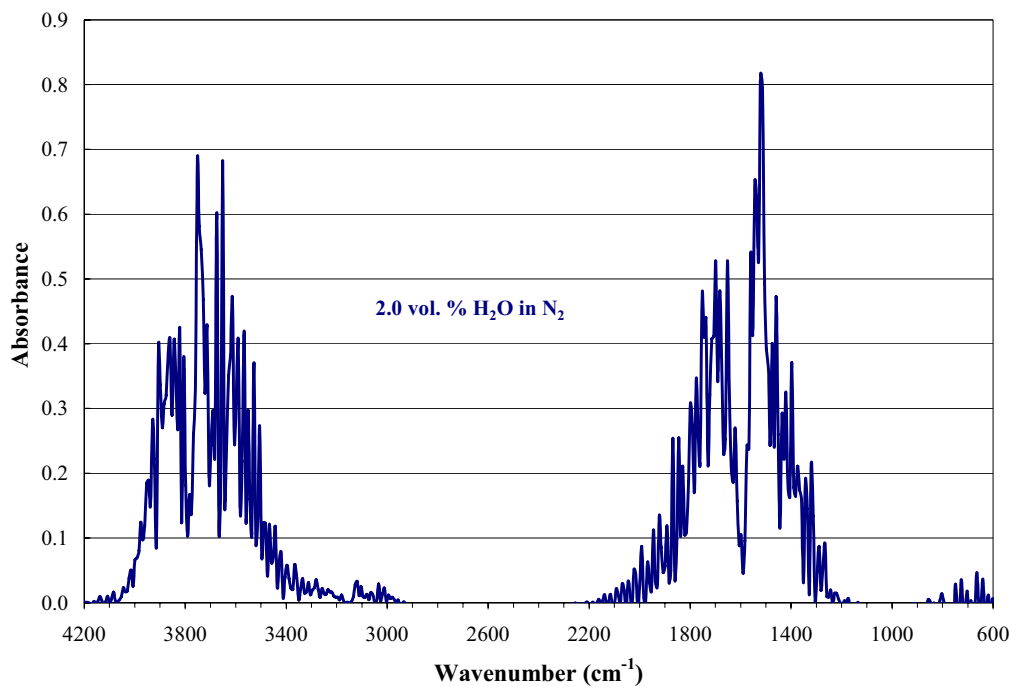
Figure A.1 Water Reference Spectrum (2.0 vol. %, 180°C, 5 m path length)
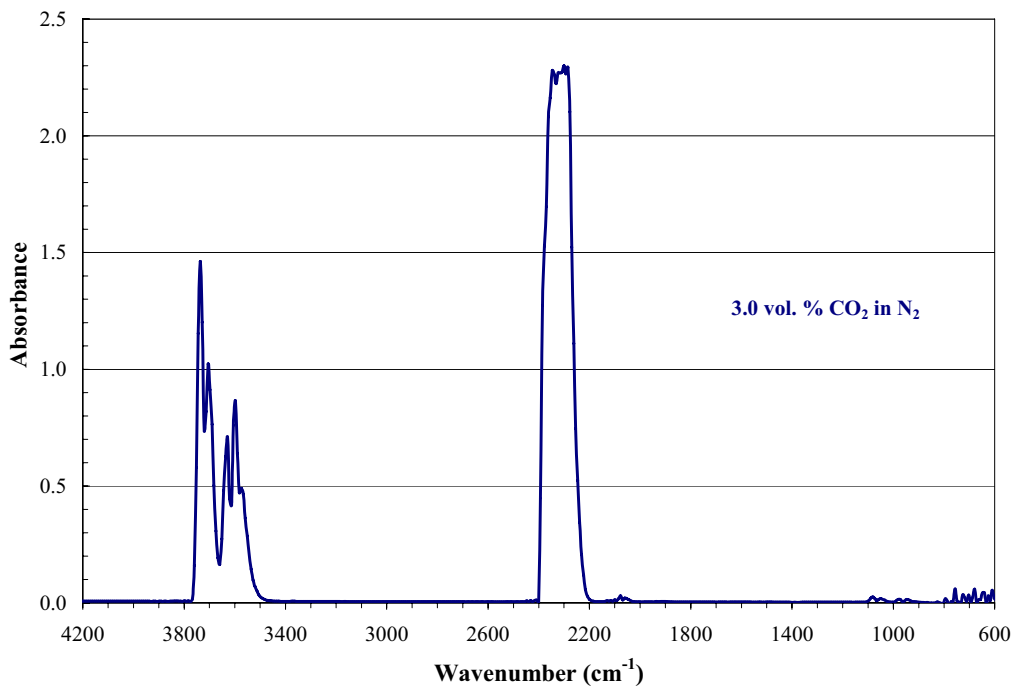
Figure A.2 CO₂ Reference Spectrum (3.0 vol. %, 180°C, 5 m path length)
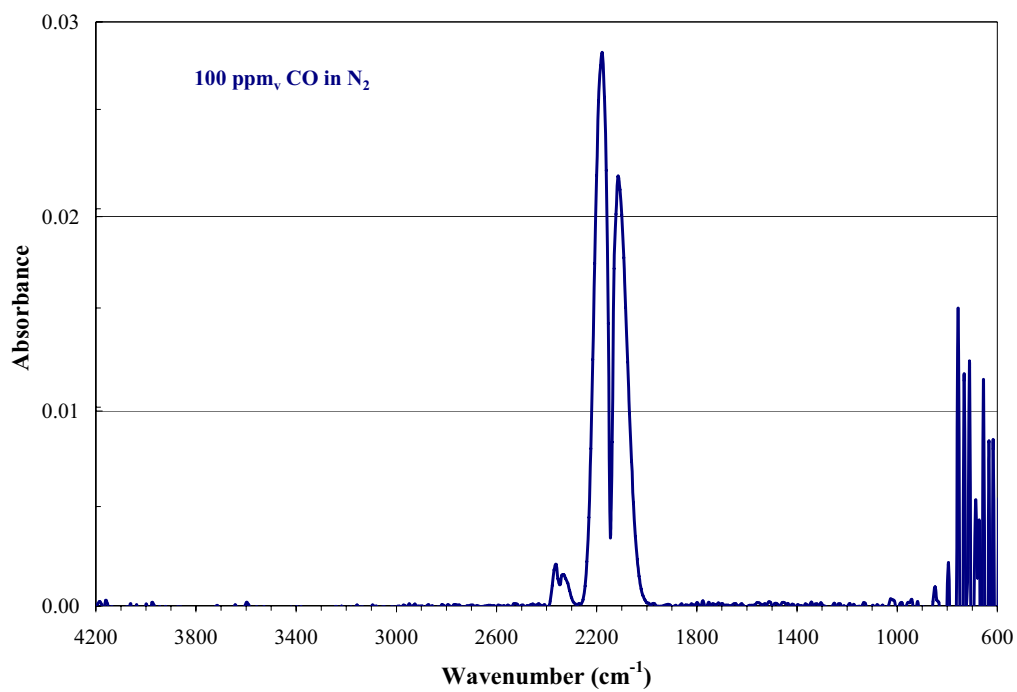
Figure A.3 CO Reference Spectrum (100 ppm$_v$, 180°C, 5 m path length)
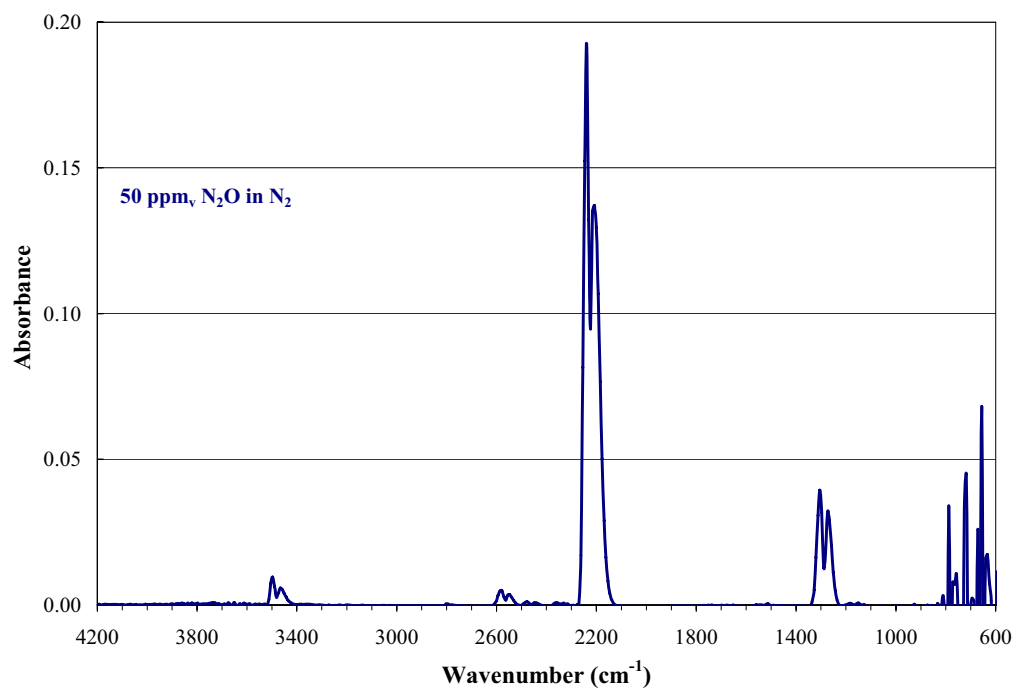
Figure A.4 N$_2$O Reference Spectrum (50 ppm$_v$, 180°C, 5 m path length)

177
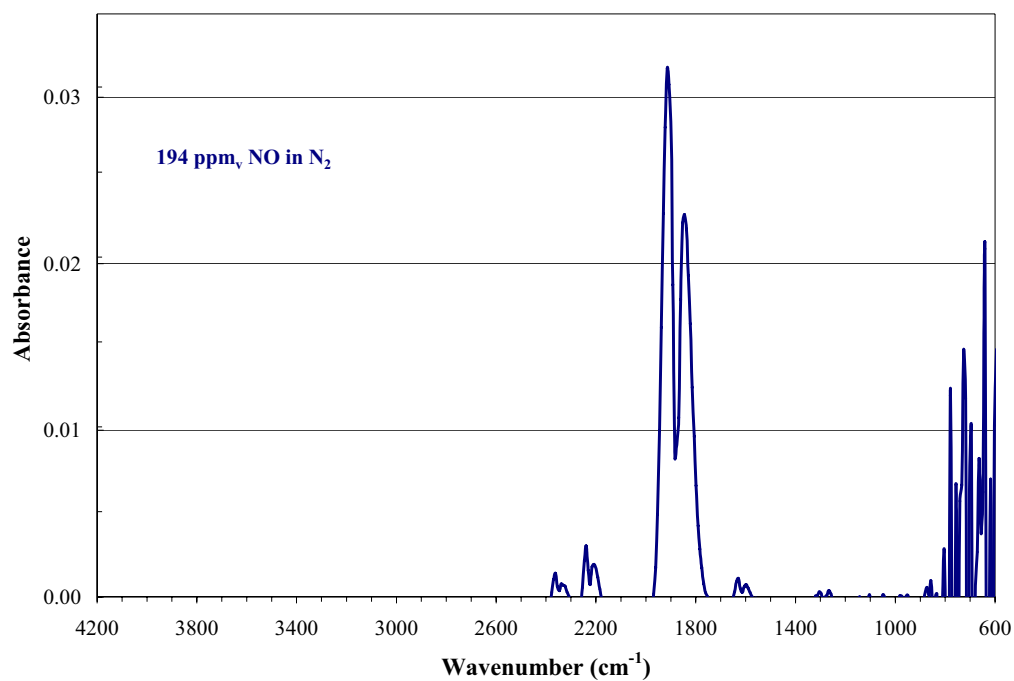
Figure A.5 NO Reference Spectrum (194 ppm$_v$, 180°C, 5 m path length)
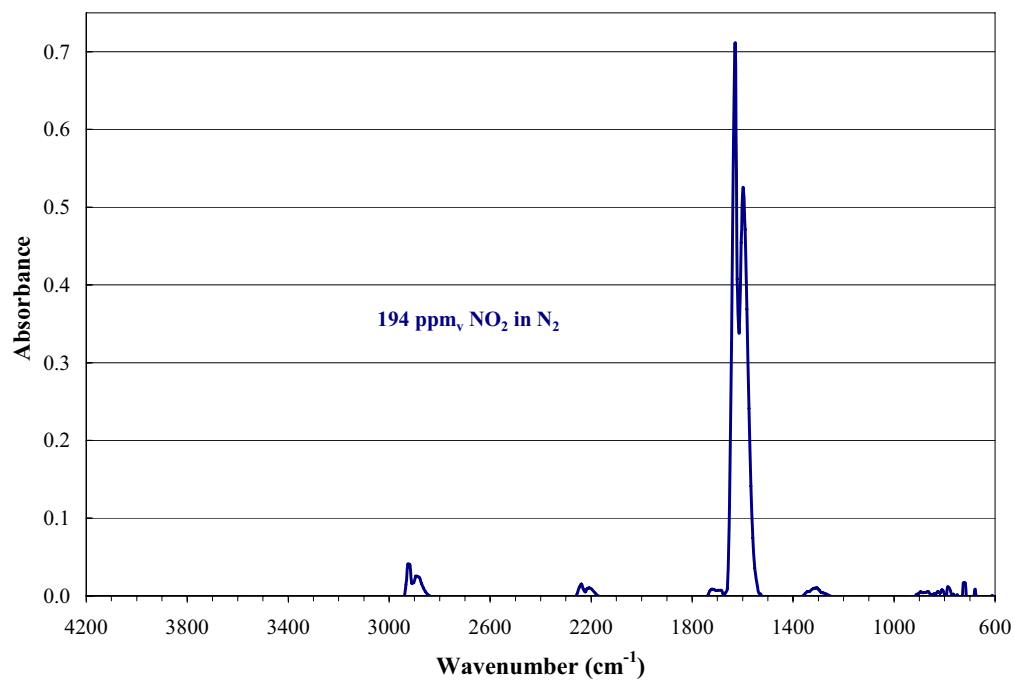
Figure A.6 NO$_2$ Reference Spectrum (194 ppm$_v$, 180°C, 5 m path length)

178
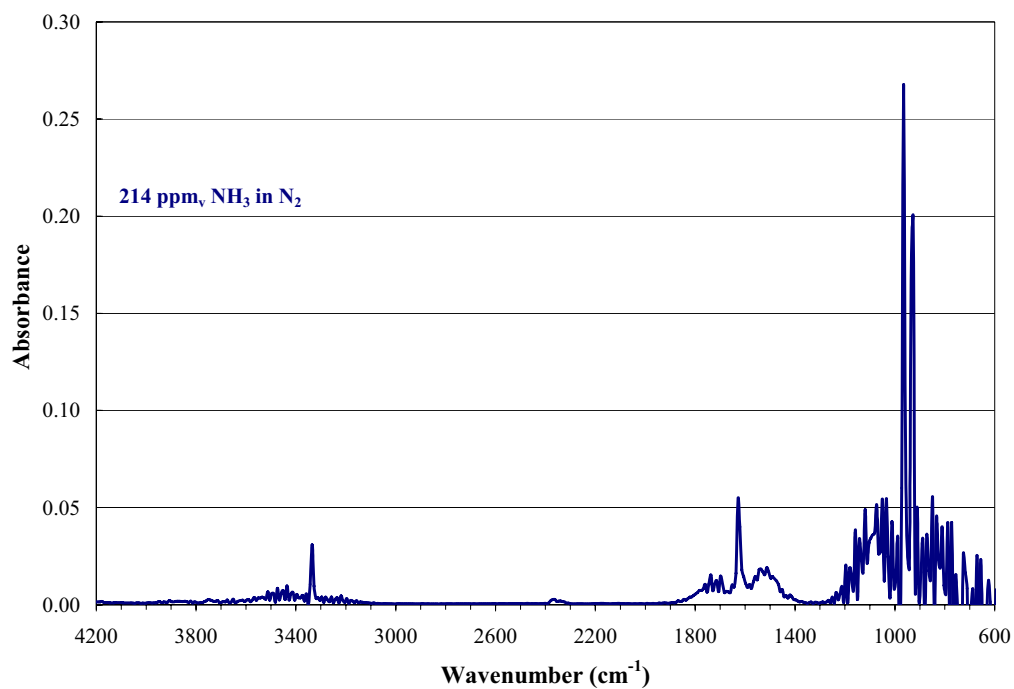
Figure A.7 NH$_3$ Reference Spectrum (214 ppm$_v$, 180°C, 5 m path length)
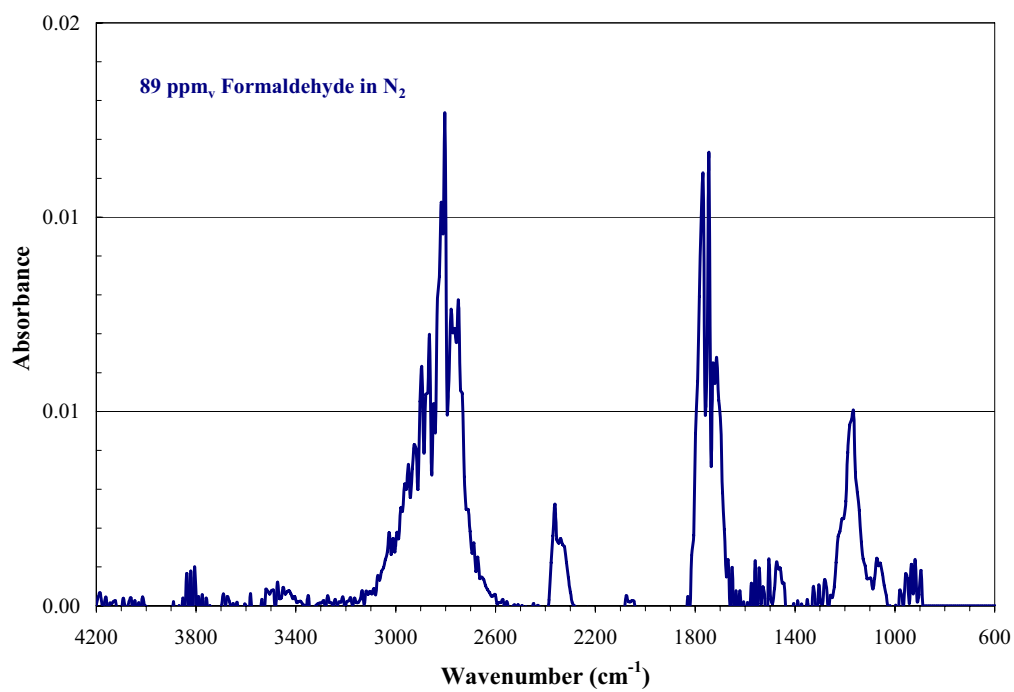
Figure A.8 Formaldehyde Reference Spectrum (89 ppm$_v$, 180°C, 2.4 m path length)
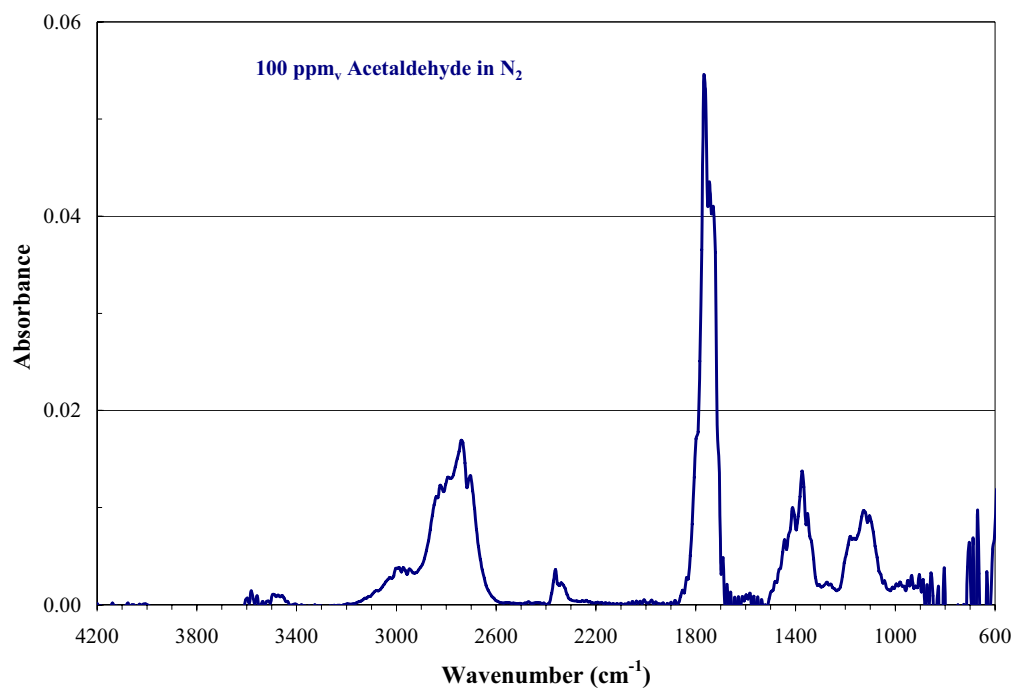
Figure A.9 Acetaldehyde Reference Spectrum (100 ppm$_v$, 180°C, 2.5 m path length)
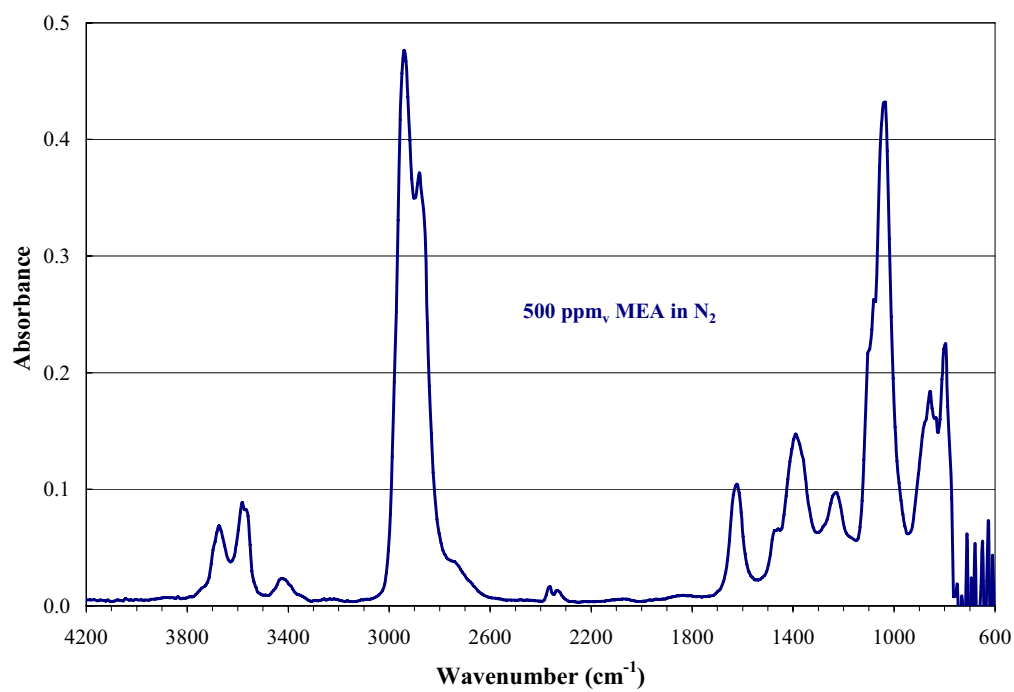
Figure A.10 MEA Reference Spectrum (500 ppm$_v$, 180°C, 5 m path length)
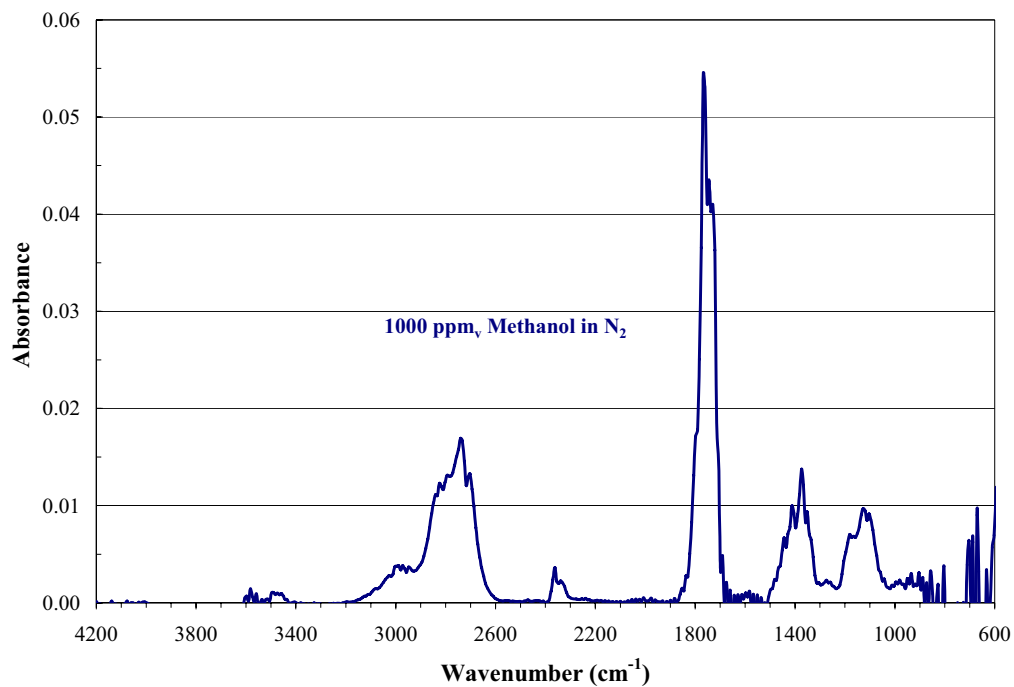
Figure A.11 Methanol Reference Spectrum (1000 ppm$_v$, 180°C, 5 m path length)
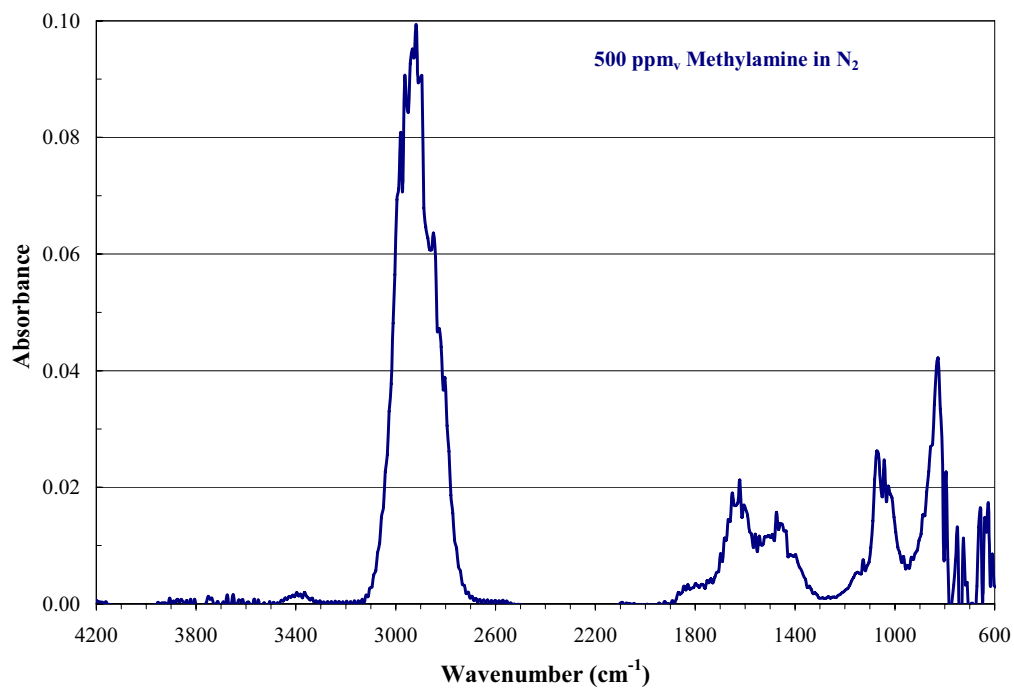
Figure A.12 Methylamine Reference Spectrum (500 ppm$_v$, 180°C, 40 cm path length)

181
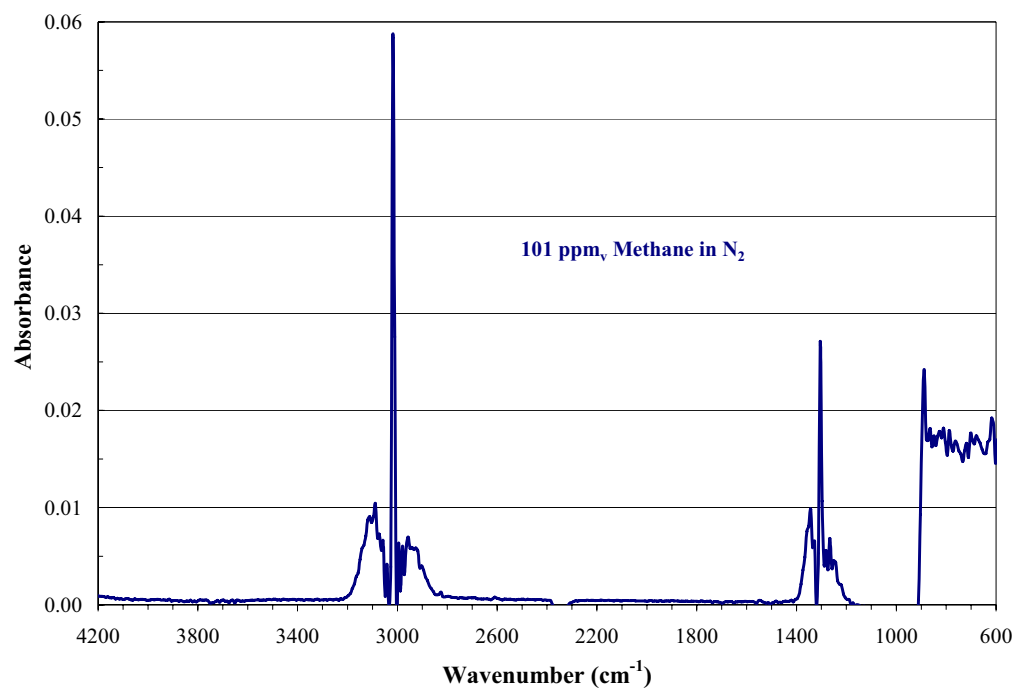
Figure A.13 Methane Reference Spectrum (101 ppm$_v$, 180°C, 2.5 m path length)

Appendix B: FT-IR Multi-Component Analysis Methods

This appendix documents the input files for the Calcmet™ software for the two analysis methods developed in this study. The method for the Agitated Reactor is named Degradation_20040825.LIB, and the method for the Sparged Reactor is named OLD-MEA-Degradation.LIB. Unless otherwise notated, reference files are located in the folder C:\Library01235. These reference spectra were generated on the FT-IR analyzer used in this study. Reference spectra from the folder C:\Library180 were generated on other analyzers at 180°C, and the path length is noted within the files.

Table B.1 Summary of Component Analysis Input Data for Calcmet Application Degradation_20040825.LIB (Agitated Reactor Analysis Method)

Compound	Conc.	Measuring Range 1 cm^{-1}		Abs. limit	Measuring Range 2 cm^{-1}		Abs. limit	Measuring Range 3 cm^{-1}		Abs. limit	Refs.
Water	vol. %	1883	2161	1.0	3142	3319	0.5				13
CO_2	vol. %	980	1130	1.0	1999	2208	0.5	2450	2650	0.5	3
CO	ppm_v	2007	2207	0.5	2624	2750	1.0				8
N_2O	ppm_v	2107	2246	0.5	2647	2900	0.5				5
NO	ppm_v	1760	1868	0.8	1869	1991	0.8	2550	2650	1.0	4
NO_2	ppm_v	2550	2933	0.5							3
NH_3	ppm_v	910	964	1.0	980	1196	0.5	3219	3396	0.5	4
Formaldehyde	ppm_v	988	1111	1.0	2450	2600	0.6	2650	3211	0.5	3
Acetaldehyde	ppm_v	1034	1243	1.0	2638	2916	1.0				3
MEA	ppm_v	980	1119	1.0	2624	3150	1.0				1
Methanol	ppm_v	980	1281	1.0	2450	2650	1.0	2763	3304	1.0	7
Methylamine	ppm_v	980	1303	1.0	2450	2650	1.0	2800	3450	1.0	3
CH_4	ppm_v	2833	3203	0.5	3018	3203	0.5				2

Table B.2 Summary of Component Analysis Input Data for Calcmet Application OLD-MEA-Degradation.LIB (Sparged Reactor Analysis Method)

Compound	Conc.	Measuring Range 1			Measuring Range 2			Refs.
		cm^{-1}		Abs. limit	cm^{-1}		Abs. limit	
Water	vol. %	1922	2146	1.0	3049	3250	0.5	13
CO_2	vol. %	918	1119	1.0	1950	2130	1.0	11
CO	ppm_v	2007	2099	0.5	2624	2750	1.0	8
N_2O	ppm_v	920	1119	1.0	2647	2900	0.5	3
NO	ppm_v	1869	1991	0.8				5
NO_2	ppm_v	2550	2933	0.5				2
NH_3	ppm_v	910	1000	1.0				5
Formaldehyde	ppm_v	1134	1204	1.0	2650	3211	0.5	1
Acetaldehyde	ppm_v	2638	2916	1.0				2
MEA	ppm_v	2624	3150	1.0	940	1119	1.0	1

Table B.3 Input File for Calcmet™ Application Degradation_20040825.LIB
(Agitated Reactor Analysis Method)

ComponentNumber = 1
ComponentName = Water vapor H2O
ConcentrationUnit = vol-%
ActiveLines = All
AutoAnalyze = 1 (1=Yes)
OutputChannel = 0
ViewResults = 1 (1=Yes)
AllowNegative = 0 (1=Yes)
ConversionMultiplier = 1
ResultSmoothing = 0
RangeSetting = 0
Range1 = 0 5
Range2 = 0 25
AlarmLimits = 0 25
AlarmSound = 0
Compensations = 1 1 1 0 -11
Calibrations = 0 0 4 2
ResidualWarningLimit = 0.01
ResidualErrorLimit = 0.02
UseDoubleReferences = 1 (1=Yes)
AutoInterferenceUpdate = 0 0.001
DefaultReference = 1
BaselineCorrections = 1 0
MethodNumber = 0 (1=Yes)
AnalysisArea = 1 1883 2161 1
AnalysisArea = 0 2092 2223 1
AnalysisArea = 1 3142 3319 0.5
Interference = 0110110110000000000000001
CrossInterferences = 0 0 0 0 0
ReferenceFile = C:\Library 01253\Water Ref - 20040616\H2O_01.ref
ReferenceFile = C:\Library 01253\Water Ref - 20040616\H2O_02.ref
ReferenceFile = C:\Library 01253\Water Ref - 20040616\H2O_03.ref
ReferenceFile = C:\Library 01253\Water Ref - 20040616\H2O_04.ref
ReferenceFile = C:\Library 01253\Water Ref - 20040616\H2O_06.ref
ReferenceFile = C:\Library 01253\Water Ref - 20040616\H2O_08.ref
ReferenceFile = C:\Library 01253\Water Ref - 20040616\H2O_10.ref
ReferenceFile = C:\Library 01253\Water Ref - 20040616\H2O_12.ref
ReferenceFile = C:\Library 01253\Water Ref - 20040616\H2O_14.ref
ReferenceFile = C:\Library 01253\Water Ref - 20040616\H2O_16.ref
ReferenceFile = C:\Library 01253\Water Ref - 20040616\H2O_18.ref

ReferenceFile = C:\Library 01253\Water Ref - 20040616\H2O_20.ref
ReferenceFile = C:\Library 01253\Water Ref - 20040616\H2O_22.ref
ReferenceFile = C:\Library 01253\Water Ref - 20040616\H2O_24.ref
ReferenceFile = C:\Library 01253\Water Ref - 20040616\H2O_26.ref
ReferenceFile = C:\Library 01253\Water Ref - 20040616\H2O_28.ref
ReferenceFile = C:\Library 01253\Water Ref - 20040616\H2O_30.ref

---

ComponentNumber = 2
ComponentName = Carbon dioxide CO2
ConcentrationUnit = vol-%
ActiveLines = All
AutoAnalyze = 1 (1=Yes)
OutputChannel = 0
ViewResults = 1 (1=Yes)
AllowNegative = 0 (1=Yes)
ConversionMultiplier = 1
ResultSmoothing = 0
RangeSetting = 0
Range1 = 0 1
Range2 = 0 5
AlarmLimits = 0 30
AlarmSound = 0
Compensations = 1 1 1 0 -11
Calibrations = 0 4 0 2
ResidualWarningLimit = 0.01
ResidualErrorLimit = 0.02
UseDoubleReferences = 0 (1=Yes)
AutoInterferenceUpdate = 1 0.01
DefaultReference = 3
BaselineCorrections = 1 0
MethodNumber = 0 (1=Yes)
AnalysisArea = 1 980 1130 1
AnalysisArea = 1 2450 2650 0.5
AnalysisArea = 1 1999 2208 0.5
Interference = 1010101110000000000000100111
CrossInterferences = 0 0 0 0 0
ReferenceFile = CO2_03.ref
ReferenceFile = C:\Library 01253\George's References\CO2_1.0vol%.ref
ReferenceFile = C:\Library 01253\George's References\CO2_0.15vol%.ref

---

ComponentNumber = 3
ComponentName = Carbon monoxide CO
ConcentrationUnit = ppm

ActiveLines = All
AutoAnalyze = 1 (1=Yes)
OutputChannel = 0
ViewResults = 1 (1=Yes)
AllowNegative = 0 (1=Yes)
ConversionMultiplier = 1
ResultSmoothing = 0
RangeSetting = 0
Range1 = 0 10
Range2 = 0 500
AlarmLimits = 0 5000
AlarmSound = 0
Compensations = 1 1 1 0 -11
Calibrations = 0 0 4 2
ResidualWarningLimit = 0.01
ResidualErrorLimit = 0.02
UseDoubleReferences = 0 (1=Yes)
AutoInterferenceUpdate = 1 0.001
DefaultReference = 2
BaselineCorrections = 1 0
MethodNumber = 0 (1=Yes)
AnalysisArea = 1 2007 2207 0.5
AnalysisArea = 1 2624 2750 1
AnalysisArea = 0 2550 2600 1
Interference = 110011110000000000001100111
CrossInterferences = 0 0 0 0 0
ReferenceFile = CO_998.ref
ReferenceFile = CO_11.ref
ReferenceFile = CO_200.ref
ReferenceFile = CO_402.ref
ReferenceFile = CO_51.ref
ReferenceFile = CO_602.ref
ReferenceFile = CO_805.ref
ReferenceFile = CO_100.ref

ComponentNumber = 5
ComponentName = Nitrous oxide N2O
ConcentrationUnit = ppm
ActiveLines = All
AutoAnalyze = 1 (1=Yes)
OutputChannel = 0
ViewResults = 1 (1=Yes)
AllowNegative = 1 (1=Yes)

ConversionMultiplier = 1
ResultSmoothing = 0
RangeSetting = 0
Range1 = 0 100
Range2 = 0 500
AlarmLimits = 0 100000
AlarmSound = 1
Compensations = 1 1 1 0 -11
Calibrations = 0 0 0 2
ResidualWarningLimit = 0.01
ResidualErrorLimit = 0.02
UseDoubleReferences = 0 (1=Yes)
AutoInterferenceUpdate = 1 0.001
DefaultReference = 5
BaselineCorrections = 1 0
MethodNumber = 0 (1=Yes)
AnalysisArea = 1 2107 2246 0.5
AnalysisArea = 1 2647 2900 0.5
AnalysisArea = 0 2400 2700 1
Interference = 11110111000000000000110011101
CrossInterferences = 0 0 0 0 0
ReferenceFile = C:\Library 01253\George's References\N2O_100000ppmG.ref
ReferenceFile = C:\Library 01253\George's References\N2O_4882ppmG.ref
ReferenceFile = C:\Library 01253\George's References\N2O_50000ppmG.ref
ReferenceFile = C:\Library180\Nitrous oxide N2O 122 ppm.ref
ReferenceFile = C:\Library180\Nitrous oxide N2O 0050 ppm.ref

ComponentNumber = 6
ComponentName = Nitrogen monoxide NO
ConcentrationUnit = ppm
ActiveLines = All
AutoAnalyze = 1 (1=Yes)
OutputChannel = 0
ViewResults = 1 (1=Yes)
AllowNegative = 1 (1=Yes)
ConversionMultiplier = 1
ResultSmoothing = 0
RangeSetting = 0
Range1 = 0 20
Range2 = 0 150
AlarmLimits = 0 1000
AlarmSound = 0
Compensations = 1 1 1 0 -11

Calibrations = 0 0 4 2
ResidualWarningLimit = 0.01
ResidualErrorLimit = 0.02
UseDoubleReferences = 0 (1=Yes)
AutoInterferenceUpdate = 0 0.001
DefaultReference = 3
BaselineCorrections = 1 0
MethodNumber = 0 (1=Yes)
AnalysisArea = 1 1760 1868 0.8
AnalysisArea = 1 1869 1991 0.8
AnalysisArea = 1 2550 2650 1
Interference = 11101001100000000000001001
CrossInterferences = 0 0 0 0 0
ReferenceFile = NO_99.ref
ReferenceFile = NO_194.ref
ReferenceFile = NO_50.ref
ReferenceFile = NO_10.ref

ComponentNumber = 7
ComponentName = Nitrogen dioxide NO2
ConcentrationUnit = ppm
ActiveLines = All
AutoAnalyze = 1 (1=Yes)
OutputChannel = 0
ViewResults = 1 (1=Yes)
AllowNegative = 0 (1=Yes)
ConversionMultiplier = 1
ResultSmoothing = 0
RangeSetting = 0
Range1 = 0 20
Range2 = 0 1000
AlarmLimits = 0 1000
AlarmSound = 0
Compensations = 1 1 1 0 -11
Calibrations = 0 0 4 2
ResidualWarningLimit = 0.01
ResidualErrorLimit = 0.02
UseDoubleReferences = 0 (1=Yes)
AutoInterferenceUpdate = 1 0.001
DefaultReference = 2
BaselineCorrections = 1 0
MethodNumber = 0 (1=Yes)
AnalysisArea = 0 941 1397 1

190

AnalysisArea = 0 1497 1706 1.8
AnalysisArea = 1 2550 2933 0.5
Interference = 110110010000000000000110011101
CrossInterferences = 0 0 0 0 0
ReferenceFile = C:\Library180\Nitrogen dioxide NO2 0050 ppm.ref
ReferenceFile = C:\Library180\Nitrogen dioxide NO2 0005 ppm.ref
ReferenceFile = NO2_194.ref

ComponentNumber = 9
ComponentName = Ammonia NH3
ConcentrationUnit = ppm
ActiveLines = All
AutoAnalyze = 1 (1=Yes)
OutputChannel = 0
ViewResults = 1 (1=Yes)
AllowNegative = 0 (1=Yes)
ConversionMultiplier = 1
ResultSmoothing = 0
RangeSetting = 0
Range1 = 0 100
Range2 = 0 300
AlarmLimits = 0 500
AlarmSound = 0
Compensations = 1 1 1 0 -11
Calibrations = 0 4 0 2
ResidualWarningLimit = 0.01
ResidualErrorLimit = 0.02
UseDoubleReferences = 0 (1=Yes)
AutoInterferenceUpdate = 1 0.001
DefaultReference = 3
BaselineCorrections = 1 0
MethodNumber = 0 (1=Yes)
AnalysisArea = 1 910 964 1
AnalysisArea = 1 980 1196 0.5
AnalysisArea = 1 3219 3396 0.5
Interference = 11001011000000000000001100111
CrossInterferences = 0 0 0 0 0
ReferenceFile = NH3_11.ref
ReferenceFile = NH3_3.ref
ReferenceFile = C:\Library180\Ammonia NH3 0214 ppm.ref
ReferenceFile = C:\Library180\Ammonia NH3 0531 ppm.ref

ComponentNumber = 21
ComponentName = Formaldehyde
ConcentrationUnit = ppm
ActiveLines = All
AutoAnalyze = 1 (1=Yes)
OutputChannel = 0
ViewResults = 1 (1=Yes)
AllowNegative = 1 (1=Yes)
ConversionMultiplier = 1
ResultSmoothing = 0
RangeSetting = 0
Range1 = 0 10
Range2 = 0 100
AlarmLimits = 0 100
AlarmSound = 0
Compensations = 1 1 1 0 -11
Calibrations = 0 0 4 2
ResidualWarningLimit = 0.01
ResidualErrorLimit = 0.02
UseDoubleReferences = 0 (1=Yes)
AutoInterferenceUpdate = 1 0.001
DefaultReference = 1
BaselineCorrections = 1 0
MethodNumber = 0 (1=Yes)
AnalysisArea = 1 988 1111 1
AnalysisArea = 1 2450 2600 0.6
AnalysisArea = 1 2650 3211 0.5
Interference = 11011011100000000000010011101
CrossInterferences = 0 0 0 0 0
ReferenceFile = C:\Library180\HCHO_10.ref
ReferenceFile = C:\Library180\HCHO_50.ref
ReferenceFile = C:\Library180\Formaldehyde CH2O.ref

ComponentNumber = 22
ComponentName = Acetaldehyde
ConcentrationUnit = ppm
ActiveLines = All
AutoAnalyze = 1 (1=Yes)
OutputChannel = 0
ViewResults = 1 (1=Yes)
AllowNegative = 0 (1=Yes)
ConversionMultiplier = 1
ResultSmoothing = 0

RangeSetting = 0
Range1 = 0 10
Range2 = 0 100
AlarmLimits = 0 100
AlarmSound = 0
Compensations = 1 1 1 0 -11
Calibrations = 0 4 0 2
ResidualWarningLimit = 0.01
ResidualErrorLimit = 0.02
UseDoubleReferences = 0 (1=Yes)
AutoInterferenceUpdate = 1 0.001
DefaultReference = 3
BaselineCorrections = 1 0
MethodNumber = 0 (1=Yes)
AnalysisArea = 1 1034 1243 1
AnalysisArea = 0 1798 2038 0.5
AnalysisArea = 1 2638 2916 1
Interference = 110110111000000000000100011101
CrossInterferences = 0 0 0 0 0
ReferenceFile = C:\Library180\Acetaldehyde C2H4O 0500 ppm.ref
ReferenceFile = C:\Library180\Acetaldehyde C2H4O 0100 ppm.ref
ReferenceFile = C:\Library180\Acetaldehyde C2H4O_05.ref

ComponentNumber = 25
ComponentName = MEA
ConcentrationUnit = ppm
ActiveLines = All
AutoAnalyze = 1 (1=Yes)
OutputChannel = 0
ViewResults = 1 (1=Yes)
AllowNegative = 0 (1=Yes)
ConversionMultiplier = 1
ResultSmoothing = 0
RangeSetting = 0
Range1 = 0 100
Range2 = 0 250
AlarmLimits = 0 250
AlarmSound = 0
Compensations = 1 1 1 0 -11
Calibrations = 0 0 0 2
ResidualWarningLimit = 0.01
ResidualErrorLimit = 0.02
UseDoubleReferences = 0 (1=Yes)

AutoInterferenceUpdate = 1 0.005
DefaultReference = 1
BaselineCorrections = 1 0
MethodNumber = 0 (1=Yes)
AnalysisArea = 1 2624 3150 1
AnalysisArea = 1 980 1119 1
AnalysisArea = 0 3500 4000 1
Interference = 110110111000000000000110001101
CrossInterferences = 0 0 0 0 0
ReferenceFile = C:\Library 01253\George's References\MEA_500.ref

ComponentNumber = 26
ComponentName = Methanol
ConcentrationUnit = Auto
ActiveLines = All
AutoAnalyze = 1 (1=Yes)
OutputChannel = 0
ViewResults = 1 (1=Yes)
AllowNegative = 1 (1=Yes)
ConversionMultiplier = 1
ResultSmoothing = 0
RangeSetting = 0
Range1 = 0 50
Range2 = 0 500
AlarmLimits = 0 1000
AlarmSound = 0
Compensations = 1 1 1 0 -11
Calibrations = 0 0 4 2
ResidualWarningLimit = 0.01
ResidualErrorLimit = 0.02
UseDoubleReferences = 0 (1=Yes)
AutoInterferenceUpdate = 1 0.005
DefaultReference = 3
BaselineCorrections = 1 0
MethodNumber = 0 (1=Yes)
AnalysisArea = 1 980 1281 1
AnalysisArea = 1 2450 2650 1
AnalysisArea = 1 2763 3304 1
Interference = 110110111000000000000110010101
CrossInterferences = 0 0 0 0 0
ReferenceFile = Methanol_5000.ref

ComponentNumber = 27

ComponentName = Methylamine
ConcentrationUnit = Auto
ActiveLines = All
AutoAnalyze = 1 (1=Yes)
OutputChannel = 0
ViewResults = 1 (1=Yes)
AllowNegative = 1 (1=Yes)
ConversionMultiplier = 1
ResultSmoothing = 0
RangeSetting = 0
Range1 = 0 10
Range2 = 0 100
AlarmLimits = 0 100
AlarmSound = 0
Compensations = 1 1 1 0 -11
Calibrations = 0 0 4 2
ResidualWarningLimit = 0.01
ResidualErrorLimit = 0.02
UseDoubleReferences = 0 (1=Yes)
AutoInterferenceUpdate = 1 0.001
DefaultReference = 2
BaselineCorrections = 1 0
MethodNumber = 0 (1=Yes)
AnalysisArea = 1 980 1303 1
AnalysisArea = 1 2450 2650 1
AnalysisArea = 1 2800 3450 1
Interference = 110110111000000000000110011001
CrossInterferences = 0 0 0 0 0
ReferenceFile = C:\Library180\Methylamine CH5N 0894 ppm.ref
ReferenceFile = C:\Library180\Methylamine CH5N 0100 ppm.ref
ReferenceFile = C:\Library180\Methylamine CH5N 0500 ppm.ref

ComponentNumber = 29
ComponentName = Methane CH4
ConcentrationUnit = Auto
ActiveLines = All
AutoAnalyze = 1 (1=Yes)
OutputChannel = 0
ViewResults = 1 (1=Yes)
AllowNegative = 1 (1=Yes)
ConversionMultiplier = 1
ResultSmoothing = 0
RangeSetting = 0

```
Range1 = 0 10
Range2 = 0 100
AlarmLimits = 0 100
AlarmSound = 0
Compensations = 0 0 0 0 -11
Calibrations = 0 0 4 2
ResidualWarningLimit = 0.01
ResidualErrorLimit = 0.02
UseDoubleReferences = 0 (1=Yes)
AutoInterferenceUpdate = 1 0.001
DefaultReference = 1
BaselineCorrections = 1 0
MethodNumber = 0 (1=Yes)
AnalysisArea = 0 1292 1412 0.5
AnalysisArea = 1 2833 3203 0.5
AnalysisArea = 1 3018 3203 0.5
Interference = 1101101110000000000001100111
CrossInterferences = 0 0 0 0 0
ReferenceFile = C:\Library180\Methane CH4 0050 ppm.ref
ReferenceFile = C:\Library180\Methane CH4 0101 ppm.ref
```

Table B.4 Input File for Calcmet™ OLD-MEA-Degradation.LIB

ComponentNumber = 1
ComponentName = Water vapor H2O
ConcentrationUnit = vol-%
ActiveLines = All
AutoAnalyze = 1 (1=Yes)
OutputChannel = 0
ViewResults = 1 (1=Yes)
AllowNegative = 0 (1=Yes)
ConversionMultiplier = 1
ResultSmoothing = 0
RangeSetting = 0
Range1 = 0 5
Range2 = 0 25
AlarmLimits = 0 25
Calibrations = 0 0 0 2
ResidualWarningLimit = 0.01
ResidualErrorLimit = 0.02
AlarmSound = 0
UseDoubleReferences = 1 (1=Yes)
AutoInterferenceUpdate = 0 (1=Yes)
DefaultReference = 4
BaselineCorrections = 1 0 0
Compensations = 1 1 1 0 -11
MethodNumber = 0 (1=Yes)
AnalysisArea = 0 1814 1875 1
AnalysisArea = 1 1922 2146 1
AnalysisArea = 1 3049 3250 0.5
Interference = 0110110110000000000000001
CrossInterferences = 0 0 0 0 0
ReferenceFile = H2O_10.ref
ReferenceFile = H2O_14.ref
ReferenceFile = H2O_18.ref
ReferenceFile = H2O_22.ref
ReferenceFile = H2O_26.ref
ReferenceFile = H2O_30.ref
ReferenceFile = H2O_34.ref
ReferenceFile = H2O_38.ref
ReferenceFile = H2O_04.ref
ReferenceFile = H2O_02.ref
ReferenceFile = H2O_06.ref
ReferenceFile = H2O_0.5.ref

ReferenceFile = H2O_08.ref

ComponentNumber = 2
ComponentName = Carbon dioxide CO2
ConcentrationUnit = vol-%
ActiveLines = All
AutoAnalyze = 1 (1=Yes)
OutputChannel = 0
ViewResults = 1 (1=Yes)
AllowNegative = 0 (1=Yes)
ConversionMultiplier = 1
ResultSmoothing = 0
RangeSetting = 0
Range1 = 0 5
Range2 = 0 35
AlarmLimits = 0 30
Calibrations = 0 0 4 2
ResidualWarningLimit = 0.01
ResidualErrorLimit = 0.02
AlarmSound = 0
UseDoubleReferences = 0 (1=Yes)
AutoInterferenceUpdate = 0 (1=Yes)
DefaultReference = 4
BaselineCorrections = 1 0 0
Compensations = 1 1 1 0 -11
MethodNumber = 0 (1=Yes)
AnalysisArea = 1 918 1119 1
AnalysisArea = 1 1950 2130 1
AnalysisArea = 0 3300 3800 1
Interference = 101110011110000000011111
CrossInterferences = 0 0 0 0 0
ReferenceFile = CO2_30.ref
ReferenceFile = CO2_03.ref
ReferenceFile = CO2_06.ref
ReferenceFile = CO2_09.ref
ReferenceFile = CO2_12.ref
ReferenceFile = CO2_15.ref
ReferenceFile = CO2_18.ref
ReferenceFile = CO2_21.ref
ReferenceFile = CO2_24.ref
ReferenceFile = CO2_27.ref
ReferenceFile = CO2_0.5.ref

ComponentNumber = 3
ComponentName = Carbon monoxide CO
ConcentrationUnit = ppm
ActiveLines = All
AutoAnalyze = 1 (1=Yes)
OutputChannel = 0
ViewResults = 1 (1=Yes)
AllowNegative = 0 (1=Yes)
ConversionMultiplier = 1
ResultSmoothing = 0
RangeSetting = 0
Range1 = 0 10
Range2 = 0 500
AlarmLimits = 0 5000
Calibrations = 0 0 4 2
ResidualWarningLimit = 0.01
ResidualErrorLimit = 0.02
AlarmSound = 0
UseDoubleReferences = 0 (1=Yes)
AutoInterferenceUpdate = 1 (1=Yes)
DefaultReference = 1
BaselineCorrections = 1 0 0
Compensations = 1 1 1 0 -11
MethodNumber = 0 (1=Yes)
AnalysisArea = 1 2007 2099 0.5
AnalysisArea = 1 2624 2750 1
AnalysisArea = 0 2550 2600 1
Interference = 110010011000000000000110011
CrossInterferences = 0 0 0 0 0
ReferenceFile = CO_998.ref
ReferenceFile = CO_11.ref
ReferenceFile = CO_200.ref
ReferenceFile = CO_402.ref
ReferenceFile = CO_51.ref
ReferenceFile = CO_602.ref
ReferenceFile = CO_805.ref
ReferenceFile = CO_100.ref

ComponentNumber = 5
ComponentName = Nitrous oxide N2O
ConcentrationUnit = ppm
ActiveLines = All
AutoAnalyze = 1 (1=Yes)

OutputChannel = 0
ViewResults = 1 (1=Yes)
AllowNegative = 0 (1=Yes)
ConversionMultiplier = 1
ResultSmoothing = 0
RangeSetting = 2
Range1 = 0 5000
Range2 = 0 100000
AlarmLimits = 0 100000
Calibrations = 0 0 0 2
ResidualWarningLimit = 0.01
ResidualErrorLimit = 0.02
AlarmSound = 1
UseDoubleReferences = 0 (1=Yes)
AutoInterferenceUpdate = 0 (1=Yes)
DefaultReference = 2
BaselineCorrections = 1 0 0
Compensations = 1 1 1 0 -11
MethodNumber = 0 (1=Yes)
AnalysisArea = 1 920 1119 1
AnalysisArea = 1 2647 2900 0.5
AnalysisArea = 0 2400 2700 1
Interference = 111001011000000000011001
CrossInterferences = 0 0 0 0 0
ReferenceFile = C:\Library 01253\George's References\N2O_100000ppmG.ref
ReferenceFile = C:\Library 01253\George's References\N2O_4882ppmG.ref
ReferenceFile = C:\Library 01253\George's References\N2O_50000ppmG.ref

ComponentNumber = 6
ComponentName = Nitrogen monoxide NO
ConcentrationUnit = ppm
ActiveLines = All
AutoAnalyze = 1 (1=Yes)
OutputChannel = 0
ViewResults = 1 (1=Yes)
AllowNegative = 0 (1=Yes)
ConversionMultiplier = 1
ResultSmoothing = 0
RangeSetting = 0
Range1 = 0 20
Range2 = 0 150
AlarmLimits = 0 1000
Calibrations = 0 0 4 2

ResidualWarningLimit = 0.01
ResidualErrorLimit = 0.02
AlarmSound = 0
UseDoubleReferences = 0 (1=Yes)
AutoInterferenceUpdate = 0 (1=Yes)
DefaultReference = 1
BaselineCorrections = 0 0 0
Compensations = 1 1 1 0 -11
MethodNumber = 0 (1=Yes)
AnalysisArea = 0 1760 1868 0.8
AnalysisArea = 1 1869 1991 0.8
AnalysisArea = 0 2550 2600 1
Interference = 11101001100000000000001001
CrossInterferences = 0 0 0 0 0
ReferenceFile = NO_99.ref
ReferenceFile = NO_194.ref
ReferenceFile = NO_50.ref
ReferenceFile = NO_98.ref
ReferenceFile = NO_10.ref

ComponentNumber = 7
ComponentName = Nitrogen dioxide NO2
ConcentrationUnit = ppm
ActiveLines = All
AutoAnalyze = 1 (1=Yes)
OutputChannel = 0
ViewResults = 1 (1=Yes)
AllowNegative = 0 (1=Yes)
ConversionMultiplier = 1
ResultSmoothing = 0
RangeSetting = 0
Range1 = 0 20
Range2 = 0 1000
AlarmLimits = 0 1000
Calibrations = 0 0 4 2
ResidualWarningLimit = 0.01
ResidualErrorLimit = 0.02
AlarmSound = 0
UseDoubleReferences = 0 (1=Yes)
AutoInterferenceUpdate = 0 (1=Yes)
DefaultReference = 1
BaselineCorrections = 1 0 0
Compensations = 1 1 1 0 -11

MethodNumber = 0 (1=Yes)
AnalysisArea = 0 941 1397 1
AnalysisArea = 0 1497 1706 1.8
AnalysisArea = 1 2550 2933 0.5
Interference = 110110101010000000011001
CrossInterferences = 0 0 0 0 0
ReferenceFile = C:\Library180\Nitrogen dioxide NO2 0050 ppm.ref
ReferenceFile = C:\Library180\Nitrogen dioxide NO2 0005 ppm.ref

ComponentNumber = 9
ComponentName = Ammonia NH3
ConcentrationUnit = ppm
ActiveLines = All
AutoAnalyze = 1 (1=Yes)
OutputChannel = 0
ViewResults = 1 (1=Yes)
AllowNegative = 0 (1=Yes)
ConversionMultiplier = 1
ResultSmoothing = 0
RangeSetting = 0
Range1 = 0 50
Range2 = 0 250
AlarmLimits = 0 500
Calibrations = 0 4 0 2
ResidualWarningLimit = 0.01
ResidualErrorLimit = 0.02
AlarmSound = 0
UseDoubleReferences = 0 (1=Yes)
AutoInterferenceUpdate = 0 (1=Yes)
DefaultReference = 1
BaselineCorrections = 0 0 0
Compensations = 1 1 1 0 -11
MethodNumber = 0 (1=Yes)
AnalysisArea = 1 910 1000 1
AnalysisArea = 0 1551 1667 0.75
AnalysisArea = 0 3265 3396 0.5
Interference = 111011110000000000011001
CrossInterferences = 0 0 0 0 0
ReferenceFile = NH3_100.ref
ReferenceFile = NH3_11.ref
ReferenceFile = NH3_200.ref
ReferenceFile = NH3_3.ref
ReferenceFile = NH3_49.ref

ComponentNumber = 21
ComponentName = Formaldehyde
ConcentrationUnit = ppm
ActiveLines = All
AutoAnalyze = 1 (1=Yes)
OutputChannel = 0
ViewResults = 1 (1=Yes)
AllowNegative = 0 (1=Yes)
ConversionMultiplier = 1
ResultSmoothing = 0
RangeSetting = 0
Range1 = 0 10
Range2 = 0 100
AlarmLimits = 0 100
Calibrations = 0 0 4 2
ResidualWarningLimit = 0.01
ResidualErrorLimit = 0.02
AlarmSound = 0
UseDoubleReferences = 0 (1=Yes)
AutoInterferenceUpdate = 1 (1=Yes)
DefaultReference = 1
BaselineCorrections = 1 0 0
Compensations = 1 1 1 0 -11
MethodNumber = 0 (1=Yes)
AnalysisArea = 1 1134 1204 1
AnalysisArea = 0 1605 1868 0.6
AnalysisArea = 1 2650 3211 0.5
Interference = 1101101110000000000010011
CrossInterferences = 0 0 0 0 0
ReferenceFile = C:\Library180\Formaldehyde CH2O.ref

ComponentNumber = 22
ComponentName = Acetaldehyde
ConcentrationUnit = ppm
ActiveLines = All
AutoAnalyze = 1 (1=Yes)
OutputChannel = 0
ViewResults = 1 (1=Yes)
AllowNegative = 0 (1=Yes)
ConversionMultiplier = 1
ResultSmoothing = 0
RangeSetting = 0

Range1 = 0 10
Range2 = 0 100
AlarmLimits = 0 100
Calibrations = 0 4 0 2
ResidualWarningLimit = 0.01
ResidualErrorLimit = 0.02
AlarmSound = 0
UseDoubleReferences = 0 (1=Yes)
AutoInterferenceUpdate = 1 (1=Yes)
DefaultReference = 1
BaselineCorrections = 1 0 0
Compensations = 1 1 1 0 -11
MethodNumber = 0 (1=Yes)
AnalysisArea = 0 1073 1157 0.5
AnalysisArea = 0 1798 2038 0.5
AnalysisArea = 1 2638 2916 1
Interference = 11011011100000000000100011
CrossInterferences = 0 0 0 0 0
ReferenceFile = C:\Library180\Acetaldehyde C2H4O 0500 ppm.ref
ReferenceFile = C:\Library180\Acetaldehyde C2H4O 0100 ppm.ref

ComponentNumber = 25
ComponentName = MEA
ConcentrationUnit = ppm
ActiveLines = All
AutoAnalyze = 1 (1=Yes)
OutputChannel = 0
ViewResults = 1 (1=Yes)
AllowNegative = 0 (1=Yes)
ConversionMultiplier = 1
ResultSmoothing = 0
RangeSetting = 0
Range1 = 0 100
Range2 = 0 1000
AlarmLimits = 0 100
Calibrations = 0 0 0 2
ResidualWarningLimit = 0.01
ResidualErrorLimit = 0.02
AlarmSound = 0
UseDoubleReferences = 0 (1=Yes)
AutoInterferenceUpdate = 0 (1=Yes)
DefaultReference = 1
BaselineCorrections = 1 0 0

```
Compensations = 0 0 0 0 -11
MethodNumber = 0 (1=Yes)
AnalysisArea = 1 2624 3150 1
AnalysisArea = 1 940 1119 1
AnalysisArea = 0 3500 4000 1
Interference = 110011111000000000000011
CrossInterferences = 0 0 0 0 0
ReferenceFile = C:\Library 01253\George's References\MEA_500.ref
```

Appendix C: Original Sparged Reactor Experiments

This appendix presents results from the initial screening experiments using the original Sparged Reactor system developed by Chi (Chi 2000). An overall flow diagram for the apparatus used in the degradation experiments is shown in Figure C.1. The apparatus was capable of bubbling air, air with additional CO_2, pure CO_2, or N_2 through a jacketed reactor containing the amine solution. The degradation products were vented and sent to the bench top FT-IR system. This setup allows for bypassing the reactor with a mixture of NH_3 and N_2 in order to calibrate the FT-IR signal to a known source of NH_3.

The degradation experiments were performed using a semi-batch jacketed reactor. The reactor was heated by circulating a hot solution of ethylene glycol and water through the jacket of the reactor. The reactor was operated by bubbling air through the amine solution inside the reactor. The reactor air was then passed through an ice-water condenser before mixing with dilution air. The water was condensed prior to mixing in order to decrease condensation of water and adsorption of ammonia inside the gas lines leading to the Perkin Elmer bench top FT-IR. The exit gas was analyzed

for ammonia concentration continuously throughout each experiment. Figure C.2 shows a diagram of the reactor setup.

In these experiments, oxidative degradation was quantified by analyzing the rate of evolution of ammonia from a solution of MEA solvent in contact with a source of oxygen. The ammonia is stripped from the solution and analyzed by a FT-IR. The amount of ammonia monitored is the related to the amount of solution in the reactor, and this is called the degradation rate in units of millimoles of NH_3 / liter of amine solution in the reactor. All of the experiments used 7 molal MEA solutions (30% wt).

Table C.1 is a summary of the completed experiments and summarizes the observed degradation rates as well as the process conditions under which the experiments were run. Complete data files for each experiment are available from Gary Rochelle at The University of Texas at Austin.
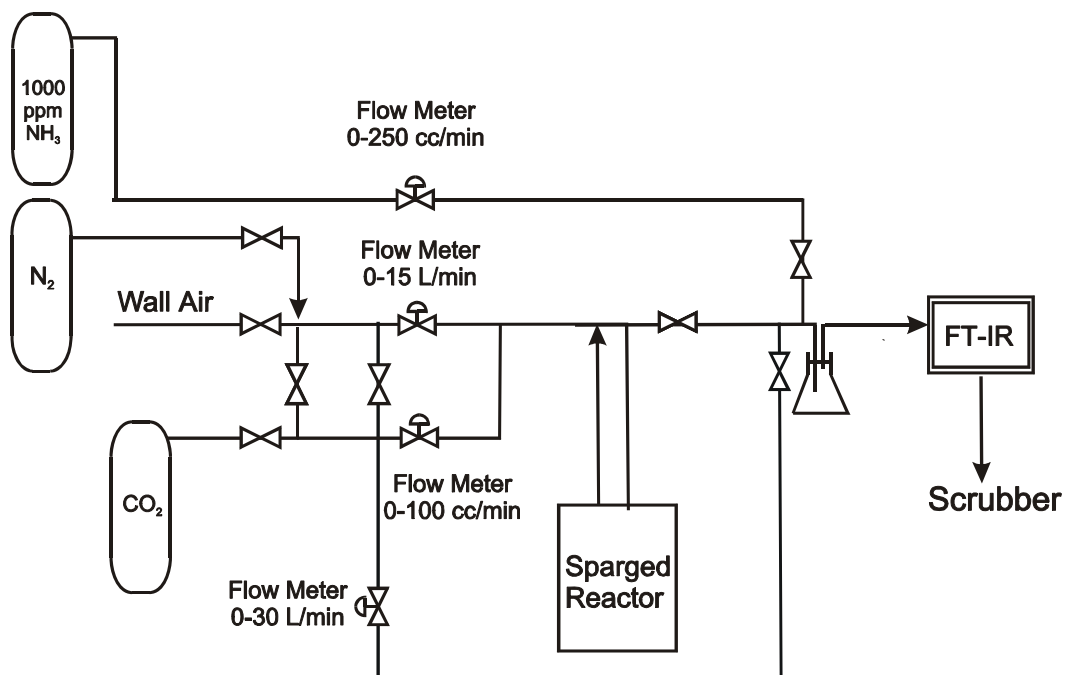
Figure C.1 Flow Diagram for the Oxidative Degradation Experimental Apparatus
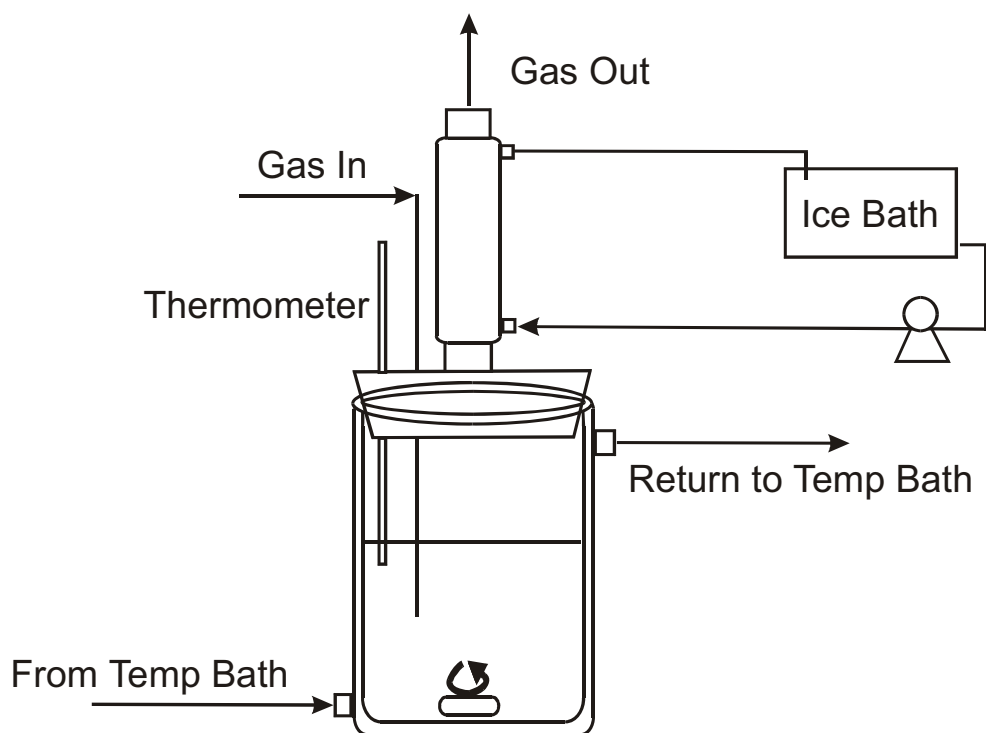
Figure C.2 Diagram of the Original Sparged Reactor Apparatus Developed by Chi (Chi 2000)

Table C.1 Experimental Results for Experiments Run in the Original Sparged Reactor

Cu (mM)	Fe (mM)	Inhibitor	Ratio to Cu	Conc. (mM)	NH₃ Evolution (mM/hr)	Δ Rate relative to previous addition (mM/hr)
11/13/2000	α	0.40	(°C)	55	% O₂ in Air	20
0.0	0.0001	-----	-----	-----	0.20	-----
10.0	0.0001	-----	-----	-----	1.93	1.73
10.0	0.0001	Bicine	2	20	1.91	-0.02
10.0	0.0001	EDTA	2	20	0.09	-1.82
5/16/2001	α	0.40	(°C)	55	% O₂ in Air	20
0.0	0.0001	-----	-----	-----	0.68	-----
4.0	0.0001	-----	-----	-----	1.68	1.48
4.0	0.0001	EDTA	0.8	3.2	1.45	-0.23
4.0	0.0001	EDTA	1.0	4.0	1.16	-0.29
5/18/2001	α	0.40	(°C)	55	% O₂ in Air	20
DATA SHOWS REVERSE TRENDS-----Rate data inconclusive						
5/22/2001	α	0.40	(°C)	55	% O₂ in Air	20
0.0	0.0001	-----	-----	-----	0.23	-----
4.0	0.0001	-----	-----	-----	1.49	1.26
4.0	0.0001	EDTA	0.8	3.2	1.23	-0.26
4.0	0.0001	EDTA	1.2	4.8	0.21	-1.02
5/23/2001	α	0.40	(°C)	55	% O₂ in Air	20
0.0	0.0001	-----	-----	-----	0.23	-----
4.0	0.2001	-----	-----	-----	2.27	2.037
4.0	0.2001	MDEA	110.4	442	2.20	-0.069
4.0	0.2001	Bicine	23.3	93	1.21	-0.988
5/29/2001	α	0.40	(°C)	55	% O₂ in Air	20
0.000	0.0001	-----	-----	-----	0.03	-----
0.001	0.0001	-----	-----	-----	0.59	0.57
0.010	0.0001	-----	-----	-----	1.45	0.86
0.100	0.0001	-----	-----	-----	2.19	0.74
1.000	0.0001	-----	-----	-----	2.06	-0.13
1.000	0.0001	EDTA	0.8	0.8	1.62	-0.44

Cu (mM)	Fe (mM)	Inhibitor	Ratio to Cu	Conc. (mM)	NH₃ Evolution (mM/hr)	Δ Rate relative to previous addition (mM/hr)
5/31/2001	**α**	**0.40**	**(°C)**	**55**	**% O₂ in Air**	**20**
0.0	0.0001	-----	-----	-----	0.11	-----
0.0	0.2001	-----	-----	-----	1.84	1.73
0.1	0.2001	-----	-----	-----	3.26	1.42
0.2	0.2001	-----	-----	-----	2.90	-0.36
0.3	0.2001	-----	-----	-----	2.56	-0.34
1.0	0.2001	-----	-----	-----	2.17	-0.39
6/1/2001	**α**	**0.40**	**(°C)**	**55**	**% O₂ in Air**	**20**
0.0	0.0001	-----	-----	-----	0.13	-----
1.0	0.0001	-----	-----	-----	1.81	1.68
1.0	0.0011	-----	-----	-----	2.41	0.60
1.0	0.0101	-----	-----	-----	2.53	0.11
1.0	0.1001	-----	-----	-----	2.16	-0.37
6/13/2001	**α**	**0.40**	**(°C)**	**55**	**% O₂ in Air**	**20**
0.000	0.0001	-----	-----	-----	0.04	-----
0.001	0.0001	-----	-----	-----	0.68	0.65
0.001	0.0010	-----	-----	-----	1.00	0.32
0.010	0.0010	-----	-----	-----	1.52	0.52
0.010	0.0100	-----	-----	-----	1.99	0.47
0.010	0.0100	EDTA	1.1	0.011	1.54	-0.45
6/20/2001	**α**	**0.40**	**(°C)**	**55**	**% O₂ in Air**	**20**
0.000	0.0001	-----	-----	-----	0.07	-----
0.001	0.0001	-----	-----	-----	1.76	1.70
0.010	0.0001	-----	-----	-----	1.80	0.04
0.100	0.0001	-----	-----	-----	2.08	0.28
1.000	0.0001	-----	-----	-----	1.79	-0.29
1.000	0.0001	H₃PO₄	100	100	1.45	-0.34
6/22/2001	**α**	**0.40**	**(°C)**	**55**	**% O₂ in Air**	**20**
0.000	0.0001	-----	-----	-----	0.12	-----
0.001	0.0001	-----	-----	-----	0.49	0.37
0.010	0.0001	-----	-----	-----	1.43	0.94
0.100	0.0001	-----	-----	-----	2.12	0.69
1.000	0.0001	-----	-----	-----	1.99	-0.13
1.000	0.0001	Na₃PO₄	100	100	1.72	-0.27

Cu (mM)	Fe (mM)	Inhibitor	Ratio to Cu	Conc. (mM)	NH$_3$ Evolution (mM/hr)	Δ Rate relative to previous addition (mM/hr)
6/27/2001	α	0.15	(^{o}C)	55	% O$_2$ in Air	20
0.000	0.0001	-----	-----	-----	0.24	-----
0.010	0.0001	-----	-----	-----	3.67	3.43
0.010	0.1000	-----	-----	-----	4.99	1.32
0.100	0.1000	-----	-----	-----	5.12	0.13
0.100	0.1000	Benzoic Acid	100	10	5.03	-0.09
0.100	0.1000	K$_2$CO$_3$	100	10	4.86	-0.17
6/28/2001	α	0.40	(^{o}C)	25	% O$_2$ in Air	20

The rate data was too low to be calculated accurately at the current FT-IR set-up.

Cu (mM)	Fe (mM)	Inhibitor	Ratio to Cu	Conc. (mM)	NH$_3$ Evolution (mM/hr)	Δ Rate relative to previous addition (mM/hr)
6/29/2001	α	0.40	(^{o}C)	80	% O$_2$ in Air	20
0.000	0.0001	-----	-----	-----	0.12	-----
0.001	0.0001	-----	-----	-----	0.49	0.37
0.010	0.0001	-----	-----	-----	1.43	0.94
0.100	0.0001	-----	-----	-----	2.12	0.69
1.000	0.0001	-----	-----	-----	1.99	-0.13
1.000	0.0001	Na$_3$PO$_4$	100	100	1.72	-0.27
7/11/2001	α	0.15	(^{o}C)	55	% O$_2$ in Air	20
0.001	0.0001	-----	-----	-----	0.00	-----
0.010	0.0001	-----	-----	-----	1.26	1.26
1.000	0.0001	-----	-----	-----	4.53	3.27
4.000	0.0001	-----	-----	-----	5.77	1.24
1.000	0.0001	EDTA	1.0	1.0	5.32	-0.45
1.000	0.0001	EDTA	1.2	1.2	5.12	-0.20
7/17/2001	α	0.15	(^{o}C)	55	% O$_2$ in Air	20
0.001	0.2000	-----	-----	-----	3.13	-----
0.010	0.2000	-----	-----	-----	3.92	0.79
0.100	0.2000	-----	-----	-----	5.34	1.42
1.000	0.2000	-----	-----	-----	4.95	-0.39
4.000	0.2000	-----	-----	-----	4.90	-0.05
4.000	0.2000	EDTA	1.0	4.0	1.35	-3.60
4.000	0.2000	EDTA	1.2	4.8	1.21	-0.14

Cu (mM)	Fe (mM)	Inhibitor	Ratio to Cu	Conc. (mM)	NH$_3$ Evolution (mM/hr)	Δ Rate relative to previous addition (mM/hr)
7/19/2001	α	**0.15**	(°C)	55	**% O$_2$ in Air**	**20**
0.000	0.0010	-----	-----	-----	0.39	-----
0.000	0.0100	-----	-----	-----	2.08	1.69
0.000	0.1000	-----	-----	-----	3.58	1.50
0.000	0.2000	-----	-----	-----	3.58	0.00
0.000	1.0000	-----	-----	-----	3.62	0.04
7/20/2001	α	**0.15**	(°C)	55	**% O$_2$ in Air**	**20**
0.001	0.0100	-----	-----	-----	0.73	-----
0.010	0.0100	-----	-----	-----	4.02	3.29
0.100	0.0100	-----	-----	-----	6.42	2.40
1.000	0.0100	-----	-----	-----	6.10	-0.32
4.000	0.0100	-----	-----	-----	6.03	-0.07
7/23/2001	α	**0.40**	(°C)	70	**% O$_2$ in Air**	**20**
0.100	0.0010	-----	-----	-----		-----
4.000	0.2000	-----	-----	-----		0.00
7/30/2001	α	**0.40**	(°C)	55	**% O$_2$ in Air**	**20**
0.000	0.0001	-----	-----	-----	1.32	-----
0.000	0.0010	-----	-----	-----	1.81	0.49
0.000	0.0100	-----	-----	-----	2.00	0.19
0.000	0.1000	-----	-----	-----	2.22	0.22
0.000	1.0000	-----	-----	-----	2.69	0.47
8/1/2001	α	**0.40**	(°C)	55	**% O$_2$ in Air**	**20**
0.000	0.0001	-----	This Data is not included in rate data. The purpose of experiment was to check for MT problems. 1/2 Air rate.		1.07	-----
0.010	0.0001	-----			1.97	0.90
0.100	0.2000	-----			2.32	0.35
	0.2000	-----				
1.000					2.08	-0.24
8/6/2001	α	**0.40**	(°C)	55	**% O$_2$ in Air**	**20**
0.010	0.2000	-----	-----	-----	3.53	-----
0.100	0.2000	-----	-----	-----	3.51	-0.02
1.000	0.2000	-----	-----	-----	2.92	-0.59
4.000	0.2000	-----	-----	-----	2.84	-0.08

Cu (mM)	Fe (mM)	Inhibitor	Ratio to Cu	Conc. (mM)	NH$_3$ Evolution (mM/hr)	Δ Rate relative to previous addition (mM/hr)
8/7/2001	α	0.40	(°C)	55	% O$_2$ in Air	20
0.000	0.0001	-----	-----	-----	2.03	-----
0.010	0.2000	-----	-----	-----	3.21	1.18
0.100	0.2000	-----	-----	-----	3.29	0.08
1.000	0.2000	-----	-----	-----	2.83	-0.46
4.000	0.2000	-----	-----	-----	2.59	-0.24
4.000	0.2000	Na$_2$SO$_3$	5	20	2.52	-0.07

C.1. Results

The results of this study are somewhat different from later findings due to the lower mass transfer capabilities of the system and analytical techniques with greater error. The preliminary findings from this study are as follows.

The addition of copper to MEA solutions containing dissolved iron appears to catalyze the oxidative degradation rate of MEA. This effect appears to be saturated at a copper concentration of approximately 0.1 mM, and could possibly decrease at copper concentrations higher than 0.1 mM. Consequently, in the operating range of 1-4 mM copper, it appears that 4 mM copper is actually slightly preferential in terms of the oxidative degradation rate. Additionally, it appears that the most important process parameter is solution loading. As can been from the data tables, all of the degradation rates for the lower loadings are higher than the corresponding rates of the higher loadings. This potentially means that the degradation rates at the top of the absorber are actually faster than the rates in the absorber sump.

Any process that uses iron or steel equipment will contain some dissolved iron. The addition of copper to these systems appears to create a synergistic effect on the overall rate of oxidative degradation. While an increase of iron concentration at a constant copper concentration increases the degradation rate, this increase is small. It appears that the overall oxidative degradation rate is less than first order in both iron and copper concentrations.

In terms of degradation inhibitors, EDTA is the only inhibitor that has been tested that shows potential for decreasing the rate of degradation. EDTA was tested at several ratios of EDTA to copper concentration, and was proven to be effective in almost eliminating the oxidative degradation due to copper at a ratio of 1.2/1. MDEA was tested in a solution using 5% wt MDEA, and the decrease in the oxidative degradation rate was negligible. Bicine was tested by itself as a degradation inhibitor, but was ineffective. The combination of a 23/1 ratio of bicine to copper, in addition to the 5% wt MDEA decreased the degradation rate by almost 45%. Finally, both H_3PO_4 and Na_3PO_4 were tested as degradation inhibitors, but both had only small inhibition potentials.

Appendix D: Sparged Reactor O$_2$ Mass Transfer Experiments

This appendix documents the experimental results from the O$_2$ mass transfer study performed in the Sparged Reactor. All experiments were performed with 7.0 m MEA at 55°C. Data points in gray font color indicate data points that should not be used for quantitative analysis. In general these data points have excluded because the system was not at steady state or there was a problem with the mass balance. Table D.1 tabulates the results from experiments performed in the SpargedReactor. Complete data files for each experiment are available from Gary Rochelle at The University of Texas at Austin.

Table D.1 Experimental Results for the O$_2$ Mass Transfer Study in the Sparged Reactor at 55°C

Date	Gas (LPM)	Ave Soln. Mass (g)	% Mass Change	MEA (m)	α	ρ (g/cc)	Fe [mM]	Cu [mM]	Misc. Variable	Value	NH$_3$ Evolution [mM/hr]	Relative Rate
06/25/02	8.8	250.0		7.0	0.40	1.07	0.0001	0.000			1.47	
06/25/02	8.8	250.0		7.0	0.40	1.07	0.0011	0.000			1.24	
06/25/02	8.8	250.0		7.0	0.40	1.07	0.0107	0.000			1.63	
06/25/02	8.8	250.0		7.0	0.40	1.07	0.1054	0.000			1.98	
06/26/02	8.8	250.0		7.0	0.40	1.07	0.0001	0.000			0.76	
06/26/02	8.8	250.0		7.0	0.40	1.07	0.0011	0.000			0.68	
06/26/02	8.8	250.0		7.0	0.40	1.07	0.0011	0.011			1.62	
06/26/02	8.8	250.0		7.0	0.40	1.07	0.0011	0.107			1.99	
06/26/02	8.8	250.0		7.0	0.40	1.07	0.0118	0.107			2.78	
06/26/02	8.8	250.0		7.0	0.40	1.07	0.1062	0.107				
06/27/02	8.7	289.4		7.0	0.40	1.07	0.0001	0.000			1.11	
06/27/02	8.7	289.4		7.0	0.40	1.07	0.0001	0.093			2.08	
06/27/02	8.7	289.4		7.0	0.40	1.07	0.0093	0.093			2.24	
06/27/02	8.7	289.4		7.0	0.40	1.07	0.0913	0.093			1.92	
06/27/02	8.7	289.4		7.0	0.40	1.07	0.0913	0.905				
06/27/02	8.7	289.4		7.0	0.40	1.07	0.0913	1.726				
07/01/02	8.0	274.0		7.0	0.40	1.07	0.0001	0.000			1.32	
07/01/02	8.0	274.0		7.0	0.40	1.07	0.0010	0.000			1.37	
07/01/02	8.0	274.0		7.0	0.40	1.07	0.0098	0.000			1.76	
07/01/02	8.0	274.0		7.0	0.40	1.07	0.0962	0.000			2.05	
07/01/02	8.0	274.0		7.0	0.40	1.07	0.0962	0.010			2.19	
07/01/02	8.0	274.0		7.0	0.40	1.07	0.0962	0.098			2.27	
07/01/02	8.0	274.0		7.0	0.40	1.07	0.0962	5.453				

Date	Gas (LPM)	Ave Soln. Mass (g)	% Mass Change	MEA (m)	α	ρ (g/cc)	Fe [mM]	Cu [mM]	Misc. Variable	Value	NH$_3$ Evolution [mMJ/hr]	Relative Rate
07/11/02	7.8	262.0	-8.1%	7.0	0.40	1.07	0.0002	0.000			0.51	
07/11/02	7.8	262.0	-8.1%	7.0	0.40	1.07	0.0011	0.000			0.60	
07/11/02	7.8	262.0	-8.1%	7.0	0.40	1.07	0.0103	0.000			1.03	
07/11/02	7.8	262.0	-8.1%	7.0	0.40	1.07	0.1005	0.000			1.35	
07/11/02	7.8	262.0	-8.1%	7.0	0.40	1.07	1.0309	0.000		mM	1.87	
07/11/02	7.8	262.0	-8.1%	7.0	0.40	1.07	1.0309	0.000	EDTA	1.00	0.91	
07/11/02	7.8	262.0	-8.1%	7.0	0.40	1.07	1.0309	0.000	EDTA	10.31	0.76	
07/15/02	7.8	317.4	33.1%	7.0	0.40	1.07	0.0001	0.000			0.71	
07/15/02	7.8	317.4	33.1%	7.0	0.40	1.07	0.0001	0.008			1.14	
07/15/02	7.8	317.4	33.1%	7.0	0.40	1.07	0.0009	0.008			1.19	
07/15/02	7.8	317.4	33.1%	7.0	0.40	1.07	0.0085	0.008			1.35	
07/15/02	7.8	317.4	33.1%	7.0	0.40	1.07	0.0832	0.008			1.51	
07/15/02	7.8	317.4	33.1%	7.0	0.40	1.07	0.8223	0.008		mM	1.68	
07/15/02	7.8	317.4	33.1%	7.0	0.40	1.07	0.8223	0.008	EDTA	0.05	1.22	
07/15/02	7.8	317.4	33.1%	7.0	0.40	1.07	0.8223	0.008	EDTA	0.23	0.81	
07/16/02		BAD DATA MASS BALANCE 45% off										
07/17/02[1]	7.7	302.9	-20.7%	7.0	0.15	1.02	0.0001	0.000			1.70	
07/17/02[1]	7.7	302.9	-20.7%	7.0	0.15	1.02	0.0010	0.000			1.87	
07/17/02[1]	7.7	302.9	-20.7%	7.0	0.15	1.02	0.0094	0.000			1.86	
07/17/02[1]	7.7	302.9	-20.7%	7.0	0.15	1.02	0.1004	0.000				
07/17/02[1]	7.7	302.9	-20.7%	7.0	0.15	1.02	0.9350	0.000			2.06	
07/18/02[2]	7.6	245.0	-23.5%	7.0	0.15	1.02	0.0001	0.000			0.73	
07/18/02[2]	7.6	245.0	-23.5%	7.0	0.15	1.02	0.0001	0.013			2.99	
07/18/02[2]	7.6	245.0	-23.5%	7.0	0.15	1.02	0.0013	0.013			2.98	
07/18/02[2]	7.6	245.0	-23.5%	7.0	0.15	1.02	0.0117	0.013			3.18	
07/18/02[2]	7.6	245.0	-23.5%	7.0	0.15	1.02	0.1235	0.013			2.89	
07/18/02[2]	7.6	245.0	-23.5%	7.0	0.15	1.02	1.6192	0.013		mM	2.88	
07/18/02[2]	7.6	245.0	-23.5%	7.0	0.15	1.02	1.6192	0.013	EDTA	0.11	2.04	
07/18/02[2]	7.6	245.0	-23.5%	7.0	0.15	1.02	1.6192	0.013	EDTA	0.23	1.79	

Date	Gas (LPM)	Ave Soln. Mass (g)	% Mass Change	MEA (m)	α	ρ (g/cc)	Fe [mM]	Cu [mM]	Misc. Variable	Value	NH$_3$ Evolution [mM]/hr	Relative Rate
07/19/02	7.5	265.3		7.0	0.15	1.02	0.0001	0.000			0.75	
07/19/02	7.5	265.3		7.0	0.15	1.02	0.0001	0.001			5.23	
07/19/02	7.5	265.3		7.0	0.15	1.02	0.0011	0.001			4.83	
07/19/02	7.5	265.3		7.0	0.15	1.02	0.0106	0.001			4.64	
07/19/02	7.5	265.3		7.0	0.15	1.02	0.1138	0.001			4.29	
07/19/02	7.5	265.3		7.0	0.15	1.02	1.4956	0.001		mM	4.68	
07/19/02	7.5	265.3		7.0	0.15	1.02	1.4956	0.001	EDTA	1.36	2.35	
10/15/02	7.9	358.7		7.0	0.40	1.07	0.0001	0.00			1.40	
10/15/02	7.9	358.7		7.0	0.40	1.07	0.0001	9.02			1.33	
10/15/02	7.9	358.7		7.0	0.40	1.07	0.0056	9.02			1.37	
10/15/02	7.9	358.7		7.0	0.40	1.07	0.0603	9.02			1.50	
10/15/02	7.9	358.7		7.0	0.40	1.07	0.5990	9.02			1.41	
10/15/02	7.9	358.7		7.0	0.40	1.07	0.9721	9.02		mM	1.44	
10/15/02	7.9	358.7		7.0	0.40	1.07	0.9721	9.02	EDTA	10.22		
10/15/02	7.9	358.7		7.0	0.40	1.07	0.9721	9.02	EDTA	41.08	0.44	
10/18/02[1,2]	7.7	301.4		7.0	0.21[3]		0.0001	0.000	pH	10.3	0.17	
10/18/02[1,2]	7.7	301.4		7.0	0.21[3]		0.0001	0.001			0.27	
10/18/02[1,2]	7.7	301.4		7.0	0.21[3]		0.0061	0.001			0.49	
10/18/02[1,2]	7.7	301.4		7.0	0.21[3]		0.0540	0.001			0.67	
10/18/02[1,2]	7.7	301.4		7.0	0.21[3]		0.1732	0.001			0.63	
10/18/02[1,2]	7.7	301.4		7.0	0.21[3]		0.9894	0.001			0.63	
10/18/02[1,2]	7.7	301.4		7.0	0.21[3]		12.8376	0.001	pH	10.6	0.96	
10/21/02	7.7	301.8		7.0	0.50[4]		0.0001	0.000	pH	8.9	0.18	
10/21/02	7.7	301.8		7.0	0.50[4]		0.0001	0.001			0.18	
10/21/02	7.7	301.8		7.0	0.50[4]		0.0037	0.001			0.18	
10/21/02	7.7	301.8		7.0	0.50[4]		0.0156	0.001			0.16	
10/21/02	7.7	301.8		7.0	0.50[4]		0.1111	0.001			0.17	
10/21/02	7.7	301.8		7.0	0.50[4]		0.9844	0.001	pH	9.4	0.16	

Date	Gas (LPM)	Ave Soln. Mass (g)	% Mass Change	MEA (m)	α	ρ (g/cc)	Fe [mM]	Cu [mM]	Misc. Variable	Value	NH$_3$ Evolution [mM/hr]	Relative Rate
10/30/02	7.6	280.5	20.1%	7.0	0.05^5		0.0001	0.000	pH	11.0	0.55	
10/30/02	7.6	280.5	20.1%	7.0	0.05^5		0.0001	0.001			1.65	
10/30/02	7.6	280.5	20.1%	7.0	0.05^5		0.0036	0.001			1.54	
10/30/02	7.6	280.5	20.1%	7.0	0.05^5		0.0320	0.001				
10/30/02	7.6	280.5	20.1%	7.0	0.05^5		0.1026	0.001			2.43	
10/30/02	7.6	280.5	20.1%	7.0	0.05^5		0.9311	0.001	pH	11.1	2.19	
11/13/02	7.7	270.8		7.0	0.15	1.02	0.0001	0.00	vol. % O$_2$	19.5%	0.97	
11/13/02	7.7	270.8		7.0	0.15	1.02	0.0962	0.001	vol. % O$_2$	19.5%	1.03	
11/13/02	7.7	270.8		7.0	0.15	1.02	0.0962	0.001	vol. % O$_2$	19.5%		
11/13/02	7.7	270.8		7.0	0.15	1.02	0.0962	0.001	vol. % O$_2$	10.8%		
11/13/02	7.7	270.8		7.0	0.15	1.02	0.0962	0.001	vol. % O$_2$	3.5%	0.63	
11/13/02	7.7	270.8		7.0	0.15	1.02	0.0962	0.001	vol. % O$_2$	0.0%	0.37	
11/18/02	7.7	269.4		7.0	0.15	1.02	0.0001	0.000	vol. % O$_2$	17.0%	1.18	
11/18/02	7.7	269.4		7.0	0.15	1.02	0.0968	0.001	vol. % O$_2$	17.0%	1.97	
11/18/02	7.7	269.4		7.0	0.15	1.02	0.0968	0.001	vol. % O$_2$	6.2%	1.18	
11/18/02	7.7	269.4		7.0	0.15	1.02	0.0968	0.001	vol. % O$_2$	3.0%	0.80	
11/18/02	7.7	269.4		7.0	0.15	1.02	0.0968	0.001	vol. % O$_2$	0.0%	0.15	
12/05/02	7.8	254.3	-17.1%	7.0	0.15	1.02	0.0001	0.000			1.15	
12/05/02	7.8	254.3	-17.1%	7.0	0.15	1.02	0.0001	0.005			1.69	
12/05/02	7.8	254.3	-17.1%	7.0	0.15	1.02	0.0030	0.005			1.98	
12/05/02	7.8	254.3	-17.1%	7.0	0.15	1.02	0.0177	0.005			2.19	
12/05/02	7.8	254.3	-17.1%	7.0	0.15	1.02	0.1638	0.005			2.47	
12/05/02	7.8	254.3	-17.1%	7.0	0.15	1.02	1.0891	0.005		mM	2.58	
12/05/02	7.8	254.3	-17.1%	7.0	0.15	1.02	1.0891	0.005	Na$_2$SO$_3$	7.21	2.96	
12/05/02	7.8	254.3	-17.1%	7.0	0.15	1.02	1.0891	0.005	Na$_2$SO$_3$	55.31	2.56	

Date	Gas (LPM)	Ave Soln. Mass (g)	% Mass Change	MEA (m)	α	ρ (g/cc)	Fe [mM]	Cu [mM]	Misc. Variable	Value	NH₃ Evolution [mMJ/hr]	Relative Rate
12/06/02	6.4	296.4		7.0	0.40	1.07	0.0002	0.000			0.83	
12/06/02	6.4	296.4		7.0	0.40	1.07	0.0002	0.012			1.32	
12/06/02	6.4	296.4		7.0	0.40	1.07	0.0029	0.012			1.29	
12/06/02	6.4	296.4		7.0	0.40	1.07	0.0148	0.012			1.35	
12/06/02	6.4	296.4		7.0	0.40	1.07	0.1468	0.012			1.43	
12/06/02	6.4	296.4		7.0	0.40	1.07	0.9849	0.012			1.46	
12/06/02	6.4	296.4		7.0	0.40	1.07	0.9849	0.998				
12/09/02	7.9	271.7	-12.3%	7.0	0.15	1.02	0.0001	0.000			0.86	
12/09/02	7.9	271.7	-12.3%	7.0	0.15	1.02	0.0001	0.013			3.38	
12/09/02	7.9	271.7	-12.3%	7.0	0.15	1.02	0.0028	0.013			3.20	
12/09/02	7.9	271.7	-12.3%	7.0	0.15	1.02	0.0150	0.013			3.17	
12/09/02	7.9	271.7	-12.3%	7.0	0.15	1.02	0.1098	0.013			2.91	
12/09/02	7.9	271.7	-12.3%	7.0	0.15	1.02	1.0336	0.013			2.80	
12/10/02[1,2]	7.6	251.0		7.0	0.00	0.99	0.0001	0.000			1.12	
12/10/02[1,2]	7.6	251.0		7.0	0.00	0.99	0.0001	0.012			1.50	
12/10/02[1,2]	7.6	251.0		7.0	0.00	0.99	0.0030	0.012			1.95	
12/10/02[1,2]	7.6	251.0		7.0	0.00	0.99	0.0145	0.012			1.93	
12/10/02[1,2]	7.6	251.0		7.0	0.00	0.99	0.1292	0.012			2.13	
12/10/02[1,2]	7.6	251.0		7.0	0.00	0.99	0.9697	0.012			2.41	

[1] precipitate formed during experiment
[2] abnormally high foaming of MEA solution
[3] loading is H_2SO_4 loading, pH = 10.3 instead of 12.1, final pH = 10.6
[4] loading is H_2SO_4 loading, pH = 8.9 instead of 12.1, final pH = 9.4
[5] loading is H_2SO_4 loading, pH = 11.0 instead of 12.2, final pH = 11.1

Appendix E: Sulfite Oxidation Mass Transfer Experiments

This appendix documents the experimental results from the sulfite oxidation experiments performed in the Sparged Reactor. Experiments were run using 0.05 m Na_2SO_3 buffered by 0.20 m $NaHSO_3$. The pH was measured continuously through the experiment; as the sulfite was oxidized, the pH of the solution decreased since the bisulfite was converted to sulfite in order to maintain thermodynamic equilibrium. The reactor solution was then titrated with a 1.0 m Na_2SO_3 solution to replace the oxidized sulfite, the solution returned to the original pH as some of the sulfite converted back to bisulfite. The O_2 absorption rate was then calculated by relating the rate of sulfite addition to the rate of oxygen absorption by the O_2 stoichiometry shown in Equation 4.1. Table E.1 and Table E.2 show measured viscosity data for concentrated $MgSO_4$ using a previously developed method (Cullinane 2005). Table E.3 shows data from the sulfite oxidation study. Complete data files for each experiment are available from Gary Rochelle at The University of Texas at Austin.

$$SO_3^{-2} + \frac{1}{2}O_2 \xrightarrow{\text{catalyst}} SO_4^{-2} \qquad\qquad \text{E.1}$$

Table E.1 Measured Viscosity of 20 wt. % $MgSO_4$ (aq.) (1.968 molal)

T (°C)	time (s)	ν (cS)	ρ_{water} (g/cc)	μ_{water} (cP)	η (ν_{sol}/ν_{water})	B (cm^2/s^2)
24.0	224.41	3.099	1.00	0.96	3.21	0.01381
24.0	222.73	3.076	1.00	0.96	3.19	0.01381
24.5	220.96	3.051	1.00	0.95	3.19	0.01381
26.0	210.96	2.913	1.00	0.93	3.12	0.01381
26.2	209.91	2.899	1.00	0.93	3.12	0.01381
26.2	209.18	2.889	1.00	0.93	3.10	0.01381
34.0	173.42	2.395	0.99	0.86	2.78	0.01381
34.0	172.65	2.384	0.99	0.86	2.77	0.01381
34.0	171.94	2.374	0.99	0.86	2.76	0.01381
34.0	171.30	2.366	0.99	0.86	2.75	0.01381
46.5	130.69	1.805	0.99	0.92	1.93	0.01381
47.5	128.50	1.775	0.99	0.94	1.87	0.01381
47.5	127.18	1.756	0.99	0.94	1.85	0.01381
47.5	126.66	1.749	0.99	0.94	1.84	0.01381
56.0	107.29	1.482	0.98	1.13	1.28	0.01381
56.5	106.44	1.470	0.98	1.15	1.26	0.01381
63.0	94.84	1.310	0.98	1.39	0.92	0.01381
64.0	93.81	1.295	0.98	1.43	0.89	0.01381
64.5	92.89	1.283	0.98	1.45	0.86	0.01381

B is the measured constant specific to this viscometer

Table E.2 Measured Viscosity of 15 wt. % $MgSO_4$ (aq.) (1.387 molal)

T (°C)	time (s)	ν (cS)	ρ_{water} (g/cc)	μ_{water} (cP)	η (ν_{sol}/ν_{water})	B (cm^2/s^2)
25.8	147.67	2.039	1.00	0.93	2.18	0.01381
26.0	146.89	2.029	1.00	0.93	2.17	0.01381
26.0	146.40	2.022	1.00	0.93	2.17	0.01381
31.0	129.40	1.787	0.99	0.87	2.03	0.01381
32.0	126.70	1.750	0.99	0.87	2.01	0.01381
33.5	122.67	1.694	0.99	0.86	1.96	0.01381
40.5	105.08	1.451	0.99	0.86	1.67	0.01381
41.0	103.97	1.436	0.99	0.86	1.64	0.01381
41.5	102.42	1.414	0.99	0.87	1.61	0.01381
52.5	83.72	1.156	0.98	1.04	1.10	0.01381
53.0	82.54	1.140	0.98	1.05	1.07	0.01381
53.5	81.98	1.132	0.98	1.06	1.05	0.01381
58.0	75.31	1.040	0.98	1.20	0.85	0.01381
59.0	74.74	1.032	0.98	1.23	0.82	0.01381
59.0	74.70	1.032	0.98	1.23	0.82	0.01381

B is the measured constant specific to this viscometer

Table E.3 O_2 Asorption Rates Measured by Sulfite Oxidation in the Sparged Reactor
(0.05 molal Na_2SO_3 and 0.20 molal $NaHSO_3$)

Date	Solution	T (°C)	Air Rate (LPM)	O_2 Uptake (mM/hr)
1/16/2003	Water	55.0	8.06	39.9
1/20/2003	10 wt % $MgSO_4$	55.0	8.06	9.8
1/22/2003	10 wt % $MgSO_4$	57.0	8.06	7.2
1/22/2003	10 wt % $MgSO_4$	57.0	5.84	8.7
1/27/2003	10 wt % $MgSO_4$	56.5	8.06	13.7
1/27/2003	10 wt % $MgSO_4$	57.0	5.88	10.1
1/27/2003	10 wt % $MgSO_4$	57.4	2.89	8.2
3/17/2003	Water	56.0	8.06	37.2
3/17/2003	Water	56.0	5.48	25.3
3/17/2003	Water	56.0	2.93	19.9
3/30/2003	5 wt % $MgSO_4$	54.7	9.39	26.1
3/30/2003	5 wt % $MgSO_4$	54.5	8.06	18.0
3/30/2003	5 wt % $MgSO_4$	54.6	6.44	14.2
3/30/2003	5 wt % $MgSO_4$	54.8	3.78	11.0
4/05/2003	15 wt % $MgSO_4$	54.5	9.10	10.3
5/12/2003	15 wt % $MgSO_4$	53.5	9.12	8.7
5/12/2003	15 wt % $MgSO_4$	53.7	7.32	10.9
5/12/2003	15 wt % $MgSO_4$	53.8	5.84	11.0
5/12/2003	15 wt % $MgSO_4$	54.2	3.34	13.0
5/16/2003	15 wt % $MgSO_4$	54.6	9.71	14.0
5/16/2003	15 wt % $MgSO_4$	55.6	7.79	3.8
5/16/2003	15 wt % $MgSO_4$	55.8	5.84	7.7
5/16/2003	15 wt % $MgSO_4$	55.7	3.01	9.8

Appendix F: Agitated Reactor O$_2$ Mass Transfer Experiments

This appendix documents the experimental results from the O$_2$ mass transfer study performed in the Agitated Reactor. All experiments were performed at 55°C. Dates in *italics* indicate a continuation of the previous experiment. Data points in gray font color indicate data points that should not be used for quantitative analysis. In general these data points have excluded because the system was not at steady state or there was a problem with the mass balance.

Table F.1 tabulates the results from experiments performed in the Agitated Reactor. Complete data files for each experiment are available from Gary Rochelle at The University of Texas at Austin.

Table F.1 Experimental Results for the O$_2$ Mass Transfer Study in the Agitated Reactor at 55°C

Date	Gas (LPM)	Ave Soln. Mass (g)	% Mass Change	MEA (m)	α	ρ (g/cc)	Fe [mM]	Cu [mM]	O$_2$ (%)	RPM	NH$_3$ Evolution [mM]/hr	Relative Rate
09/16/03	7.4	537.8	-1.6%	7.0	0.15	1.02	0.0002	0.00	air	0	0.22	0.06
09/16/03	7.4	537.8	-1.6%	7.0	0.15	1.02	0.0002	0.20	air	0	3.98	1.00
09/16/03	7.4	537.8	-1.6%	7.0	0.15	1.02	0.0002	0.20	air	174	3.22	0.81
09/16/03	7.4	537.8	-1.6%	7.0	0.15	1.02	0.0002	0.20	air	1185	6.11	1.54
09/16/03	7.4	537.8	-1.6%	7.0	0.15	1.02	0.0002	0.20	air	1448	6.73	1.69
09/16/03	7.4	537.8	-1.6%	7.0	0.15	1.02	0.0002	0.20	air	600	2.12	0.53
09/22/03	7.3	548.8	4.3%	7.0	0.15	1.02	0.0002	0.00	air	0	0.24	1.00
09/22/03	7.3	548.8	4.3%	7.0	0.15	1.02	0.0002	0.00	air	170	0.58	2.42
09/22/03	7.3	548.8	4.3%	7.0	0.15	1.02	0.0002	0.00	air	623	0.80	3.33
09/22/03	7.3	548.8	4.3%	7.0	0.15	1.02	0.0002	0.00	air	1034	0.92	3.83
09/22/03	7.3	548.8	4.3%	7.0	0.15	1.02	0.0002	0.00	air	1427	0.98	4.08
09/22/03	7.3	548.8	4.3%	7.0	0.15	1.02	0.0002	0.00	air	800	---	
09/22/03	7.3	548.8	4.3%	7.0	0.15	1.02	0.0002	0.00	air	0	---	
09/23/03	6.7	548.4	4.3%	7.0	0.15	1.02	0.0002	0.00	air	0	0.93	1.00
09/23/03	6.7	548.4	4.3%	7.0	0.15	1.02	0.0002	0.00	air	412	0.85	0.91
09/23/03	6.7	548.4	4.3%	7.0	0.15	1.02	0.0002	0.00	air	841	0.78	0.84
09/23/03	6.7	548.4	4.3%	7.0	0.15	1.02	0.0002	0.00	air	1418	---	
09/23/03	6.7	548.4	4.3%	7.0	0.15	1.02	0.0002	0.00	air	0	0.60	0.65
09/24/03	7.4	548.4	4.3%	7.0	0.15	1.02	0.0002	0.00	air	0	1.62	
09/24/03	7.4	548.4	4.3%	7.0	0.15	1.02	0.0002	0.00	air	1446	1.81	
09/29/03	7.5	592.4	29.0%	7.0	0.15	1.02	0.0002	0.00	air	0	0.15	0.05
09/29/03	7.5	592.4	29.0%	7.0	0.15	1.02	0.0002	0.18	air	0	2.83	1.00
09/29/03						ADD 37.1 mM Formaldehyde						
09/29/03	7.5	592.4	29.0%	7.0	0.15	1.02	0.0002	0.18	air	1387	4.74	1.67
09/29/03	7.5	592.4	29.0%	7.0	0.15	1.02	0.0002	0.18	air	820	3.71	1.31
09/29/03	7.5	592.4	29.0%	7.0	0.15	1.02	0.0002	0.18	air	384	3.01	1.06
09/29/03	7.5	592.4	29.0%	7.0	0.15	1.02	0.0002	0.18	air	0	2.93	1.04

Date	Gas (LPM)	Ave Soln. Mass (g)	% Mass Change	MEA (m)	α	ρ (g/cc)	Fe [mM]	Cu [mM]	O$_2$ (%)	RPM	NH$_3$ Evolution [mM]/hr	Relative Rate
09/30/03	7.2	592.4	29.0%	7.0	0.15	1.02	0.0002	0.18	air	0	2.71	0.96
09/30/03	7.2	592.4	29.0%	7.0	0.15	1.02	0.0002	0.18	air	909	2.94	1.04
09/30/03	7.2	592.4	29.0%	7.0	0.15	1.02	0.0002	0.18	air	0	3.00	1.06
09/30/03	7.2	592.4	29.0%	7.0	0.15	1.02	0.0002	0.18	air	1200	3.65	1.29
09/30/03	7.2	592.4	29.0%	7.0	0.15	1.02	0.0002	0.18	air	0	2.75	0.97
09/30/03	7.2	592.4	29.0%	7.0	0.15	1.02	0.0002	0.18	air	618	2.01	0.71
09/30/03	7.2	592.4	29.0%	7.0	0.15	1.02	0.0002	0.18	air	0	2.56	0.90
10/03/03	7.4	592.4	29.0%	7.0	0.15	1.02	0.0002	0.18	air	0	2.23	0.79
10/03/03	7.4	592.4	29.0%	7.0	0.15	1.02	0.0002	0.18	air	1200	3.46	1.22
10/20/03	7.3	518.8		7.0	0.15	1.02	0.0002	0.00	air	0	0.20	0.12
10/20/03	7.3	518.8		7.0	0.15	1.02	0.1429	0.00	air	0	1.66	1.00
10/20/03	7.3	518.8		7.0	0.15	1.02	0.1429	0.00	air	1429	2.03	1.22
10/20/03	7.3	518.8		7.0	0.15	1.02	0.1429	0.00	air	220	1.29	0.78
10/20/03	7.3	518.8		7.0	0.15	1.02	0.1429	0.00	air	751	1.46	0.88
10/20/03	7.3	518.8		7.0	0.15	1.02	0.1429	0.00	air	1414	1.78	1.07
10/20/03	7.3	518.8		7.0	0.15	1.02	0.1429	0.00	air	0	1.55	0.93
10/21/03	7.2	625.4	41.1%	7.0	0.15	1.02	0.1187	0.00	air	1430		0.00
10/21/03	7.2	625.4	41.1%	7.0	0.15	1.02	0.1187	0.00	air	900		0.00
10/21/03	7.2	625.4	41.1%	7.0	0.15	1.02	0.1187	0.00	air	0	1.47	0.89
10/21/03	7.2	625.4	41.1%	7.0	0.15	1.02	0.1187	0.00	air	510	1.20	0.72
10/21/03	7.2	625.4	41.1%	7.0	0.15	1.02	0.1187	0.00	air	1410	1.69	1.02
10/21/03	7.2	625.4	41.1%	7.0	0.15	1.02	0.1187	0.00	air	615	1.30	0.78
10/21/03	7.2	625.4	41.1%	7.0	0.15	1.02	0.1187	0.00	air	1425	1.56	0.94
10/21/03	7.2	625.4	41.1%	7.0	0.15	1.02	0.1187	0.00	air	0	1.40	0.84

Date	Gas (LPM)	Ave Soln. Mass (g)	% Mass Change	MEA (m)	α	ρ (g/cc)	Fe [mM]	Cu [mM]	O$_2$ (%)	RPM	NH$_3$ Evolution [mM]/hr	Relative Rate
10/24/03	7.0	659.5	53.5%	7.0	0.15	1.02	0.0002	0.00	8.2%	1343	0.23	0.07
10/24/03	7.0	659.5	53.5%	7.0	0.15	1.02	0.0002	0.17	8.2%	1343	3.41	1.00
10/24/03	7.0	659.5	53.5%	7.0	0.15	1.02	0.0002	0.17	8.2%	877	1.79	0.52
10/24/03	7.0	659.5	53.5%	7.0	0.15	1.02	0.0002	0.17	8.2%	244	1.43	0.42
10/24/03	7.0	659.5	53.5%	7.0	0.15	1.02	0.0002	0.17	8.2%	603	1.60	0.47
10/24/03	7.0	659.5	53.5%	7.0	0.15	1.02	0.0002	0.17	8.2%	0	1.52	0.45
10/24/03	7.0	659.5	53.5%	7.0	0.15	1.02	0.0002	0.17	8.2%	1406	2.79	0.82
10/27/03	7.4	544.7	2.5%	7.0	0.15	1.02	0.0002	0.00	17.2%	1400	0.21	0.03
10/27/03	7.4	544.7	2.5%	7.0	0.15	1.02	0.0002	0.20	17.2%	1400	7.79	1.25
10/27/03	7.4	544.7	2.5%	7.0	0.15	1.02	0.0002	0.20	4.6%	1400	2.90	0.46
10/27/03	7.4	544.7	2.5%	7.0	0.15	1.02	0.0002	0.20	7.2%	1400	3.64	0.58
10/27/03	7.4	544.7	2.5%	7.0	0.15	1.02	0.0002	0.20	2.1%	1400	1.82	0.29
10/27/03	7.4	544.7	2.5%	7.0	0.15	1.02	0.0002	0.20	0.0%	1400	0.11	0.02
10/27/03	7.4	544.7	2.5%	7.0	0.15	1.02	0.0002	0.20	12.7%	1400	5.47	0.88
10/27/03	7.4	544.7	2.5%	7.0	0.15	1.02	0.0002	0.20	17.2%	1400	6.24	1.00
10/28/03	7.4	496.8	-11.9%	3.5	0.15	1.01	0.0001	0.22	17.0%	1400	4.12	1.00
10/28/03	7.4	496.8	-11.9%	3.5	0.15	1.01	0.0001	0.22	7.1%	1400	2.13	0.52
10/28/03	7.4	496.8	-11.9%	3.5	0.15	1.01	0.0001	0.22	12.6%	1400	2.54	0.62
10/28/03	7.4	496.8	-11.9%	3.5	0.15	1.01	0.0001	0.22	2.1%	1400	1.16	0.28
10/28/03	7.4	496.8	-11.9%	3.5	0.15	1.01	0.0001	0.22	17.0%	1400		0.00
10/30/03	7.2	458.6		3.5	0.15	1.01	0.0001	0.00	17.7%	1400	1.34	0.40
10/30/03	7.2	458.6		3.5	0.15	1.01	0.0001	0.24	17.7%	1400	3.33	1.00
10/30/03	7.2	458.6		3.5	0.15	1.01	0.0001	0.24	4.7%	1400	1.50	0.45
10/30/03	7.2	458.6		3.5	0.15	1.01	0.0001	0.24	0.0%	1400	0.15	0.05
11/01/03	7.1	531.8	3.3%	14.0	0.15	1.04	0.0003	0.20	7.5%	1400	4.31	0.59
11/01/03	7.1	531.8	3.3%	14.0	0.15	1.04	0.0003	0.20	13.2%	1400	7.28	1.00
11/01/03	7.1	531.8	3.3%	14.0	0.15	1.04	0.0003	0.20	2.2%	1400	2.08	0.28
11/01/03	7.1	531.8	3.3%	14.0	0.15	1.04	0.0003	0.20	4.8%	1400	3.25	0.44
11/01/03	7.1	531.8	3.3%	14.0	0.15	1.04	0.0003	0.20	16.3%	1400	7.31	1.00

Date	Gas (LPM)	Ave Soln. Mass (g)	% Mass Change	MEA (m)	α	ρ (g/cc)	Fe [mM]	Cu [mM]	O$_2$ (%)	RPM	NH$_3$ Evolution [mM]/hr	Relative Rate
11/03/03	7.1	554.3	4.4%	14.0	0.15	1.04	0.0003	0.20	17.9%	1400	8.70	1.00
11/03/03	7.1	554.3	4.4%	14.0	0.15	1.04	0.0003	0.20	13.3%	1400	7.07	0.81
11/03/03	7.1	554.3	4.4%	14.0	0.15	1.04	0.0003	0.20	4.8%	1400	3.78	0.43
11/03/03	7.1	554.3	4.4%	14.0	0.15	1.04	0.0003	0.20	0.0%	1400	0.14	0.02
11/10/03	7.1	549.6	9.9%	7.0	0.15	1.02	0.0002	0.19	air	1408	9.22	1.00
11/10/03	7.1	549.6	9.9%	7.0	0.15	1.02	0.0002	0.19	air	1175	6.64	0.72
11/10/03	7.1	549.6	9.9%	7.0	0.15	1.02	0.0002	0.19	air	899	4.08	0.44
11/10/03	7.1	549.6	9.9%	7.0	0.15	1.02	0.0002	0.19	air	526	2.28	0.25
11/10/03	7.1	549.6	9.9%	7.0	0.15	1.02	0.0002	0.19	air	248	2.48	0.27
11/10/03	7.1	549.6	9.9%	7.0	0.15	1.02	0.0002	0.19	air	0	3.61	0.39
11/13/03	6.7	536.3	8.0%	7.0	0.15	1.02	0.0002	0.20	19.0%	1400	4.12	0.45
11/13/03	6.7	536.3	8.0%	7.0	0.15	1.02	0.0002	0.20	14.0%	1400	3.74	0.41
11/13/03							MEA Solution contains 0.5 m NaCl					
11/14/03	7.2	543.8	3.9%	3.5	0.15	1.01	0.0001	0.20	17.6%	1400	2.43	0.94
11/14/03	7.2	543.8	3.9%	3.5	0.15	1.01	0.0001	0.20	13.1%	1400	2.59	1.00
11/14/03	7.2	543.8	3.9%	3.5	0.15	1.01	0.0001	0.20	7.4%	1400	1.97	0.76
11/14/03	7.2	543.8	3.9%	3.5	0.15	1.01	0.0001	0.20	2.1%	1400	0.92	0.36
11/14/03	7.2	543.8	3.9%	3.5	0.15	1.01	0.0001	0.20	0.0%	1400	0.12	0.05
						MEA Solution contains 1.6 m NaCl so ionic strength is same as 7.0 molal MEA						
05/12/04							BAD ANALYSIS					
05/13/04				BAD ANALYSIS - LASER OUT OF ALIGNMENT - SEND FOR REPAIR									
05/24/04					REFERENCE SPECTRA LOST							
05/26/04	7.3	473.4	-13.0%	2.0	0.15	1.00	0.0001	0.21	17.4%	700	1.20	0.85
05/26/04	7.3	473.4	-13.0%	2.0	0.15	1.00	0.0001	0.21	17.4%	1400	1.41	1.00
05/26/04	7.3	473.4	-13.0%	2.0	0.15	1.00	0.0001	0.21	7.2%	1400	0.92	0.65
05/26/04	7.3	473.4	-13.0%	2.0	0.15	1.00	0.0001	0.21	7.2%	700	0.66	0.47
05/26/04	7.3	473.4	-13.0%	2.0	0.15	1.00	0.0001	0.21	4.6%	1400	0.62	0.44
05/26/04	7.3	473.4	-13.0%	2.0	0.15	1.00	0.0001	0.21	4.6%	700	0.51	0.36

Date	Gas (LPM)	Ave Soln. Mass (g)	% Mass Change	MEA (m)	α	ρ (g/cc)	Fe [mM]	Cu [mM]	O₂ (%)	RPM	NH₃ Evolution [mMl/hr	Relative Rate
06/03/04	7.2	507.8	-2.8%	1.0	0.15	0.99	0.0000	0.21	17.5%	1400	0.30	0.43
06/03/04	7.2	507.8	-2.8%	1.0	0.15	0.99	0.0000	0.21	17.5%	700	0.65	0.94
06/03/04	7.2	507.8	-2.8%	1.0	0.15	0.99	0.0000	0.21	17.5%	1400	0.69	1.00
06/04/04	7.2	438.8	-4.5%	1.0	0.15	0.99	0.0000	0.20	4.6%	1400	0.21	0.84
06/04/04	7.2	438.8	-4.5%	1.0	0.15	0.99	0.0000	0.20	4.6%	700	0.21	0.84
06/04/04	7.2	438.8	-4.5%	1.0	0.15	0.99	0.0000	0.20	4.6%	1400	0.25	1.00
06/07/04	7.2	536.4	4.0%	7.0	0.15	1.02	0.0002	0.00	17.9%	1400	0.30	1.00
06/07/04	7.2	536.4	4.0%	7.0	0.15	1.02	0.0002	0.01	17.9%	1400	1.87	6.23
06/07/04	7.2	536.4	4.0%	7.0	0.15	1.02	0.0002	0.06	17.9%	1400	4.12	13.73
06/07/04	7.2	536.4	4.0%	7.0	0.15	1.02	0.0002	0.12	17.9%	1400	5.01	16.70
06/07/04	7.2	536.4	4.0%	7.0	0.15	1.02	0.0002	0.66	17.9%	1400	6.01	20.03
06/07/04	7.2	536.4	4.0%	7.0	0.15	1.02	0.0002	1.24	17.9%	1400	6.10	20.33
06/07/04	7.2	536.4	4.0%	7.0	0.15	1.02	0.0002	3.39	17.9%	1400	7.45	24.83
06/26/04	7.0	551.8	15.5%	7.0	0.15	1.02	0.0035	0.00	18.4%	1400	2.50	1.00
06/26/04	7.0	551.8	15.5%	7.0	0.15	1.02	0.0359	0.00	18.4%	1400	3.29	1.32
06/26/04	7.0	551.8	15.5%	7.0	0.15	1.02	0.1229	0.00	18.4%	1400	3.74	1.50
06/26/04	7.0	551.8	15.5%	7.0	0.15	1.02	0.4268	0.00	18.4%	1400	3.57	1.43
06/26/04	7.0	551.8	15.5%	7.0	0.15	1.02	0.6131	0.00	18.4%	1400	3.19	1.28
06/26/04	7.0	551.8	15.5%	7.0	0.15	1.02	0.8953	0.00	18.4%	1400	2.88	1.15
06/28/04	7.1	493.2	-6.2%	7.0	0.00	0.99	0.0002	0.000	18.0%	1400	0.13	1.00
06/28/04	7.1	493.2	-6.2%	7.0	0.00	0.99	0.0002	0.006	18.0%	1400	0.17	1.31
06/28/04	7.1	493.2	-6.2%	7.0	0.00	0.99	0.0002	0.131	18.0%	1400	0.39	3.00
06/28/04	7.1	493.2	-6.2%	7.0	0.00	0.99	0.0002	0.378	18.0%	1400	0.59	4.54
06/28/04	7.1	493.2	-6.2%	7.0	0.00	0.99	0.0002	1.074	18.0%	1400	7.68	59.08
06/28/04	7.1	493.2	-6.2%	7.0	0.00	0.99	0.0002	4.058	18.0%	1400	8.33	64.08

Appendix G: Experiments with Degradation Inhibitors

This appendix documents the experimental results from the degradation inhibitors study performed in the Agitated Reactor. All experiments were performed with 7.0 m MEA at 55°C and 1400 RPM. Dates in *italics* indicate a continuation of the previous experiment. Data points in gray font color indicate data points that should not be used for quantitative analysis. In general these data points have excluded because the system was not at steady state or there was a problem with the mass balance. Table G.1 tabulates the results from experiments performed in the Sparged Reactor. Complete data files for each experiment are available from Gary Rochelle at The University of Texas at Austin.

Table G.1 Experimental Results for the Oxidation Inhibitor Experiments (Agitated Reactor, 7.0 m MEA, 55°C, 1400 RPM)

Date	α	Gas (LPM)	Ave Soln. Mass (g)	% Mass Change	ρ (g/cc)	Fe [mM]	Cu [mM]	Inhibitor	[mM]	NH₃ Evolution [mM/hr]	Relative Rate
01/28/04	0.15	7.1	545.5	-4.9%	1.02	0.0002	0.2012	Na₂SO₃	0.0	9.4	1.00
01/28/04	0.15	7.1	545.5	-4.9%	1.02	0.0002	0.2012	Na₂SO₃	811.9	2.12	0.23
01/28/04	0.15	7.1	545.5	-4.9%	1.02	0.0002	2.3073	Na₂SO₃	811.9	2.45	0.26
01/29/04	0.15	7.2	545.5	-4.9%	1.02	0.0002	2.3073	Na₂SO₃	811.9	6.15	0.65
02/05/04	0.15	7.1	460.1	-6.6%	1.02	0.0002	0.2037	Na₂SO₃	0.0	6.51	1.00
02/05/04	0.15	7.1	460.1	-6.6%	1.02	0.0002	0.2037	Na₂SO₃	164.0	4.18	0.64
02/06/04	0.15	7.1	460.1	-6.6%	1.02	0.0002	0.2037	Na₂SO₃	164.0	4.94	0.76
02/09/04	0.15	7.2	511.5	NA	1.02	0.0002	0.2002	Na₂SO₃	0.0	7.01	1.00
02/09/04	0.15	7.2	511.5	NA	1.02	0.0002	0.2002	Na₂SO₃	27.2	4.87	0.69
02/10/04								BAD DATA			
02/19/04	0.15	7.2	440.4	-12.8%	1.02	0.0002	0.2180			5.06	
02/20/04	0.15	7.2	477.8	-5.3%	1.02	0.0002	0.2049	Na₂SO₃	0.0	7.03	1.00
02/20/04	0.15	7.2	477.8	-5.3%	1.02	0.0002	0.2049	Na₂SO₃	8.3	5.81	0.83
02/20/04	0.15	7.2	477.8	-5.3%	1.02	0.0002	0.2049	Na₂SO₃	26.5	4.39	0.62
02/20/04	0.15	7.2	477.8	-5.3%	1.02	0.0002	0.2049	Na₂SO₃	109.7	1.13	0.16
02/20/04	0.15	7.2	477.8	-5.3%	1.02	0.0002	0.2049	Na₂SO₃	195.2	1.53	0.22
02/20/04	0.15	7.2	477.8	-5.3%	1.02	0.0002	0.2049	Na₂SO₃	365.5	2.31	0.33
02/20/04	0.15	7.2	477.8	-5.3%	1.02	0.0002	0.2049	Na₂SO₃	450.1	2.3	0.33
02/21/04	0.15	7.2	508.4	5.8%	1.02	0.0002	0.1934	Na₂SO₃	0.0	6.04	1.00
02/21/04	0.15	7.2	508.4	5.8%	1.02	0.0002	0.1934	Ascorbic Acid	65.5	15.26	2.53
02/21/04	0.15	7.2	508.4	5.8%	1.02	0.0002	0.1934	Inhibitor A	69.9		

Date	α	Gas (LPM)	Ave Soln. Mass (g)	% Mass Change	ρ (g/cc)	Fe [mM]	Cu [mM]	Inhibitor	[mM]	NH_3 Evolution [mM]/hr	Relative Rate
02/23/04	0.15	7.2	521.9	8.9%	1.02	0.0002	0.2018	Inhibitor A	0.0	7.49	1.00
02/23/04	0.15	7.2	521.9	8.9%	1.02	0.0002	0.2018	Inhibitor A	6.1	5.35	0.71
02/23/04	0.15	7.2	521.9	8.9%	1.02	0.0002	0.2018	Inhibitor A	19.8	1.85	0.25
02/23/04	0.15	7.2	521.9	8.9%	1.02	0.0002	0.2018	Inhibitor A	62.1	0.75	0.10
02/23/04	0.15	7.2	521.9	8.9%	1.02	0.0002	0.2018	Inhibitor A	125.3	0.46	0.06
02/23/04	0.15	7.2	521.9	8.9%	1.02	0.0002	0.2018	Inhibitor A	245.9	0.37	0.05
02/27/04	0.40	7.5	494.4	-5.7%	1.07	0.0002	0.2083	Na_2SO_3	0.0	7.58	1.00
02/27/04	0.40	7.5	494.4	-5.7%	1.07	0.0002	0.2083	Na_2SO_3	19.9	4.97	0.66
02/27/04	0.40	7.5	494.4	-5.7%	1.07	0.0002	0.2083	Na_2SO_3	81.7	1.29	0.17
02/27/04	0.40	7.5	494.4	-5.7%	1.07	0.0002	0.2083	Na_2SO_3	166.0	1.95	0.26
02/27/04	0.40	7.5	494.4	-5.7%	1.07	0.0002	0.2083	Na_2SO_3	338.2	2.41	0.32
02/27/04	0.40	7.5	494.4	-5.7%	1.07	0.0002	0.2083	Na_2SO_3	1026.5	1.25	0.16
02/28/04							BAD DATA				
03/16/04	0.40	7.4	511.0	-1.1%	1.07	0.0002	0.2024	Inhibitor A	0.0	1.32	1.00
03/16/04	0.40	7.4	511.0	-1.1%	1.07	0.0002	0.2024	Inhibitor A	8.7	0.22	0.17
03/16/04	0.40	7.4	511.0	-1.1%	1.07	0.0002	0.2024	Inhibitor A	27.3	0.15	0.11
03/22/04	0.40	7.4	515.7	-0.7%	1.07	0.0002	0.1978	Inhibitor A	0.0	1.49	1.00
03/22/04	0.40	7.4	515.7	-0.7%	1.07	0.0002	0.1978	Inhibitor A	1.3	1.21	0.81
03/22/04	0.40	7.4	515.7	-0.7%	1.07	0.0002	0.1978	Inhibitor A	3.6	0.56	0.38
03/22/04	0.40	7.4	515.7	-0.7%	1.07	0.0002	0.1978	Inhibitor A	5.0	0.42	0.28

Date	α	Gas (LPM)	Ave Soln. Mass (g)	% Mass Change	ρ (g/cc)	Fe [mM]	Cu [mM]	Inhibitor	[mM]	NH₃ Evolution [mM]/hr	Relative Rate
07/06/04	0.15	7.1	515.5	-0.3%	1.02	0.0002	0.2108	KBr	0.0	7.25	1.00
07/06/04	0.15	7.1	515.5	-0.3%	1.02	0.0002	0.2108	KBr	3.1	5.92	0.82
07/06/04	0.15	7.1	515.5	-0.3%	1.02	0.0002	0.2108	KBr	9.3	5.42	0.75
07/06/04	0.15	7.1	515.5	-0.3%	1.02	0.0002	0.2108	KBr	21.9	5.01	0.69
07/06/04	0.15	7.1	515.5	-0.3%	1.02	0.0002	0.2108	KBr	50.0	4.90	0.68
07/06/04	0.15	7.1	515.5	-0.3%	1.02	0.0002	0.2108	KBr	98.6	4.76	0.66
07/06/04	0.15	7.1	515.5	-0.3%	1.02	0.0002	0.2108	KBr	199.2	4.62	0.64
07/06/04	0.15	7.1	515.5	-0.3%	1.02	0.0002	0.2108	KBr	390.4	4.57	0.63
07/06/04	0.15	7.1	515.5	-0.3%	1.02	0.0002	0.2108	KBr	988.1	4.40	0.61
07/06/04	0.15	7.1	515.5	-0.3%	1.02	0.0002	0.2108	KBrO₃	177.6	5.08	0.70
07/07/04	0.15	7.1	511.3	-1.9%	1.02	0.0002	0.2085	KCl	0.0	6.34	1.00
07/07/04	0.15	7.1	511.3	-1.9%	1.02	0.0002	0.2085	KCl	14.0	5.40	0.85
07/07/04	0.15	7.1	511.3	-1.9%	1.02	0.0002	0.2085	KCl	146.5	5.55	0.88
07/07/04	0.15	7.1	511.3	-1.9%	1.02	0.0002	0.2085	KCl	548.9	5.65	0.89
07/07/04	0.15	7.1	511.3	-1.9%	1.02	0.0002	0.2085	KCl	1524.6	5.71	0.90
07/08/04	0.15	7.2	502.8	-0.3%	1.02	0.0002	0.1934	MnSO₄	0.0	6.23	1.00
07/08/04	0.15	7.2	502.8	-0.3%	1.02	0.0002	0.1934	MnSO₄	6.4	1.04	0.17
07/08/04	0.15	7.2	502.8	-0.3%	1.02	0.0002	0.1934	MnSO₄	7.4	0.84	0.13
07/09/04								BAD DATA			
07/12/04	0.15	7.2	517.0	NA	1.02	0.0002	0.2067	MnSO₄	0.000	5.89	1.00
07/12/04	0.15	7.2	517.0	NA	1.02	0.0002	0.2067	MnSO₄	0.002	3.69	0.63
07/12/04	0.15	7.2	517.0	NA	1.02	0.0002	0.2067	MnSO₄	0.120	3.37	0.57
07/12/04	0.15	7.2	517.0	NA	1.02	0.0002	0.2067	MnSO₄	0.895	3.44	0.58
07/14/04	0.15	7.1	495.8	-8.4%	1.02	0.0002	0.2128	KMnO₄	0.0000	6.71	1.00
07/14/04	0.15	7.1	495.8	-8.4%	1.02	0.0002	0.2128	KMnO₄	0.0034	3.82	0.65
07/14/04	0.15	7.1	495.8	-8.4%	1.02	0.0002	0.2128	KMnO₄	0.0270	4.05	0.69
07/14/04	0.15	7.1	495.8	-8.4%	1.02	0.0002	0.2128	KMnO₄	0.0270	9.21	1.56

Date	α	Gas (LPM)	Ave Soln. Mass (g)	% Mass Change	ρ (g/cc)	Fe [mM]	Cu [mM]	Inhibitor	[mM]	NH₃ Evolution [mM/hr]	Relative Rate
07/19/04	0.15	7.1	502.4	-7.3%	1.02	0.0002	0.0000	EDTA	0.00	1.29	0.20
07/19/04	0.15	7.1	502.4	-7.3%	1.02	0.0002	0.2113	EDTA	0.00	6.34	1.00
07/19/04	0.15	7.1	502.4	-7.3%	1.02	0.0002	0.2105	EDTA	0.19	2.13	0.34
07/19/04	0.15	7.1	502.4	-7.3%	1.02	0.0002	0.2104	EDTA	0.21	1.93	0.30
07/19/04	0.15	7.1	502.4	-7.3%	1.02	0.0002	0.2103	EDTA	0.22	1.67	0.26
07/21/04	0.15	7.1	485.6	-6.2%	1.02	0.0002	0.2205	K-Formate	0.0	5.83	1.00
07/21/04	0.15	7.1	485.6	-6.2%	1.02	0.0002	0.2205	K-Formate	19.5	5.33	0.91
07/21/04	0.15	7.1	485.6	-6.2%	1.02	0.0002	0.2205	K-Formate	221.0	5.16	0.89
07/22/04	0.15	7.1	485.6	-6.2%	1.02	0.0002	0.2205	K-Formate	774.5	5.12	0.88
07/26/04	0.15	7.1	477.1	-9.3%	1.02	0.0002	0.2104	Quinone	0.0	4.67	0.80
07/26/04	0.15	7.1	477.1	-9.3%	1.02	0.0002	0.2104	Quinone	16.4	21.34	3.66
07/28/04	0.15	7.2	468.2	-13.2%	1.02	0.0002	0.2150	Formaldehyde	0.0	3.98	0.76
07/28/04	0.15	7.2	468.2	-13.2%	1.02	0.0002	0.2150	Formaldehyde	0.0	5.22	1.00
07/28/04	0.15	7.2	468.2	-13.2%	1.02	0.0002	0.2142	Formaldehyde	53.5	4.08	0.78
07/28/04	0.15	7.2	468.2	-13.2%	1.02	0.0002	0.2137	Formaldehyde	91.0	3.61	0.69
07/29/04	0.15	7.1	468.2	-13.2%	1.02	0.0002	0.2112	Formaldehyde	259.6	0.79	0.15
07/29/04	0.15	7.1	468.2	-13.2%	1.02	0.0002	0.2082	Formaldehyde	468.9	0.44	0.08
07/31/04	0.15	7.2	506.4	NA	1.02	0.0002	0.2099	Inhibitor A	0.0	5.38	1.00
07/31/04	0.15	7.2	506.4	NA	1.02	0.0002	0.2099	Inhibitor A	1.0	5.31	0.99
07/31/04	0.15	7.2	506.4	NA	1.02	0.0002	0.2099	Inhibitor A	5.1	2.68	0.50
08/02/04	0.15	7.2	506.4	NA	1.02	0.0002	0.2099	Inhibitor A	5.1	5.41	1.01
08/03/04							BAD DATA				
08/04/04	0.15	7.2	511.7	NA	1.02	0.0002	0.2101	Na₃PO₄	0.0	4.69	1.00
08/04/04	0.15	7.2	511.7	NA	1.02	0.0002	0.2101	Na₃PO₄	12.3	4.46	0.95
08/04/04	0.15	7.2	511.7	NA	1.02	0.0002	0.2101	Na₃PO₄	31.8	4.27	0.91
08/04/04	0.15	7.2	511.7	NA	1.02	0.0002	0.2101	Na₃PO₄	99.5	3.64	0.78
08/07/04	0.15	7.2	482.5	NA	1.02	0.0002	0.2090	Inhibitor A	0.0	4.15	1.00
08/07/04	0.15	7.2	482.5	NA	1.02	0.0002	0.2090	Inhibitor A	49.0	0.74	0.18

Date	α	Gas (LPM)	Ave Soln. Mass (g)	% Mass Change	ρ (g/cc)	Fe [mM]	Cu [mM]	Inhibitor	[mM]	NH₃ Evolution [mM/hr]	Relative Rate
08/08/04	0.15	7.2	482.5	NA	1.02	0.0002	0.2090	Inhibitor A	49.0	0.55	0.13
08/09/04	0.15	7.1	491.5	-5.6%	1.02	0.0002	0.2092	Inhibitor A	0.0	4.60	1.00
08/09/04	0.15	7.1	491.5	-5.6%	1.02	0.0002	0.2092	Inhibitor A	20.7	4.51	0.98
08/10/04	0.15	7.2	491.5	-5.6%	1.02	0.0002	0.2092	Inhibitor A	101.6	2.79	0.61
08/10/04	0.15	7.2	491.5	-5.6%	1.02	0.0002	0.2092	Inhibitor A	201.5	2.02	0.44
08/12/04	0.15	7.1	476.2	-8.3%	1.02	0.0002	0.2165	MnSO₄	0.000	5.06	1.00
08/12/04	0.15	7.1	476.2	-8.3%	1.02	0.0002	0.2165	MnSO₄	0.011	10.80	2.13
08/13/04	0.15	7.2	476.2	-8.3%	1.02	0.0002	0.2165	MnSO₄	0.011	5.40	1.07
08/18/04	0.15	7.2	437.1	-24.9%	1.02	0.0002	0.2417	BAD DATA....PLAYING WITH BOMB AND MIST ELIMINATOR			
08/19/04	0.15	7.2	529.4	11.6%	1.02	0.0002	0.1921	Inhibitor A	0.0	5.50	1.00
08/19/04	0.15	7.2	529.4	11.6%	1.02	0.0002	0.1921	Inhibitor A	10.4	2.89	0.53
08/20/04	0.15	7.2	529.4	11.6%	1.02	0.0002	0.1921	Inhibitor A	48.1	0.98	0.18
08/20/04	0.15	7.2	529.4	11.6%	1.02	0.0002	0.1921	Inhibitor A	70.7	0.67	0.12
08/20/04	0.15	7.2	529.4	11.6%	1.02	0.0002	0.1921	Inhibitor A	93.4	0.53	0.10
08/20/04	0.15	7.2	529.4	11.6%	1.02	0.0002	0.1921	Inhibitor A	186.8	0.43	0.08
08/20/04	0.15	7.2	529.4	11.6%	1.02	0.0002	0.1921	Inhibitor A	280.6	0.35	0.06
08/24/04	0.15	7.2	504.2	NA	1.02	0.0002	0.2012	MnSO₄	0.0	5.17	1.00
08/24/04	0.15	7.2	504.2	NA	1.02	0.0002	0.2012	MnSO₄	2.6	12.48	2.41
08/25/04	0.15	7.2	504.2	NA	1.02	0.0002	0.2012	MnSO₄	2.6	4.50	0.87
10/25/04	0.15	7.2	557.6	16.0%	1.02	0.2658	0.0000	Inhibitor A	0.00	2.13	1.00
10/25/04	0.15	7.2	557.6	16.0%	1.02	0.2658	0.0000	Inhibitor A	0.11	1.95	0.92
10/25/04	0.15	7.2	557.6	16.0%	1.02	0.2658	0.0000	Inhibitor A	0.46	1.87	0.88
10/25/04	0.15	7.2	557.6	16.0%	1.02	0.2658	0.0000	Inhibitor A	1.09	1.78	0.84
10/25/04	0.15	7.2	557.6	16.0%	1.02	0.2658	0.0000	Inhibitor A	4.78	1.69	0.79
10/25/04	0.15	7.2	557.6	16.0%	1.02	0.2658	0.0000	Inhibitor A	18.25	1.56	0.73
10/25/04	0.15	7.2	557.6	16.0%	1.02	0.2658	0.0000	Inhibitor A	73.96	1.07	0.50
10/26/04	0.15	7.2	557.6	16.0%	1.02	0.2658	0.0000	Inhibitor A	179.46	0.70	0.33
10/26/04	0.15	7.2	557.6	16.0%	1.02	0.2658	0.0000	Inhibitor A	272.65	0.56	0.26

Date	α	Gas (LPM)	Ave Soln. Mass (g)	% Mass Change	ρ (g/cc)	Fe [mM]	Cu [mM]	Inhibitor	[mM]	NH₃ Evolution [mM/hr]	Relative Rate
11/01/04	0.40	7.3	466.2	-9.7%	1.07	0.3147	0.0000	Inhibitor A	0.00	1.18	1.00
11/01/04	0.40	7.3	466.2	-9.7%	1.07	0.3147	0.0000	Inhibitor A	11.47	0.93	0.79
11/01/04	0.40	7.3	466.2	-9.7%	1.07	0.3147	0.0000	Inhibitor A	48.61	0.48	0.41
11/02/04	0.40	7.3	466.2	-9.7%	1.07	0.3147	0.0000	Inhibitor A	105.65	0.23	0.19
12/01/04	0.15	7.2	461.1	-1.6%	1.02	0.3061	0.0000	Paraformaldehyde	0.0	2.34	1.00
12/01/04	0.15	7.2	461.1	-1.6%	1.02	0.3061	0.0000	Paraformaldehyde	51.1	1.60	0.68
12/01/04	0.15	7.2	461.1	-1.6%	1.02	0.3061	0.0000	Paraformaldehyde	103.7	1.31	0.56
12/01/04	0.15	7.2	461.1	-1.6%	1.02	0.3061	0.0000	Paraformaldehyde	257.4	1.06	0.45
12/01/04	0.15	7.2	461.1	-1.6%	1.02	0.3061	0.0000	Paraformaldehyde	498.0	0.94	0.40
12/01/04	0.15	7.2	461.1	-1.6%	1.02	0.3061	0.0000	Paraformaldehyde	715.6	0.89	0.38
12/01/04	0.15	7.2	461.1	-1.6%	1.02	0.3061	0.0000	Paraformaldehyde	991.7	0.84	0.36
12/02/04				try to oxidize formaldehyde…rate doesn't come back to initial value							
12/07/04	0.15	7.2	473.9	-8.6%	1.02	0.3141	0.0000	Inhibitor A	0.0	2.24	1.00
12/08/04	0.15	7.1	473.9	-8.6%	1.02	0.3141	0.0000	Inhibitor A	56.7	1.77	0.79
12/08/04	0.15	7.1	473.9	-8.6%	1.02	0.3141	0.0000	Inhibitor A	77.8	1.52	0.68
12/08/04	0.15	7.1	473.9	-8.6%	1.02	0.3141	0.0000	Inhibitor A	103.8	1.45	0.65
01/10/05	0.15	7.1	477.8	1.1%	1.02	0.3056	0.0000	Inhibitor A	0.0	1.18	1.00
01/11/05	0.15	7.2	477.8	1.1%	1.02	0.3056	0.0000	Inhibitor A	50.0	0.83	0.70
01/11/05	0.15	7.2	477.8	1.1%	1.02	0.3054	0.0000	Paraformaldehyde	24.7	0.51	0.43
01/11/05	0.15	7.2	477.8	1.1%	1.02	0.3051	0.0000	Paraformaldehyde	49.6	0.37	0.31
01/11/05	0.15	7.2	477.8	1.1%	1.02	0.3049	0.0000	Paraformaldehyde	74.4	0.27	0.23
01/11/05	0.15	7.2	477.8	1.1%	1.02	0.3045	0.0000	Paraformaldehyde	123.1	0.21	0.18
01/13/05	0.15	7.1	495.7	8.0%	1.02	0.2878	0.0000	Inhibitor A	0.0	1.75	1.00
01/14/05	0.15	7.1	495.7	8.0%	1.02	0.2878	0.0000	Inhibitor A	48.0	1.43	0.82
01/14/05	0.15	7.1	495.7	8.0%	1.02	0.2878	0.0000	Paraformaldehyde	23.5	1.33	0.76
01/14/05	0.15	7.1	495.7	8.0%	1.02	0.2878	0.0000	Paraformaldehyde	70.0	1.30	0.74
01/14/05	0.15	7.1	495.7	8.0%	1.02	0.2878	0.0000	Paraformaldehyde	138.3	1.29	0.74
01/14/05	0.15	7.1	495.7	8.0%	1.02	0.2878	0.0000	Paraformaldehyde	289.9	1.12	0.64
01/14/05	0.15	7.1	495.7	8.0%	1.02	0.2878	0.0000	Paraformaldehyde	558.8	0.89	0.51
01/14/05	0.15	7.1	495.7	8.0%	1.02	0.2878	0.0000	Paraformaldehyde	938.7	0.65	0.37

Date	α	Gas (LPM)	Ave Soln. Mass (g)	% Mass Change	ρ (g/cc)	Fe [mM]	Cu [mM]	Inhibitor	[mM]	NH$_3$ Evolution [mM/hr]	Relative Rate
01/24/05	0.15	7.2	495.1	0.6%	1.02	0.2987	0.0000	Na$_2$SO$_3$	0.0	2.38	1.00
01/24/05	0.15	7.2	495.1	0.6%	1.02	0.2987	0.0000	Na$_2$SO$_3$	11.8	2.61	1.10
01/24/05	0.15	7.2	495.1	0.6%	1.02	0.2987	0.0000	Na$_2$SO$_3$	49.3	2.50	1.05
01/24/05	0.15	7.2	495.1	0.6%	1.02	0.2987	0.0000	Na$_2$SO$_3$	99.6	2.21	0.93
01/24/05	0.15	7.2	495.1	0.6%	1.02	0.2987	0.0000	Na$_2$SO$_3$	245.7	1.62	0.68
01/24/05	0.15	7.2	495.1	0.6%	1.02	0.2987	0.0000	Na$_2$SO$_3$	481.7	1.66	0.70
01/24/05	0.15	7.2	495.1	0.6%	1.02	0.2987	0.0000	Na$_2$SO$_3$	667.0	1.63	0.68
01/31/05	0.15	7.3	490.3	NA	1.02	0.3021	0.2047	Inhibitor A	0.0	7.58	1.00
01/31/05	0.15	7.3	490.3	NA	1.02	0.3021	0.2047	Inhibitor A	1.2	7.45	0.98
01/31/05	0.15	7.3	490.3	NA	1.02	0.3021	0.2047	Inhibitor A	5.3	7.19	0.95
01/31/05	0.15	7.3	490.3	NA	1.02	0.3021	0.2047	Inhibitor A	20.3	6.54	0.86
01/31/05	0.15	7.3	490.3	NA	1.02	0.3021	0.2047	Inhibitor A	59.7	4.74	0.63
01/31/05	0.15	7.3	490.3	NA	1.02	0.3021	0.2047	Inhibitor A	122.8	3.41	0.45
01/31/05	0.15	7.3	490.3	NA	1.02	0.3021	0.2047	Inhibitor A	247.3	1.70	0.22

Appendix H: UV-VIS Analysis Data

This appendix documents the results from UV-VIS scans for a large number of samples collected at the end of many of the experiments performed throughout this study. Analysis was performed using a HP 8452A Diode Array Spectrophotometer equipped with a deuterium lamp, and capable of a 2 nm resolution. Data was collected in the range of 200 - 800 nm using 5 ml polycarbonate cuvettes with a 1 cm path length. The sample time was 0.5 sec. Samples with an absorbance above 1.0 cannot be used for qualitative analysis due to deviations from the Beer-Lambert law, as discussed in detail in Chapter 3.

The first section of this appendix contains UV-VIS spectra for a number of standards that were run to identify peak locations for Cu^{+1}, Cu^{+2}, Fe^{+2}, and Fe^{+3}, in de-ionized water and in unloaded MEA. Additional standards were run for pure, loaded, and unloaded MEA, SO_4^{-2}, and formate. These spectra can be seen below in Figure H.1 to Figure H.7. The second section deals with tabulated data for each sample that was analyzed. The color nomenclature assigned to each for Table H.1 lists the nomenclature and order of colors assigned to all of the samples, and Table H.2 gives detailed

information about peak analysis. Typically, UV-VIS data is quantified by taking the maximum height of the peak and multiplying by the width of the peak at half height. This approximated area corresponds to a concentration. This analysis could not be performed for most of the analyzed samples due to significant peak overlap and absorbance heights above the maximum allowable limit. In these cases, a peak width and height were noted.

The final section lists some observations and conclusions based on the observed data. Complete data files for the tabulated sample spectra are available from Gary Rochelle at The University of Texas at Austin. For a complete list of experimental conditions for each sample, please refer to Appendix C, D, E, or F.

H.1. UV-VIS Reference Spectra
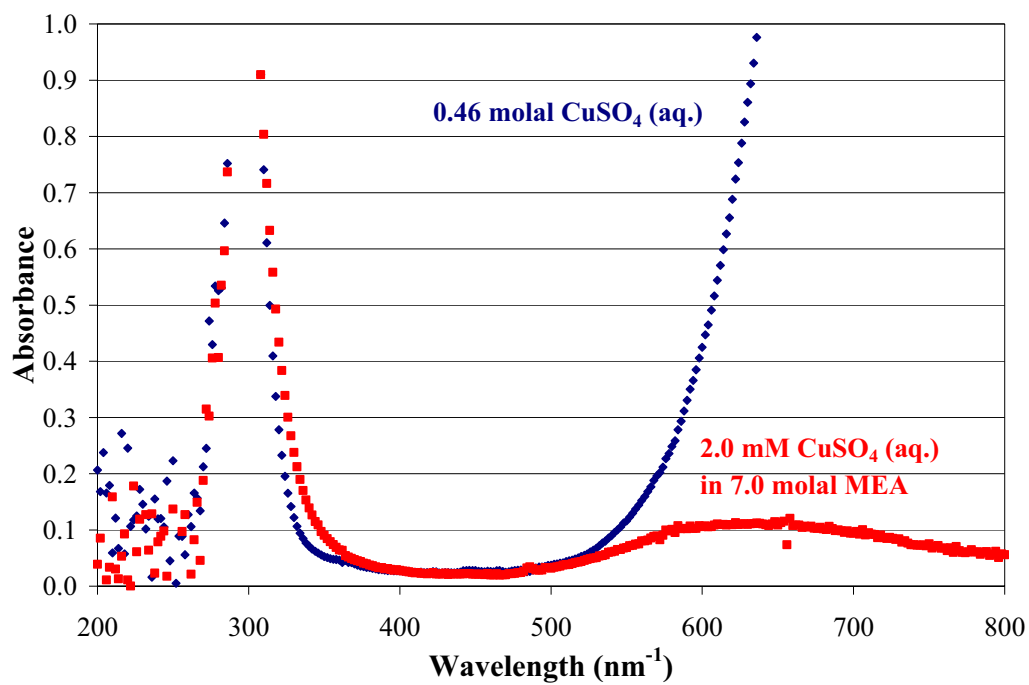
Figure H.1 Reference Spectra for CuSO$_4$ in Water and in 7.0 m MEA at 25°C
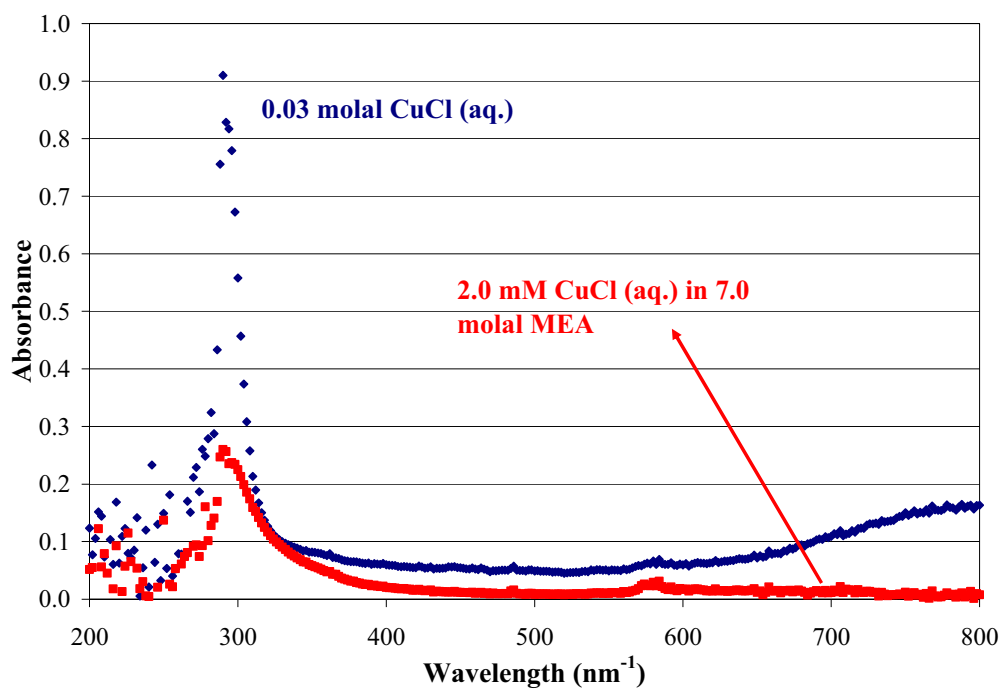
Figure H.2 Reference Spectra for CuCl in Water and in 7.0 m MEA at 25°C

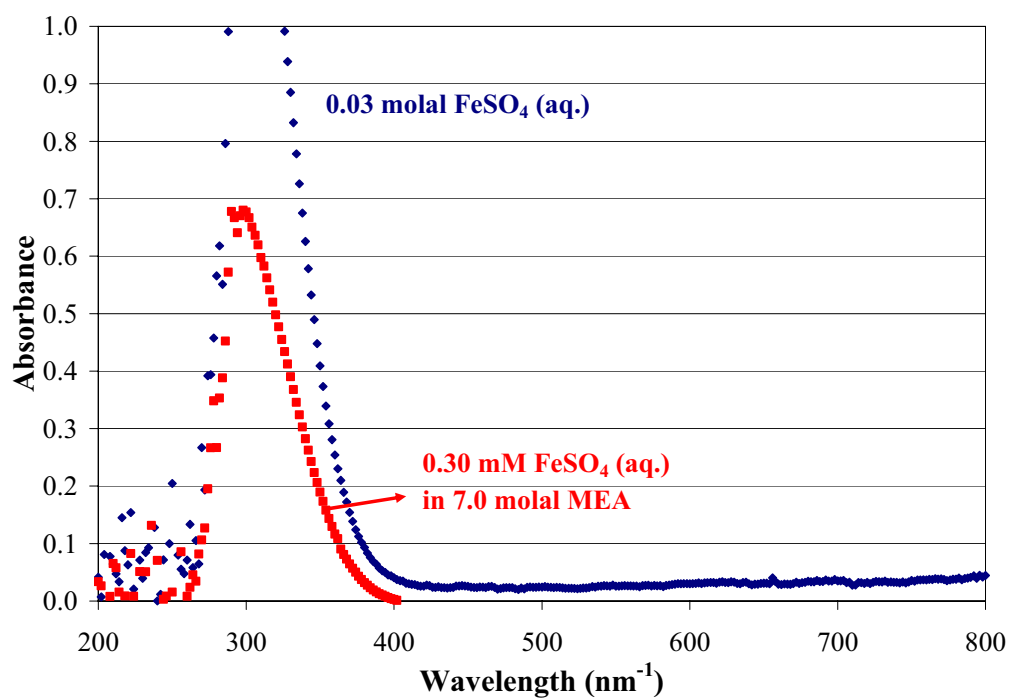**Figure H.3** Reference Spectra for FeSO$_4$ in Water and in 7.0 m MEA at 25°C
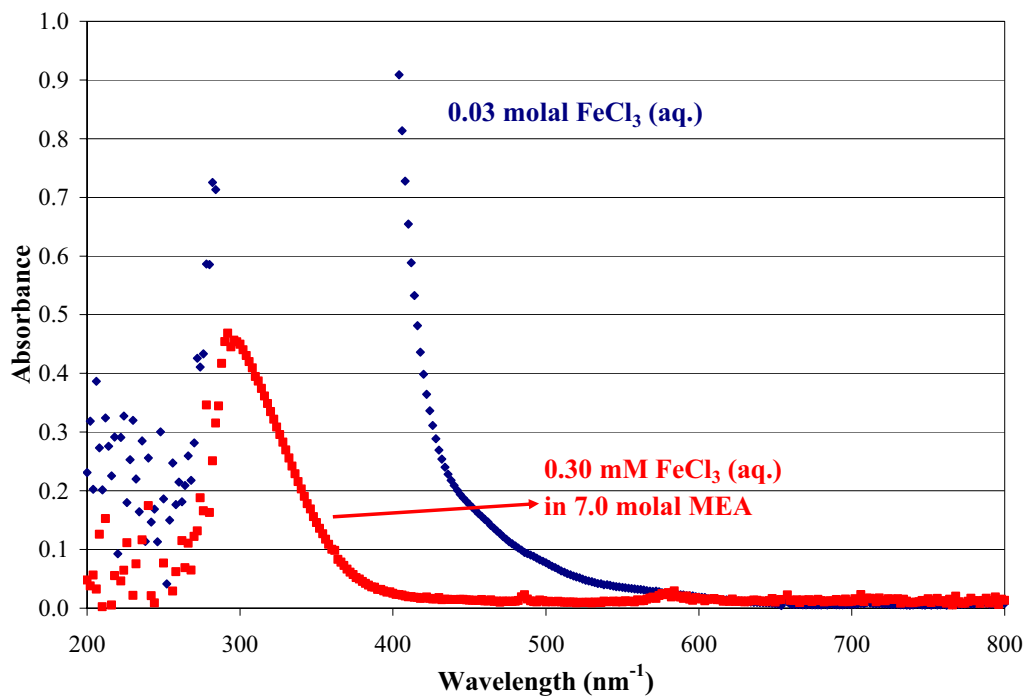
241

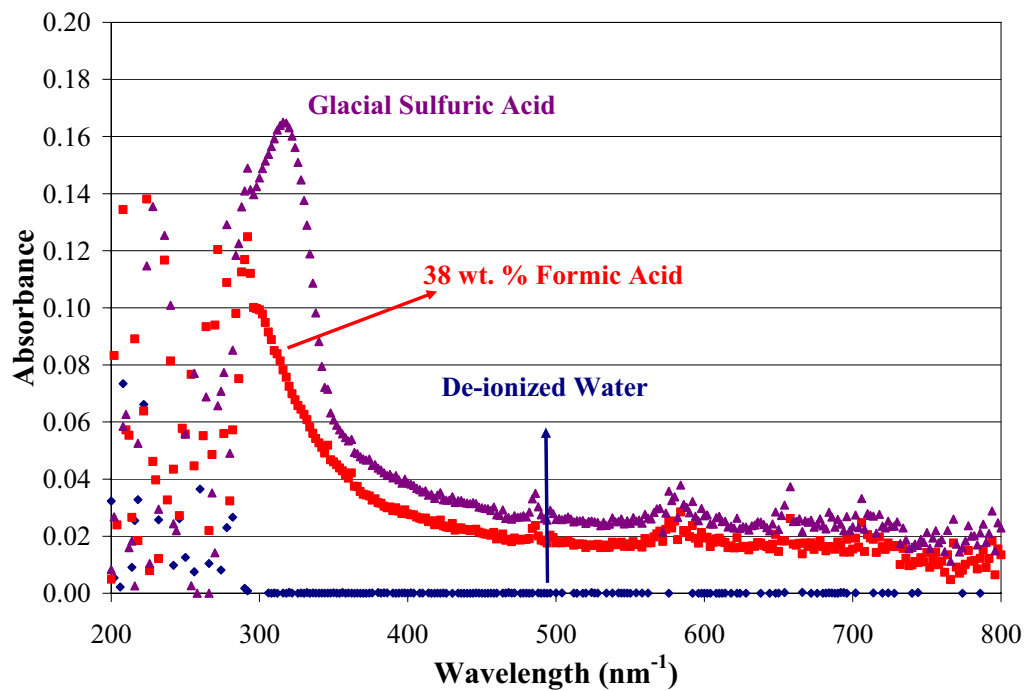**Figure H.4** Reference Spectra for $FeCl_3$ in Water and in 7.0 m MEA at 25°C

Figure H.5 Reference Spectra for De-ionized H_2O, 38 wt. % Formic Acid, and Glacial Sulfuric Acid at 25°C
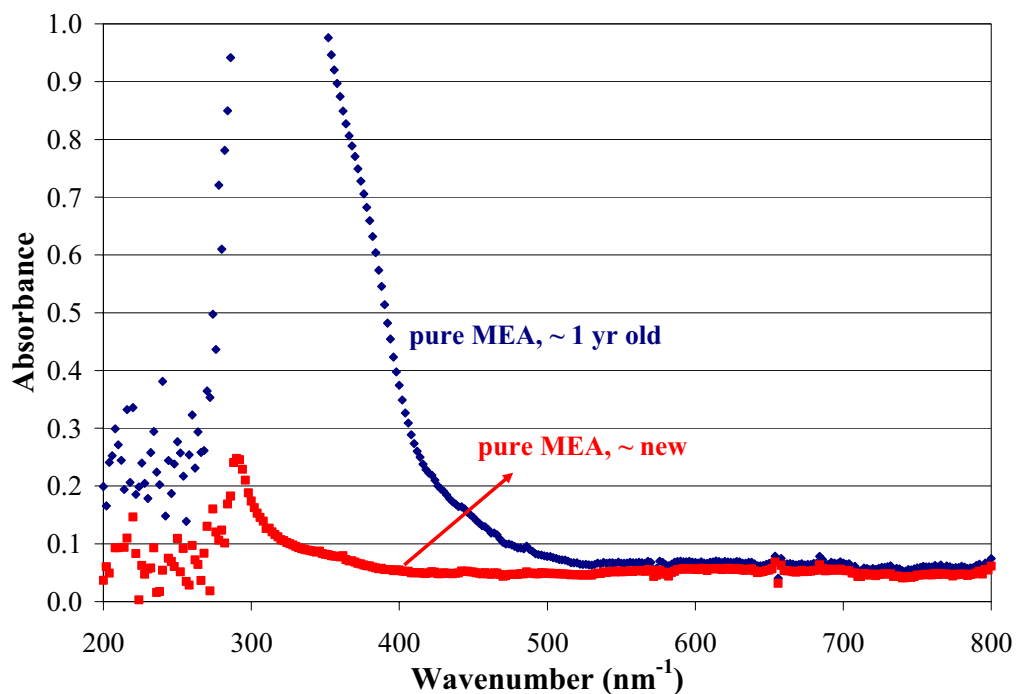
Figure H.6 Reference Spectra for Aged Pure MEA at 25°C
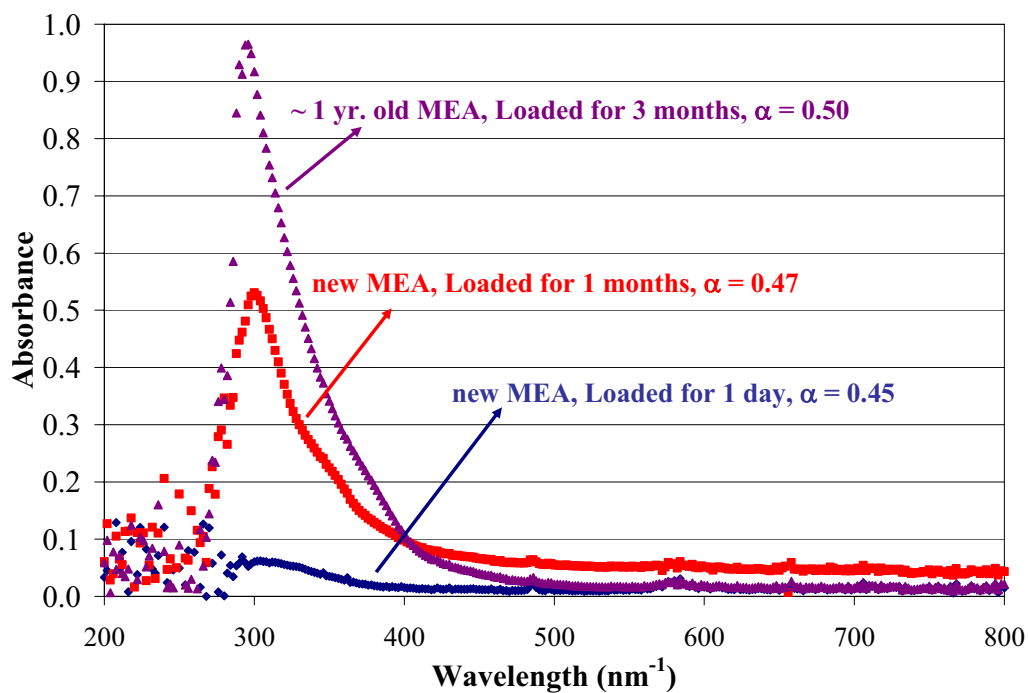
Figure H.7 Reference Spectra for Aged and Loaded 7.0 m MEA at 25°C

243

MEA is a known chelating agent that will form complexes with Fe and Cu in aqueous solution. The reference spectra for the Cu and Fe solutions shows that in the presence of MEA (aq.) the absorbance peaks are dampened. In MEA the Cu^{+1} peak at $600 - 800$ nm^{-1} completely disappears, and Cu^{+2} now shows a distinct peak from $500 - 800$ nm^{-1}. Solutions of Fe^{+2} and Fe^{+3} in MEA both show a peak from $200 - 800$ nm^{-1}. Figure H.5 shows that de-ionized water has no absorbance in the UV-VIS region, and both formic acid and sulfuric acid have a weak absorbance peak at $200 - 400$ nm^{-1}.

Figure H.6 shows scans for new and one year old pure MEA. New MEA is clear and colorless, but after MEA has been opened and exposed to the atmosphere, the MEA turns yellow over time. Both samples have a peak at 300 nm^{-1}, but the aged sample saturates the detector and trails to beyond 500 nm^{-1}. The loaded solutions show the same peak, but the intensity of the peak is less. As the loaded solutions age, the absorption peak increases in both intensity and width. The component responsible for this peak has not been determined, but is likely formed by an irreversible reaction of MEA with CO_2 (Rochelle et al. 2001).

H.2. Data Tabulation for UV-VIS Spectra

The color notation for all solutions was defined as follows:

Dark red (includes purple) < Red-orange < Orange < Yellow-orange < Gold < Yellow < Yellow-Green < Light Green < Green < Dark Green < Light blue < Blue < Dark blue

Miscellaneous: Cloudy brown, Dark brown, Pinkish purple, Brownish black, Cloudy red, and Cloudy orange

Table H.1 Color Notation for Samples that Do Not Have a UV-VIS Scan

Sample	Color
6/27/2001	Dark red
7/30/2001	Dark red (purple)
7/19/2001	Cloudy red
7/31/2001	Orange
6/13/2001	Yellow-orange
8/01/2001	Yellow-orange
6/01/2001	Yellow-orange
8/07/2001	Cloudy orange
6/22/2001	Light green
5/29/2001	Light green
6/20/2001	Light green
7/17/2001	Light green
7/16/2001	Dark green
6/28/2001	Dark green
7/11/2001	Dark green
7/23/2001	Dark green
7/10/2001	Dark green
11/13/2000	Light blue
11/13/2000	Light blue
11/13/2000	Blue
7/20/2001	Dark blue
6/29/2001	Dark blue
8/06/2001	Dark blue

Table H.2 Color Notation for Samples that Do Have a UV-VIS Scan

Date	Color	Date	Color
07/15/02	Yellow-orange	05/26/04	Gold
07/16/02	Yellow-green	06/03/04	Yellow
07/17/02	Dark red	06/04/04	Yellow
07/19/02	Yellow-orange	06/07/04	Dark green
10/15/02	Light green	06/26/04	Dark red (purple)
10/18/02	Yellow-orange	06/28/04	Green
10/21/02	Gold	07/07/04	Orange
10/30/02	Orange	07/08/04	Cloudy brown
11/13/02	Dark red	07/12/04	Orange
12/05/02	Dark red	07/14/04	Orange
12/06/02	Dark red	07/19/04	Orange
12/09/02	Dark red	07/26/04	Brownish black
10/03/03	Orange	07/21/04	Dark brown
10/20/03	Dark red	07/29/04	Orange
10/24/03	Yellow	07/31/04	Red-orange
10/27/03	Yellow-orange	08/04/04	Dark red
10/28/03	Yellow-orange	08/08/04	Yellow-orange
10/30/03	Gold	08/12/04	Red-orange
11/01/03	Yellow-orange	08/20/04	Yellow
11/03/03	Gold	10/25/04	Pinkish purple
11/10/03	Gold	11/02/04	Yellow
11/14/03	Yellow	12/01/04	Yellow-orange
01/29/04	Green	01/11/05	Yellow
02/06/04	Orange	01/13/05	Red-orange
03/22/04	Yellow	01/24/05	Yellow
05/24/04	Yellow	01/31/05	Dark brown

Table H.3 Tabulation of UV-VIS Data for Various Samples in this Work

Date	MEA	Cu	Fe	α	Inhibitors	Main Peak Ends	Shoulder Peak	Max Shoulder Height	Shoulder Ends	Peak	Abs.	Width
	m	mM	mM			nm^{-1}	nm^{-1}	Abs.	nm^{-1}	nm^{-1}	Abs.	nm^{-1}
07/15/02	7.0	0.010	0.820	0.40	EDTA	548						
07/16/02	7.0	0.850	0.001	0.40		528						
07/17/02	7.0	0.000	0.940	0.16		468	538		632			
07/19/02	7.0	0.001	1.500	0.14	EDTA	540						
10/15/02	7.0	9.000	0.970	0.40	EDTA	528				706	0.18	800+
10/18/02	7.0	0.001	12.84	0.21		608						
10/21/02	7.0	0.001	0.980	0.50	α = mol SO$_4^{-2}$ / mol MEA	374	374	1.64	590			
10/30/02	7.0	0.001	0.930	0.05		620						
11/13/02	7.0	0.001	0.100	0.15		478	486	0.59	720			
12/05/02	7.0	0.005	1.090	0.15	Na$_2$SO$_3$	464	544	0.72	670			
12/06/02	7.0	1.000	0.980	0.40		466	466	1.27	766			
12/09/02	7.0	0.013	1.030	0.15		466	538	0.89	706			
10/03/03	7.0	0.180	0.000	0.15	Formaldehyde	616						
10/20/03	7.0	0.000	0.143	0.15		476	476	1.18	712			
10/24/03	7.0	0.170	0.000	0.15		524						
10/27/03	7.0	0.200	0.000	0.15		654						
10/28/03	3.5	0.220	0.000	0.15		570						
10/30/03	3.5	0.240	0.000	0.15		562						
11/01/03	14.0	0.200	0.000	0.15		616						
11/03/03	14.0	0.200	0.000	0.15		560						
11/10/03	7.0	0.190	0.000	0.15		556						
11/14/03	3.5	0.200	0.000	0.15	NaCl	498						
01/29/04	7.0	2.310	0.000	0.15	Na$_2$SO$_3$	512	616	0.19	738			
02/06/04	7.0	0.200	0.000	0.15	Na$_2$SO$_3$	654						
03/22/04	7.0	0.200	0.000	0.40	A	496						
05/24/04	2.0	0.200	0.000	0.15		528						

Date	MEA (m)	Cu (mM)	Fe (mM)	α	Inhibitors	Main Peak Ends (nm^{-1})	Shoulder Peak (nm^{-1})	Max Shoulder Height (Abs.)	Shoulder Ends (nm^{-1})	Peak (nm^{-1})	Abs.	Width (nm^{-1})
05/26/04	2.0	0.210	0.000	0.15		526						
06/03/04	1.0	0.210	0.000	0.15		504						
06/04/04	1.0	0.200	0.000	0.15		320	320	1.95	474			
06/07/04	7.0	3.400	0.000	0.15		506	610	0.69				
06/26/04	7.0	0.000	0.895	0.15		416	534	3.22	658			
06/28/04	7.0	4.060	0.000	0.00		526	598	0.30	776			
07/07/04	7.0	0.210	0.000	0.15	KCl	662						
07/08/04	7.0	0.190	0.000	0.15	MnSO$_4$	402	402	1.38	650			
07/12/04	7.0	0.210	0.000	0.15	MnSO$_4$	650						
07/14/04	7.0	0.210	0.000	0.15	KMnO$_4$	650						
07/19/04	7.0	0.210	0.000	0.15	EDTA	680						
07/26/04	7.0	0.210	0.000	0.15	Quinone							
07/21/04	7.0	0.220	0.000	0.15	KHCO	714						
07/29/04	7.0	0.210	0.000	0.15	Formaldehyde	586						
07/31/04	7.0	0.210	0.000	0.15	Inhibitor A	710						
08/04/04	7.0	0.210	0.000	0.15	K$_3$PO$_4$	708						
08/08/04	7.0	0.210	0.000	0.15	Inhibitor A	584						
08/12/04	7.0	0.220	0.000	0.15	MnSO$_4$	688						
08/20/04	7.0	0.190	0.000	0.15	Inhibitor A	514						
10/25/04	7.0	0.000	0.266	0.15	Inhibitor A	466	542	0.64	684			
11/02/04	7.0	0.000	0.315	0.40	Inhibitor A	560						
12/01/04	7.0	0.000	0.306	0.15	Formaldehyde	548						
01/11/05	7.0	0.000	0.305	0.15	Formaldehyde, Inhibitor A	476						
01/13/05	7.0	0.000	0.288	0.15	Formaldehyde, Inhibitor A	474	548	0.39	662			
01/24/05	7.0	0.000	0.299	0.15	Na$_2$SO$_3$	488	488	0.24	692			
01/31/05	7.0	0.205	0.302	0.15	Inhibitor A	478	538	0.89	752			

248

H.3. Results

All of the samples had a large peak that saturated the detector. The samples could be categorized into two groups: one group where the main peak ended around 500 nm^{-1}, and the second group where the peak was much broader. This main peak includes contributions from Cu^{+1}, Cu^{+2}, Fe^{+2}, Fe^{+3}, SO$_4^{-2}$, formate, and the unknown compound formed in aged MEA solutions. In general, samples that were inhibited, had a lower MEA concentration, or were run for a shorter time had a narrower main peak. Based on the reference spectra above, peaks for MEA, sulfate, formate, Fe, Cu, Fe/MEA, Cu/MEA, and an unknown degradation product that shows up in the pure and unloaded MEA stock solution all are under this main peak.

Several sets of samples had a second peak that was attached to the first main peak, and was noted as a shoulder peak in Table H.3. This peak is thought to be an Fe-MEA complex based on the reference spectra above. Several samples had extremely wide main peaks that ended between 600 and 700 nm^{-1}. This corresponds roughly to the Cu/MEA complex seen in the reference spectra above. Samples with hydroquinone, potassium formate, PO$_4^{-3}$, and high Fe concentrations all had very broad peaks that absorbed across the entire wavelength region.

The sample time was changed from 0.5 sec. up to 25 sec. and there was no noticeable change in spectrum resolution. In order to try to quantify the main peak from 200 to 500 nm^{-1}, a typical single peak sample (7/14/04) was diluted multiple times. The sample had to be diluted by a factor of 160 before the main peak did not exceed 1.0

absorbance. With a dilution factor of 320 the resolution on the main peak was good enough for quantification, but at this low a concentration any metals or degradation products could not be quantified.

In general, solutions with only Cu ranged from light green to dark blue in color, and solutions with only Fe ranged from dark red to orange. Solutions with both Fe and Cu tended to be yellow in color. The addition of degradation products and most of the screened inhibitors tended to make the color darker. Manganese solutions were dark orange or red, and Inhibitor A solutions were yellow. Formate turned Cu solutions red orange and Fe solutions yellow-orange. Sulfite turned Cu solutions green or orange and Fe solutions yellow.

It should also be noted again (Chapter 5), that inhibited Fe solutions tended to turn darker colors in the absence of O_2, but Cu solutions did not exhibit this color change.

Appendix I: Inhibitor A Information

This appendix discloses the identity of the proprietary additive Inhibitor A, and includes a list of available literature. The three different oxidation states of Inhibitor A used in this work are also identified. The information in this appendix is available from Gary Rochelle at The University of Texas at Austin.

Bibliography

ABB *CO₂ Recovery from Flue Gas/Turbine Exhaust Gas: Kerr-McGee/Lummus Carbon Dioxide Recovery Technology.* ABB Lummus Global: 1998; 12.

Alawode, A. Oxidative Degradation of Piperazine. Masters Thesis, The University of Texas at Austin, Austin, TX, 2005 (in progress).

Alawode, A. Oxidative Degradation of Piperazine (in progress). Masters Thesis, The University of Texas at Austin, Austin, TX, 2005.

Alejandre, J.; Rivera, J. L.; Mora, M. A.; De la Garza, V. Force Field of Monoethanolamine. *Journal of Physical Chemistry B* **2000,** *104*(6), 1332-1337.

Alstom Power Inc.; ABB Lumus Global Inc.; American Electric Power *Engineering Feasibility and Economics of CO₂ Capture on an Existing Coal-fired Power Plant. Final Report. Volume I: American Electric Power's Conesville Power Plant Unit No. 5 CO₂ Capture Retrofit Study.* PPL-01-CT-09; U.S. Department of Energy, National Energy Transportation Laboratory: Pittsburgh, PA, 2001; 65.

Arnold, D. S.; Barrett, D. A.; Isom, R. H. Carbon Dioxide Can be Produced from Flue Gas. *Oil and Gas Journal* **1982,** *80*(47), 130-136.

Astarita, G. Regimes of Mass Transfer with Chemical Reaction. *Journal of Industrial and Engineering Chemistry (Washington, D. C.)* **1966,** *58*(8), 18-26.

Austgen, D. M., Jr A Model of Vapor-Liquid Equilibria for Acid Gas-Alkanolamine-Water Systems. Doctoral Thesis, The University of Texas at Austin, Austin, 1989.

Barron, C. H.; O'Hern, H. A. Reaction Kinetics of Sodium Sulfite Oxidation by the Rapid Mixing Method. *Chemical Engineering Science* **1966,** *21*, 397-404.

Bello, A.; Idem, R. O. Pathways for the Formation of Products of the Oxidative Degradation of CO₂-Loaded Concentrated Aqueous Monoethanolamine Solutions during CO₂ Absorption from Flue Gases. *Industrial & Engineering Chemistry Research* **2005,** *44*(4), 945-969.

Bengtsson, S.; Bjerle, I. Catalytic Oxidation of Sulphite in Diluted Aqueous Solutions. *Chemical Engineering Science* **1975,** *30*, 1429-1435.

Billet, R. *Packed Towers: In Processing and Environmental Technology*. John Wiley & Sons: 1997.

Blachly, C. H.; Ravner, H. *The Effect of Trace Amounts of Copper on the Stability of Monoethanolamine Scrubber Solutions*. NRL-MR-1482; U.S. Naval Research Laboratory: Washington, D.C., December, 1963, 1963; 9.

Blachly, C. H.; Ravner, H. *The Stabilization of Monoethanolamine Solutions for Submarine Carbon Dioxide Scrubbers*. AD609888; NRL-FR-6189; NRL-6189; Naval Research Laboratory: Washington, D.C., 1964.

Blachly, C. H.; Ravner, H. Stabilization of Monoethanolamine Solutions in Carbon Dioxide Scrubbers. *Journal of Chemical Engineering Data* **1966,** *11*(3), 401-3.

Blachly, C. H.; Ravner, H. *Studies of Submarine Carbon Dioxide Scrubber Operation: Effect of an Additive Package for the Stabilization of Monoethanolamine Solutions*. NRL-MR-1598; U.S. Naval Research Laboratory: Washington, D.C., March, 1965, 1965.

Button, J. K.; Gubbins, K. E.; Tanaka, H.; Nakanishi, K. Molecular Dynamics Simulation of Hydrogen Bonding in Monoethanolamine. *Fluid Phase Equilib.* **1996,** *116*(1-2), 320-325.

Chakravarti, S.; Gupta, A. Carbon Dioxide Recovery Plant. US-20010026779, 2001.

Chapman, C. M.; Gibilaro, L. G.; Nienow, A. W. A Dynamic Response Technique for the Estimation of Gas-Liquid Mass Transfer Coefficients in a Stirred Vessel. *Chemical Engineering Science* **1982,** *37*(6), 891-6.

Chen, T.-I.; Barron, C. H. Some Aspects of the Homogeneous Kinetics of Sulfite Oxidation. *Industrial & Engineering Chemistry Fundamentals* **1972,** *11*(4), 466-470.

Chi, Q. S. Oxidative Degradation of Monoethanolamine. Masters Thesis, The University of Texas at Austin, Austin, TX, 2000.

Chi, S.; Rochelle, G. T. Oxidative Degradation of Monoethanolamine. *Industrial & Engineering Chemistry Research* **2002,** *41*(17), 4178-4186.

CMR Prices & People. *Chemical Market Reporter* **2003,** *264*(10), 20-23.

Comeaux, R. V. The Mechanism of MEA (Monoethanolamine) Corrosion. *Proc. Am. Petrol. Inst., Sect. III* **1962,** *42*(3), 481-489.

Conklin, M. H.; Hoffmann, M. R. Metal Ion-Sulfur(IV) Chemistry. 2. Kinetic Studies of the Redox Chemistry of Copper(II)-Sulfur(IV) Complexes. *Environmental Engineering Science* **1988,** *22*(8), 891-898.

Cringle, D. C.; Pearce, R. L.; Dupart, M. S. Method for Maintaining Effective Corrosion Inhibition in Gas Scrubbing Plant. 4690740, 1987.

Cullinane, J. T. Thermodynamics and Kinetics of Aqueous Piperazine with Potassium Carbonate for Carbon Dioxide Absorption. Doctoral Thesis, The University of Texas at Austin, Austin, 2005.

Dang, H. CO_2 Absorption Rate and Solubility in Monoethanolamin/Piperazine/Water. Master of Science of Engineering Thesis, The University of Texas at Austin, Austin, TX, 2000.

Davison, J.; Freund, P.; Smith, A. *Putting Carbon Back into the Ground.* IEA Greenhouse Gas R&D Programme: 2001; 28.

Dean, J. A. *Lange's Handbook of Chemistry*. 14 ed.; 1992.

Dennis, W. H., Jr.; Hull, L. A.; Rosenblatt, D. H. Oxidations of Amines. IV. Oxidative Fragmentation. *Journal of Organic Chemistry* **1967,** *32*(12), 3783-3787.

Energy Information Administration *Emisssions of Greenhouse Gases in the United States 2003*. 2004a ftp://ftp.eia.doe.gov/pub/oiaf/1605/cdrom/pdf/ggrpt/057303.pdf (Accessed March 2005).

Energy Information Administration *International Energy Annual 2002*. 2004b http://www.eia.doe.gov/iea/contents.html (Accessed March 2005).

EPA *Technology Transfer Network Air Toxics Website, The original list of hazardous air pollutants*. 1990 http://www.epa.gov/ttn/atw/orig189.html (Accessed March 2005).

Fessenden, R. J.; Fessenden, J. S. *Organic Chemistry*. 5th ed.; Brooks/Cole Publishing Company: Pacific Grove, CA, 1994.

Freguia, S. Modeling of CO_2 Removal from Flue Gases with Monoethanolamine. Masters Thesis, The University of Texas at Austin, Austin, TX, 2002.

Gaddis, E. S. Mass Transfer in Gas-Liquid Contactors. *Chemical Engineering and Processing* **1999,** *38*(4-6), 503-510.

Garcia-Ochoa, F.; Gomez, E. Mass Transfer Coefficient In Stirred Tank Reactors for Xanthan Gum Solutions. *Biochemical Engineering Journal* **1998,** *1*(1), 1-10.

Girdler Corporation *Carbon Dioxide Absorbants.* Contract No. 50023; Girdler Corporation, Gas Processes Division: Louisville, KY, June, 1, 1950.

Goff, G. S.; Rochelle, G. T. Monoethanolamine Degradation: O_2 Mass Transfer Effects under CO_2 Capture Conditions. *Industrial & Engineering Chemistry Research* **2004,** *43*(20), 6400-6408.

Goff, G. S.; Rochelle, G. T. *Oxidative Degradation of Aqueous Monoethanolamine in CO_2 Capture Systems Under Absorber Conditions*, 6th International Conference on Greenhouse Gas Control Technologies, Kyoto, Japan, 2003; Gale, J., et al., Eds. Elsevier: Oxford UK: Kyoto, Japan, 2003; 115-120.

Grace, J. Understanding and Managing the Global Carbon Cycle. *Journal of Ecology* **2004,** *92*(2), 189-202.

Hakka, L. E.; Ouimet, M. A. Recovery of CO_2 from Waste Gas Streams Using Amines as Absorbents. US-2004253159, 2004.

Ho, F. *The Effect on the Stability of Monoethanolamine by Vanadium Metal.* Submitted to Gary T. Rochelle at The University of Texas at Austin: 2003.

Hofmeyer, B. G.; Scholten, H. G.; Lloyd, W. G. Contamination and Corrosion in Monoethanolamine Gas Treating Solutions. *Am. Chem. Soc., Div. Petrol. Chem., Preprints-Symposia* **1956,** *1*(2), 91-99.

Hull, L. A.; Davis, G. T.; Rosenblatt, D. H. Oxidations of Amines. IX. Correlation of Rate Constants for Reversible One-electron Transfer in Amine Oxidation with Reactant Potentials. *J. Amer. Chem. Soc.* **1969a,** *91*(23), 6247-50.

Hull, L. A.; Davis, G. T.; Rosenblatt, D. H.; Mann, C. K. Oxidations of Amines. VII. Chemical and Electrochemical Correlations. *J. Phys. Chem.* **1969b,** *73*(7), 2142-6.

Hull, L. A.; Davis, G. T.; Rosenblatt, D. H.; Williams, H. K. R.; Weglein, R. C. Oxidations of Amines. III. Duality of Mechanism in the Reaction of Amines with Chlorine Dioxide. *J. Am. Chem. Soc.* **1967,** *89*(5), 1163-1170.

Hull, L. A.; Giordano, W. P.; Rosenblatt, D. H.; Davis, G. T.; Mann, C. K.; Milliken, S. B. Oxidations of Amines. VIII. Role of the Cation Radical in the Oxidation of Triethylenediamine by Chlorine Dioxide and Hypochlorous Acid. *J. Phys. Chem.* **1969c,** *73*(7), 2147-52.

IEA *Carbon Dioxide Capture from Power Stations.* IEA Greenhouse Gas R&D Programme: http://www.ieagreen.org.uk/capt1.htm (Accessed 2/15/2001), 1999.

IEA *CO$_2$ Capture at Power Stations and Other Major Point Sources.* International Energy Agency, Working Party on Fossil Fuels: Paris, France, 2003; 13.

IPCC *Climate Change 2001: The Scientific Basis.* Published for International Panel on Climate Change by Cambridge University Press: New York, 2001.

Jones, G.; Ray, W. A. The Surface Tension of Solutions of Electrolytes as a Function of the Concentration. IV. Magnesium Sulfate. *Journal of the American Chemical Society* **1942,** *64*, 2744-5.

Jones, T. Oxidative Degradation of Piperazine in Aqueous Potassium Carbonate. Masters Thesis, The University of Texas at Austin, Austin, TX, 2003.

Jou, F.-Y.; Mather, A. E.; Otto, F. D. The Solubility of CO$_2$ in a 30 Mass Percent Monoethanolamine Solution. *Canadian Journal of Chemical Engineering* **1995,** *73*(1), 140-7.

Keeling, C. D.; Whorf, T. P. Atmospheric CO$_2$ Records from Sites in the SIO Air Sampling Network. In *Trends: A Compendium of Data on Global Change*;

Carbon Dioxide Information Analysis Center, Oak Ridge National Laboratory, U.S. Department of Energy: Oak Ridge, Tenn., U.S.A., 2004.

Kohl, A.; Nielsen, R. *Gas Purification*. 5th ed.; Gulf Publishing Co.: Houston, 1997.

Korosi, A.; Fabuss, B. M. Viscosities of Binary Aqueous Solutions of Sodium Chloride, Potassium Chloride, Sodium Sulfate, and Magnesium Sulfate at Concentrations and Temperatures of Interest in Desalination Processes. *Journal of Chemical and Engineering Data* **1968,** *13*(4), 548-52.

Kyoto Protocol *The United Nations Framework Convention on Climate Change*. 2004 http://unfccc.int/resource/convkp.html (Accessed March 2005).

Lawal, A. O.; Idem, R. O. Effects of Operating Variables on the Product Distribution and Reaction Pathways in the Oxidative Degradation of CO_2-Loaded Aqueous MEA-MDEA Blends during CO_2 Absorption from Flue Gas Streams. *Industrial & Engineering Chemistry Research* **2005,** *44*(4), 986-1003.

Lawal, O.; Bello, A.; Idem, R. The Role of Methyl Diethanolamine (MDEA) in Preventing the Oxidative Degradation of CO_2 Loaded and Concentrated Aqueous Monoethanolamine (MEA)-MDEA Blends during CO_2 Absorption from Flue Gases. *Industrial & Engineering Chemistry Research* **2005,** *44*(6), 1874-1896.

Lee, Y. J. Oxidative Degradation of Organic Acids Conjugated with Sulfite Oxidation in Flue Gas Desulfurization. Doctoral Thesis, The University of Texas at Austin, Austin, 1986.

Lewis, W. K.; Whitman, W. G. Principles of Gas Absorption. *Journal of Industrial and Engineering Chemistry (Washington, D. C.)* **1924,** *16*, 1215-20.

Linek, V.; Vacek, V. Chemical Engineering Use of Catalyzed Sulfite Oxidation Kinetics for the Determination of Mass Transfer Characteristics of Gas-Liquid Contactors. *Chemical Engineering Science* **1981,** *36*(11), 1747-68.

Lloyd, W. G. The Low-Temperature Autoxidation of Diethylene Glycol. *Journal of the American Chemical Society* **1956,** *78*, 72-75.

Lockhart, L. B., Jr.; Piatt, V. R. *The Present Status of Chemical Research in Atmosphere Purification and Control on Nuclear-Powered Submarines.* AD

614261; Naval Res. Lab.,Washington,DC, FIELD URL:: March 23, 1965, 1965; 42-50 pp.

McGlamery, G. G.; Torstrick, R. L.; Broadfoot, W. J.; Simpson, J. P.; Henson, L. J.; Tomlinson, S. V.; Young, J. F. *Detailed Cost Estimates for Advanced Effluent Desulfurization Processes.* EPA-600/2-75-006; U.S. Environmental Protection Agency: Washington, D.C., 1975.

Nakayanagi, M. Formation of $FeCO_3$ Scale Layer and Corrosion of Carbon Steel in CO_2-loaded Aqueous Alkanolamine Solutions. *Sekiyu Gakkaishi* **1996,** *39*(5), 322-329.

Nelson, M. Personal Communication to George S. Goff. Austin, TX, 2005.

NRC *Climate Change Science: An Analysis of Key Questions.* 0-309-07574-2; National Research Council Committee on the Science of Climate Change, National Academy Press: Washington, D.C., 2001.

Onda, K.; Takeuchi, H.; Okumoto, Y. Mass Transfer Coefficients Between Gas and Liquid Phases in Packed Columns. *Journal of Chemical Engineering of Japan* **1968,** *1*(1), 56-62.

Pearce, R. L. Removal of Carbon Dioxide From Industrial Gases. U.S. Patent 4440731, 1984.

Pearce, R. L.; Pauley, C. R.; Wolcott, R. A. Recovery of Carbon Dioxides from Gases. U.S. Patent 2135900, 1984.

Perry, R. H.; Green, D. W.; Maloney, J. O. *Perry's Chemical Engineers' Handbook.* 7th ed.; McGraw-Hill: New York, 1997.

Petryaev, E. P.; Pavlov, A. V.; Shadyro, O. I. Homolytic Deamination of Amino Alcohols. *Zh. Org. Khim.* **1984,** *20*(1), 29-34.

Polderman, L. D.; Dillon, C. P.; Steele, A. B. Why Monoethanolamine Solution Breaks Down in Gas-Treating Service. *Oil and Gas Journal* **1955,** *54*(No. 2), 180-3.

Ranney, M. W. *Corrosion Inhibitors - Manufacture and Technology.* Noyes Data Corporation: Park Ridge, NJ, 1976.

Rao, A. B.; Rubin, E. S. A Technical, Economic, and Environmental Assessment of Amine-Based CO_2 Capture Technology for Power Plant Greenhouse Gas Control. *Environmental Science and Technology* **2002,** *36*(20), 4467-4475.

Riggs, O. L., Jr. Theoretical Aspects of Corrosion Inhibitors and Inhibition. In *Corrosion Inhibitors*, Nathan, C. C., Ed.; National Association of Corrosion Engineers: Houston, 1973; 7-27.

Rochelle, G. T.; Bishnoi, S.; Chi, S.; Dang, H.; Santos, J. *Research Needs for CO_2 Capture from Flue Gas by Aqueous Absorption/Stripping.* DE-AF26-99FT01029; U.S. Department of Energy - Federal Energy Technology Center: Pittsburgh, PA, 2001.

Rooney, P. C.; DuPart, M. S.; Bacon, T. R. Oxygen's Role in Alkanolamine Degradation. *Hydrocarbon Process., Int. Ed.* **1998,** *77*(7), 109-113.

Rosenblatt, D. H.; Hayes, A. J., Jr.; Harrison, B. L.; Streaty, R. A.; Moore, K. A. Reaction of Chlorine Dioxide with Triethylamine in Aqueous Solution. *Journal of Organic Chemistry* **1963,** *28*(10), 2790-2794.

Rosenblatt, D. H.; Hull, L. A.; DeLuca, D. C.; Davis, G. T.; Weglein, R. C.; Williams, H. K. R. Oxidations of Amines. II. Substituent Effects in Chlorine Dioxide Oxidations. *J. Am. Chem. Soc.* **1967,** *89*(5), 1158-1163.

Ruddiman, W. F. How Did Humans First Alter Global Climate. *Scientific American* **2005,** *292*(3), 46-53.

Saarinen, P.; Kauppinen, J. Multicomponent Anaylsis of FT-IR Spectra. *Applied Spectroscopy* **1991,** *45*(6), 953-963.

Seader, J. D.; Henley, E. J. *Separation Process Principles*. 1st ed.; John Wiley & Sons: 1997.

Seibig, S.; van Eldik, R. Kinetics of [FeII(EDTA)] Oxidation by Molecular Oxygen Revisited. New Evidence for a Multistep Mechanism. *Inorganic Chemistry* **1997,** *36*(18), 4115-4120.

Somogyi, L. P. Kirk-Othmer Encyclopedia of Chemical Technology, *Food Additives in Kirk-Othmer Encyclopedia of Chemical Technology*. 2004

http://www.mrw.interscience.wiley.com/kirk/articles/foodfrie.a01/frame.html (Accessed October 2004).

Strazisar, B. R.; Anderson, R. R.; White, C. M. Degradation Pathways for Monoethanolamine in a CO_2 Capture Facility. *Energy & Fuels* **2003,** *17*(4), 1034-1039.

Supap, T. Kinetic Study of Oxidative Degradation in Gas Treating Unit Using Aqueous Monoethanolamine Solution. MS Thesis, University of Regina, Regina, Saskatchewan, 1999.

Supap, T.; Idem, R.; Veawab, A.; Aroonwilas, A.; Tontiwachwuthikul, P.; Chakma, A.; Kybett, B. D. Kinetics of the Oxidative Degradation of Aqueous Monoethanolamine in a Flue Gas Treating Unit. *Industrial & Engineering Chemistry Research* **2001,** *40*(16), 3445-3450.

Tanthapanichakoon, W.; Veawab, A. Heat Stable Salts and Corrosivity in Amine Treating Units. *Greenhouse Gas Control Technologies, Proceedings of the International Conference on Greenhouse Gas Control Technologies, 6th, Kyoto, Japan, Oct. 1-4, 2002* **2003,** *2*, 1591-1594.

Taylor, S. M.; Halpern, J. Kinetics of the Permanganate Oxidation of Formic Acid and Formate Ion in Aqueous Solution. *Journal of the American Chemical Society* **1959,** *81*, 2933-8.

Tromans, D. Modeling Oxygen Solubility in Water and Electrolyte Solutions. *Industrial & Engineering Chemistry Research* **2000,** *39*(3), 805-812.

U.S. Census Bureau International Population Reports WP/02, *Global Population Profile: 2002*. 2004 http://www.census.gov/ipc/www/wp02.html (Accessed March 2005).

Ulrich, R. K. Sulfite Oxidation Under Flue Gas Desulfurization Conditions: Enhanced Oxygen Absorption Catalyzed by Transition Metals. Doctoral Thesis, The University of Texas at Austin, Austin, 1983.

Van't Riet, K. Review of Measuring Methods and Results in Nonviscous Gas-Liquid Mass Transfer in Stirred Vessels. *Industrial & Engineering Chemistry Process Design & Development* **1979,** *18*(3), 357-364.

Vazquez, G.; Alvarez, E.; Navaza, J. M.; Rendo, R.; Romero, E. Surface Tension of Binary Mixtures of Water + Monoethanolamine and Water + 2-Amino-2-methyl-1-propanol and Tertiary Mixtures of These Amines with Water from 25^oC to 50^oC. *Journal of Chemical and Engineering Data* **1997,** *42*(1), 57-59.

Veawab, A.; Aroonwilas, A. Identification of Oxidizing Agents in Aqueous Amine-CO_2 Systems Using a Mechanistic Corrosion Model. *Corrosion Science* **2002,** *44*(5), 967-987.

Veawab, A.; Tontiwachwuthikul, P.; Chakma, A. Influence of Process Parameters on Corrosion Behavior in a Sterically Hindered Amine-CO_2 System. *Industrial & Engineering Chemistry Research* **1999,** *38*(1), 310-315.

Veldman, R. R.; Trahan, D. Oxygen Scavenging Solutions for Reducing Corrosion by Heat Stable Amine Salts. 5686016, 1997.

Veldman, R. R.; Trahan, D. O. Addition of Oxygen Scavengers as Corrosion Inhibitors to Alkanolamine Solutions for Treatment of Natural Gas and Petroleum Fluids. 6299836, 2001.

Vorobyov, I.; Yappert, M. C.; DuPre, D. B. Hydrogen Bonding in Monomers and Dimers of 2-Aminoethanol. *Journal of Physical Chemistry A* **2002,** *106*(4), 668-679.

Weiland, R. H. *Physical Properties of MEA, DEA, MDEA, and MDEA-Based Blends Loaded with CO_2.* GPA Research Report No. 152; Gas Processors Association: Tulsa, OK, 1996.

Weiland, R. H.; Dingman, J. C.; Cronin, D. B.; Browning, G. J. Density and Viscosity of Some Partially Carbonated Aqueous Alkanolamine Solutions and Their Blends. *Journal of Chemical and Engineering Data* **1998,** *43*(3), 378-382.

White, J. C. Deaerator Providing Control of Physicochem. Oxygen Scavenging in Boiler Feedwaters. US-20010045396, 2001.

Wiberg, K. B.; Stewart, R. The Mechanism of Permanganate Oxidation. I. The Oxidation of Some Aromatic Aldehydes. *Journal of the American Chemical Society* **1955,** *77*, 1786-95.

Wolcott, R. A.; Pauley, C. R.; Pearce, R. L. Recovery of copper inhibitor in the recovery of carbon dioxide from flue gases. 8502555, 1985.

Wong, H. A.; Kohler, R.; Kosseim, A. J.; Kubek, D. J.; McCullough, J. G. Corrosion-Inhibition System Passes Severest Test at Chevron's Princess MEA Plant. *Oil and Gas Journal* **1985,** *83*(45), 100-108.

Yazvikova, N. V.; Zelenskaya, L. G.; Balyasnikova, L. V. Mechanism of Side reactions During removal of Carbon Dioxide from Gases by Treatment with Monoethanolamine. *Zhurnal Prikladnoi Khimii* **1975,** *48*(3), 674-676.

Vita

George Scott Goff was born on November 23, 1977 in Parkersburg, West Virginia to Glenn Scott Goff and Sandra West Goff. The author graduated from St. Marys High School, in St. Marys WV in 1996, and then entered the chemical engineering program at West Virginia University where he graduated cum laude with B.S. in May 2000. While attending WVU, he worked three summers at the GE Silicones - OSi Specialties plant in Friendly, WV and during his senior year worked as an intern in the Environmental Health and Safety Department of Mylan Pharmaceuticals in Morgantown, WV. The author began attendance at The University of Texas at Austin in the fall of 2000 where he commenced his graduate studies in the department of chemical engineering, where he has served as a teaching assistant and assistant instructor of the capstone design course.

Permanent Address: 630 Ruby St.

Belmont, West Virginia 26134

This dissertation was typed by the author.